Thermal Imaging Cameras

Characteristics and Performance

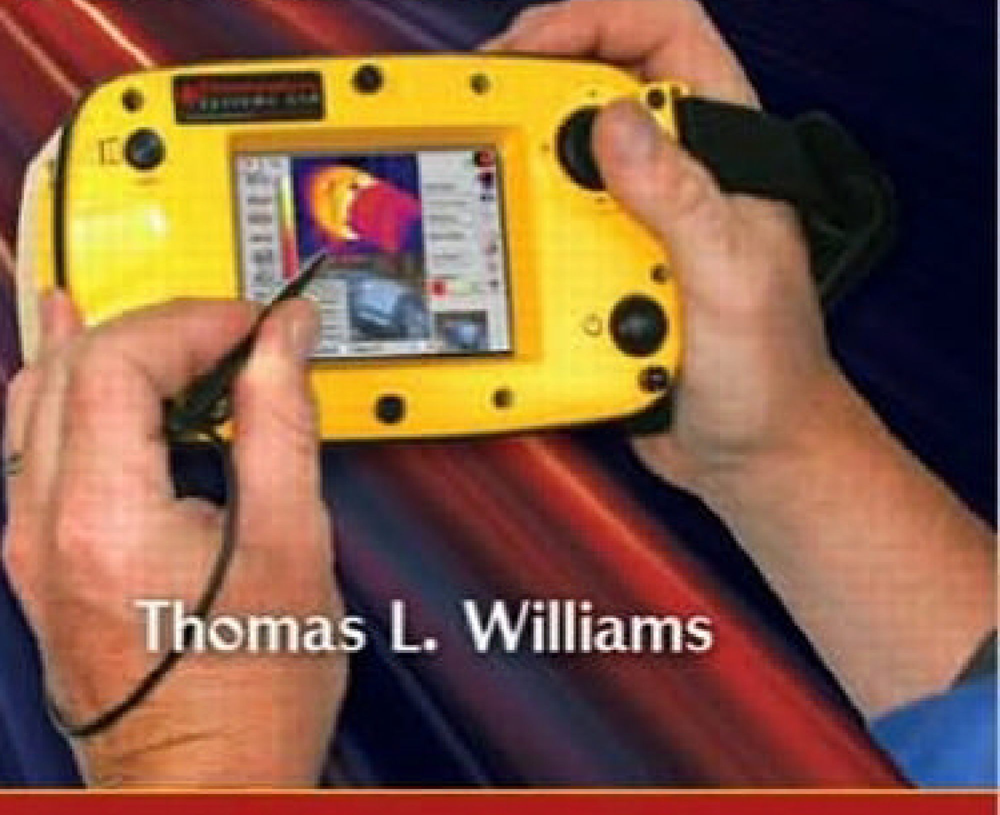

Thomas L. Williams

CRC Press
Taylor & Francis Group

Thermal Imaging Cameras

Characteristics and Performance

Thermal Imaging Cameras

Characteristics and Performance

Thomas L. Williams

CRC Press
Taylor & Francis Group
Boca Raton London New York

CRC Press is an imprint of the
Taylor & Francis Group, an **informa** business

CRC Press
Taylor & Francis Group
6000 Broken Sound Parkway NW, Suite 300
Boca Raton, FL 33487-2742

© 2009 by Taylor & Francis Group, LLC
CRC Press is an imprint of Taylor & Francis Group, an Informa business

No claim to original U.S. Government works
Printed in the United States of America on acid-free paper
10 9 8 7 6 5 4 3 2 1

International Standard Book Number-13: 978-1-4200-7185-6 (Hardcover)

This book contains information obtained from authentic and highly regarded sources. Reasonable efforts have been made to publish reliable data and information, but the author and publisher cannot assume responsibility for the validity of all materials or the consequences of their use. The authors and publishers have attempted to trace the copyright holders of all material reproduced in this publication and apologize to copyright holders if permission to publish in this form has not been obtained. If any copyright material has not been acknowledged please write and let us know so we may rectify in any future reprint.

Except as permitted under U.S. Copyright Law, no part of this book may be reprinted, reproduced, transmitted, or utilized in any form by any electronic, mechanical, or other means, now known or hereafter invented, including photocopying, microfilming, and recording, or in any information storage or retrieval system, without written permission from the publishers.

For permission to photocopy or use material electronically from this work, please access www.copyright.com (http://www.copyright.com/) or contact the Copyright Clearance Center, Inc. (CCC), 222 Rosewood Drive, Danvers, MA 01923, 978-750-8400. CCC is a not-for-profit organization that provides licenses and registration for a variety of users. For organizations that have been granted a photocopy license by the CCC, a separate system of payment has been arranged.

Trademark Notice: Product or corporate names may be trademarks or registered trademarks, and are used only for identification and explanation without intent to infringe.

Library of Congress Cataloging-in-Publication Data

Williams, T. L.
Thermal imaging cameras : characteristics and performance / Thomas Williams.
p. cm.
"A CRC title."
Includes bibliographical references and index.
ISBN 978-1-4200-7185-6 (hardcover : alk. paper)
1. Thermography--Equipment and supplies. 2. Video recording--Equipment and supplies. 3. Electronic cameras. 4. Infrared detectors. 5. Infrared radiation. 6. Night vision devices. I. Title.

TA1570.W538 2009
621.36'2--dc22 2009003683

Visit the Taylor & Francis Web site at
http://www.taylorandfrancis.com

and the CRC Press Web site at
http://www.crcpress.com

Contents

Preface xiii

Author xv

Symbols and Abbreviations xvii

Chapter 1
An Introduction to Thermal Imaging 1
- 1.1 Aim of This Book 1
- 1.2 What Is Thermal Imaging? 1
- 1.3 Atmospheric Transmission 3
- 1.4 Choice of 3–5 μm or 8–12 μm 4
- 1.5 Important Factors in the Application of Thermal Imaging 5
- 1.6 Specifying and Measuring the Performance of a Thermal Imager 5

Chapter 2
Thermal Imaging Cameras and Their Component Parts 7
- 2.1 A Basic Thermal Imager 7
- 2.2 Image-Forming Optical System 8
- 2.3 Windows for Thermal Imaging 14
- 2.4 Scanning Mechanisms 15
- 2.5 Radiation Detectors 18
  - 2.5.1 The Basic Detector 18
  - 2.5.2 Photon/Quantum Detectors 19
  - 2.5.3 Thermal Detector Arrays 21
  - 2.5.4 Some Detector Array Configurations 24
- 2.6 Cooling Detectors 28
- 2.7 Special Signal Processing and Other Requirements 32
  - 2.7.1 Signal Offset Correction 32
  - 2.7.2 Conversion to Standard Video Format 32
- 2.8 Displays 32
- 2.9 Computer and Software 33
- References 33

Chapter 3
Industrial and Commercial Thermal Imagers and the Facilities They Provide 35
- 3.1 Introduction 35
- 3.2 Thermal Imagers That Measure Actual Temperature 36

3.2.1 Temperature Measurement 36
3.2.2 Emissivity and Atmospheric Absorption 39
3.2.3 Object Dimensions 42
3.2.4 Thermal and Visible Displays 42
3.3 Software Facilities for Industrial Applications 43
3.3.1 General 43
3.3.2 Monitoring Temperatures 43
3.4 Thermal Imagers for Surveillance Types of Application 45
3.4.1 General 45
3.4.2 Military Applications 47
3.4.3 Civil Applications 48
3.5 Imagers Used by Firefighters 48
3.6 Manufacturers' Data Sheets 50
References 52

Chapter 4
Performance Parameters for Components of a Thermal Imager 53
4.1 Introduction 53
4.2 Lenses 53
4.2.1 Focal Length 53
4.2.2 Magnification (M) 54
4.2.3 Numerical Aperture (NA) 55
4.2.4 *f*/number 56
4.2.5 Transmission 56
4.2.6 Relative Field Irradiance (RFI) 56
4.2.7 Modulation Transfer Function (MTF) 57
4.2.8 Veiling Glare Index (VGI) 59
4.2.9 Narcissus Effect 59
4.2.10 Distortion 60
4.3 Detectors 61
4.3.1 Detective Quantum Efficiency (DQE) 61
4.3.2 RMS Noise 61
4.3.3 Noise Spectrum 62
4.3.4 Noise-Equivalent Power (NEP) 62
4.3.5 D* (D-star) 62
4.3.6 Responsivity 63
4.3.7 Spectral Response 63
4.3.8 Frequency Response 63
4.3.9 Time Constant 63
4.3.10 Modulation Transfer Function (MTF) 64
4.4 Scanners 65
4.4.1 Horizontal Scan Linearity 65
4.4.2 Vertical Scan Linearity 65
4.4.3 Scan Judder 65
4.5 Displays 66

4.5.1 General 66
4.5.2 Maximum Luminance 66
4.5.3 Polar Luminance Distribution 66
4.5.4 Grey Scale/Linearity 66
4.5.5 MTF 67
4.5.6 Distortion 67
4.5.7 Veiling Glare 68
References 69

Chapter 5
Performance Parameters for a Complete Thermal Imager 71
5.1 Introduction 71
5.2 Factors Affecting Performance 71
5.3 Performance Parameters 73
5.3.1 MTF 73
5.3.2 Nyquist Limit 73
5.3.3 Aliasing 74
5.3.4 Signal Transfer Function (SiTF) 75
5.3.5 Noise-Equivalent Temperature Difference (NETD) 76
5.3.6 Minimum Resolvable Temperature Difference (MRTD): The Johnson Criterion 76
5.3.7 Minimum Detectable Temperature Difference (MDTD) 79
5.3.8 Objective MRTD 79
5.3.8.1 MRTD Model A (Video or Display) 80
5.3.8.2 MRTD Model B 81
5.3.9 Objective MDTD 81
5.3.10 Slit Response Function (SRF) 81
5.3.11 Aperture Response Function (ARF) 82
5.3.12 Absolute Temperature Range 82
5.3.13 Maximum and Minimum Temperature Difference Range and Offset Temperature Range 83
5.3.14 Temperature Measurement Uncertainty 83
5.3.15 Emissivity Range 83
5.3.16 Narcissus 83
5.3.17 Veiling Glare Index (VGI) and Uniformity Index (VGUI) 84
5.3.18 Scene Influence Factor (SIF) 84
5.3.19 Field of View (FOV) 85
5.3.20 Close Focus Distance 85
5.3.21 Spectral Response 85
5.4 Frame Rates and Readout Timing 86
5.5 Other Factors 86
References 86

Chapter 6
Basic Equipment for Testing and Calibrating at Thermal Wavelengths 87
6.1 Introduction 87
6.2 Radiation Sources 87
6.2.1 Tungsten Filament Lamps 87
6.2.2 Nichrome Wire or Strip Sources 88
6.2.3 Nernst Glower 89
6.2.4 Globar (SiC/Carborundum Rod) 90
6.2.5 Opperman Source 90
6.2.6 Blackbody 90
6.2.7 High-Emissivity Plates 91
6.2.8 Modulated IR Sources 91
6.2.9 Laser, Laser Diode, and LED Sources 92
6.3 Infrared Detectors 93
6.4 Cooling Detectors 93
6.5 Optical Systems and Collimators 93
6.5.1 General 93
6.5.2 Off-Axis Paraboloid Collimators 93
6.5.3 Multimirror Collimators 96
6.5.4 Refracting Collimators 96
6.5.4.1 3–5 µm Collimators 96
6.5.4.2 8–14 µm Collimators 97
6.5.5 High-Magnification Objectives 97
6.6 Integrating Spheres 97
6.7 Spectral Filters 99
References 101

Chapter 7
Measurement Procedures and Techniques for the Principal Components That Make Up a Thermal Imager 103
7.1 Introduction 103
7.2 General Measurement Procedures 103
7.3 Lenses and Optical Systems 104
7.3.1 Focal Length 104
7.3.2 Angular Magnification 107
7.3.3 *f*/number or NA 109
7.3.4 Entrance and Exit Pupil Diameters of Afocal Systems 111
7.3.5 Distortion 112
7.3.6 Spectral Transmission 113
7.3.7 Relative Field Irradiance 117
7.3.8 Veiling Glare 118
7.3.9 Narcissus 119
7.3.10 MTF 120

7.3.10.1 Testing Image-Forming Objectives 121
7.3.10.2 Testing Afocal Systems 126
7.3.10.3 Measuring MTF with a Detector Array or Thermal Imager 126
7.3.10.4 Removing a Pedestal or dc Offset from the LSF 127
7.4 Detectors and Detector Arrays 128
7.4.1 Responsivity 128
7.4.2 Detective Quantum Efficiency (DQE) 130
7.4.3 RMS Noise 131
7.4.4 Noise-Equivalent Power (NEP) 131
7.4.5 Frequency Response 131
7.4.6 MTF 132
7.4.6.1 Slit Scan While Monitoring the Output of a Single Element 132
7.4.6.2 Slit and Array Scan Technique for Linear and 2D Arrays 133
7.4.6.3 Tilted (Sloping) Slit Technique for 2D Arrays 134
7.4.6.4 SPRITE or Detector with TDI 135
7.4.6.5 Random Pattern Technique 135
7.4.6.6 Software Requirements 136
7.5 Scanners 136
7.6 Displays 137
7.6.1 Luminance and Spectral Characteristics 137
7.6.2 Polar Luminance Distribution 137
7.6.3 Grey Scale/Linearity 138
7.6.4 MTF 138
7.6.4.1 Eyepiece Displays 140
7.6.5 Distortion 141
7.6.6 Veiling Glare 142
References 143

Chapter 8
Measurement Techniques and Procedures for Complete Thermal Imagers 145
8.1 Introduction 145
8.2 MTF 146
8.2.1 General 146
8.2.2 Measurement from the Video Output 146
8.2.3 Measurement off the Display 147
8.3 Nyquist Limit 148
8.4 Aliasing 148
8.5 Signal Transfer Function (SiTF) 149

- 8.6 Noise-Equivalent Temperature Difference (NETD) 150
- 8.7 Minimum Resolvable Temperature Difference (MRTD) 151
- 8.8 Minimum Detectable Temperature Difference (MDTD) 153
- 8.9 Objective MRTD 154
- 8.10 Objective MDTD 154
- 8.11 Slit Response Function (SRF) 154
- 8.12 Aperture Response Function (ARF) 155
- 8.13 Temperature Measurement Performance Characteristics 155
- 8.14 Emissivity Range 156
- 8.15 Narcissus 157
- 8.16 Veiling Glare Index (VGI) and Uniformity Index (VGUI) 157
- 8.17 Scene Influence Factor (SIF) 158
- 8.18 Field of View (FOV) 159
- 8.19 Close Focus Distance 159
- 8.20 Spectral Response 160
- References 162

Chapter 9
Calibration and Alignment of Test Facilities 163

- 9.1 Introduction 163
- 9.2 Calibrating and Aligning a Collimator 163
  - 9.2.1 Wavefront Deformation (Aberration) 163
  - 9.2.2 Calibrating Focal Length 165
  - 9.2.3 Collimator Alignment and Focus 166
  - 9.2.4 Test Piece Alignment 170
    - 9.2.4.1 Lens System 170
    - 9.2.4.2 Thermal Imager 171
  - 9.2.5 Checking an MTF Test Facility 172
    - 9.2.5.1 Audit Lenses 172
    - 9.2.5.2 Standard Lenses 172
    - 9.2.5.3 Slits 173
    - 9.2.5.4 Square-Topped Pulses 173
- 9.3 Radiometric Characteristics 173
  - 9.3.1 General 173
  - 9.3.2 Temperature Sensors 174
  - 9.3.3 Blackbodies 175
  - 9.3.4 Radiometers 175
  - 9.3.5 Radiometric Calibration of an MRTD or Similar Test Facility 178
  - 9.3.6 Spectral Characteristics 179
- References 179

Chapter 10
Applications of Thermal Imaging Cameras 181
10.1 Introduction 181
10.2 Industrial Applications 181
  10.2.1 Buildings and Structures 181
  10.2.2 Inspection of Composite Panels and Structures 182
  10.2.3 Inspection of Furnace and Other High-Temperature Constructions 183
  10.2.4 Plant and Site Inspection 184
10.3 Advanced and Specialist Applications 186
  10.3.1 Detection of Buried Objects 186
  10.3.2 Studying and Preserving Works of Art 186
  10.3.3 Fire Detection and Volcano Monitoring 187
  10.3.4 Visualizing Electric and Magnetic Fields 187
  10.3.5 Thermal Wave Imaging (TWI) and Time-Resolved Infrared Radiometry (TRIR) 187
  10.3.6 Sonic Thermal NDT 188
  10.3.7 Thermoelastic Stress Analysis 188
10.4 Medical and Biological Applications 189
10.5 Military and Civil Surveillance and Other Applications 191
References 192

Appendix A: Objective Measurement of MRTD and MDTD 195
A.1 Performance Parameters That Determine MRTD and MDTD 195
A.2 Theory for MRTD Measurement 195
  A.2.1 MRTD Model A (Video or Display) 196
  A.2.2 MRTD Model B 197
A.3 Theory for MDTD Measurement 200
  A.3.1 MDTD Model A 200
  A.3.2 MDTD Model B 201
  A.3.3 MDTD Model C 201
References 201

Appendix B: Sampled Imaging Systems and Aliasing 203
B.1 What Are Sampled Imaging Systems? 203
B.2 Image Formation by Sampled Imaging System 203
B.3 Basic Theory 205
B.4 Measures of Aliasing 210
B.5 MTF Measurement Techniques 211
References 212

Preface

The main impetus for the development of thermal imaging cameras has been a military one. However, as their performance has increased and their cost decreased, thermal imaging cameras have found applications in a wide range of industrial and civil applications, even to the extent of being used for TV wildlife programs. The aim of this book is not only to provide an introduction to the topic for those who wish to have a better understanding of thermal imaging, or for those who wish to discover how it could be applied in their area of work, but also to provide wider and more comprehensive knowledge of the topic for those who use, make, test, design, and sell such imagers. The intention throughout this book is to employ a more practical approach born of experience using and testing thermal imagers, and to keep theory to a minimum. The book deals with only the standard form of camera and not with the specialized forms of thermal imager, such as the push-broom systems used for surveying the Earth from satellites, although much of the information in the book should prove useful to those involved with such systems. The reader will also find information that will be valuable in a general sense to anyone engaged in work on thermal wavelengths.

The first chapter is a description of the physical basis on which thermal imaging depends, followed by a chapter that describes how a thermal imager works and the components that it uses. Some of this is of a slightly historical nature, where some of the scanning systems used on earlier imagers are described, whereas the latest trend is to use detector arrays without the need for scanning. Chapter 3 is intended to provide users or potential users with helpful information about the types of imager available commercially and the facilities they can provide.

In order to evaluate the suitability of a thermal imaging camera for a particular application, it is important to have ways of specifying and measuring meaningful performance characteristics. The next five chapters deal with describing, defining, and measuring these characteristics for both a complete thermal imager and the components, such as the lens and detector, that are major parts of an imager. The list of performance parameters covered is comprehensive and includes the more usual items, such as field of view (FOV), modulation transfer function (MTF), minimum resolvable temperature difference (MRTD), as well as the less common items, such as slit response function (SRF), narcissus, scene influence factor (SIF). These chapters include practical information about the devices and systems that can be used for testing at the wavelengths used by thermal imagers, as well as the setup and alignment of test benches. The final chapter reviews some of the many different ways and applications in which thermal imagers have been used. It also provides a number of references to help those wishing to further investigate a particular application. The book concludes with an appendix dealing with the objective measurement of MRTD and minimum detectable temperature difference (MDTD) as well as an appendix dealing with aliasing, the potential problem of all imaging systems that use detector arrays.

The book includes a list of some of the abbreviations and symbols used in the text as well as a brief description, where appropriate.

I thank my current and former colleagues, all of whom it has been a pleasure to work with; my contacts in the industry, universities, and research establishments who are always unstinting in their help; and, last but not least, the publishers, who have been very helpful and understanding in the production of this book.

Author

Thomas Williams holds a bachelor's degree in physics from University College London. He started work with what was then the Dynamics Group of de Havilland Propellers on the design and testing of missile infrared guidance systems. He next joined Sira Electro-optics, where he has spent most of his working life. Here he was involved in designing and building a wide range of electro-optical systems as well as in the practical task of assessing and testing such systems. He has been responsible for designing and using a range of test equipment for assessing the performance of thermal imaging systems and their component parts as well as systems working at other wavelengths. The author has lectured on several courses dealing with different aspects of thermal imaging in addition to courses dealing more generally with optical systems. He has published more than thirty technical papers, coedited and provided a chapter for a book entitled *Applications of Thermal Imaging*, provided a chapter for the book *Visual Instrumentation*, and written a book entitled *The Optical Transfer Function of Imaging Systems*. In 2000, he received the Callendar Medal from the Institute of Measurement and Control for his work on instrumentation. He currently works as a consultant to Surrey Satellite Technology Ltd. and serves on several International Standards committees dealing with fundamental optics, telescopic and night vision systems, and photography.

Symbols and Abbreviations

The table below defines some of the abbreviations and symbols used in this book. In some cases the symbols defined in this table may be defined differently in some parts of the text. The definition in the associated text is the correct one to use in that particular instance.

Symbol	Term	Relevant Sections
μm	Micrometers (10^{-6} meters)	
$1/f$ (noise)	Noise varying as the inverse of the frequency	4.3.2
1D	One-dimensional	
2D	Two-dimensional	
A	Area of a detector	4.3.5
Absolute zero	Temperature of –273°C	1.2
AF	Aliasing function	5.3.3, Appendix B
Ag	Silver	
AGI	Ambient glare index	7.6.6
Al	Aluminum	
Al_2O_3	Aluminum oxide (sapphire)	6.2.1, 6.7
AP	Aliasing potential	5.3.3, 8.4, Appendix B
AR	Aliasing ratio	5.3.3, 8.4, Appendix B
ARF	Aperture response function	5.3.11, 8.12
Au	Gold	
BFD	Back focal distance	4.2.1
BK7	Crown glass	
BLIP	Background-limited photodetector	4.3.1
c	Velocity of light	2.5.2
c_1 and c_2	Constants in Planck's equation	1.2
c/mm	Cycles per millimeter	
c/mrad	Cycles per milliradian	
CaF_2	Calcium fluoride	2.2, 6.7
CCD	Charge-coupled device	2.5.4
CCIR	Digital video format	2.7.2
CIE	Committee International d'Eclairage	7.6.1
CMOS	Complementary metal oxide semiconductor	2.5.4
CMT	Cadmium mercury telluride	2.5.2
CO_2	Carbon dioxide	
CRT	Cathode ray tube	4.5
CW (laser)	Continuous wave	6.2.9
D* (D-star)	Detectivity of a detector	4.3.5
DMTF	Dynamic MTF	4.5.5

(*Continued*)

(*Continued*)

Symbol	Term	Relevant Sections
dn/dt	Rate of change of refractive index with temperature	2.2
DQE	Detective quantum efficiency	4.3.1, 7.4.2
DUT	Detector under test	
e	Exponential function	4.3.9
$e(\lambda)$	Emissivity at a wavelength λ	1.2
EFL	Effective focal length	4.2.1
E_g	Quantum energy gap	2.5.2
E_g	Energy gap between quantum levels	2.5.1
EM	Electromagnetic (radiation)	1.2
f	Signal frequency or focal length	4.3.5, 6.5.2, 7.3.1, 7.3.3, 9.2.2
F	Radiant flux	6.6
f/number	Ratio of the focal length to the aperture diameter	5.3.5, 7.3.3
f-number	Same as *f*/number	
FOV	Field of view	2.1, 3.6, 4.2.1, 5.3.19, 8.17
FTIR	Fourier transform infrared (spectrometer)	9.3.4
FWHH	Full width half height	6.2.9, 6.7
Ge	Germanium	2.2, 6.5.4, 6.7
GPS	Global positioning system	
G-R (noise)	Generation-recombination noise	4.3.2
h	Planck's constant, also used for object height	2.5.2, 4.2.10
h'	Image height	4.2.10
HeNe (laser)	Helium-neon	6.2.9, 9.2.1
I	Irradiance	4.2.3, 7.3.7
InSb	Indium antimonide	2.5.2
IR	Infrared	
ISO	International Standards Organization	
K	Degrees Kelvin	
k	A constant	
KrS5	Thallium bromoiodide	2.2
L	Luminance	7.6.6
LCD	Liquid crystal display	2.8, 4.5
LN_2	Liquid nitrogen	
LNO_2	Liquid nitrogen	2.5.2
LSF	Line spread function	7.3.10
M	Magnification	4.2.2, 7.3.2
m	A length or distance	5.3.6
MCT	Cadmium mercury telluride	2.5.2
MDTD	Minimum detectable temperature difference	5.3.7, 5.3.9, 8.8, 8.10, Appendix A
MEMS	Microelectromechanical systems	2.5.2
MgF_2	Magnesium fluoride	
MgO	Magnesium oxide (periclase)	6.2.1, 6.7
MRTD	Minimum resolvable temperature difference	5.3.6, 5.3.8, 8.7, 8.9, 9.3.5, Appendix A

MTF	Modulation transfer function	4.2.7, 4.3.10, 4.5.5, 5.2, 5.3.1, 7.3.10, 7.4.6, 7.6.4, 8.2, Appendix A, Appendix B
N	Noise signal	8.6
NA	Numerical aperture	4.2.3, 7.3.3
NaCl	Sodium chloride	2.2
NDT	Non-destructive testing	
NEP	Noise-equivalent power	4.3.4, 7.4.4
NETD	Noise-equivalent temperature difference	3.6, 5.2, 5.3.5, 5.3.8, 5.3.9, 8.6, Appendix A
NFOV	Narrow field of view	3.4.2
NI	Narcissus index	7.3.9, 8.15
NPS	Noise power spectrum	5.3.8
OAA	Off-axis angle of a collimator	9.2.3
OAD	Off-axis distance of a collimator	9.2.3
PAL	Television video format used largely in Europe	2.7.2
PC	Personal computer	
PHD	Picture height distortion	4.5.6
PtR	Platinum resistance (thermometer)	9.3.2
PtSi	Platinum silicide	2.5.2
QWIP	Quantum well detector devices	2.5.2
R	Radiance/radiant flux or responsivity of a detector, or response of a camera	4.2.5, 6.6, 7.4.1, 8.19
r	Reflectance	4.2.5
RFI	Relative field irradiance	4.2.6
RGB	Red/green/blue color coordinate system	7.6.1
RMS	Root mean square	4.3.2, 7.4.3
S	Signal	4.3.1
s	Spatial frequency	4.2.7
S/N	Signal/noise ratio	4.3.1, 4.3.5
Si	Silicon	2.2, 6.5.4
SiC	Silicon carbide/carborundum	6.2.4
SIF	Scene influence factor	5.3.18, 8.16
SiO	Silicon monoxide	
SiO_2	Silicon dioxide	
SiTF	Signal transfer function	4.5.4, 5.3.4, 8.5
SLR (camera)	Single-lens reflex	9.2.3
SO_2	Sulfur dioxide	
SPRITE	Signal processing in the element (detector)	2.5.2
SRF	Slit response function	3.2.3, 5.3.10, 8.11
T	Temperature	
t	Optical transmission	4.2.3
TDI (detector)	Time delay and integration	2.5.4, 4.3.10
TGS	Triglycine sulfate	2.5.2
TR	Temperature difference ratio	5.3.9
TRIR	Time-resolved infrared radiometry	10.3.5
TV	Television	

(*Continued*)

(*Continued*)

Symbol	Term	Relevant Sections
TWI	Thermal wave imaging	10.3.5
UUT	Unit under test	
V	Image distortion	4.5.6
V value	Abbe constant for glass	2.2, 4.5.6
VGI	Veiling glare index	4.2.8, 5.3.17, 7.3.8, 7.6.6, 8.16
VGUI	Veiling glare uniformity index	5.3.17, 8.16
w	Width of a slit	4.3.10
$\boldsymbol{W}(\lambda, T)$	Radiance for wavelength λ and temperature T	1.2
WFOV	Wide field of view	3.4.2
ZnS	Zinc sulfide	2.2
ZnSe	Zinc selenide	2.2, 6.5.4
α	*f*/number, or area ratios in an integrating sphere	4.2.4, 6.6
Δf	Frequency bandwidth	4.3.5
θ	Angle subtended by the object	4.2.10
θ'	Angle subtended by the image	4.2.10

1

An Introduction to Thermal Imaging

1.1 AIM OF THIS BOOK

The main aim of this book is to provide suppliers and potential and existing users of thermal imagers (principally thermal imaging video cameras) with information that will offer a useful guide in understanding and applying thermal imaging. It deals with the important performance parameters of a thermal imager, how they should be specified, and how they should be measured, as well as providing an understanding of how a thermal imager works and how its performance is affected by the tasks it is used to perform and by the various associated external parameters. The book also includes a brief description of some of the many applications of thermal imaging. As a result, the reader should find the book a fairly comprehensive introduction and reference to thermal imaging. However, note that it is not intended to be a guide to designing thermal imagers.

A major incentive in the development of thermal imagers has been their military applications, where the ability to see through smoke and mist and to differentiate between targets at above ambient temperatures and their background has proved invaluable. However, there are also numerous industrial and civil applications that are being exploited ever increasingly as the potential of thermal imaging is more clearly understood. This book will hopefully add to this understanding and, most important, will provide a sound quantitative basis for evaluating the suitability of a thermal imager for a particular application.

1.2 WHAT IS THERMAL IMAGING?

It seems appropriate to start by describing what is meant by thermal imaging. It is a well-known fact of physics that a body at a temperature greater than absolute zero (–273°C) emits electromagnetic (EM) radiation. Absolute zero is the temperature where the lowest quantum energy states for electrons, atoms, and molecules are occupied and no transitions between energy states are possible that would result in the emission of EM radiation. At temperatures above absolute zero EM radiation is emitted, and the amount of radiation and its distribution over the wavelength spectrum will depend primarily on the temperature of the body and a characteristic of its surface known as its emissivity. The latter will normally be a function of wavelength and may, to a lesser extent, also depend on the temperature of the object.

The maximum radiation energy that can be emitted by a body at a given wavelength is a function of its temperature and its surface emissivity for that particular wavelength. The equation that describes this relationship is known as Planck's equation and can be written as

$$W(\lambda, T) = e(\lambda)\ c_1/\pi\lambda^5[\exp(c_2/\lambda T) - 1] \tag{1.1}$$

where $W(\lambda, T)$ is the radiance for a wavelength λ in μm and a temperature T in Kelvin. The radiance is given in units of watts m^{-2} steradians^{-1} μm^{-1}, where

$$c_1 = 3.7418 \times 10^8$$

$$c_2 = 14387.9$$

c_1 and c_2 are the constants for this form of Planck's equation when the units of $W(\lambda, T)$ are as given above. $e(\lambda)$ is the emissivity at a wavelength λ and can vary in the range 0 to 1.

A real or effective surface (e.g., the aperture of a cavity) where the emissivity is unity over an extended range of wavelengths is referred to as a black body for that range of wavelengths. Such surfaces are particularly useful because their radiance can be calculated from knowledge of their temperature, using Planck's equation. They can therefore be used as standard sources of radiation for calibration purposes. More information about black body surfaces will be found in Section 6.2.6.

Figure 1.1 shows a plot of the radiance of surfaces with an emissivity of unity, for four different temperatures. The temperatures are 2,727°C (i.e., 3,000K, very approximately the temperature of a lamp filament), 0°C (273K, the freezing point of water), 20°C (293K, approximately normal ambient temperature), and 100°C (373K, the temperature of boiling water). The plot also shows the wavelength range to which the human eye is sensitive (i.e., visible radiation), which is approximately 0.4 to 0.75 μm. From these curves we see that, as we well know, a lamp emits radiation to which the eye is sensitive. However, a body at ambient temperature, or even at the

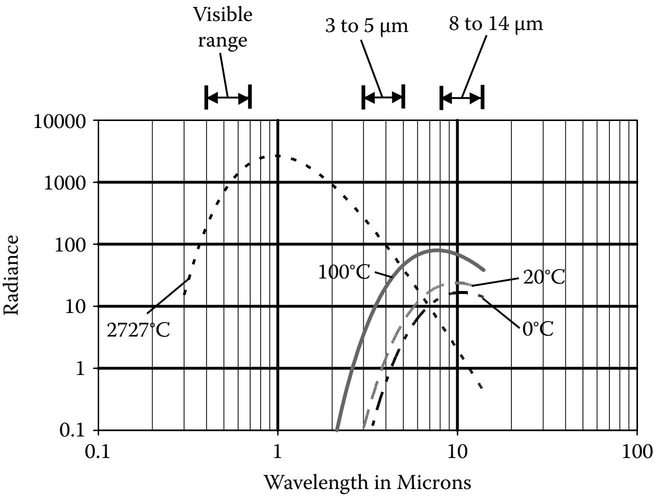

FIGURE 1.1 The radiance of a surface as a function of wavelength, for four different temperatures. Note that the radiance for T = 2,727°C has been plotted on a scale reduced by a factor of 1,000.

temperature of boiling water, emits virtually no radiation in the band of wavelengths to which the eye is sensitive. We can therefore only see them directly if they are illuminated externally by sources such as the sun or an incandescent lamp. In a limited sense thermal imaging is basically concerned with converting images produced by the longer-wavelength "thermal" radiation emitted by these cooler bodies to visual wavelength images that we can see. In a broader sense the term *thermal imaging* can also apply to systems where no visual image is generated, but a thermal image is captured and processed entirely electronically to measure some specified parameter or detect the presence of some object.

1.3 ATMOSPHERIC TRANSMISSION

The transmission of the atmosphere plays an important part in thermal imaging. In particular, many of the molecules present in the atmosphere absorb radiation in the wavelength range of interest. Particularly important are the absorption from water vapor, carbon dioxide, oxygen, and carbon monoxide. Figure 1.2 shows a typical atmospheric transmission curve.

On the basis of this curve and that of Figure 1.1, as well as other considerations (such as the performance of radiation detectors), thermal imaging systems are generally considered to work in one of two useful wavelength bands. The first of these is taken as extending from 3 to 5 μm, and the second from 8 to 14 μm. In practice there are many reasons for departing from these exact ranges. One important factor is the performance of detectors. For example, performance can be greatly enhanced by using detector arrays. However, viable arrays of *photon detectors* (see Section 2.5.2) for the longer of the two wavelength bands are currently limited to having a response that extends no farther than approximately 11 μm. There are, of course, applications where the atmosphere is not a limitation and different wavelength ranges can be used. Examples are where measurements are from space, or where the path length is very short, or where its constituents can be controlled (e.g., by the use of a pure dry-nitrogen atmosphere).

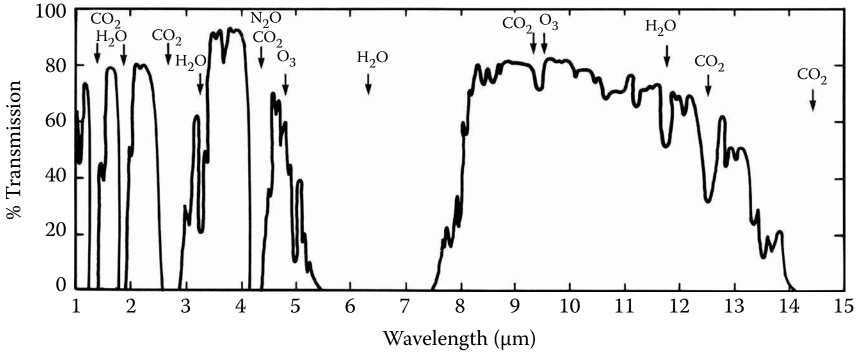

FIGURE 1.2 Example of the transmission through the atmosphere for a 1 km path.

1.4 CHOICE OF 3–5 μm OR 8–12 μm

There are several factors that affect the choice of which of these two wavelength bands to use, and these considerations are discussed in more detail in Chapters 3 and 10. Here we merely outline briefly the relevant factors.

Surface radiance: Generally speaking, the radiant flux emitted by a surface at ambient temperatures is greater in the 8–14 μm band than it is in the 3–5 μm band. However, at ambient temperatures, the change in radiant flux for a given small change in the temperature of a surface is greater in the 3–5 μm band (Table 1.1 lists some relevant data). The relative importance of these two factors on the performance of the imager will depend on the design and mode of operation of the imager.

Radiation from the sun: A small but significant amount of the sun's radiation falls into the short-wavelength end of the 3–5 μm band. In some applications this may be an advantage, helping to increase image contrast and possibly providing some additional information about the object. In other applications, such as when measuring the temperature of an object, it is merely unwanted additional radiation. The sun's radiation can normally be eliminated by introducing a filter that reduces the range of wavelengths to which the imager is sensitive.

Atmospheric transmission: Where an imager is used for imaging over relatively long distances the transmission characteristics of the atmosphere become very important. The degree to which the atmosphere attenuates radiation can be very different for different climatic conditions, and some conditions will favor the 3–5 μm band, while others will favor the 8–14 μm band. Because of the longer wavelength, transmission through mist and smoke is better in the 8–14 μm band. This is a particular advantage in surveillance applications.

Technology and commercial considerations: Technical developments will obviously affect the relative performance capabilities in the two bands, and this can change with time. Technical developments also affect the complexity and cost of imagers, and such commercial considerations can be an important factor in the choice of an imager and the band in which it operates.

TABLE 1.1
Radiance and Contrast for Different Thermal Wavelength Bands for a Surface at Ambient Temperature (20°C)

Wavelength Band	Radiance in watts/m²/steradian	Contrast (% Change in Radiance) for 1°C Temperature Difference
3–5 μm	4.06	37.7
8–12 μm	93.4	16.9
8–14 μm	133.2	15.7

1.5 IMPORTANT FACTORS IN THE APPLICATION OF THERMAL IMAGING

There are several characteristics of thermal imaging that govern its applications. The three most important are:

Response to the temperature of a surface: We see from Equation (1.1) that the radiance of a surface is a function of its temperature. As a result, a thermal imager can be used as a means of measuring the temperature of an object, or more importantly, to provide a two-dimensional map of relative or actual temperature distribution in a scene. This ability can be used in many different applications, some of which are described in Chapter 10.

Passive imaging: The radiation used to generate the thermal image of an object comes from the object itself, and therefore no external source of radiation is required to see the object. As a result, thermal imaging provides a means of seeing at nighttime, or under conditions of poor illumination. Moreover, the visibility of certain objects that may be of particular interest, such as human beings or military vehicles, is enhanced because of their relatively high temperature with respect to the background.

Visibility through smoke and mist: Because the wavelengths involved are ten to twenty times longer than wavelengths in the visible part of the spectrum, the radiation undergoes less scattering by particles in the atmosphere. As a result, the range of visibility through smoke and mist is greatly increased. This property is of particular importance in various forms of surveillance and is used by firefighters to enable them to see in smoke-filled buildings.

1.6 SPECIFYING AND MEASURING THE PERFORMANCE OF A THERMAL IMAGER

For the user to be able to assess the suitability of a thermal imager for a particular application, he or she must be provided with relevant performance parameters. These parameters should be well defined and should preferably be parameters that can be measured precisely and in a completely objective manner. In the author's experience this is not always the case with the information provided by the manufacturer, and one aim of this book is to help in remedying this situation.

The relevance of a particular performance parameter will depend very much on the specific application. Generally speaking, applications can be divided into two main areas:

Surveillance: Here the ability to detect small temperature differences, and to be able to resolve detail in order to recognize targets, will be of primary importance.

Temperature measurement: Most industrial and scientific applications fall in this class, where accurate temperature measurement is important, as well as knowledge of the effect on the accuracy of temperature measurement of variables such as the size and shape of an object. The ability to resolve detail is also an important consideration.

The relevant performance parameters for these various applications and how they are defined and measured form a major part of this book.

2 Thermal Imaging Cameras and Their Component Parts

2.1 A BASIC THERMAL IMAGER

The essential elements of an original form of thermal imager are illustrated as a block diagram in Figure 2.1. They are:

- An optical system that can form an image of an external scene using radiation in the thermal wavelength range.
- One or more detector elements that can convert this radiation into electrical signals proportional to the radiation falling on them.
- Some systems require a scanning mechanism that scans the thermal image in a regular pattern across the detector element(s), although most modern imagers do not require this, since they use large detector arrays that completely cover the field of view of the imager (see below).
- An electronic processor that can process the detector outputs, in conjunction with data from the scan mechanism (where this is used), and can convert them into a video signal.
- A display unit that generates a visual image from the video signal.

As will be shown in Sections 2.5.3 and 2.5.4, the greater the proportion of the area of the complete image plane that is occupied by detector elements, the better will be the performance of the imager in terms of sensitivity to temperature differences. The ultimate arrangement is to completely fill the image plane with detector elements and to do away with the scanning mechanism, as illustrated in Figure 2.2. Most modern imagers conform to this arrangement where and when technical and economic consideration allow the construction of large two-dimensional (2D) detector arrays. This type of imager is often referred to as a staring array imager.

For a staring array imager the spatial resolution for a given field of view (FOV) will depend on the actual number of detector elements in the image plane. For a system with a scanner the spatial resolution for a given FOV will depend partly on the dimension of detector elements and partly on the number of lines taken to scan the image. In both cases other factors also affect resolution, including the signal bandwidth of the processing electronics and, of course, the resolution of the lens system and the display. However, in many cases thermal imagers use standard TV formats that usually, but not necessarily, control some of these last factors.

Each of these building blocks of a thermal imager is described in more detail in the following sections.

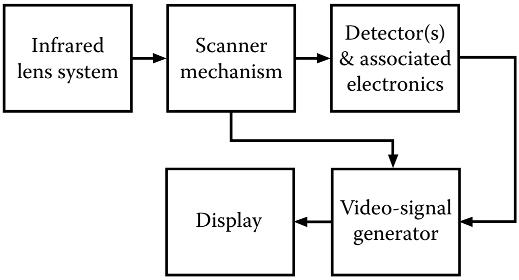

FIGURE 2.1 Block diagram illustrating the main subunits that make up a thermal imaging camera.

2.2 IMAGE-FORMING OPTICAL SYSTEM

The term *imaging forming* is used here to differentiate this part of an imager from the scanning system, which also includes optical components. In some instances it may in fact be difficult to separate the two parts of the system.

The optical systems used in thermal imagers are designed and function in the same way as optical systems for visible wavelengths. The main difference is that most of the materials used for thermal wavelengths are different from those used at visible wavelengths, and in fact, there are differences between optical materials used in the 3–5 μm band and those used in the 8–14 μm band.

Table 2.1 lists some of the optical materials that are used and their suitability for each of these bands. More detailed information about infrared optical materials can be found in the *Handbook of Infrared Optical Materials*, edited by Paul Klocek.[1]

Mirrors function as well in the thermal bands as they do in the visible, and in principle, the design of all-mirror optical systems will be the same whether they are for use at thermal or visible wavelengths. However, there are differences when systems are optimized for a particular wavelength band. The differences are principally to do with the choice of reflective coating and the protective film applied over the coating. Protective films are required on coatings of Al and Ag to prevent deterioration from oxidation and

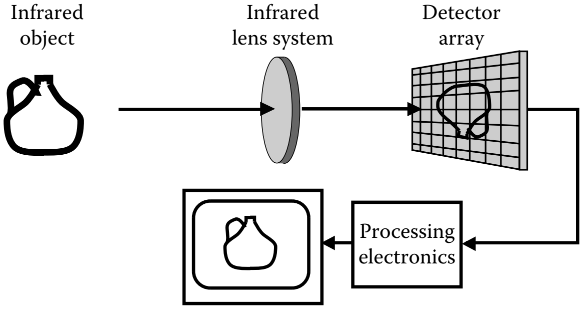

FIGURE 2.2 Schematic of a staring array system.

TABLE 2.1
Some of the Most Commonly Used Materials for Optical Systems Working at Thermal Wavelengths (Quoted Numbers Are Approximate)

Material	Useful Wavelength Range in μm	Refractive Index	Comments
Silicon	1.4–7 and 20–25	3.43 at 4 μm 3.42 at 10 μm	Has significant absorption bands from approximately 7 to 20 μm; however, it can be used in the 8–12 μm range in thin sections
Germanium	1.6–20	4.02 at 4 μm 4.01 at 10 μm	Most commonly used material for lenses and windows in the 8–14 μm band
Zinc sulfide	0.4–12	2.25 at 4 μm 2.20 at 10 μm	
Zinc selenide	0.5–20	2.43 at 4 μm 2.41 at 10 μm	Used extensively in conjunction with Ge in multielement objectives for the 8–14 μm band
Calcium fluoride	0.13–12	1.41 at 4 μm 1.31 at 10 μm	
Sapphire (aluminum oxide)	0.17–6.5	1.67 at 4 μm	Very hard and abrasive resistant
KRS5 (thallium bromoiodide)	0.5–40	2.38 at 4 μm 2.37 at 10 μm	Note that thallium salts are very toxic
Sodium chloride	0.17–18	1.52 at 4 μm 1.49 at 10 μm	Very hygroscopic, but can be coated with protective films

attack from atmospheric pollutants such as SO_2. Coatings of Au are largely resistant to atmospheric pollutants but are very soft and require protection from physical damage.

Protective coatings for mirrors are usually MgF_2, SiO, or SiO_2. The latter is particularly hard and durable, but suffers from some absorption around a wavelength of 8 μm.

An important aspect of some of the lens materials is their relatively high refractive index compared with those of the glasses used for visible wavelength optics (e.g., the refractive index of BK7 is 1.54 at 0.546 μm, compared with a refractive index for germanium of 4.01 at 10 μm). This has two important effects. One is that uncoated surfaces will have a high reflectivity, while the other is that it is generally possible to achieve a high degree of optical correction with fewer elements than would be required in the case of a visible optical system.

The high reflectivity means that these materials must be used with an antireflection coating, in order to both obtain good transmission through the optical system and reduce levels of unwanted glare radiation caused by multiple reflections between optical surfaces. Unwanted reflections at optical surfaces are usually the cause of the narcissus effect in a thermal imager, where a cooled detector element virtually sees an image of itself (see Section 4.2.9). This usually results in a dark or bright halo in the center of the image.

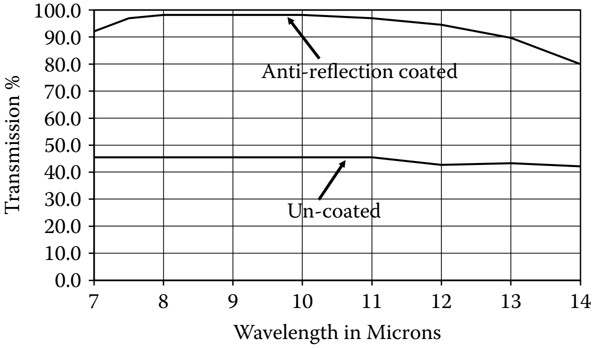

FIGURE 2.3 The effect of an antireflection coating on the transmission of a Ge window.

Developing efficient coatings for some of these materials has been an important aspect of thermal imaging. Of particular interest has been the development of an amorphous diamond coating for use with germanium. Although not the best coating from the point of view of providing the highest transmission, it is extremely hard and resistant to atmospheric attack. It is usually used on the outside surface of an optical system, or on a window through which the imager looks. This type of coating is sufficiently hard to allow the coated surface to be cleaned with a windscreen wiper. Figure 2.3 shows the transmission of germanium with and without an antireflection coating.

When designing an optical system, there are two important characteristics of the material that will affect the design: the value of the refractive index and the dispersion (i.e., a measure of how much the refractive index changes with wavelength). Generally speaking, a high refractive index reduces the monochromatic aberrations contributed by an optical element, while a low dispersion reduces the chromatic aberrations (i.e., those aberrations that are a function of the wavelength of the radiation) contributed by an optical element (note that dispersion is normally characterized by what is referred to as the Abbe constant, or V value, and this *increases* in value as dispersion gets smaller). Table 2.2 lists the aberrations (in terms of the root mean square [RMS] image

TABLE 2.2
RMS Spot Diameter (μm) for an *f*/2 Lens of 100 mm Focal Length in the 8–12 μm Band

Material	On-Axis 8–12 μm	4° Off-Axis 8–12 μm	On-Axis 10 μm	4° Off-Axis 10 μm
Germanium	43	133	43	132
Germanium aspheric	9	122	Diffraction limited	121
Zinc selenide	147	204	93	170
Sodium chloride	499	536	368	418

TABLE 2.3
RMS Spot Diameter (μm) for an *f*/2 Lens of 100 mm Focal Length in the 3–5 μm Band

Material	On-Axis 3–5 μm	4° Off-Axis 3–5 μm	On-Axis 4 μm	4° Off-Axis 4 μm
Germanium	79	159	42	132
Zinc selenide	98	172	91	169
Sodium chloride	342	394	339	390
Silicon	61	148	53	139
Silicon aspheric	30	131	Diffraction limited	121

spot diameter) of an optimized single-element *f*/2 lens of 100 mm focal length, made from sodium chloride, zinc selenide, and germanium, respectively, and working in the 8–12 μm band. Table 2.3 lists the data for similar lenses working in the 3–5 μm band and reoptimized for this wavelength range, together with the addition of data for a silicon lens. The modulation transfer function (MTF) curves (for those unfamiliar with the MTF concept, see Section 4.2.7 and Williams[2]) for the same lenses are plotted in Tables 2.4 and 2.5, respectively. The results illustrate the effects of refractive index and dispersion on image quality. In particular, we note that a single-element germanium lens has a reasonably good polychromatic performance in the 8–12 μm band and can be used in some applications where a relatively small image field is required. However, because of its higher dispersion in the 3–5 μm band, its polychromatic performance is worse, and although silicon has a lower refractive index, the silicon lens has a better polychromatic performance because of its lower dispersion.

The monochromatic aberrations associated with a lens used over a small field of view can be virtually eliminated by making one of the surfaces aspheric rather than spherical (see Tables 2.2 and 2.3). Machining aspheric surfaces in materials such as germanium and silicon is a far more practical proposition for thermal wavelength optics than for the equivalent visible lens, and it is quite common to use aspheric components for thermal imagers. As explained below, the final lens in a thermal imager that employs a scanner mechanism is frequently just a single element, since it is required to cover only a relatively small field of view. However, the lens system ahead of the scanner is usually required to cover a relatively large field of view and, in practice, will have more than one element in order to obtain a good performance over the larger field of view and will, if necessary, use at least two different materials in order to correct for chromatic effects. The lens objective in a staring array camera does, of course, have to cover the full field of view of the camera, and will therefore have this rather more complex construction. Figure 2.4 illustrates the possible construction of a typical lens objective for use in a staring array camera in the 8–12 μm band. The objective consists of two Ge elements (with an aspheric surface on one element); it has a focal length of 100 mm, an *f*/number of 2, and a total FOV of 20°. A lens for the 3–5 μm band, made up of two Si elements, could look very similar, but its performance may not be quite as good.

Some thermal imagers are provided with a fixed intermediate field of view objective together with optical units that can be attached to this objective to increase or decrease the

TABLE 2.4
MTF Curves for an *f*/2 Lens of 100 mm Focal Length in the 8–12 μm Band

Material	Wavelength 10 μm	Wavelength 8–12 μm
Germanium	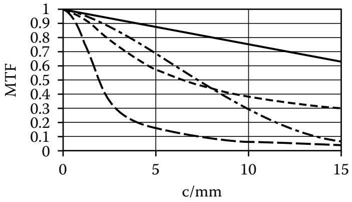	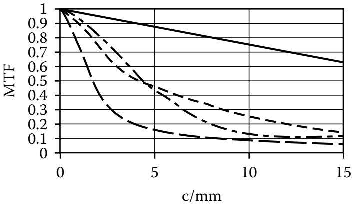
Zinc selenide	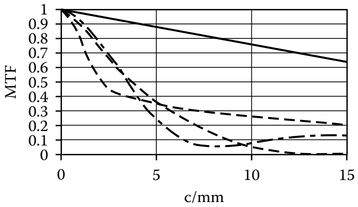	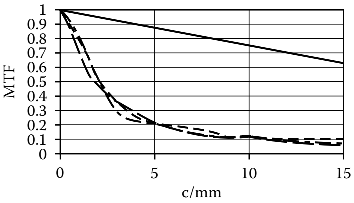
Sodium chloride	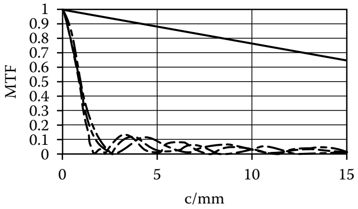	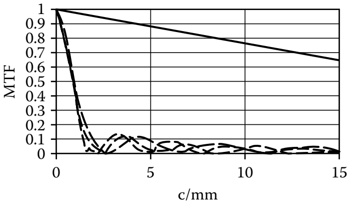

Diffraction ——— On-axis —·—·—·

4° Off-axis T – – – – 4° Off-axis R —— —— -

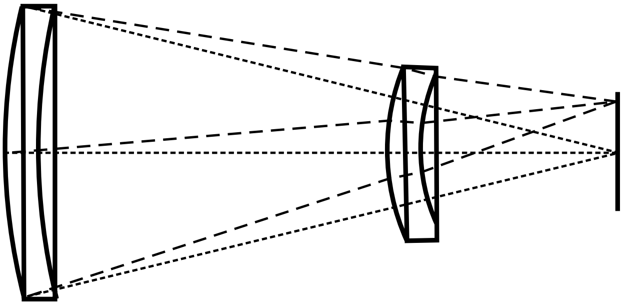

FIGURE 2.4 Example of the construction of an all-Ge lens with a total FOV of 20°.

TABLE 2.5
MTF Curves for an *f*/2 Lens of 100 mm Focal Length in the 3–5 μm Band

Material	**Wavelength 4 μm**	**Wavelength 3–5 μm**
Germanium	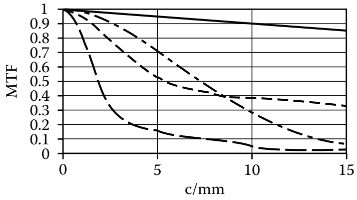	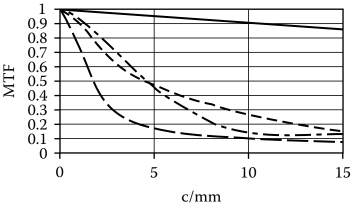
Zinc selenide	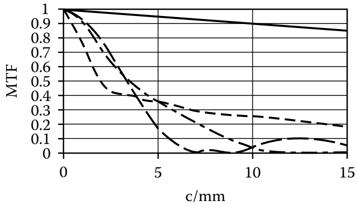	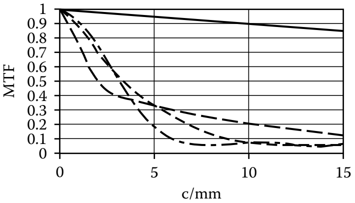
Silicon	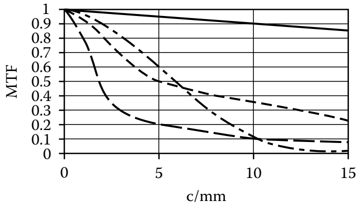	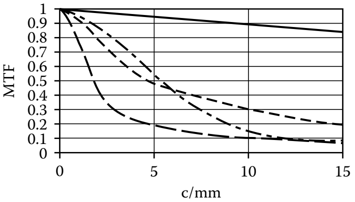
Sodium chloride	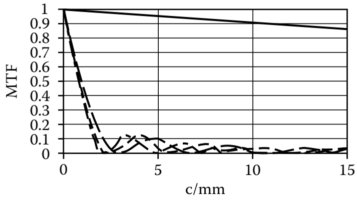	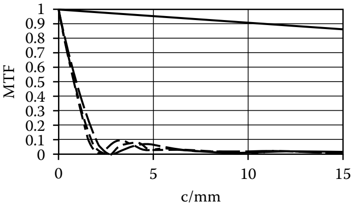

Diffraction ———	On-axis — - — - — ·
4° Off-axis T – – – –	4° Off-axis R —— —— -

field of view of the imager. It is, of course, also possible to have zoom lenses that work in the thermal wavelength ranges, and such lenses have been incorporated into thermal imagers.

Many of the imagers that include a scanner have an image-forming optical system that is split in two with the scanner mechanism in between. The front end is basically an afocal system (in effect a telescope) that provides the scanner system with a collimated beam from each object point, while the rear end focuses the collimated beam from the scanner onto the detector. By changing the front end (i.e., using an afocal system with a different angular magnification), one can change the field of view of the imager. As mentioned earlier, the optical system at the rear can often be of

© 2009 by Taylor & Francis Group, LLC

relatively simple construction, as it is only required to work over a field of view sufficiently large to cover the area occupied by the detector elements in the focal plane.

One of the parameters of an optical material not mentioned so far is the rate of change of refractive index with temperature, usually referred to as the dn/dT. For most materials the change is small and has relatively little effect on the performance (mainly a change in focal length, with an associated focus change) compared with the expansion or contraction of the metal housing. However, germanium has a relatively large dn/dT (approximately 390×10^{-6}/°C). This is significant when the lens has a relatively long focal length and where an imager may have to work over a large range of ambient conditions. Where manual adjustment of focus is not possible or convenient, some means of automatic focus correction frequently needs to be applied. One of two techniques is usually used in these circumstances. In the first of these the temperature of the optical system is monitored by temperature sensors and the focus adjusted accordingly by means of some form of motorized mechanism and control circuit working from the output of the temperature sensors. This is referred to as active compensation. The alternative is passive compensation, where by very careful optical and mechanical design, the focus change caused by the change in refractive index of the germanium is partly compensated by the changes in refractive index of lens elements made from other materials, and partly by adjustment of the mechanical spacing of the lens elements using spacers made from materials with appropriate thermal coefficients of expansion.

A further property of germanium that may be significant in special circumstances is that the bulk transmission gradually decreases as temperatures exceed approximately 50°C, although the effect is not great until temperatures are above about 100°C. The exact transmission characteristics of the germanium can to some extent be adjusted by the degree and type of doping of the material.

2.3 WINDOWS FOR THERMAL IMAGING

In many applications it is desirable to have a plane-parallel-sided window between the thermal imager and the scene being imaged. Such a window will be designed to protect the imager from the external environment, which could be the outside of an aircraft in flight, or a harmful chemical atmosphere or fluid. The same materials listed above (Section 2.2) will of course be suitable for windows, but the choice of material and its coating will depend on the particular application and very specifically the conditions it will have to withstand (see, for example, Madding[3] and Rozlosnik[4]). One of the points to note is that some materials can be used at wavelengths where normally they may have relatively poor transmission, provided conditions allow them to be used with a sufficiently small thickness. If for unavoidable reasons it is necessary to use a material that does not have very high transmittance in the wavelength range of interest, it may be necessary to take account of the fact that the window itself can be a significant source of the thermal radiation.[3] In addition to this the transmittance can change with temperature, and in some instances actually increases as the temperature increases. Another point to note is that in general windows should be at an angle to the optical axis of the imager in order to avoid reflections that can result in the narcissus effect (see Section 4.2.9). However, the antireflection coating applied to such a window must take into account this angle.

© 2009 by Taylor & Francis Group, LLC

2.4 SCANNING MECHANISMS

The function of a scanning mechanism is to move the image formed by the lens system over the detector element(s) in a well-controlled fashion. Scanner systems normally fall into one of three classes as represented by the one-dimensional (1D) oscillating mirror scanner arrangements illustrated in Figure 2.5. In the first of these (Figure 2.5(a)) the scanner occupies the space between the image-forming optical system and the detector. In the next arrangement (Figure 2.5(b)) the scanner is between the external object and the image-forming optical system, and in the third arrangement the scanner is placed between an afocal front end and the image-forming back end of the optical system. Each of these arrangements has its advantages and disadvantages, and these can be different if the scanner is a 2D system rather than the 1D systems illustrated in Figure 2.5. Very briefly, these are as follows:

Object space scanner (Figure 2.5(b)): If, as is normal, the aperture stop is at the lens, the latter is used virtually on-axis over the whole scan, whether it is a 1D or 2D scan. This means that the lens can be of simple construction and the cold stop, normally used with cooled detectors to prevent them from seeing radiation from anywhere (e.g., the body of the imager) other than through the optical system from the external object, can be small and effective. This allows a high performance to be achieved from the detector and reduces the presence of unwanted artifacts in the image. However, for various reasons, including size and having moving parts at the front end, this arrangement has rarely been used in production imagers.

Image space scanner (Figure 2.5(a)): There are several problems with this arrangement. The first is that the effective position of the focus at the detector will vary as the scan mirror rotates, so that unless some special form of mechanical or optical compensation is applied, the quality of the image will deteriorate toward the edge of the field. The second is that the lens must perform well over the full field of view, and may therefore have to be of more complex construction. Finally, if the aperture stop is at the lens

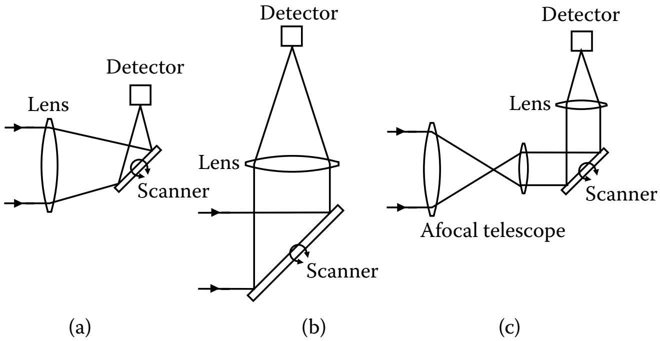

FIGURE 2.5 Three classes of scanning systems: (a) image space, (b) object space, and (c) afocal.

© 2009 by Taylor & Francis Group, LLC

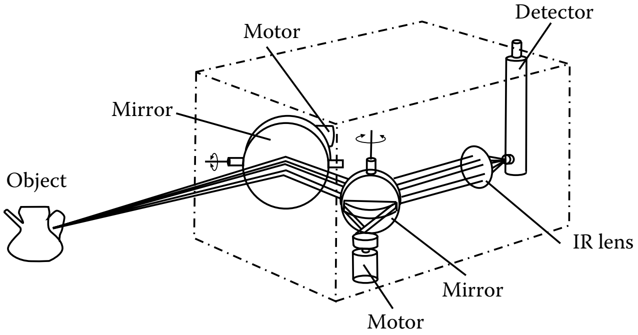

FIGURE 2.6 Basic thermal imaging system.

rather than the scanning mirror, the radiation falls on the detector at angles that vary over the scan, which leads to greater problems in producing an effective cold stop.

Afocal scanner (Figure 2.5(c)): This has similar advantages to the object space scanner, with the further advantage that the field of view, and hence the spatial resolution, can be varied by varying the magnification of the afocal front end.

A very basic object space 2D scanner arrangement is illustrated in Figure 2.6. It consists of two plane mirrors, one of which is pivoted about a horizontal axis and the other about a vertical axis. Radiation from the object goes to the first mirror, is reflected to the second mirror, and then is reflected to the image-forming objective lens. The latter forms an image of the original object in its focal plane, where in this example there is a single detector element. Moving the first mirror about its horizontal axis will cause the image to move vertically across the detector, while moving the second mirror about its vertical axis will make the image move horizontally across the detector. By the use of appropriate electrical torque motors and drive circuits, the mirrors can be driven to generate a typical TV raster scan pattern.

This simple scan mechanism has many drawbacks and would not be appropriate if one wished to produce images at typical TV frame rates of twenty-five or more frames a second. The particular arrangement would require relatively large mirrors to be driven very rapidly in a reciprocating manner with a linear movement between the ends of their travel. Real 2D scanning systems need to be more sophisticated than this, and several different arrangements have been devised and incorporated into imaging systems. Most of these are now largely of historical interest as a result of the move toward staring array imagers, or the use of long arrays in conjunction with 1D scanners. A form of scanner used on one of the very first makes of industrial thermal imager (AGA Thermovision 680) is illustrated in Figure 2.7. It consists of a lens system that forms an image of the external scene onto

© 2009 by Taylor & Francis Group, LLC

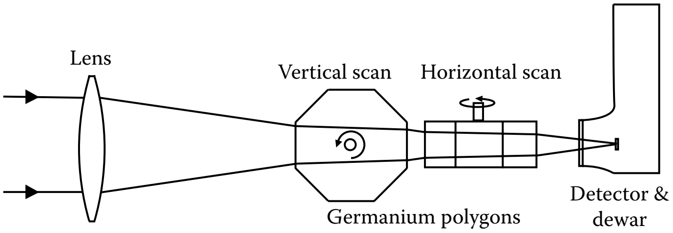

FIGURE 2.7 Schematic of an early thermal imager using rotating Ge polygons.

a single-element detector via two germanium polygons. The polygons are arranged with their axes of rotation orthogonal to each other, and rotation of the first of these generates the vertical frame scan, while the faster rotation of the second polygon generates the horizontal line scan. Most of the subsequent 2D scanners used arrangements of mirror polygons, combined in some cases with simple flapping plane mirrors, to generate the required scans (see, for example, Lettington and Moore[5] and Moore and Reeve[6]). A simple diagrammatic illustration of such a scanner is shown in Figure 2.8. In this case the fast horizontal scan is achieved using a mirror polygon, and the slower vertical scan by using a plane oscillating (flapping) mirror.

Microscan: This type of scanner has not had a mention so far. It is not a scanner in the same sense as the devices described above. It is used in some staring array imagers in order to effectively increase the resolution of the imager, by removing, or at least decreasing, the effects of aliasing. As the

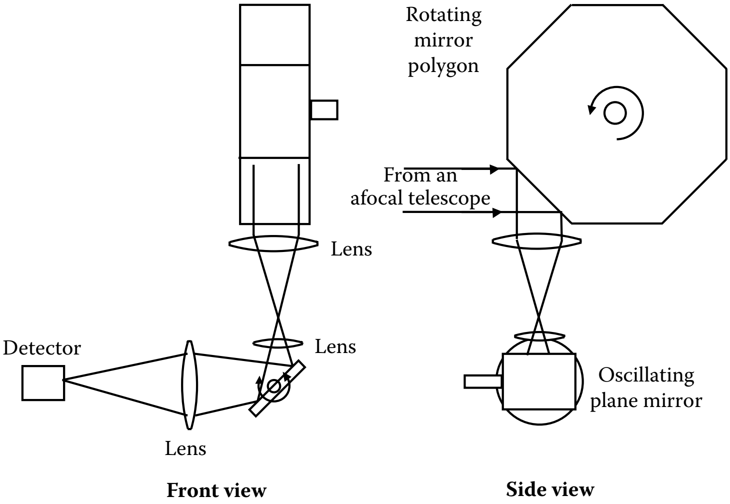

FIGURE 2.8 Scheme for a scanner system using a rotating polygon and an oscillating mirror.

© 2009 by Taylor & Francis Group, LLC

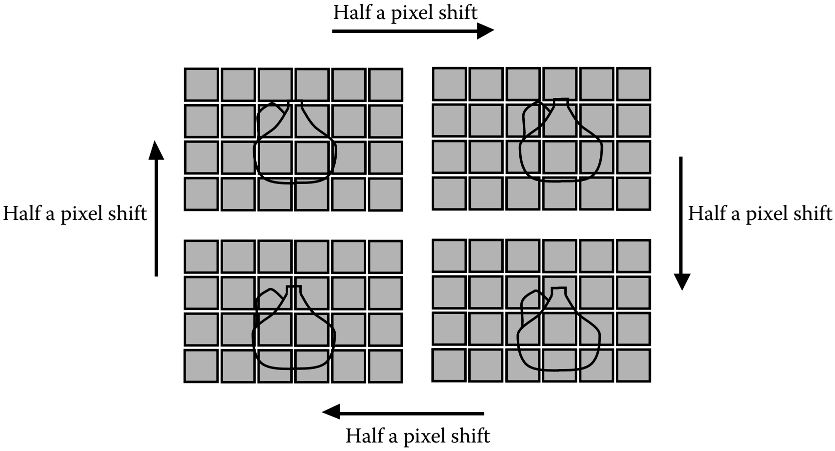

FIGURE 2.9 Illustration of the four image shifts, relative to the detector array, produced by a microscan system.

name implies, it generates a very small scan of the image in a square pattern with sides equal to half the spacing between two detector elements of the array (see Figure 2.9). By suitably processing the four images obtained in this way and combining them into a single image, one effectively halves the spacing between elements (i.e., double the number of elements in each direction). The result is to double what is known as the Nyquist frequency (equal to half the reciprocal of the spacing between elements of the array). This is the maximum spatial frequency to which a staring array system should respond if aliasing artifacts are to be avoided in the image. This topic is discussed in greater detail in Section 5.3.3 and Appendix B. Microscans are often generated by small movements of an optical element or mirror produced by means of a piezoelectric actuator.

Many very clever forms of scanner have been developed and can be found described in the literature (e.g., see Lettington and Moore[5] and Moore and Reeve[6]). Because of the advent of staring arrays, microscans are rapidly becoming of mainly historical interest and are not a topic for this book to cover in any greater detail.

2.5 RADIATION DETECTORS

2.5.1 The Basic Detector

Possibly the most important part of a thermal imager is the detector or detector array. It largely determines the potential level of thermal and spatial resolution that can be achieved as well as the complexity that is required to fulfill this potential.

There are basically two types of thermal infrared (IR) detectors. The first depends on the IR radiation heating the detector element, with the resulting temperature rise

© 2009 by Taylor & Francis Group, LLC

then triggering some other physical mechanism that is taken as a measure of the radiation falling on the element. This type of detector is generally known as a thermal detector.

The second type of detector is one where the photons, which are the incident radiation, interact at an atomic or molecular level with the material of the detector to produce charge carriers that generate a voltage across the detector element, or a change in its electrical resistance. The mechanism usually involves an electron absorbing a photon and, as a result, moving from one quantum energy level to another. This type of detector is usually referred to as a photon or quantum detector.

In general, photon detectors provide greater sensitivity than thermal detectors. However, to achieve this better performance they usually need to be cooled in order for the charge carriers to populate the quantum energy levels where they can have the desired interaction with the incident photons. The need to cool detectors of this type is a major factor in both the design and application of thermal imagers that use photon detectors, and the different methods of cooling are discussed in a later section. Thermal detectors have the great advantage that they do not normally require cooling, although some types of thermal detectors require their temperature to be controlled to ensure that they operate under optimum conditions.

In selecting the type of detector to use in a thermal imager there are several factors to consider. The main ones are:

- The wavelength band in which it responds
- The frequency response; i.e., can it function at sufficiently high frequencies to provide standard video frame rates or even higher frame rates for some applications?
- The thermal sensitivity and spatial resolution that can be achieved
- Cooling requirements and the associated complexity, cost, and possible inconvenience
- Reliability and cost

The detectors covered in the sections below have satisfied these criteria to a sufficient extent to be used in the many different thermal imaging cameras.

2.5.2 PHOTON/QUANTUM DETECTORS

These are detectors where the signal is generated by the direct interaction of photons with charge carriers such as electrons, to change their energy state. The energy of the photon must be greater than the quantum level change that produces the effect. This level determines the long-wavelength cutoff of the detector. Since the energy of a photon is given by hc/λ, where h is Planck's constant, c is the velocity of light, and λ is the wavelength of the photon, we have that the cutoff wavelength is given by

$$\lambda_0 = hc/E_g \tag{2.1}$$

where E_g is the energy gap corresponding to the quantum level change. We note that since the signal response in this type of detector depends on the number of

© 2009 by Taylor & Francis Group, LLC

incident photons and not on the total photon energy, the responsivity of the detector (expressed as signal output per unit radiant energy input) will therefore in theory fall off linearly as the wavelength decreases.

Photon detectors are mainly semiconductors with suitable doping to achieve the desired characteristics. They usually operate either as photoconductors, where the incident radiation varies the electrical conductivity of the detector element, or as photovoltaic devices, where the radiation actually generates a voltage, usually across a p-n junction. A third mode of operation is where the voltage is generated across a metal to semiconductor junction known as a Schottky barrier. Most photon detectors operating at thermal wavelengths need to be cooled (at least if they are to have a good responsivity). For the 3–5 μm band a temperature of the order of 195K is usually satisfactory, and this can be achieved by means of three-stage thermoelectric devices requiring only a few watts to provide the necessary cooling. For the 8–12 μm band temperatures of the order of 77K are required. This is the temperature of liquid nitrogen, and methods of achieving this temperature are described in more detail in Section 2.6. Very briefly, however, this entails mounting the detector element(s) in a Dewar and either bulk cooling it with liquid nitrogen or using a Joule-Thomson cooler supplied with high-pressure nitrogen or air, or the use of a closed-circuit Stirling engine cooling system.

The above discussion is relevant principally to single-element detectors, or small arrays. Additional factors come into play when dealing with large arrays, and these are covered in Section 2.5.4.

In this section we describe briefly the main characteristics of the principal types of photon detector used in thermal imagers.

Cadmium mercury telluride: This is usually referred to as CMT or MCT and can be constructed to operate as a photovoltaic device (i.e., where the incident radiation generates a voltage) or as a photoconductive device (i.e., where the incident radiation alters the effective resistance of the device). By adjusting the composition of the material, we can optimize CMT detectors to work in either the 3–5 μm band or the 8–14 μm band, although in the latter case they are usually optimized to only have a response out to approximately 12.5 μm. CMT can in fact be optimized to work out to wavelengths as long as 16 μm or slightly more.

CMT requires cooling to operate efficiently. In the 8–14 μm band temperatures have to be as low as 77K, which is the temperature of liquid nitrogen (often written as LNO_2). In the 3–5 μm band, detectors can be optimized to function efficiently at temperatures as high as 195K. This is an important consideration and greatly simplifies the design of 3–5 μm imagers since these temperatures can be achieved using small thermoelectric cooling devices that require only a few amps of current to operate.

Indium antimonide (InSb): This material is only useful in the 3–5 μm band and can be constructed to operate as a photovoltaic device or as a photoconductive device. To achieve its full potential it needs to be cooled to liquid nitrogen temperatures, although it can also be made to have a useful response at the higher temperature of 195K. In the latter case it is used only as a photoconductive device.

© 2009 by Taylor & Francis Group, LLC

Platinum silicide (PtSi): This type of detector works as a Schottky barrier photodiode. It responds in the 3–5 μm band and needs to be cooled to liquid nitrogen temperatures.

PtSi has a relatively poor quantum efficiency (i.e., it makes use of only about 2% of the incident photons) and is unsuitable as a single-element detector. It comes into its own in the form of large detector arrays for use in staring array imagers. The reason for this is that large arrays can be made using well-established silicon wafer technology and result in devices having a very good uniformity of response. In addition to this, the material is fully compatible with the inclusion on the chip of a charge-coupled device (CCD) readout for the array. Another feature of PtSi that has proved useful in some applications is that it will respond to wavelengths as short as 1 μm.

Quantum well (QWIP) devices: This is a relatively new type of detector and could well prove to be the detector of choice for many applications. The basic principle is that the required quantized energy levels and photon absorption is achieved by using certain geometrical structures that include gratings and thin film layers. Different material combinations can be used for making these devices, one of these being aluminum gallium arsenide and gallium arsenide. They can be made to cover various wavelength bands in the range of approximately 3–20 μm and can be built as large staring arrays.[7] The devices normally require cooling to liquid nitrogen temperatures, although devices can be designed that can operate at higher temperatures.

Although QWIP devices are made up of relatively complex structures, they use well-established manufacturing techniques that produce repeatable results. A comprehensive technical comparison of QWIP and other infrared detectors can be found in Rogalski.[8]

Other materials: There are several other materials that can be used as detectors for thermal imaging. These include indium arsenide, lead tin telluride, lead sulfide, lead selenide, and others. Although some of these have found limited use in thermal imaging devices, they do not in general have any significant advantages over the materials listed above.

2.5.3 THERMAL DETECTOR ARRAYS

Thermal detectors are generally useful for thermal imaging only in the form of 2D staring arrays. Here the advantage of having to respond at frame rate frequencies rather than video signal frequencies (e.g., 25–50 Hz rather than several MHz) gives them a thermal and spatial resolution that is sufficient for a wide range of industrial and other applications. It should be noted, however, that for several reasons[9] it is not always possible to make full use of this potential increase in time for each detector element to be exposed to the radiation from the external scene.

The development of useful thermal arrays is relatively recent and has been made possible largely as a result of the development of techniques for micromachining materials such as silicon, generally referred to as MEMS (micro-electromechanical systems) technology. The most commonly used of these devices are described below.

© 2009 by Taylor & Francis Group, LLC

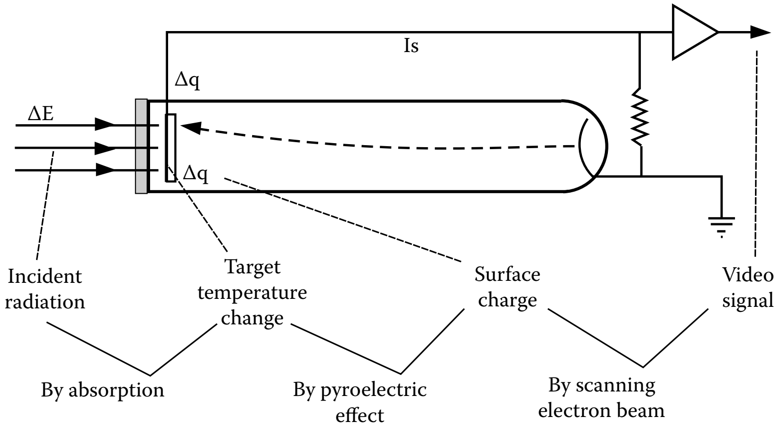

FIGURE 2.10 Pyrovidicon tube.

Pyrovidicon: This is an early form of thermal imaging device and effectively functioned in the 8–14 μm band. It is now largely of historical interest. Unlike the other devices described in this section, it is, strictly speaking, not in the form of an array. The principle of operation is illustrated in Figure 2.10. The pyrovidicon consists of a thin slice or wafer of a pyroelectric material (usually triglycine sulfate [TGS]) with the front face, on which the thermal image is formed, coated with an absorbing material. The important property of a pyroelectric material is that a change in temperature causes it to become electrically polarized, i.e., a charge is generated across the wafer. The charge pattern over the face of the wafer will follow the pattern of temperature change produced by the incident radiation, and hence the thermal image formed on its face. The charge pattern is read out by scanning the rear face of the wafer with an electron beam in the same way as is done on a TV camera vidicon tube. The electrical output is converted to a video signal for display on a cathode ray tube (CRT). Performance can be improved by reticulating the surface of the wafer. This inhibits lateral heat diffusion.

As indicated above, the charge pattern is generated as a result of a change in temperature, and the charge pattern is soon neutralized if the image is stationary. As a result, the image will fade away and disappear. Pyrovidicon cameras will therefore normally include a mechanical chopper to modulate the image and generate this change, although they can operate without a chopper if the image is continually changing, e.g., by slowly moving the camera.

The thermal and spatial resolution of a pyrovidicon is relatively poor. However, as one of the first thermal imagers that did not require cooling, it proved useful in several applications, such as fire fighting.

Resistive bolometer arrays: One very successful form of array makes use of the change in electrical resistance with temperature that occurs in many

© 2009 by Taylor & Francis Group, LLC

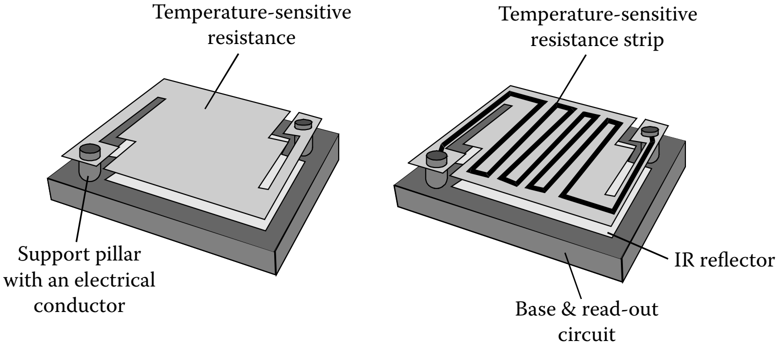
Temperature-sensitive resistance
Temperature-sensitive resistance strip
Support pillar with an electrical conductor
IR reflector
Base & read-out circuit

FIGURE 2.11 Example of the construction of a single pixel in a resistive bolometer array.

materials. The form of construction of this type of array is illustrated in Figure 2.11. Each resistive element is deposited on a silicon platform that has a very small heat capacity and is thermally isolated by an air gap from the base silicon wafer. Small pillars, or narrow strips of material, support the platforms and provide the electrical connection to the resistive element. The base wafer will have the readout and processing circuits. Typically each detector element will have dimensions of the order of 30 × 30 μm.

The viability of such arrays depends on the ability to make elements having a very small heat capacity that are well isolated thermally from their base support. This has been made possible by the development of techniques for micromachining silicon and other materials. The resistive elements are typically made by depositing materials such as vanadium oxide and titanium oxide on the substrate. However, amorphous silicon has also been used very successfully. An important requirement of these elements is that they should have a high absorption at the operating wavelengths. This can be achieved with appropriate coatings and by having a reflective surface on the substrate below each element to return back to the element any radiation transmitted through it. The gap between the reflective surface and the resistive element can in fact be designed to optimize the absorption of the incident radiation.

Although this type of bolometer array does not require a chopper to modulate the incident radiation, it usually does require a shutter that can be introduced at intervals in front of the array and is used for adjusting the uniformity corrections made to equalize the output of individual elements of the array.

Bolometer detector arrays frequently incorporate a thermoelectric cooler largely in order to maintain an optimum temperature for matching of the resistive element and the readout electronics.

Ferroelectric/pyroelectric arrays: This type of array is similar in construction to the resistive bolometer arrays described above, except that detection is based on using the pyroelectric or ferroelectric effect. As indicated earlier, this type of detection process requires the incident radiation to be chopped.

© 2009 by Taylor & Francis Group, LLC

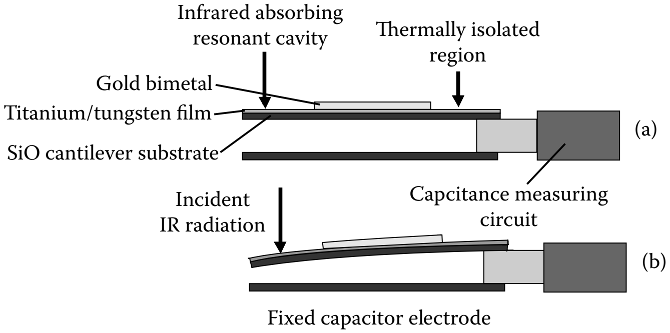
Infrared absorbing resonant cavity
Thermally isolated region
Gold bimetal
Titanium/tungsten film
SiO cantilever substrate
(a)
Incident IR radiation
Capcitance measuring circuit
(b)
Fixed capacitor electrode

FIGURE 2.12 Principle of operation of a single pixel of a bimetallic cantilever array.

Bimetallic cantilever arrays: Figure 2.12 illustrates the principle of this detector mechanism. Each element of the array is a very fine bimetallic strip that will bend as its temperature changes. The degree of bending is a measure of its temperature, and this can be detected by measuring the capacitance between the end of the strip and the base wafer on which it is supported. The actual practical configuration may differ from this in order to optimize the packing density and responsivity of the array. A diagram of a pixel of an array designed to meet such considerations is shown in Figure 2.13, while Figure 2.14 is a micrograph of part of such an array.

2.5.4 SOME DETECTOR ARRAY CONFIGURATIONS

As indicated earlier, the thermal sensitivity of an imager is improved by increasing the area of the effective image plane occupied by detector elements (see also

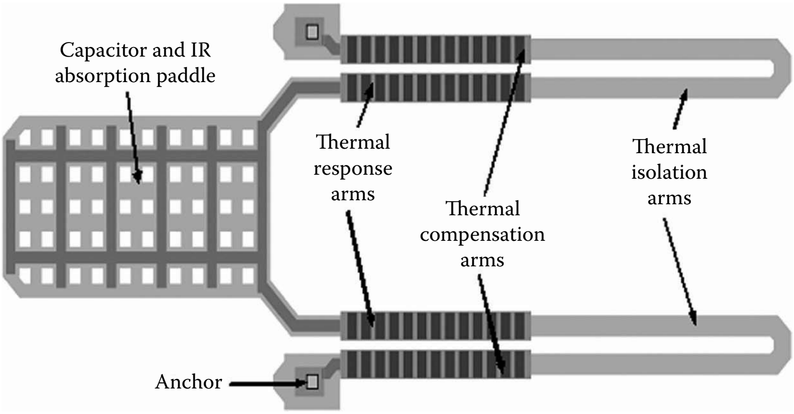

FIGURE 2.13 Diagram showing the shape of a pixel of a bimetallic cantilever array designed to optimize performance. (Reproduced by kind permission of Multispectral Imaging, Inc.)

© 2009 by Taylor & Francis Group, LLC

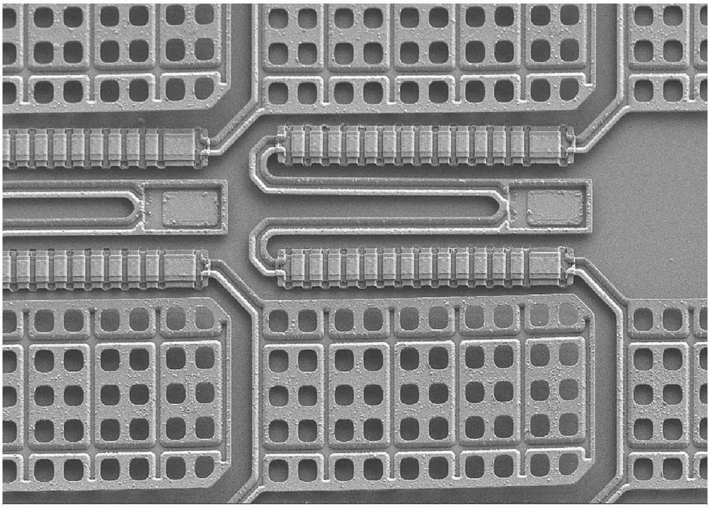

FIGURE 2.14 Micrograph of a bimetallic cantilever array. (Reproduced by kind permission of Multispectral Imaging, Inc.)

Section 2.5.3). At the same time, however, the size of these elements must be limited in order to achieve the desired spatial resolution. The ultimate arrangement is to use a staring array where the whole image plane is occupied by detector elements. The latter is not always possible, or the optimum solution, because of the limitations of current technology both with respect to what is physically possible and for reasons of cost. A major problem with all arrays is making the electrical connections to each element. If the signal processing is all done off the chip, there is a practical limit to the number of connections one can accommodate, particularly if these have to be made through a Dewar. As a result, arrays with a large number of elements are only possible using on-chip processing that allows the number of external connections to be greatly reduced. Typically this is what a CCD or complementary metal oxide semiconductor (CMOS) form of readout does. Other problems relate to electrically interfacing to individual detector elements, matching the characteristics of a detector material to the signal readout circuits, and of course of reliably and cost-effectively manufacturing large arrays of small detector elements.

Below we describe some possible nonstaring array configurations designed to improve the performance of thermal imagers by increasing the number of pixels in the focal plane. Many of these are largely of historical interest as far as thermal cameras are concerned, although most may still be relevant for specialized thermal imaging systems.

Linear parallel scan arrays: This is one of the simplest configurations to use (see Figure 2.15(a)). It has the advantage that it only requires a 1D scanner system, such as a flapping or rotating plane mirror, and is a relatively easy configuration to manufacture, with a reasonable amount of space around the elements for associated electronic circuits and connections. The main

© 2009 by Taylor & Francis Group, LLC

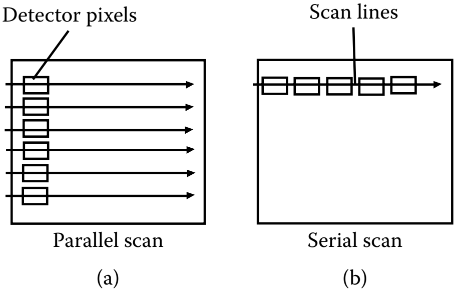

FIGURE 2.15 Types of scan: (a) parallel and (b) serial.

disadvantage is that in general each detector element will have a different signal response, which unless corrected will produce an image with distinct lines at right angles to the scan direction (usually referred to as lineness). Unfortunately, the response of most detectors will vary differently as the scene temperature changes so that some type of dynamic compensation is required. This is usually achieved by suitable signal processing algorithms that take into account the signal levels from neighboring lines.

A linear array need not necessarily extend over the full height of the image format, in which case the scan has to be 2D and the image format is scanned in a number of swathes.

Linear serial scan arrays: This is illustrated in Figure 2.15(b). Here the linear array of elements is arranged along the scan direction, although the array does not normally extend over the full width of the image format. In order to use such a configuration, circuitry is required on the chip that will amplify the signal from each element and then add it to the signal from the next element with a time delay that is equal to the time taken for the scanned image to move the distance separating the detector elements. This type of processing is referred to as time delay and integration (TDI). The advantage of this type of arrangement is that it gets over any problems of "lineness." However, it has the disadvantage of requiring special circuitry on the chip and necessarily a 2D scan.

SPRITE detector: This is not strictly a type of detector array, but it is listed here because it behaves in the same way as a linear serial scan array.[4] The name is an acronym for *signal **pr**ocessing **i**n **t**he **e**lement*, and the arrangement is illustrated in Figure 2.16. The device consists of a CMT detector element with an extended width in the direction of the scan. A bias voltage across the width of the element causes the charge carriers generated by the incident radiation to move down the length of the element to the end, where they can then be read out by a suitably placed contact. By adjusting the bias voltage the speed at which the charges move can be synchronized to the speed at which the scan moves the image. The result is that the charge carriers add constructively in the same way that they do in a TDI arrangement.

Combined parallel and serial scan arrays: The detector array arrangements illustrated in Figure 2.15 can be combined to form a configuration

© 2009 by Taylor & Francis Group, LLC

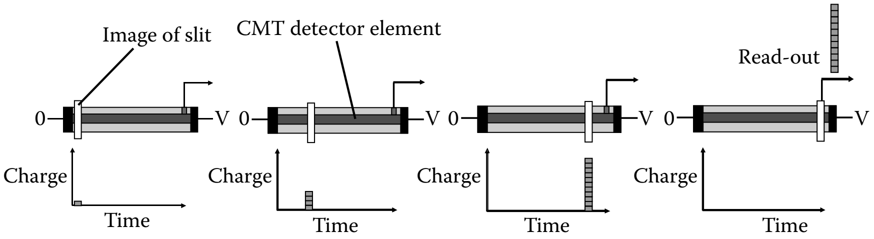

FIGURE 2.16 Illustration of the charge buildup as the image of a slit moves along the detector strip.

of both serial and parallel scanned elements. This, of course, requires the image to be scanned in swathes of several lines. This type of arrangement has proved particularly successful using SPRITE detectors for the serial part of the scan (see Figure 2.17(a)).

One configuration that has been used in order to achieve both high thermal and spatial resolution is to have staggered arrays. Here the elements are arranged in a limited number of columns, with each covering the full image height but staggered in a vertical direction with respect to each other to effectively increase the number of scan lines making up the image (see Figure 2.17(b)). Only a 1D scan is required, and a simple delay between the outputs of each column corrects for their relative displacement in the horizontal direction.

Staring arrays: The main advantages of this type of detector configuration are that no scanner mechanism is required and potentially much better thermal sensitivity can be achieved so that viable imagers can be built using uncooled

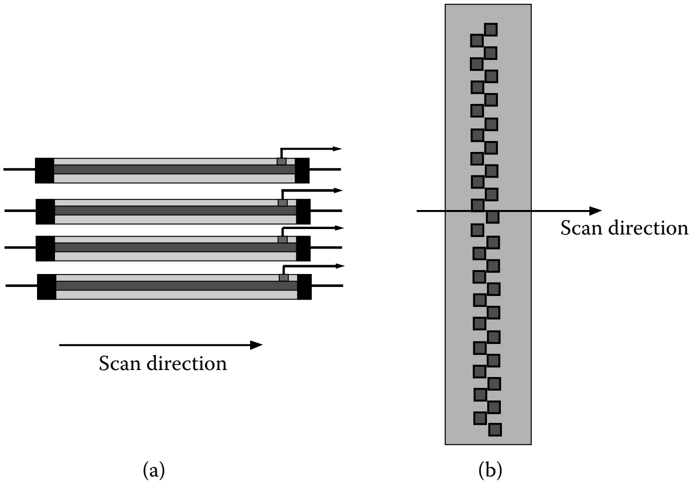

FIGURE 2.17 Illustration of combined serial and parallel scan configurations. (a) Four SPRITE detectors. (b) Two staggered arrays covering the full height of the image.

thermal detectors. It is the configuration currently used in most thermal imagers. However, this type of configuration is not without its own set of problems. Some of the problems and special requirements are as follows:

- With a staring array there is obviously no way in which external connections can be made to each element of the array, so some form of readout, such as a CCD or CMOS arrangement, must be incorporated into the array. The surface of the detector wafer will normally have little or no space for any readout circuits, so that these normally have to be accommodated at a different level in the wafer, or in a second wafer. One of the major problems with staring arrays of detector elements of materials such as InSb and CMT is that of making reliable connections between the wafer supporting the detector elements and the wafer with the readout electronics (e.g., the CCD array). One solution has been to use what is referred to as the indium bump technique. Here an array of small bumps of indium (which is malleable) is deposited on the bottom readout wafer, and these connect to the appropriate positions on the detector wafer when the two are brought together. To be successful, the bumps need to be of consistent shape and to be very precisely positioned, and of course the wafers need to be very precisely positioned with respect to each other. Techniques for doing this are now well developed. Another solution has been to make the interconnections by making tiny holes in the center of each detector element and connecting through these holes by depositing a suitable conductor material. This problem is avoided in PtSi arrays because of the ability to build a CCD array into the same wafer. The problem also does not occur with most of the uncooled types of array because of their form of construction.
- With CMT arrays there is a problem in matching the characteristics of the optimum detector material for the 8–14 μm band to suitable readout electronics. As a result, it has been found necessary to use material with a shorter cutoff wavelength, and typically these arrays only respond in the 8–10 μm or 8–11 μm band.
- The responsivity and direct current (dc) offset of each detector element of an array will in general be different and can change with both the temperature of the array and scene temperature. This means that special signal processing, together with stored data about each element, is required to correct the video signal output. Most cameras incorporate automatic procedures for refreshing the stored data at appropriate time intervals using a shutter as a reference target.
- Some types of array, such as pyroelectric arrays, require a chopper mechanism to modulate the scene radiation.

2.6 COOLING DETECTORS

As indicated earlier, most of the detectors used in thermal imaging require some form of cooling or temperature control. The type of cooler used depends on both the temperature levels required and the logistics of using the imager. There are four principal methods of cooling detectors:

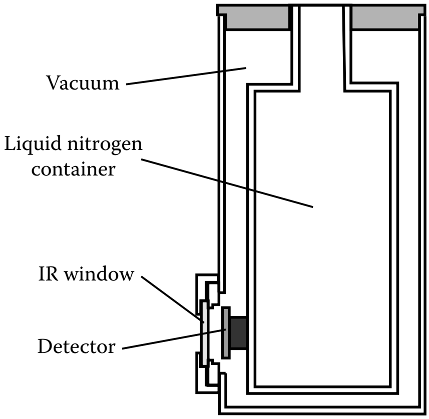

FIGURE 2.18 Example of a bulk-cooled detector.

Bulk cooling: This is the simplest form of cooling. The detector is mounted in a Dewar as illustrated in Figure 2.18, and is cooled directly by filling the later with liquid nitrogen. The technique is very effective and can be used to cool large arrays with no difficulty. The disadvantages are the logistics of having to have a supply of liquid nitrogen, the problem of spillage from the Dewar or of the liquid nitrogen not being at the bottom of the Dewar if one is moving the device around, and finally, the relatively large size of the Dewar when hold times of one or more hours are required. Bulk cooling is very practical in a laboratory, or static, environment.

Thermoelectric cooler (Peltier cooler): This makes use of the well-known Seebeck or Peltier effect, where an electric current passing through a junction between two dissimilar materials produces cooling at the junction when the current flows in one direction and heating when it travels in the opposite direction. As one would expect, the junction at the opposite end of the loop will have the current flowing in the opposite sense and will therefore heat up when the first one is cooling, and vice versa.

Special semiconductor materials have been developed to enable efficient devices to be produced. The requirement is for the materials to show a large Seebeck/Peltier effect and at the same time to have a relatively low thermal conductivity. The coolers can be constructed as multistage devices, with the number of stages determining the temperature differences that can be generated. Figure 2.19 is an illustration of a typical three-stage device. Temperature differences as large as –40°C can be generated in this way.

Where it can achieve the temperatures required for the type of detector being used, the thermoelectric cooler is almost invariably used. It is small and lightweight and requires a relatively small current of a few amps to

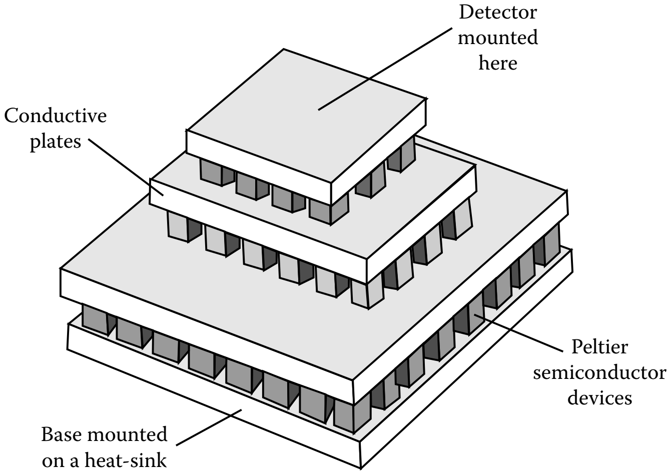

FIGURE 2.19 Illustration showing the arrangement of a three-stage thermoelectric cooler.

work. Among other things, it enables small, compact, portable, and battery-driven thermal imagers to be built.

Joule-Thomson cooler: When a gas expands through a small orifice it cools, and if the cooled gas goes through a heat exchanger where it cools the oncoming gas, a regenerative process occurs that leads to the gas gradually getting colder. If the arrangement is enclosed in a Dewar and the pressure differentials are large enough, the gas eventually turns into the liquid form as it emerges from the orifice. A diagram of a Joule-Thomson cooler arrangement is shown in Figure 2.20.

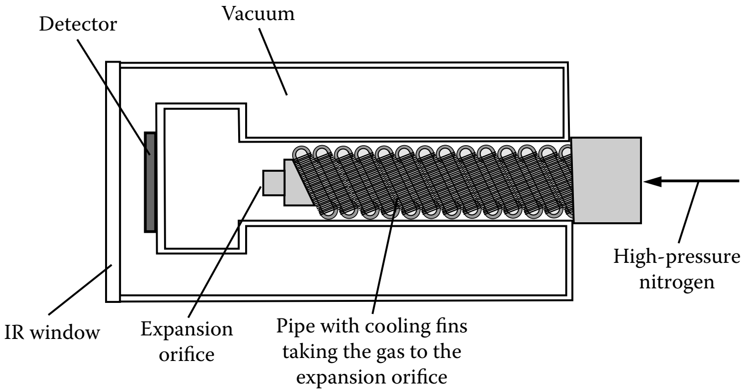

FIGURE 2.20 Diagram of a detector with a Joule-Thomson cooler.

The main disadvantage of this type of cooler is the need to have a supply of clean high-pressure gas. Nitrogen or air can be used, but it needs to be free of moisture, CO_2, and any small particles that could block the expansion orifice. High-pressure bottles of clean air or nitrogen can be used for running these devices. It is also possible to run them from small air pumps fitted with suitable air filtering systems.

Stirling engine coolers: These devices cool using the same principle as the household refrigerator, i.e., the Stirling cycle. They are self-contained closed-loop devices only requiring an electrical power supply to run them. Although they suffered originally from having poor reliability, current designs have overcome this problem and such devices are now very much in favor when liquid nitrogen temperatures are required.

In most detector arrangements the Stirling engine is an integral part of the detector construction. Figure 2.21 is an example of a Stirling engine cooled detector array.

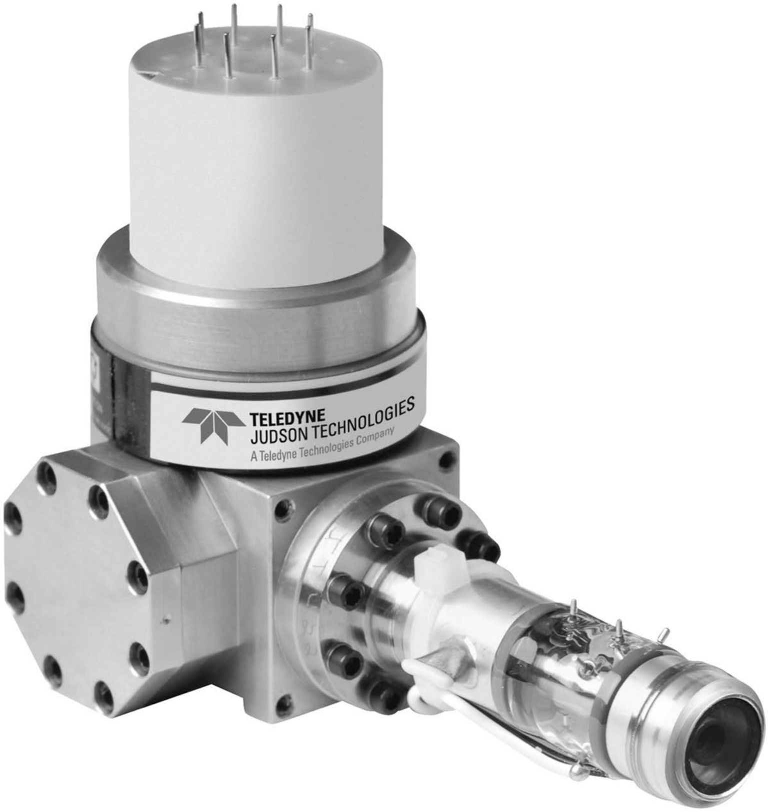

FIGURE 2.21 Example of a Stirling engine cooled detector array. (With kind permission of Teledyne Judson Technologies.)

2.7 SPECIAL SIGNAL PROCESSING AND OTHER REQUIREMENTS

2.7.1 Signal Offset Correction

The thermal image produced by the optical system will in general consist of a very high average background level of radiation corresponding approximately to the radiation emitted by a surface that is at ambient temperature, together with relatively small departures from this average level that represent the temperature and emissivity differences between the objects in the scene. So, for example, the difference in the radiation received from a surface at 18°C and one at 22°C in the 8–12 μm band is only 7% of the total (background) radiation in the same band from a surface at 20°C. The signal of interest in generating the video signal for the camera output is that corresponding to this difference and not the absolute radiation level.

In an imager with a scanner, alternating current (ac) coupling to the detector(s) will give just this signal. However, it is necessary to have a common start level for each scan line or swathe of lines. This is usually achieved by clamping the signal after each scan line to a common level, as the imager in effect looks at an internal surface that will be at the same temperature for each line. Where the imager is used for measuring temperature, this internal surface acts as the temperature reference and must either be controlled to remain at a known fixed temperature, or its temperature must be monitored and used to apply a correction to the temperature readout.

With staring array imagers the problem will be different depending on the type of array used. For most arrays of photon detectors the signal output will have a large dc offset corresponding to the average scene temperature, and suitable signal processing is required to remove this. With resistive bolometer arrays the devices will usually have their readout electronics designed to respond to temperature differences from an assumed ambient, or from the temperature at which they are controlled. However, some additional form of correction may be necessary.

2.7.2 Conversion to Standard Video Format

It is now usual to provide an output from a thermal imaging camera that conforms to a standard video format (e.g., PAL or CCIR), and suitable processing electronics is required to do this. We note in particular that where parallel scan is used suitable memory will be part of this processing system in order to convert a parallel output to a serial output.

2.8 DISPLAYS

The image generated by a thermal imager is normally viewed on either a separate external display that could be a computer screen or a small display that forms part of the camera and is designed to be looked at directly or through an eyepiece. The small, flat-screen, direct-view displays that are part of a camera are usually liquid crystal displays (LCDs). LCDs are also frequently used in eyepiece displays. Displays can be monochromatic or color. In the latter case, images can be color coded to show temperature differences as color differences.

2.9 COMPUTER AND SOFTWARE

Many thermal imagers come with software that allows the images generated by the camera to be analyzed in various ways. The software can form part of the camera or can be designed for use with an external PC. Typically software allows one to highlight areas of a maximum or minimum temperature or areas with a specific temperature, etc. Where imagers are being used for surveillance purposes, software can highlight and warn of specific targets, etc.

This aspect of thermal imagers is discussed in more detail in Chapter 3.

REFERENCES

1. Klocek, P. 1991. *Handbook of infrared optical materials*. New York: Marcel Dekker.
2. Williams, T. L. 1999. *The optical transfer function of imaging systems*. Bristol and Philadelphia: IOP Publishing.
3. Madding, R. P. 2005. Spectrally transmissive IR windows—How they affect your thermography results. *SPIE Proceedings* 5782:1–8.
4. Rozlosnik, A. 2005. Infrared windows in industrial applications I. *SPIE Proceedings* 5782:438–66.
5. Lettington, A. H., and Moore, W. T. 1986. Compact high performance thermal imager. *SPIE Proceedings* 685:146–151.
6. Moore, W. T., and Reeve, T. C. 1979. A 625 line CCIR compatible thermal imaging systems. In *2nd International Conference on Low Light and Thermal Imaging*, IEE Conference Publication 173, pp. 63–64.
7. Gunapala, S. D., et al. 2005. 1024×1024 pixel mid-wavelength and long-wavelength infrared QWIP focal plane arrays for imaging applications. *Semiconductor Science and Technology* 20:473–80.
8. Rogalski, A. 2003. Quantum well photoconductors in infrared detector technology. *Journal of Applied Physics* 93:4355–91.
9. Pron, H., et al. 2002. Focal plane array infrared cameras as research tools. *QIRT Journal* 1:229–40.

3 Industrial and Commercial Thermal Imagers and the Facilities They Provide

3.1 INTRODUCTION

A very wide range of sophisticated facilities are usually available on modern industrial or commercial imagers. These either form part of the camera and its associated electronics or are provided in the form of special software that can be used to further process the basic image, either in the camera itself or on an external PC. The type of facility provided will to a large extent depend on the application of the imager. Generally speaking, imagers are designed either to measure temperature or for use as a means of surveillance, although an imager can of course serve both purposes.

As a means for measuring temperature, temperature differences, or temperature profiles, they have many industrial, medical, and research applications, some of which are briefly described in Chapter 10. The design of the imager must make provision for generating an accurate temperature scale and have facilities for compensating for emissivities that differ from unity. For surveillance applications an accurate temperature scale is no longer a requirement, and the stress needs to be on having high spatial resolution with the ability to detect very small temperature differences.

Examples of small, very portable, and handheld cameras that would be very convenient for many temperature measurement applications are shown in Figure 3.1(a) and (b).

Thermal imagers frequently find applications in areas where they have to withstand demanding environmental conditions. Most frequently they may be used in hostile industrial environments or by firefighters, but can also have special applications, such as monitoring the tire temperatures on racing cars in real time, or the performance of rockets in flight. Imagers designed to operate under such conditions are also available commercially, and their ability to withstand different levels of vibration, shock, dust, water ingress, high temperatures, operation in vacuum, etc., will be specified by the manufacturer. This often means using standard imagers mounted in special enclosures. Figure 3.2 is an example of a small ruggedized imager that is suitable for use in harsh environments, while Figure 3.3 shows the essential core parts of an imager that can be customized to meet the requirements of a particular application.

The first of the two sections below deals with the types of imager used for industrial and other applications where the measurement of actual temperature is important, while the second section deals with the types of imager where some form of surveillance is the primary application, and finally there is a short section dealing with imagers for fire fighting. As mentioned above, these applications are not mutually exclusive. Even the cameras with no internal temperature reference can be used for measuring actual temperatures by placing reference sources in the external scene.

3.2 THERMAL IMAGERS THAT MEASURE ACTUAL TEMPERATURE

3.2.1 Temperature Measurement

This type of imager will have some form of internal temperature reference and will be calibrated to give an actual temperature reading of any part of the external scene that is within the particular temperature range that has been set on the device. The imager will usually have a facility for choosing different temperature ranges so that smaller temperature differences can be discerned where the scene covers a relatively small temperature range. Most imagers can produce either or both a grey scale and a color-coded display. In the former instance it is normal to represent low temperatures as dark greys and high temperatures as light greys (although a facility to reverse this is sometimes provided), with a scale showing temperature versus grey level provided

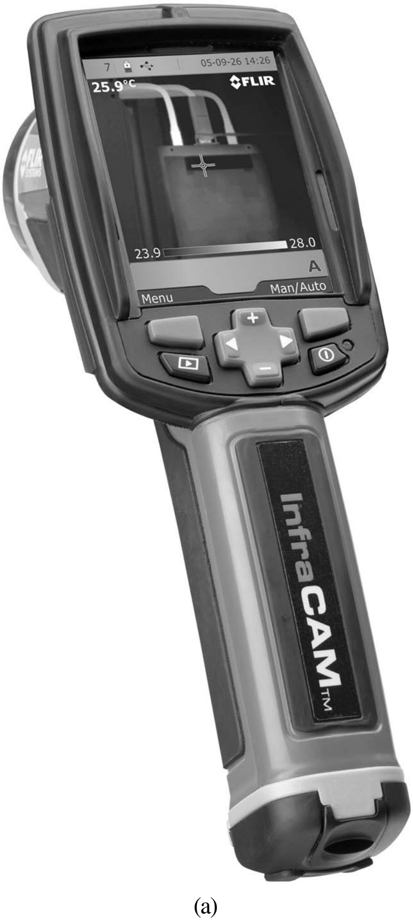

(a)

FIGURE 3.1 (a and b) Examples of small handheld thermal imaging cameras. ((a) With kind permission of FLIR Systems Ltd. and (b) with kind permission of Land Instruments International.)

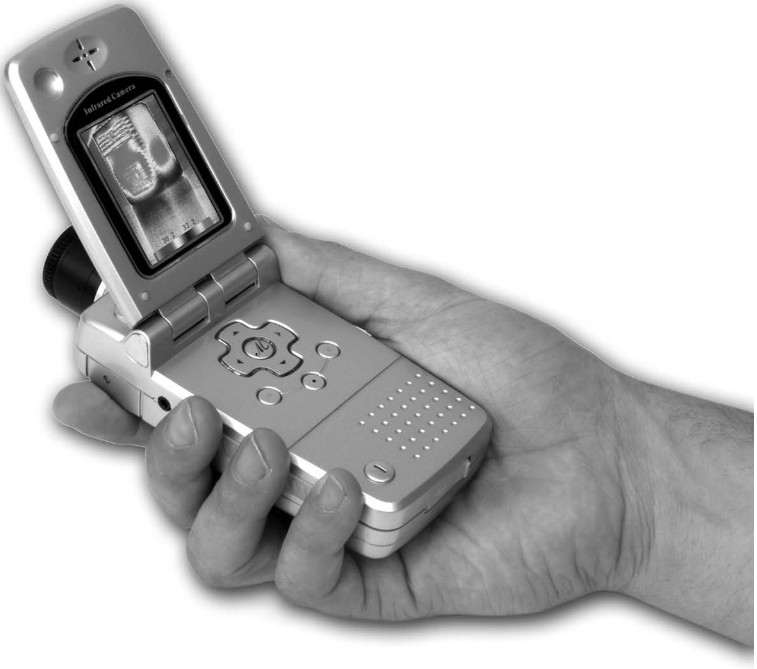

(b)

FIGURE 3.1 *(Continued)*

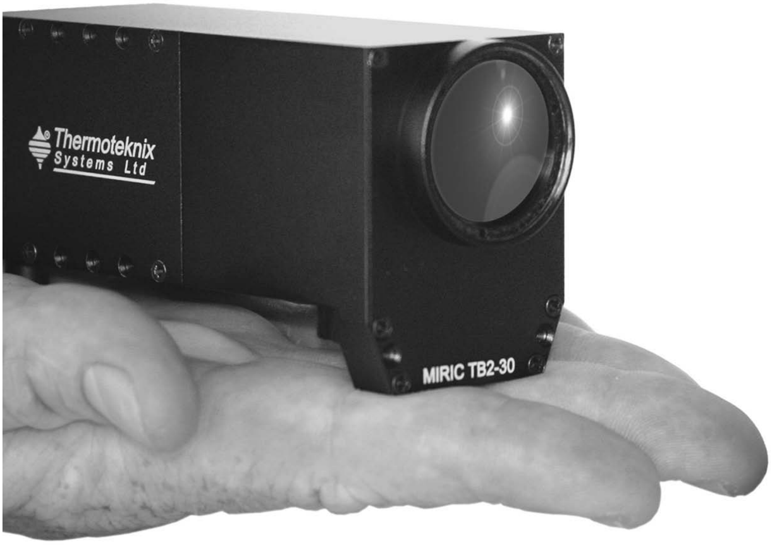

FIGURE 3.2 Small ruggedized thermal imager. (With kind permission of Thermoteknix Ltd.)

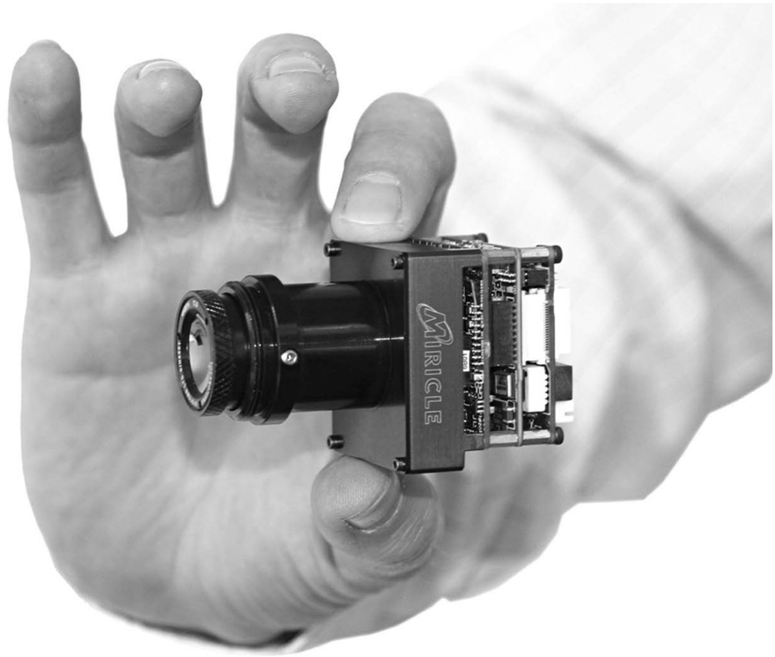

FIGURE 3.3 Core parts of an imager that can be customized to suit a particular application. (With kind permission of Thermoteknix Ltd.)

on one side of the display. In the latter case different temperatures are shown as different colors, with a scale showing temperature versus color on one side of the display. Normally, cold temperatures are represented by blue, and hot temperatures by bright orange. One or more movable cursors, or a fixed central mark, allow the user to obtain an actual temperature reading for a specific position in the image. An additional or alternative facility allows the user to highlight all parts of the image that are within a temperature range that he or she can set.

The range of temperatures covered by an imager, and in particular the maximum range covered at a single camera setting, will be an important factor in the choice of imager for a particular application.

In situations where high temperature-accuracy is required (e.g., in some medical and research applications) some manufacturers provide an arrangement where the imager is basically self-calibrating, using a blackbody source positioned in the scene.

Most of the imagers used in this type of industrial application have uncooled detector arrays, or at least when necessary, cooling or temperature control is provided by thermoelectric devices that use relatively little power. However, where very high sensitivity or resolution is necessary, cooling to liquid nitrogen temperatures may be required, and this will involve the use of either a Joule-Thomson cooler and an associated source of high-pressure nitrogen, bulk cooling with liquid nitrogen, or a Stirling cycle engine (see Section 2.6). Bulk cooling is relatively convenient in a fixed laboratory situation, although a Joule-Thomson cooler may have advantages in a similar situation. A Stirling cycle engine provides portability and greater convenience than the other two, although the camera may be more expensive.

3.2.2 EMISSIVITY AND ATMOSPHERIC ABSORPTION

It is important to note that the temperatures referred to above are the apparent temperatures and will only be the actual temperatures if the particular object of interest has an emissivity of unity and atmospheric absorption is zero at the distance and within the wavelength range used by the imager. Most imagers have a facility that allows the user to set a value for the emissivity of the object, in which case the temperature readings will be automatically compensated for this effect. To simplify matters this is sometimes provided as a list of materials and associated surface finishes, from which the user can make a selection. However, few, if any, provide a direct control for compensating for atmospheric absorption.

Figures 3.4 to 3.6 illustrate the sources of radiation that affect the temperature reading the camera measures, while Figure 3.7 shows the combined effect of all these sources.

Figure 3.4 shows the radiation that comes directly from the object of interest and how it is affected by the emissivity of the object and the absorption of the atmosphere. Figures 3.5 and 3.6 show the radiation reflected by the object from the sun and the local surrounds, respectively.

We can conclude from these illustrations that, strictly speaking, the apparent temperature will depend not only on the emissivity of the object but also on the temperature of the surrounding objects and the atmospheric absorption (see also Hamrelius[1]). The effect could be particularly marked where the object concerned has a low emissivity or when the camera is at a relatively distant position from the object, although at even short distances the CO_2 absorption that occurs around 4.2–4.4 μm can be very significant.*

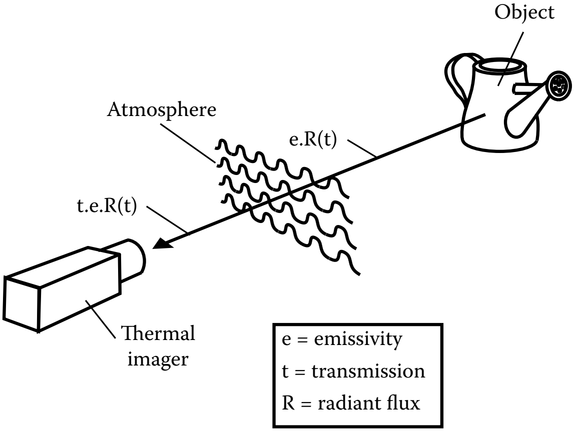

FIGURE 3.4 Radiation received by the thermal imager from the test object.

---

* The ONTAR Corporation of North Andover, Massachusetts, produces a range of software for predicting transmission for different wavelength bands and atmospheric conditions.

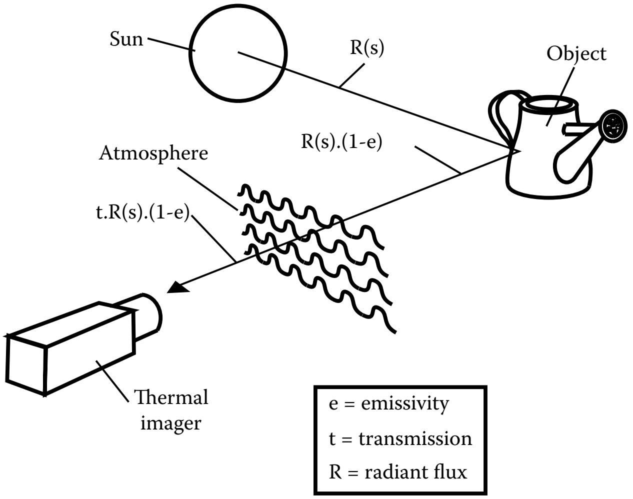

FIGURE 3.5 Radiation received by the thermal imager from the sun.

In theory the atmosphere itself can contribute to the radiation received by the imager. However, under most conditions the effect is small enough to ignore. The contribution from sun reflections is also only significant for imagers working in the 3–5 μm wavelength range and can be virtually eliminated by using a filter that cuts out all wavelengths shorter than about 4 μm. However, one must not ignore the heating effect of the sun's radiation on the thermal scene. This can result in differential temperature effects, where high-emissivity surfaces will absorb more of the radiation and therefore get hotter than low-emissivity surfaces.

One way around the emissivity problem is to attach a high-emissivity patch to the object (these are available commercially), or to paint a small patch with a

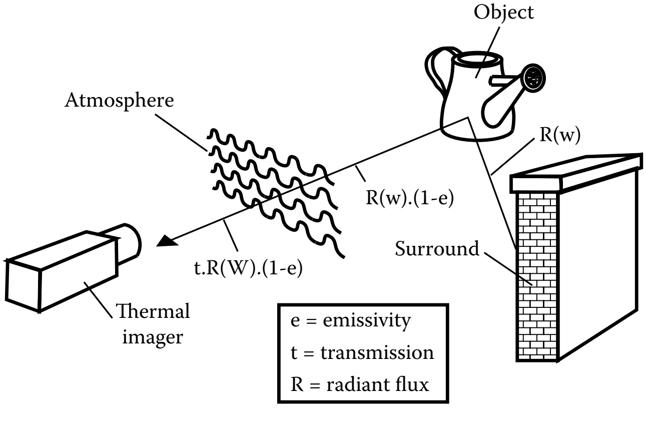

FIGURE 3.6 Radiation received by the thermal imager from the surround.

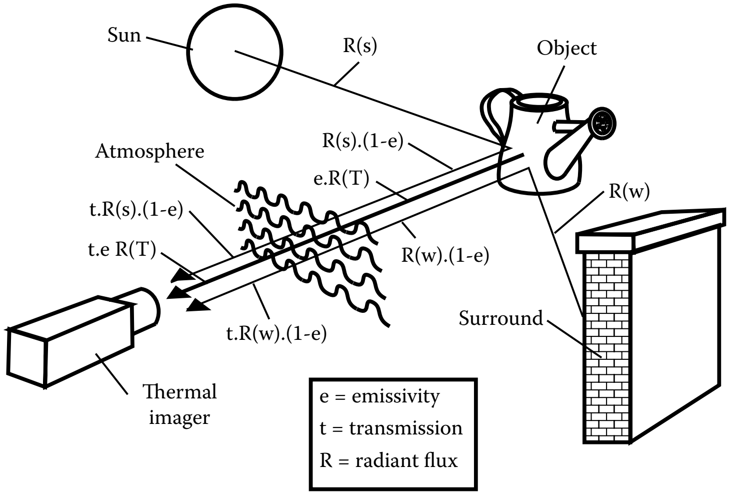

FIGURE 3.7 Radiation received by the thermal imager from all sources.

high-emissivity paint and measure the temperature of the object by measuring the temperature at the patch. Note that this can be used as a method of measuring the emissivity of a surface by comparing the temperature indication at the patch with an adjacent area of the normal surface. Laboratory methods of measuring emissivity are described in Hanssen.[2]

The atmospheric transmission problem can be tackled in several different ways. One of these is to calibrate the imager for this effect by using it to measure the temperature of a known high-emissivity source (e.g., a blackbody cavity—see Section 6.2.6) at various distances. It is important to note that the fall-off in apparent temperature with distance will be not be linear, but will be approximated by an equation of the form

$$T_m = T_a.\exp(-k.d) \qquad (3.1)$$

where T_m is the measured temperature, T_a is the actual temperature, d is the distance, and k is a constant. The value of k will depend on the atmospheric conditions that existed at the time of the measurement, and in particular the temperature and relative humidity. If these change significantly, the value of k will alter. The value of k will also be different for imagers working in different wavelength bands.

The experimental approach described above is relatively simple (see also Richards[3]). It will readily indicate if atmospheric transmission is likely to have significant effects for a particular imager (as indicated above, the wavelength range in which the imager operates will be an important factor) and for the conditions under which it will be used. However, as an alternative to this, the value of k can be determined by calculation using commercially available software. More detailed information about atmospheric transmission can be found in Richards[3] and Farmer.[4]

A point to note about temperature measurement is that what a thermal imager sees is the effective temperature of the surface of a body as modified by its emissivity and not necessarily the temperature of the body itself (excluding, of course, bodies that may have a transparent or semitransparent surface, or where the body itself is transparent or semitransparent). The surface temperature can be subject to variations caused by air currents.

3.2.3 OBJECT DIMENSIONS

The angular dimensions that an object subtends at the imager can significantly affect the measured temperature when the smallest angular dimension of an object approaches the limiting resolution of the imager. The main characteristics of the imager that will determine this are the focal length of the objective lens and its associated modulation transfer function (MTF), as well as the MTF of the detector array (see Chapter 4 for descriptions and definitions of these parameters). A standard performance parameter that evaluates this effect is the slit response function (SRF; described in Section 5.3.10). The SRF is a very good indication of when, and by how much, object size is likely to affect temperature measurements. Unfortunately, it is not a commonly quoted performance parameter, although it can be calculated from the MTF of an imager (see Section 5.3.10 and Williams[5]).

A simple way of evaluating the effect for a specific object is to produce an aperture in a metal plate, which has similar dimensions to the object, and to note the temperature indication given by the imager when the aperture is positioned in front of a blackbody of known temperature. The aperture should be in a plate of a material with high heat conductivity (e.g., copper or aluminium alloy) and coated with a high-emissivity paint. The plate should ideally be at a temperature similar to that of the background against which the object will be located.

3.2.4 THERMAL AND VISIBLE DISPLAYS

Some cameras have a dual imaging capability, where both a thermal and a visible wavelength image are recorded and where both images can be displayed side by side or superimposed. Such a facility can prove useful in several ways. One of these is that it allows the user to identify objects, or specific areas of an object, where the identity may not be obvious in the thermal image. Moreover, the greater detail and higher contrast of a visible wavelength image allows greater accuracy in positioning a cursor for designating a point in the image for temperature measurement. Dual images can also prove of greater use than single images, for record purposes.

In general, the sensor arrays used in thermal imagers have fewer pixels than the arrays used for visual wavelength imaging, and a useful dual image configuration is to superimpose a narrow field of view thermal image onto a relatively wide field of view visible image.[6,7] This allows the user to easily identify the area of interest using the visible image and to have a higher than normal resolution in the area covered by the thermal image. Figure 3.8 is an example of a camera capable of taking both visible and thermal images.

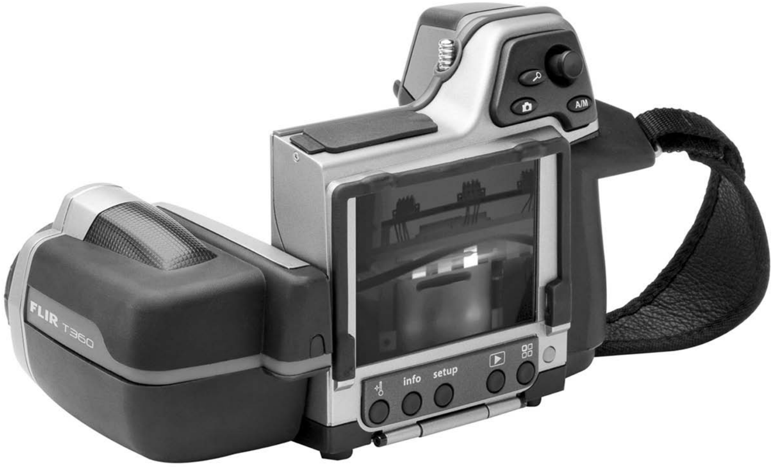

FIGURE 3.8 Example of a camera capable of taking both visible and thermal images. (With kind permission of FLIR Systems Ltd.)

3.3 SOFTWARE FACILITIES FOR INDUSTRIAL APPLICATIONS

3.3.1 General

The software provided (or available) with a thermal imaging camera for processing the basic output of the camera can either be built into the camera or be designed for use on an external PC. The software can be of a general nature or can be specific for a given application, and the facilities it provides will be important for the ease, accuracy, and convenience with which specific tasks can be achieved. The user should give this careful consideration when selecting the type of camera and associated software to use. Most imagers now make use of removable memory cards to store images and other data, as well as a means of introducing special software for controlling the operation of the imager. The storage capacity of such cards may be important in some applications.

Where no software already exists, the user should consider producing dedicated software to enhance the convenience, accuracy, and speed of specific applications in which he or she will be applying a thermal imaging camera. Digital image processing has reached a stage where there are not many tasks that cannot be achieved with appropriate software.

Users should not overlook the importance of using carefully researched procedures and software to optimize the use of thermal imagers for fault finding and regular maintenance (e.g., Almeida[8]).

3.3.2 Monitoring Temperatures

One of the important applications of thermal imaging is in monitoring various types of industrial plants to detect malfunctions or early signs of wear that will eventually lead to failure. Sophisticated software is available that will assist in controlling and recording multiple site inspections so that possible failures can be detected and problems rectified, at an early stage. For example, a higher than normal temperature on a bearing can indicate an imminent failure of that part of a system.

Software run on a PC can store a list of inspection points, as well as detailed information about each such point, including operating conditions, records of measured temperatures at relevant positions, and thermal and visible wavelength images. This information can be downloaded to the imager that is used for the inspection, as and when required. Figure 3.9 shows the display provided on the thermal imager, by one such software system.

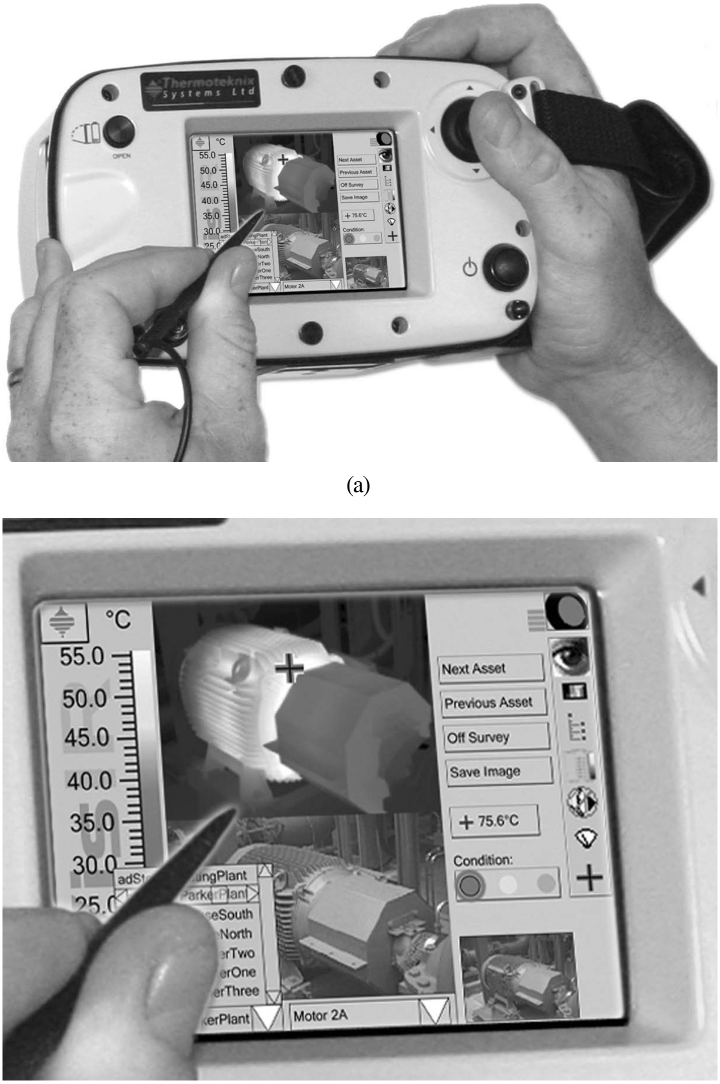

(a)

(b)

FIGURE 3.9 (a) Thermal imaging camera display with dual images of an electric motor. (b) Enlarged image of the display. (With kind permission of Thermoteknix Ltd.)

This shows the thermal image of the inspection point as it is being inspected, as well as a previously recorded visual image for identification and comparison purposes. The same imager can display a reference thermal image instead of the visual image. Showing a reference image is important in several ways. By making a comparison between the images, it is possible to place the camera in the same position used for the reference image. The camera may in fact have a facility for superimposing the images to ensure that the current thermal image is taken from exactly the same position as the reference image. This is important, since it ensures as far as possible that the effects of emissivity, of the radiation reflected from the surrounding objects and atmospheric absorption, are consistent. This will minimize measurement errors that can arise from, in particular, viewing a surface from a different angle and a different distance.

The reference image can also show the exact points where the temperature must be measured, or this can be done automatically by a PC at a later time. The software may also automatically select the correct temperature range, emissivity setting, and color palette for comparing the reference and actual images for a particular object. Other relevant data, such as currents and voltages, may also be recorded and stored with the thermal data for a more detailed analysis at a later time.

The software may also associate other image pairs with those of the motor, such as images for the fuses associated with the motor.

This type of software and imager of course can be adapted for use in a very wide range of applications. Essentially it allows temperatures (as displayed by a thermal image) to be compared with a stored reference set of temperatures. The variables can be position on a site, item of equipment, operating conditions, stages in a process, etc.

Some of the other facilities frequently provided on such imagers are the ability to display temperature profiles along a line in the image, the ability to log data in real time, and the availability of higher than normal frame rates for analyzing rapidly changing temperatures, or moving objects.

Where a reference image and an inspection image can be accurately superimposed it becomes relatively easy to generate, in software, images that show up the exact differences between the two. Within certain limits, even images that do not match exactly when superimposed can be manipulated sufficiently well to produce an accurate image showing the temperature differences.

Imagers are also used at fixed positions in an industrial site, in conjunction with remote control stations and suitable software, for multipoint temperature observation for process monitoring and plant surveillance. Much of this can be made automatic, including, in particular, the indication of alarm conditions.

Many other facilities are available on various cameras, and these include voice recording, autofocus, global positioning system (GPS), image detail enhancement, etc.

3.4 THERMAL IMAGERS FOR SURVEILLANCE TYPES OF APPLICATION

3.4.1 General

One of the main areas of application for this type of imager is in the military field. The imagers in this case are usually specifically designed for the task they will be required

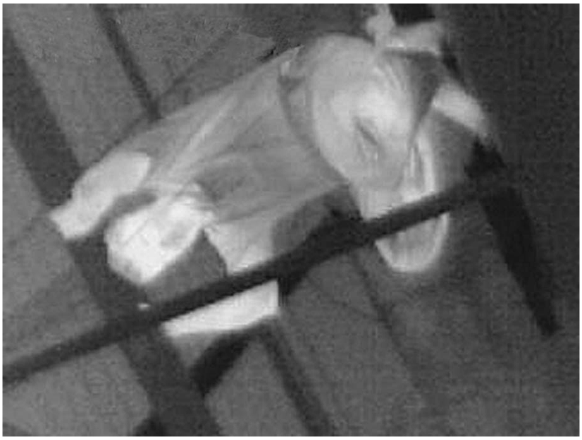

FIGURE 3.10 Visibility of an intruder hiding in a dark attic. (With kind permission of FLIR Systems Ltd.)

to perform and the vehicle on which they will be mounted, which could be a tank or an aeroplane, or they could be designed to be handheld by a soldier, or mounted as a sight on his rifle. There are, however, many nonmilitary surveillance tasks, such as border or site security and following and locating criminals from aircraft or helicopters.

There are several advantages of thermal imagers in this type of application:

- They are passive devices, so that no external illumination is required to light up the scene. A vehicle, person, or animal is observed by the radiation it emits. Figure 3.10 illustrates the easy visibility of an intruder hiding in a dark attic.
- It is difficult to produce camouflage that will hide a vehicle or human from being detected by a thermal imager. They can usually be seen as heat sources through all but the thickest vegetation.
- Smoke and mist do not attenuate and scatter the thermal radiation as much as they do the visible wavelength radiation. The result is not only that objects can be seen through a significant level of smoke or mist, but also that the range at which objects can be seen, under normal atmospheric conditions, is greatly increased.

For many applications, in particular some of the military ones, the important characteristics of a thermal imager are resolution and sensitivity. This is usually achieved by the use of large detector arrays cooled to liquid nitrogen temperatures. However, in situations that are not so demanding, or where weight is an important consideration, the type of imager described above for use in measuring temperature will be more than adequate, although the mechanical configuration (i.e., to protect against environmental conditions) may need to be different.

Thermal imaging cameras can be mounted in servo-controlled enclosures that protect them from the elements and allow them to be aimed in different directions and monitored and controlled remotely, in much the same way as the video cameras widely used for surveillance purposes. The enclosure windows do, of course, have to be of a material that transmits the appropriate thermal wavelengths (see Section 2.3). In military as well as civil applications where imagers are carried on helicopters or other vehicles, the servo-controlled platforms usually also include gyro stabilization.

3.4.2 Military Applications

The use of thermal imaging for detection and location of targets, in the form of either vehicles, including aircraft, or persons, has been one of the main driving forces behind the development of thermal imaging. The advantages are listed in Section 3.4.1. The imagers used on vehicles and aircraft are usually relatively large and will be designed to have a high thermal sensitivity and resolution, usually implying the use of detectors cooled to liquid nitrogen temperatures. Many of the imagers are designed so that they can be fitted with various focal length lenses, depending on their specific application. So, for example, very long focal length lenses will allow surveillance at very long distances, making use of the relatively low scatter that the atmosphere produces even under conditions of mist that would limit visual observation to very small distances. However, thermal imagers that are intended to be hand-held, helmet mounted, or mounted on rifles will be much more akin to the relatively light and straightforward industrial imagers.

On aircraft such as helicopters, thermal imagers can be used in conjunction with helmet-mounted displays, where the imager is servo mounted to track the head movements of the pilot. In this role it can, among other things, serve as a night sight for the pilot.

The minimum detectable temperature difference (MDTD; see Section 5.3.7) is a measure of the ability of a thermal imager to detect a target of given dimension, temperature relative to the background, and range, while the minimum resolvable temperature difference (MRTD; see Section 5.3.6) is a measure of the ability to recognize a target for the same parameters.

Many of the military imagers operate in conjunction with software that can perform specific tasks, such as enhancing the images, controlling gain, and automatically identifying targets as well as tracking them. Software that fuses visible images (including images from night vision cameras) with thermal images[6,7,9] can help considerably in identifying and locating targets. The thermal image can show up items, or areas of a scene, that are not visible, or at least not clearly visible in the visual or near-infrared (IR) wavelength image, while the latter can provide better definition and images that are more familiar to the user, allowing better interpretation of the combined scene.

Where the advantages of fusing thermal and visible images are to be used, there is a choice of either effectively mounting a visible camera next to a thermal camera and aligning their optical axes, or having an arrangement using a beam splitter that reflects the thermal radiation to the thermal camera and transmits the visible radiation to the visible camera. In the latter case the two cameras can have a common optical axis so that the position of all objects in both images will always be the same, independent of their distance from the cameras, while in the former case there will be some dependence, although this may not be a significant problem.

The requirement to achieve better image resolution with a thermal imager can also be achieved with the help of software and special camera arrangements.[9] One of these is to use two cameras, one of which has a wide field of view (WFOV) and the other a narrow field of view (NFOV), with an optical mechanism that allows the FOV of the latter to be moved to any part of the WFOV image. Another approach is to use a camera with an NFOV fitted with an optical mechanism that allows its FOV to be moved over a WFOV, together with software that will "stitch" the NFOV images into a single WFOV image.

3.4.3 Civil Applications

Commercial imagers are available that can be used for tasks similar to those done by military imagers, and high-performance imagers are available for such uses when necessary. Some of the applications include border surveillance, site security, tracking criminals from a helicopter, and locating injured or lost persons, including people in the sea, from both the ground and the air. Rescue helicopters can benefit particularly from such equipment.

Camera enclosures for these type of outdoor or airborne applications are produced commercially and can include servo-driven gimbal mountings that allow the imager to be pointed in any direction relative to the helicopter, plane, vehicle, or support tower. Software for image enhancement, automatic exposure control, and carrying out various surveillance tasks is available commercially, and new software is being generated all the time to improve performance or carry out new tasks.

The special software and camera arrangements referred to above for possible applications in military surveillance may be of equal use in civil applications.

3.5 IMAGERS USED BY FIREFIGHTERS

Thermal imagers have proved very useful in fire-fighting situations. They provide a means of seeing through smoke, locating bodies, and locating the source of a fire as well as other areas of high temperature. Imagers have also proved useful for locating bodies hidden under rubble as a result of the collapse of a building.

Imagers used for fire fighting are usually of special design and construction. They have to withstand harsh environmental conditions, they need to be light and at the same time robust, and they need to interface with a person who will be wearing a gas mask. Most of such imagers are designed to be handheld (see, for example, Figure 3.11(a) and (b)), but some are designed to be helmet mounted in order to free the hands of the firefighter (see, for example, Figure 3.12). In the latter case, a requirement is that the direction in which the imager is pointing can be altered relative to the helmet to accommodate the situation where the firefighter may be lying down; a second requirement is having the ability to move the display out of the line of sight of the user.

One of the other special features that are available on some of these imagers is a facility to accommodate very high temperatures in the scene (e.g., 1,000°C) without significantly affecting the visibility of the low-temperature part of the scene. Another useful facility is a wireless video link that allows an individual outside the fire to see the image that the firefighter, holding the camera, sees.

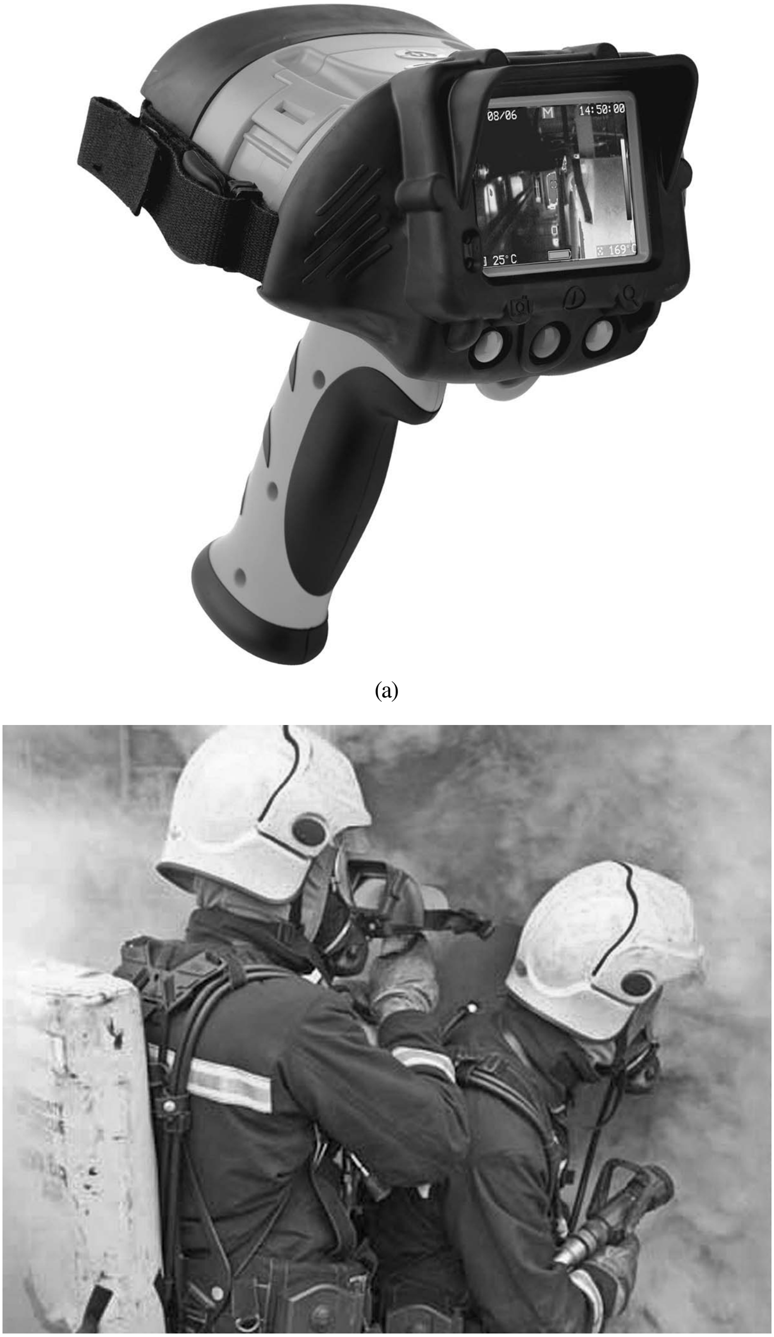

(a)

(b)

FIGURE 3.11 (a) Example of a handheld imager for fire fighting. (b) The imager in use. (Both with kind permission of E2V Technologies PLC.)

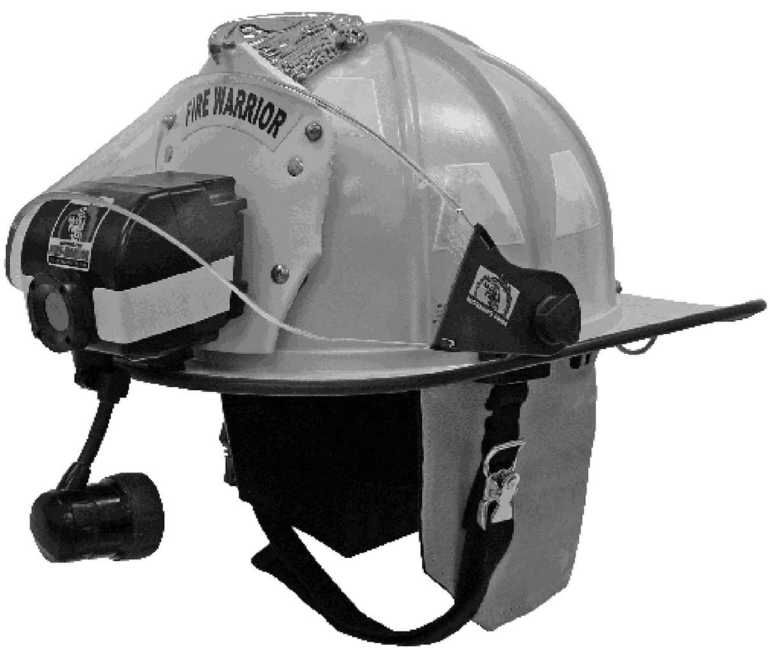

FIGURE 3.12 Example of a helmet-mounted imager intended for fire fighting. (Morning Pride by Honeywell, Fire-Warrior Micro Thermal Imaging Camera, with kind permission of Fire-Warrior/Honeywell, #1 Innovation Court, Dayton, OH 45414.)

3.6 MANUFACTURERS' DATA SHEETS

We provide here a typical list of some of the data that a manufacturer may provide in a sheet describing its product, as well as a brief description of their meaning or a reference to a section of this book where more information is available. Note that different manufacturers may use different wording and classifications than those used below, and that they may provide important additional facilities not included in this list.

Imaging characteristics:

- *Field of view* (FOV)—See Section 4.2.1.
- *Lens focal length and f/number*—See Section 4.2.1.
- *Detector*—This could include the type of detector as well as its dimensions and the number of pixels; see Section 2.4.
- *Electronic zoom range*—The electronic zoom only changes the area of the image shown on the display and not the focal length of the lens.
- *Spatial resolution*—This could be specified in terms of the MTF of the imager (see Section 5.3.1) or as the number of pixels in the detector array.
- *Minimum focus distance*—The shortest distance from the imager to an object on which a correct focus can be achieved.

- *Frame rate*—This will normally be a standard TV frame rate, but some imagers may use or allow other frame rates to be selected, and in particular faster frame rates, in order to capture events that occur over a short period of time.
- *Focus*—Facilities may be available for automatic as well as manual focusing.

Thermal characteristics:

- *NETD, sometimes referred to as thermal sensitivity*—See Section 5.3.5.
- *Spectral range*—The range of wavelengths to which the imager is sensitive.
- *Temperature range*— The maximum and minimum temperatures that can be measured with the imager and the ranges into which this can be divided (see Section 5.3.13).
- *Temperature measurement accuracy*—See Section 5.3.14.
- *MRTD/MDTD*—See Sections 5.3.6 and 5.3.7.
- *SRF/ARF*—See Sections 5.3.10 and 5.3.11.

Measurement facilities:

- *Color/monochrome display coding*
- *Temperature indication*—The methods by means of which the user can measure temperature at specified positions in the scene
- *Emissivity adjustment*—If and how provision is made for emissivity compensation.
- *Variable integration times*—For some applications it is useful to be able to use longer than normal integration times, in particular to increase sensitivity.
- *Variable stops*—The values that can be set by the user (see Sections 4.2.3 and 4.2.4).
- *Special filters*—Filters can be provided for attenuating the signal, sun radiation, etc.
- *Range adjustment*—The means by which temperature ranges are adjusted.

Displays and interfaces:

- *Type and position of camera display*
- *Memory type and characteristics*—Cameras can use removable memory cards of different types and capacity.
- *Voice recording*—A facility is available on some cameras for recording verbal comments, usually on the removable memory card.
- *External data connections*—This should specify the types of interface provided to external PCs, etc.
- *Software*—Special software may be available for use both in the imager as well as on an external computer.

Physical characteristics:

- *Dimensions*
- *Weight*

- *Type of cooler*—Applies where the detector requires cooling (see Sections 2.5 and 2.6).
- *Operating temperature*
- *Storage temperature*—Note that there is a series of ISO standards (ISO10109–1, etc.) that deal with environmental requirements for optical and optronic systems.
- *Humidity*—As above.
- *Shock*—As above.
- *Vibration*—As above.

Power requirements:

- *Battery type*—If a facility is available for using batteries.
- *Time of use for a single battery charge*
- *Mains requirements.*

Where an imager is intended for special applications the manufacturer may of course specify other characteristics and facilities specially provided to meet the requirements of that application, e.g., the type of environmental enclosure.

REFERENCES

1. Hamrelius, T. 1992. Accurate temperature measurement in thermography. *QIRT Seminar Proceedings* 27:39–45.
2. Hanssen, L. et al. 2004. Infrared spectral emissivity characterisation facility at NIST. *SPIE Conference Proceedings* 5405:1–12.
3. Richards, A. 2005. Radiometric calibration of infrared cameras accounting for atmospheric path effects. *SPIE Conference Proceedings* 5782:19–28.
4. Farmer, W. M. *The atmospheric filter*. Vols. I and II. Winter Park: JCD Publishing.
5. Williams, T. L. 1992. The MFT of thermal imaging cameras. Its relevance and measurement. In *Proceedings of the QIRT Conference*, No. 27, pp. 51–56.
6. Smith, M. I., et al. 2005. Review of image fusion technology in 2005. *SPIE Conference Proceedings* 5782:29–45.
7. Wolff, L. B., et al. 2005. Advances in low-power visible/thermal image fusion hardware. *SPIE Conference Proceedings* 5782:54–58.
8. Almeida, C. A. L., et al. 2005. Intelligent detection and diagnosis of lightning arrester faults using digital thermovision image processing techniques. *SPIE Conference Proceedings* 5782:109–20.
9. El-Maadi, A. 2007. Visible and infrared imagery for surveillance applications: Software and hardware considerations. *QIRT Journal* 4:25–40.

4 Performance Parameters for Components of a Thermal Imager

4.1 INTRODUCTION

The primary aim of this book is to deal with complete thermal imagers; however, in this chapter we also provide some limited information about the performance parameters associated with the more important components that form part of a thermal imager.

Two of the most important components of a thermal imager are detectors and lenses, and much of the performance of an imager is determined by the performance of these components and perhaps, to a lesser extent, that of the display. Ultimately these performance parameters have a direct effect on one or more of the parameters that describe the performance of a complete thermal imager, so by understanding what they are and how they can be measured, one can more easily assess the suitability of an imager for a given application. These parameters are described and defined in this chapter, and an indication of how they can be measured is given in Chapter 7.

4.2 LENSES

4.2.1 Focal Length

This is sometimes referred to as the effective focal length (EFL) to differentiate it from the back focal distance (BFD), which is the distance from the pole of the last optical surface to the image plane. For a simple thin lens, the focal length is closely equal to the distance from the lens to the image plane, for an object at infinity. For a thick lens or a multielement lens, the focal length is defined as the distance from the rear nodal point to the image plane, for an object at infinity (see Figure 4.1). In a thermal imager the real significance of the focal length is that it relates the effective dimensions of the image plane (in a staring array camera this would be the dimensions of the array) to the field of view (FOV) of the imager. The relationship is given by the equation

$$\tan\theta = h/f \tag{4.1}$$

where θ is the angle equal to half the full FOV, f is the focal length of the lens (EFL), and h is half the linear dimension in the image that corresponds to the full FOV (see Figure 4.2). For example, if we have a staring array of width w, the full FOV of the imager corresponding to this dimension is given by

$$\mathrm{FOV} = 2.\theta = 2.\tan^{-1}[w/2.f] \tag{4.2}$$

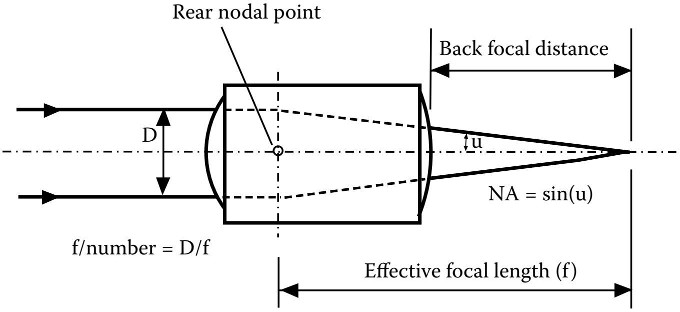

FIGURE 4.1 Focal length of a thick lens.

4.2.2 MAGNIFICATION (M)

This is a parameter of an afocal system or telescope. It is the given by the ratio

$$M = \tan\theta'/\tan\theta \tag{4.3}$$

where θ is the angle an object at infinity makes with the optical axis of the telescope and θ' is the angle the image (also at infinity) of that object makes with the optical axis (see Figure 4.3). Thermal imagers are frequently designed to have a basic image-forming optical system that, for instance, gives them a FOV equal to, say, Φ, to which one can add a telescope in order to change the FOV. Quite simply, if the telescope has a magnification M, the new FOV is given by

$$\Phi' = \tan^{-1}[\tan(\Phi)/M] \tag{4.4}$$

It should be noted that a manufacturer may identify an add-on telescope as having a magnification M, where in fact the relationship between this and the new FOV will be simply

$$\Phi' = \Phi/M \tag{4.5}$$

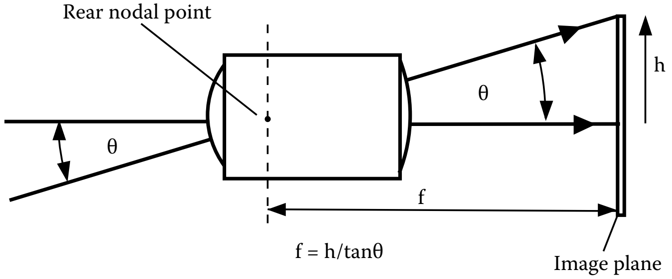

FIGURE 4.2 Relationship between focal length and image size.

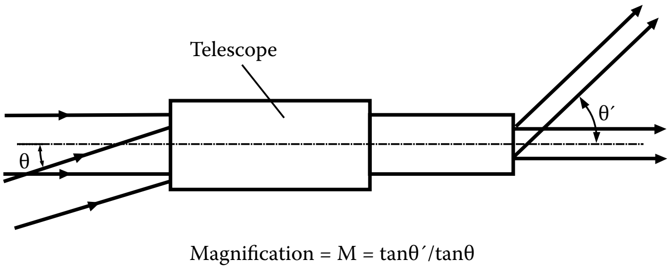

FIGURE 4.3 Magnification of a telescope (afocal system).

4.2.3 NUMERICAL APERTURE (NA)

This is equal to the sine of the half angle a ray of light passing through the edge of the aperture stop of a lens makes with the optical axis at the image plane (see Figure 4.4), i.e.,

$$\mathrm{NA} = \sin(u) \tag{4.6}$$

where u is the angle the extreme ray makes with the optical axis. The significance of the NA is that it is the parameter (other than the lens transmission) that determines the relationship between the radiance of an object and the irradiance in the image of that object. The relationship for a lens with a circular aperture is

$$I = \pi.W.t.(\mathrm{NA})^2 \tag{4.7}$$

where I is the irradiance (i.e., watts m^{-2}) in the image plane produced by a radiance W (watts m^{-2} steradian^{-1}) in the object and t is the lens transmission. Note that t will in general vary with wavelength.

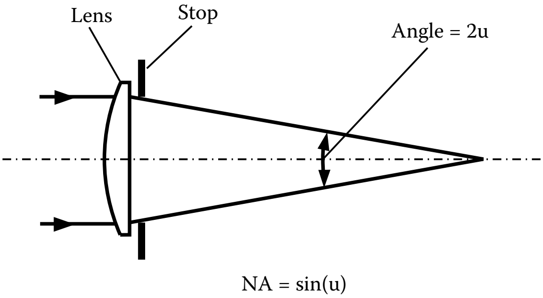

FIGURE 4.4 Numerical aperture of a lens.

4.2.4 *f*/NUMBER

This is usually taken as the ratio of the focal length of the lens to the diameter of the entrance pupil; i.e., if the *f*/number is α (normally written as f/α), then

$$\alpha = f/D \tag{4.8}$$

where f is the focal length of the lens and D is the diameter of its exit pupil (see Figure 4.1).

Strictly speaking this is an approximation and the *f*/number is more correctly defined as

$$\alpha = 1/(2.\text{NA}) \tag{4.9}$$

The two definitions only differ significantly when the NA is very large, which is sometimes the case with lenses used on thermal imagers.

The significance of the *f*/number is the same as that of the NA, and the two are just different ways of quantifying the same important aspect of a lens.

4.2.5 TRANSMISSION

Sometimes this is referred to as paraxial transmission because it is measured for a beam of radiation of limited diameter that passes centrally through the lens without striking the aperture stop. The transmission is the ratio of the radiant flux exiting the lens system to the radiant flux entering the lens system, and is often expressed as a percentage. Transmission will vary with wavelength and is normally measured as a function of the latter.

The transmission of a lens or lens system will depend on the bulk absorption of the materials from which the lens elements are made and, most importantly, on reflections at the optical surfaces. The latter depends on the quality and characteristics of the antireflection coatings applied to these surfaces. It is of particular importance in thermal imaging since most of the materials used for lenses have a very high refractive index, and the coatings therefore play a crucial role in providing high levels of transmission. The reflectance at normal incidence of a single uncoated surface of refractive index n in air is given by

$$r = (n - 1)^2/(n + 1)^2 \tag{4.10}$$

For a material such as germanium with $n = 4$ we see that $r = 0.36$ if it is uncoated.

4.2.6 RELATIVE FIELD IRRADIANCE (RFI)

This is a measure of how the irradiance in the image plane of the optical system varies with position in the image plane, when the object is a field of uniform radiance. RFI is usually expressed as the ratio of field irradiance at θ to field irradiance on-axis, where θ is the field angle.

As a result of the normal geometry of image formation, irradiance in the image plane will fall off as the fourth power of the cosine of the field angle. This effect can be counteracted to some extent in special lens designs, where effectively the size of the lens pupil increases with field angle. A fall-off in irradiance can also be the result of the antireflection coatings becoming less efficient as the field angle increases. The fall-off can also be made worse by **vignetting** of the lens pupil. *Vignetting* is the term used to describe the fall-off caused by mechanical stops, or the edge of lenses, obstructing part of the beam, as the field angle increases. Vignetting is sometimes deliberately introduced into an optical design, either as a means of removing part of the beam that has levels of aberration that would significantly reduce image quality or as a result of the need to limit the diameter/size of a lens system.

The importance of a variation of field irradiance is that it will limit the minimum temperature range that can be set when viewing a thermal scene (and therefore the smallest temperature differences that can be resolved), without losing parts of the image. It will also affect the accuracy of temperature measurement over the field of view of the imager, unless special signal processing is used to compensate for the effect.

4.2.7 MODULATION TRANSFER FUNCTION (MTF)

This is the primary means of describing and assessing the imaging quality of an optical system. In general terms MTF is defined as the ratio of the contrast in the image of a sinewave grating to the contrast in the original object (see Figure 4.5), i.e.,

$$\text{MTF} = (\text{Image contrast})/(\text{Object contrast}) \tag{4.11}$$

where contrast is defined as

$$\text{Contrast} = (I_{\max} - I_{\min})/(I_{\max} + I_{\min}) \tag{4.12}$$

and where $I_{\max}$ is the maximum intensity in the sinewave and $I_{\min}$ is the minimum intensity. (Note that comprehensive information about all aspects of MTF can be found in Williams[1].)

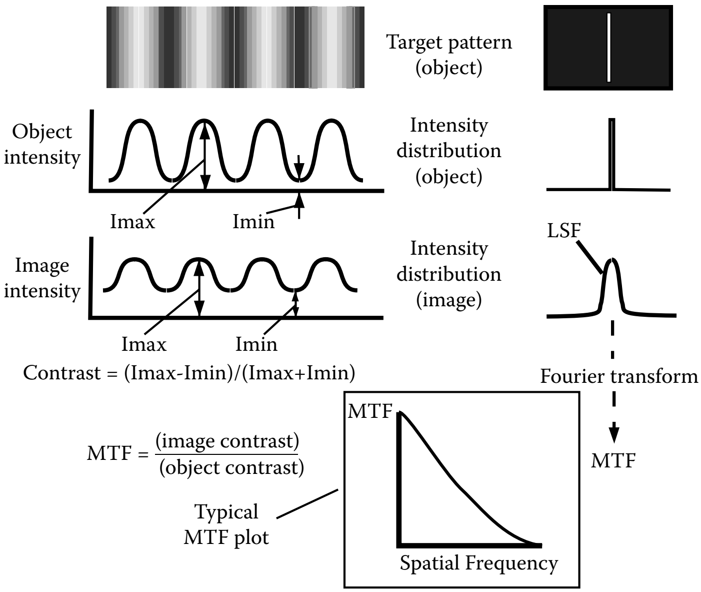

FIGURE 4.5 Illustration of how MTF is defined and measured.

MTF is a function of the spatial frequency of the grating (i.e., the reciprocal of the periodicity of the sinewave grating) and falls in value as the spatial frequency increases, being normalized to a value of unity at zero spatial frequency (see Figure 4.5). In general, the MTF of a lens will vary with field angle and with the orientation of the sinewave grating. It is usual to measure the MTF for the grating lines vertical (i.e., the MTF in the tangential, or *T* section) and for the lines horizontal (i.e., the MTF in the radial, or *R* section, sometimes also referred to as the sagittal section) and to do this for zero field angle (i.e., on-axis) and two or more off-axis field positions either side of the central position. Ideally, the off-axis measurements should also be done in a second direction in the image plane orthogonal to the first.

The spatial frequency can be expressed in terms of a linear or angular dimension depending on which is most convenient. If the spatial frequency refers to an image or object plane at a finite distance from the optical system, the units will usually be cycles/mm. If it refers to an image or object at infinity, the units are either cycles/degree or cycles/milliradian.

The MTF of an optical system that has no aberrations is limited only by the effects of the diffraction of light, and such systems are referred to as diffraction limited. The shape of the MTF curve for a perfect lens with a circular aperture is illustrated in Figure 4.6. The curve has the same shape for all such lenses when a normalized spatial frequency scale is used. The equation for the curve is

$$\mathrm{MTF}(s) = (1/\pi)[2\cos^{-1}|s/2| - \sin(2\cos^{-1}|s/2|)] \tag{4.13}$$

where s is the normalized spatial frequency going from $s = 0$ to $s = 2$.

The cutoff spatial frequency in real terms that is equivalent to $s = 2$ is given by

$$s_c = 2.\mathrm{NA}/\lambda = 1/(\lambda.f/\mathrm{number}) \tag{4.14}$$

where NA (see above) is the numerical aperture and λ is wavelength. The units for the spatial frequency s_c will be the reciprocal of the units in which λ is expressed.

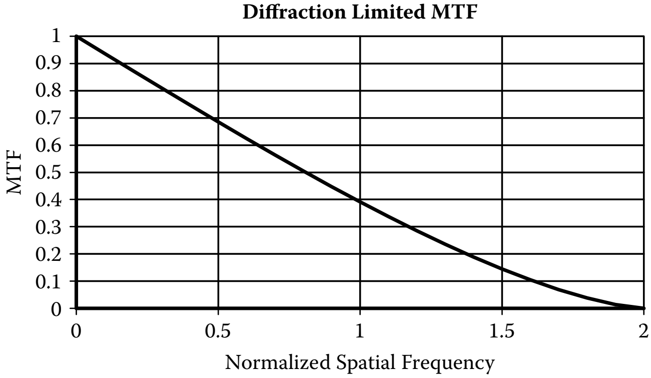

FIGURE 4.6 Diffraction-limited MTF for a lens with a circular pupil.

Thus, if λ is in millimeters, the spatial frequency units will be c/mm. If the cutoff spatial frequency is required in angular units, we then have

$$s_c = D/\lambda \tag{4.15}$$

where D is the diameter of the entrance pupil if the spatial frequency is being measured in object space, and that of the exit pupil if measured in image space. D and λ must be in the same units and the spatial frequency will be in c/radian.

As an example we note that an *f*/4 lens used with 10 μm wavelength radiation has a cutoff spatial frequency of only 25 c/mm. This is also the effective cutoff spatial frequency for a detector of width 40 μm used in a scanning system. It is also the Nyquist frequency (i.e., the maximum spatial frequency that can be used without introducing the potential for aliasing; see Appendix B) associated with a staring array with detector elements spaced 20 μm apart. The MTF associated with a detector pixel of width w millimeters is given by Equation (4.17) (see Section 4.3.10).

4.2.8 Veiling Glare Index (VGI)

This is a measure of the unwanted stray radiation that reaches the image plane. It is usually a result of scatter from lenses and lens surfaces and unwanted reflections between lens surfaces and reflections or radiation emitted from the lens and camera body. The effect of veiling glare is to reduce image contrast. However, in a thermal imager the level of glare radiation is small compared to the average background radiation the imager sees, and provided it is uniformly distributed over the image plane, its effects are usually insignificant (see Section 4.2.6).

Definitions of the VGI for visual wavelength lenses can be found in Williams[1] and ISO[2].

A different source of radiation that is incident on the image plane is that radiated by the internal parts of the imager, and if this is not uniform, or is at a significantly high level, it will affect the performance of the imager. For this reason some imagers (particularly those with cooled detectors) will include a cooled stop that prevents the detector from seeing radiation other than that passing through the lens system or from cooled internal surfaces. The internal items that are cooled may include any spectral filters in the optical path, since filters will radiate at the wavelengths they are designed to absorb.

4.2.9 Narcissus Effect

This is a specific form of veiling glare that normally shows itself as an area of apparently reduced temperature at the center of the thermal image. It is a result of one or more of the optical surfaces reflecting back to the image plane an approximately in-focus image of the cooled detector or cold stop. For instance, a poorly coated plane window placed in front of the lens and perpendicular to its optical axis will produce a very strong narcissus effect. For this and other reasons, an external window through which an imager will view a scene will be set at an angle to the optical axis.

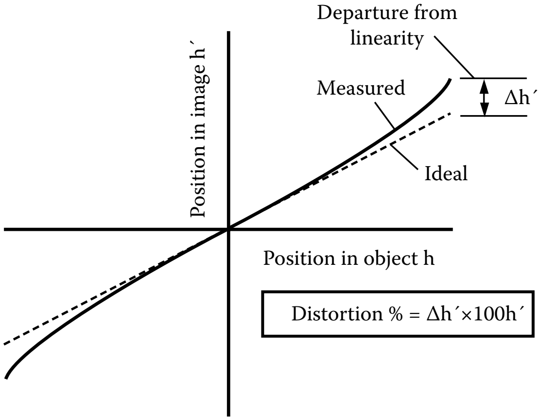

FIGURE 4.7 Measurement of distortion.

The presence of narcissus will contribute to a nonuniformity in the relative field irradiance and as such can limit the smallest temperature range that can be used without losing parts of the image.

4.2.10 DISTORTION

In an ideal imaging system the relationship between the linear position of an object in the field of view of the system and its position in the image plane should be a linear one. This can be written as $h' = k.h$, where h' is the position in the image, h is the corresponding object space position, and k is the constant of proportionality. Departures from this are a measure of distortion. Thus, if the actual image position differs from h' by dh', the percent distortion is given as $dh' \times 100/h'$ (see Figure 4.7 and ISO[3]).

Distortion is normally one of two types, referred to as Barrel and Pincushion, as illustrated in Figure 4.8. A small amount of residual distortion in a lens is in general not of critical importance unless the image is being used as a means of measuring angular or linear dimensions.

For afocal systems that do not form an image directly, the linear relationship that represents the no distortion condition can be written as $\tan\theta' = k.\tan\theta$, where θ' is

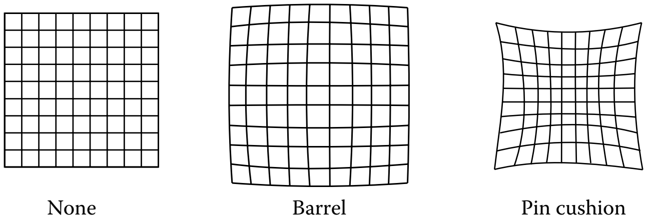

FIGURE 4.8 Types of distortion.

the angle the direction of the output makes with the optical axis and θ is the angle the direction of the input makes with the optical axis. Thus, if the actual image position differs from θ' by $d\theta'$, the percent distortion is given to a close approximation as $d\theta' \times 100/\tan\theta'$, and more precisely as $d\theta' \times 100/\sin\theta' \times \cos\theta'$.

In some thermal imagers that use scanning polygons, the afocal systems are specifically designed so that $\theta' = k.\theta$. In such instances the percent distortion is given as $d\theta' \times 100/\theta'$.

4.3 DETECTORS

4.3.1 Detective Quantum Efficiency (DQE)

For a photon detector this is the percentage of photons that interact with the material to generate a signal. A high DQE does not necessarily result in a detector with a good performance. More important is the signal/noise ratio (S/N). In an ideal detector the only source of noise is that from the statistical nature of the incident photons. In this situation the noise is proportional to the square root of the total signal so that the S/N is in fact equal to $\sqrt{S}$. It is important to point out that most of the incident photons will come from the general level of background radiation and not from the relatively small differences in radiation from the different parts of the scene that are used to generate the final thermal image. For this reason a detector that is close to the performance of an ideal detector is referred to as being a background-limited infrared photodetector (BLIP) detector. However, there are usually additional sources of noise that can dominate the performance of infrared detectors.

4.3.2 RMS Noise

Noise is usually expressed as the root mean square (RMS) value of the noise signal. As indicated above, there are several sources of noise other than that connected with the statistical nature of the incident photons. These sources and the characteristics of the noise they generate are as follows:

Johnson noise: This form of noise is always present in any resistive material and arises from the random motion of the carriers. It is proportional to the square root of the temperature and the square root of the frequency bandwidth.

Generation-recombination (G-R) noise: This arises from fluctuations in the rate at which thermally generated carriers in a semiconductor are produced and recombine. As for all noise sources, it is proportional to the square root of the frequency bandwidth. The other factors on which it depends are largely properties of the actual semiconductor material.

Flicker or 1/*f* noise: As the name implies, this noise is inversely proportional to frequency and can be the dominant source of noise at low frequencies. There is still some uncertainty regarding the mechanism that generates this type of noise, although it is generally accepted that it arises at the contacts made to the semiconductor detector element.

Readout amplifier noise: The amplifier that is used to amplify the output signal from a detector will itself introduce noise. How significant this noise is will depend on the level of the signal from the detector and on how well the output of one is electrically matched to the input of the other.

G-R and $1/f$ noise are relevant only in the case of photon detectors. The remaining sources of noise are relevant to both photon and thermal detectors.

More detailed information about detectors can be found in Keyes.[4]

4.3.3 NOISE SPECTRUM

As indicated above, the noise signal from a detector will in general be different in different frequency bands. The noise spectrum is a plot of RMS noise as a function of frequency.

4.3.4 NOISE-EQUIVALENT POWER (NEP)

This is a measure of the noise signal generated by a detector. The NEP is equal to the RMS radiant power in watts per second falling on the detector element that is required to produce a signal equal to the RMS noise signal. The NEP will depend on the central frequency and frequency bandwidth (usually taken as unity) used for measuring the noise, as well as the wavelength or wavelength range of the incident radiation. These variables must be specified for the NEP to be meaningful. The NEP of a detector will be proportional to the square root of the frequency bandwidth.

4.3.5 D* (D-STAR)

This is one of the principal figures of merit for the performance of a detector. Its purpose is to serve as a measure of the S/N performance of a detector, which is independent of the area of the detector. It does this by assuming that the NEP of a detector is proportional to the square root of the area. It is defined as

$$\mathrm{D}^* = (A.\Delta f)^{1/2}/\mathrm{NEP} \tag{4.16}$$

where A is the area of the detector and Δf the frequency bandwidth. We note that the value of D* increases as the performance of the detector increases. The value of D* will depend on the central frequency and frequency bandwidth (usually taken as unity) used for measuring the noise as well as the wavelength or wavelength range of the incident radiation. These variables must be specified for D* to be meaningful, and it is usual to write the value as $\mathrm{D}^*(\lambda, f, 1)$, where λ is the monochromatic wavelength for which it is measured, f is the frequency, and the number 1 indicates that it is for $\Delta f = 1$. Alternately, it is written as $\mathrm{D}^*(T, f, 1)$ when broadband radiation is used, and T is the temperature of the blackbody radiation source (in Kelvin) used for the measurement instead of a monochromatic source. Unless otherwise specified, D* is assumed to be measured with a hemispherical detector field of view.

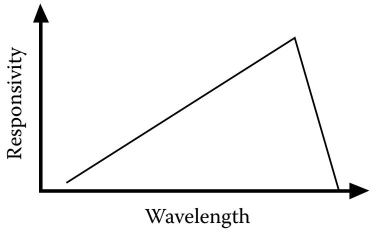

FIGURE 4.9 Typical spectral response of a photon detector.

D* is sometimes referred to as *detectivity*. However, this term is also used for the reciprocal of the NEP.

4.3.6 RESPONSIVITY

This is the ratio of detector signal to incident radiation power and is measured in volts per watt or amps per watt, depending on the type of detector. As in other instances, its value depends on variables such as wavelength and frequency.

4.3.7 SPECTRAL RESPONSE

This is a measure of how the responsivity of a detector varies with wavelength. Typically photon detectors have a spectral response that has the form shown in Figure 4.9. They have a peak response at a wavelength just short of the maximum wavelength to which they will respond, and a fall-off in response that is very nearly linear down to the shortest wavelength to which they will respond. The explanation for this is that they have an almost flat response in terms of photon numbers, but of course the energy of a photon is inversely proportional to its wavelength. Therefore, a given radiant flux is generated by fewer short-wavelength photons than long-wavelength photons.

Thermal detectors will have a spectral response that depends directly on how the absorptance of the detector surface varies with wavelength, and this will usually be fairly flat over the spectral range for which the detector is designed.

4.3.8 FREQUENCY RESPONSE

This is a measure of how the amplitude of the output signal of a detector varies with the frequency of a radiant flux input that varies sinusoidally. All detectors will have a frequency response that falls to zero above a certain frequency.

4.3.9 TIME CONSTANT

This is related directly to frequency response and is an alternative way of measuring this particular characteristic of a detector. It is defined as the time taken for the signal to reach $(1 - e^{-1})$ of its maximum value after it receives a step radiant flux input, or for the signal to fall to e^{-1} of its maximum value after the input is shut off.

4.3.10 MODULATION TRANSFER FUNCTION (MTF)

This is a measure of the contribution of the detector to the imaging characteristics of a system, whether it is a system with a scanner or a staring array. MTF has been defined in Section 4.2.7 for a lens.

In the case of a detector the object is a real image projected onto the detector, but the image produced by the detector is in the form of an electrical signal. In this case, therefore, we can define the MTF as the ratio of the modulation of the signal output to the modulation of a radiant flux input that is a spatially varying 1D sinewave that is traversed across the detector. MTF is plotted as a function of the spatial frequency (usually measured in cycles/mm).

Where detectors are intended for use in a scanning system the modulation of the output signal is measured by scanning the radiant flux input across the detector. For staring arrays this is not necessary.

With a single-element detector the MTF is largely dependent on the shape of the element. For a rectangular or square detector with a width w in the scan direction and a uniform response over its area, the MTF is given by

$$\mathrm{MTF}(s) = |\sin(\pi.w.s)/(\pi.w.s)| \tag{4.17}$$

where s is spatial frequency in c/mm when w is measured in millimeters. The shape of the MTF curve is illustrated in Figure 4.10.

The MTF in the direction orthogonal to the scan direction will be given by the same equation, where w is now the dimension of the element orthogonal to the scan direction. There is, however, a complication when considering the effective MTF for this direction in the final image generated by a thermal imager using a scanner. This relates to the fact that the image is only sampled at intervals equal to the spacing of the scan lines. The effect of this undersampling and the associated problem of aliasing, and the image artifacts it can generate, are discussed in detail in Appendix B in relation to the MTF of a complete thermal imager.

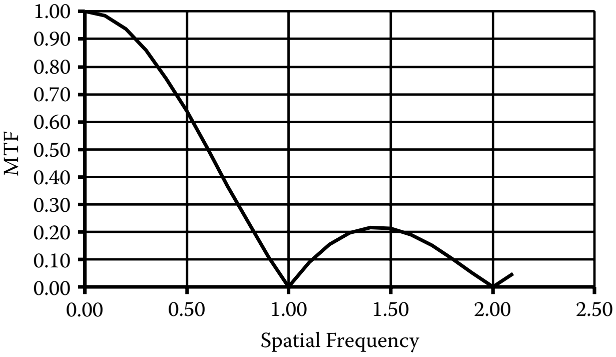

FIGURE 4.10 Theoretical MTF of a detector of unit width.

For multielement arrays used in the parallel scan mode (see Section 2.4.4), the MTFs will be the same as those given above when the elements are all in a single column. Where multielement arrays are used that include serial scan elements involving time delay and integration (TDI) (see Section 2.4.4), or where SPRITE detectors are used, the MTF in the scan direction can be more complicated. With TDI arrays the MTF will to a first approximation be given by Equation (4.17), but can be made worse by any mismatch between the delay line and the scan speed. The basic MTF of a SPRITE detector in the scan direction is largely determined by diffusion of the charge carriers as they move down the length of the detector, but will also be made worse by any mismatch between the scan speed and the speed at which the charge carriers move down the length of the element. For both detector types the MTF in the direction orthogonal to the scan direction will to a first approximation be given by Equation (4.17), but will include the effects of undersampling referred to above.

In principle, the MTF associated with a detector used in a scanning system will also depend on the scan rate if the signal frequencies generated by the image being scanned are in a frequency band where the frequency response of the detector is not flat. The effect can be predicted from knowledge of the frequency response, or time constant of the detector.

For staring arrays, the MTFs in the horizontal and vertical directions are again determined largely by the dimensions of the individual pixels and will be given by Equation (4.17). Because of the construction of such arrays there is usually a certain amount of cross talk between adjacent elements, and this will have the effect of reducing the MTF. The problem of undersampling now arises in both vertical and horizontal directions and is again dealt with in detail in Appendix B.

4.4 SCANNERS

4.4.1 Horizontal Scan Linearity

The relationship between time and the angular or linear position of the scan in the horizontal direction (assuming a normal TV-type raster scan is used) should be a linear one. Significant nonlinearity will usually result in some distortion of the image and a nonuniform response to temperature differences in the scene.

4.4.2 Vertical Scan Linearity

The relationship between time and the angular or linear position of the scan in the vertical direction should also be a linear one. Nonlinearity will result in an uneven spacing of scan lines as well as some distortion of the image.

4.4.3 Scan Judder

This refers to horizontal displacements between scan lines. The displacements can be of a regular nature, or random, depending on the mechanism that causes the effect. Judder will give rise to unwanted image artifacts as well as an effective drop in the MTF of the system.

4.5 DISPLAYS

4.5.1 General

Most thermal imagers, and in particular those intended for industrial use, have a display that is an inherent part of the imager. The display is usually either a small cathode ray tube (CRT) or liquid crystal display (LCD) screen viewed through an eyepiece, or an LCD screen viewed directly. Otherwise, or in addition, the image can be viewed on an external CRT or LCD video display. Images can also be transferred directly to a PC for viewing and processing. The performance parameters for different display types are basically the same, although their relative importance will vary both with the type of display and where and how they are used.

4.5.2 Maximum Luminance

This is a measure of how visually bright an image can be generated on a display. Luminance is measured with a photometer and is expressed in units of lumens m^{-2} steradian^{-1}. A relatively high luminance is most important when a display is viewed directly in high ambient light conditions.

4.5.3 Polar Luminance Distribution

This is a measure of how the apparent luminance of the display varies with the viewing angle and is usually normalized to unity for viewing perpendicular to the screen. This parameter is especially important when a display will be viewed from the side, e.g., when the same display is shared by two or more people, and can be a particular problem with some types of LCD.

4.5.4 Grey Scale/Linearity

A display should be capable of giving comparative information about the relative temperature differences of objects within the observed scene; i.e., equal steps in temperature should appear to the observer as equal steps in brightness. The typical relationship between video signal input and luminance output is illustrated in Figure 4.11 (the curve is sometimes referred to as a signal transfer function curve, or SiTF). There are generally three regions of the curve: an initial region where there is a relatively low response to the input signal, a region where the response is more or less linear, and finally, a high-luminance region where saturation comes into play. The shape of this curve will have an important bearing on the quality of the image that is presented to the observer. If the initial low-response region is too extended, detail will be lost in the colder parts of the thermal image, while the region where saturation occurs represents the maximum luminance that can be displayed in the image.

It may sometimes be desirable to intentionally make the linear part of the SiTF curve nonlinear since this can alter the appearance of the image in a manner that helps the user.

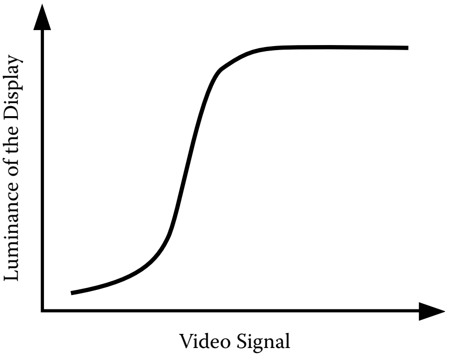

FIGURE 4.11 Typical SiTF curve for a display.

Where color displays are used in conjunction with color coding of temperature differences, the significance of this type of linearity is minimal.

4.5.5 MTF

This is a measure of the quality of the image that the display can generate, in the sense of reproducing image detail with good contrast, etc. The definition of MTF, given by Equation (4.11), applies equally to displays.

The MTF of a display should be better than, or at worst match, the MTF of the remainder of the thermal imager system if the performance of the latter (usually the more expensive part) is not to be wasted.

It should be noted that in principle the slow response of a display (e.g., due to a phosphor screen with a long decay time) can reduce the effective MTF for moving objects. The relevant MTF is usually referred to as the DMTF (dynamic MTF—see Williams[1]), and if this is likely to be a problem, it can be assessed by measuring the response or decay time of the display.

Where the display includes an eyepiece or other optical system this should either be assessed as part of the display or its MTF measured separately.

The MTF of a display will not necessarily be the same over its full area, and the MTF may need to be measured both on-axis and at several other positions in the field. This applies principally to CRT displays. Displays such as LCDs, where the image is made up of an array of identical pixels, will usually have a uniform performance over their full field.

4.5.6 DISTORTION

In the same way as a lens can generate a distorted image (see Section 4.3), so can a display. In general, distortion is only likely to be of significance with CRT displays and not with displays made up of an array of identical pixels. However, with all types of displays viewed through an eyepiece, the latter can itself introduce distortion.

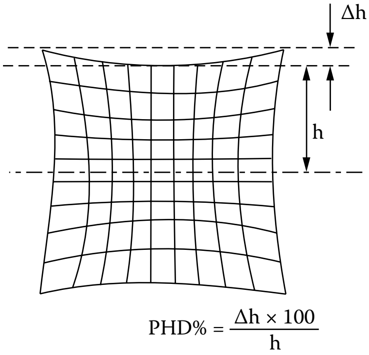

FIGURE 4.12 Picture height distortion.

As far as distortion measured directly on a flat display screen is concerned, it can be defined as

$$V = (\rho - \beta.S)/\rho \tag{4.18}$$

where ρ is the radial distance of the image point from the center of the field, S is the equivalent deflection voltage for the CRT (i.e., $S = \sqrt{(S_x^2 + S_y^2)}$, where S_x and S_y are the equivalent horizontal and vertical voltages), and the constant of proportionality $\beta = \lim(S \rightarrow 0)\ \rho/S$. One can replace β by an optimum constant of proportionality β' designed to minimize distortion over the full FOV rather than making it zero in the center of the FOV.

Levels of relative distortion of up to about 0.03 (i.e., 3%) are normally not noticeable, and larger amounts may be cosmetically acceptable.

In commercial television, distortion is often measured in terms of picture height distortion, as illustrated in Figure 4.12.[3] The latter is in fact related to the distortion as defined above, by the equation

$$\text{PHD} = 0.5[V(r) - V(H/2)] \tag{4.19}$$

where r is the radius of the format diagonal and H is the format height. The second term in this equation is small, and therefore to a close approximation:

$$\text{PHD} = V(r)/2 \tag{4.20}$$

4.5.7 VEILING GLARE

This is another name for unwanted stray light that does not contribute to image formation but merely reduces contrast. Some glare light may originate from the display device itself and can arise from multiple reflections in screens or windows, etc. In some instances, for example, in CRT displays, internal mechanisms such as scattering or secondary emission of electrons can also generate veiling glare. Usually the main cause of glare is reflection of ambient light from the display screen. Some displays have special screens that reduce this source of glare.

REFERENCES

1. Williams, T. L. 1999. *The optical transfer function of imaging systems*. Bristol and Philadelphia: IOP Publishing.
2. *ISO 9358: 1994 Optics and optical instruments; Veiling glare of image forming systems; Definitions and methods of measurement*.
3. *ISO 9039: 2008 Optics and photonics—Quality evaluation of optical systems—Determination of distortion*.
4. Keyes, R. J., ed. 1977. *Optical and infrared detectors*. Berlin: Springer-Verlag.

5 Performance Parameters for a Complete Thermal Imager

5.1 INTRODUCTION

This chapter describes the measurable parameters that are used to portray and determine the performance of a complete thermal imager. To a certain extent the parameters of importance will be different for different applications, and the relevance of each measure of performance will be related to the type of application. The differences largely depend on whether the application is one where measuring temperature is of fundamental importance, or whether the application is in a surveillance role where the ability to detect and recognize objects at long ranges is the aim.

Manufacturers of thermal imagers do not always provide the data that is relevant to the particular application of the thermal imager, or is in the best form to enable the user to assess the suitability of an imager for his or her particular use. This frequently is a result of their adopting performance parameters originally devised for evaluating an imager as a surveillance camera rather than a means of measuring temperature, or vice versa. The intention here is to make it clear which performance parameters are valid for which application, and to propose and define some new measures of performance where none have been established, but are nevertheless required. A supplier may not provide data for all the parameters defined here, but the user should request such additional data as is necessary to ensure that an imager will perform the tasks for which he or she will use it.

5.2 FACTORS AFFECTING PERFORMANCE

The two important parameters that affect the performance of an imager are the spatial resolution, as measured by the modulation transfer function (MTF), and the root mean square (RMS) noise (i.e., the random output signal fluctuations), as measured by the noise-equivalent temperature difference (NETD, sometimes written as NEΔT). The NETD is the scene temperature difference that would produce a difference signal equal to the RMS noise signal. The MTF determines the luminance difference (with respect to the background) in the image of a particular object, and the NETD determines the amplitude of the luminance fluctuations that are superimposed on the image. If the noise is too great relative to the luminance difference generated by the object, it will not be possible to detect or recognize the object in the thermal image (see Figure 5.1). When temperature measurement is the primary concern, these two parameters will determine the smallest temperature difference that can be resolved, as a function of object size. Where surveillance is concerned,

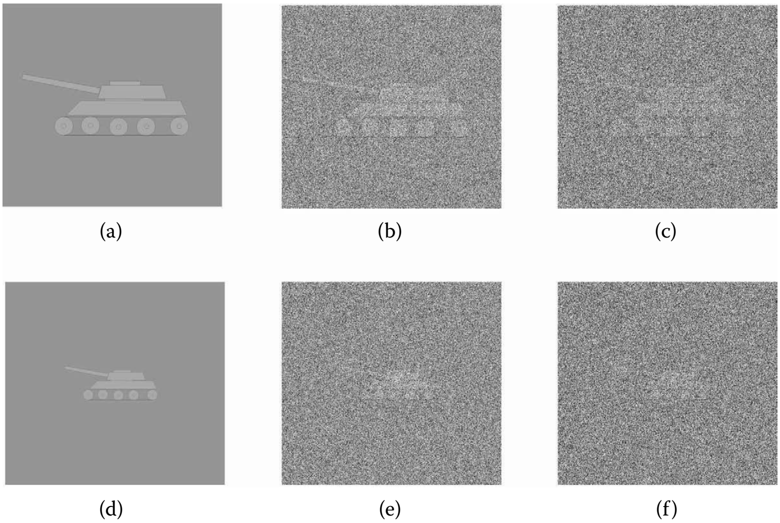

FIGURE 5.1 Examples of how size and noise affect the ability to detect and recognize a target. (a) to (c) are the same size, and so are (d) to (f).

they will determine the range at which a specific object (i.e., an object of given size and temperature difference with respect to the background) can be detected and the range at which it can be recognized.

For absolute temperature measurement with an imager it is important that the imager has a built-in absolute temperature reference and that the system responds linearly to temperature. For surveillance purposes this is not necessary, as the main concern here is to optimize the ability to see temperature difference.

In the section below we define and describe some of the measures of performance relevant to one or both of these applications. Some of these measures are not necessarily of primary interest to the general user of an imager since they are not direct indicators of the ultimate characteristics of the imager that concern him or her. However, they are all measures or parameters that are relevant to the ultimate performance of an imager.

Although the aim here is to deal with complete imaging systems, which in principle would include the display, it is customary for many performance parameters to exclude the latter and to make measurements at the video signal output. There are several reasons for this, one of which is that most of the critical data provided by the imager (e.g., temperature values) is determined by processing the video signal so that in fact the display plays no part in the quality of this data. In addition to this, several different types or forms of display can be used with the same imager, and this introduces variables that are not inherent to the imager and are frequently the choice of the user; moreover, some types of measurement are easier to make on the video signal rather than off the display screen. However, if the task at hand relies on an observer viewing the image generated on the display, it is important that the display be included in any relevant measurement. For example, many surveillance applications rely on an observer viewing the display, and the effect of the display is then important. In some applications the image is processed in, say, a PC as a video signal (e.g., to determine the temperature of a particular object), and the contribution of the display is again irrelevant.

5.3 PERFORMANCE PARAMETERS

5.3.1 MTF

The MTF of a complete imager (see Section 4.2.7 for a definition of MTF) is basically the product of the MTFs of the subunits that make up the system, and would therefore be the product of the MTFs of the lens system, the detector, the processing electronics, and the display (see Figure 5.2). As indicated above, it is possible to measure the MTF at the video output and leave out the display, and this may be a requirement for some applications. It is, of course, also possible to include the display in the measurement train.

The MTF will in general vary with target orientation and with position in the field of view, and as indicated for lenses in Chapter 4, it is usual to measure the MTF for the radial and tangential orientations and for two or more field positions either side of the axis as well as on-axis.

We note here that where aliasing is present in an imager, special methods are required to measure a unique MTF (see Appendix B and Chapter 8).

5.3.2 Nyquist Limit

In principle this is the maximum spatial frequency of sinewave that the imager can resolve, as governed by the spacing of detector elements or scan lines. In order to resolve a sinewave pattern, it must be sampled at points that are closer than half the period of the sinewave. The Nyquist limit is therefore the frequency corresponding to a period equal to half the spacing of the sampling points, i.e.,

$$\text{Nyquist frequency} = s_{\text{Nyq}} = 1/(2.p) \tag{5.1}$$

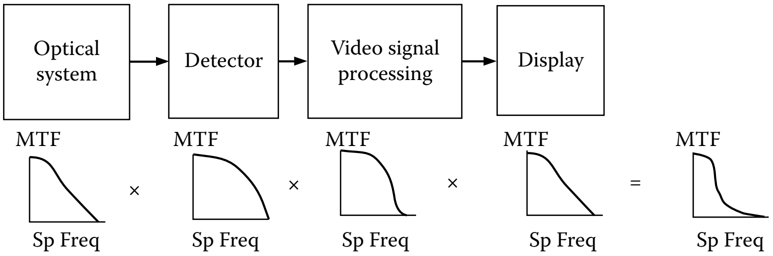

FIGURE 5.2 MTF of the thermal imager is the product of the MTFs of the units that make up the imager.

where p is the spacing between sampling points. In a normal scanning system there is effectively no limit in the line direction, but perpendicular to the line direction the limit will be given by Equation (5.1), where p is the spacing between lines. In a system involving some form of parallel scan (i.e., a vertical line of detectors) the vertical spacing of the detectors will also be the line spacing. In staring arrays the Nyquist limit will be given by making p equal to the spacing of the detector elements, and in this case, the limit will apply in both the horizontal and vertical directions.

5.3.3 ALIASING

The most obvious external signs of aliasing are the moiré fringes that appear when imaging certain regular patterns. It is a well-known phenomenon on broadcast television when the scene contains regular patterns such as the weave in clothing. Aliasing occurs when and where the scene contains spatial frequencies greater than the Nyquist limit, and when the combined MTF of the optical system and the detector is greater than zero at spatial frequencies above the Nyquist limit. Under these conditions the spatial frequencies above the Nyquist limit are reproduced in the image as spatial frequencies below the Nyquist limit (see Appendix B). Even when there are no obvious effects, such as the presence of moiré patterns, aliasing will introduce noise-like artifacts in the image.

If aliasing is present, one finds that techniques for measuring MTF that use, for instance, slit targets do not yield a unique MTF. Instead, the MTF varies over a range of values that depend on the exact position of the test target relative to the sampling array (see Figure 5.3).

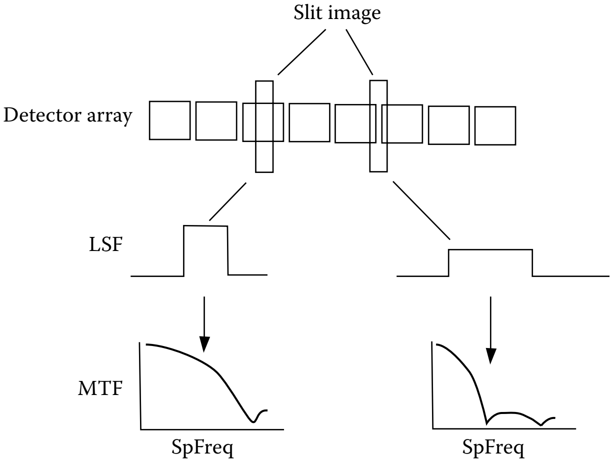

FIGURE 5.3 Illustration of how the MTF measured with a slit target can vary with the position of the slit.

© 2009 by Taylor & Francis Group, LLC

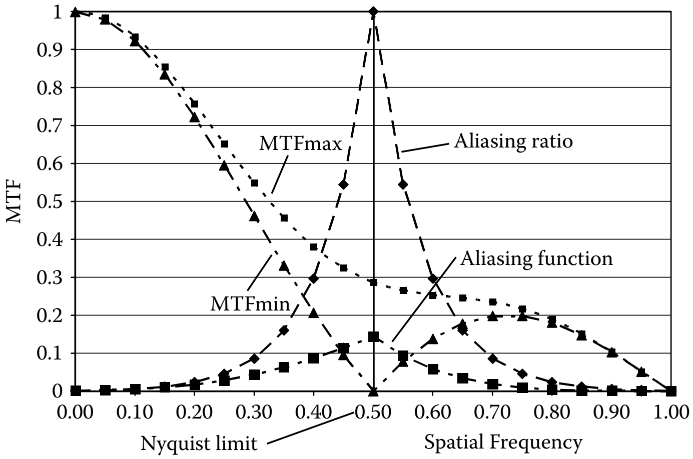

FIGURE 5.4 Measures of aliasing.

There are several measures of aliasing. The international standard ISO 15592[1] defines three of these:

Aliasing function: This is a curve that plots half the difference between the maximum and the minimum value of the MTF of the complete system, as a function of spatial frequency, measured using a narrow slit test target. It is a measure of the degree to which the system will respond to spatial frequencies higher than the Nyquist frequency, and as a result generate spurious low frequencies in the image (see Figure 5.4).

Aliasing ratio: This is a curve that plots the ratio of the aliasing function (as defined above) to the average value of the maximum and minimum MTFs, as a function of spatial frequency. It can be considered a measure of performance that relates to the inverse of a signal/noise ratio (see Figure 5.4).

Aliasing potential: This is the ratio of the area under the combined MTF of the image-forming optical system and the sampling array (but not including the MTF of any further processing) beyond the Nyquist limit, to the area up to the Nyquist limit. It is a measure of the potential the system has for generating aliasing.

A fuller discussion of aliasing will be found in Appendix B and Chapter 7, which deals with its measurements in relation to the measurement of MTF.

5.3.4 SIGNAL TRANSFER FUNCTION (SITF)

The SiTF is the relationship between output signal and the corresponding scene temperature difference. A typical SiTF curve is illustrated in Figure 5.5. For most systems it will be linear up to a temperature difference where signal saturation occurs.

© 2009 by Taylor & Francis Group, LLC

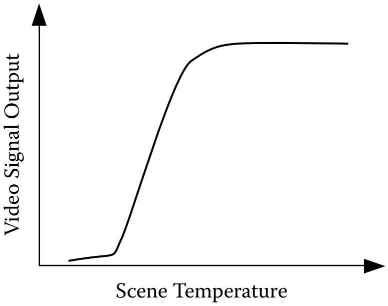

FIGURE 5.5 Typical SiTF curve.

SiTF can represent the relationship between scene temperature difference and either the video signal output or the luminance on the display, although it is often usually the former.

5.3.5 Noise-Equivalent Temperature Difference (NETD)

This is defined as the scene temperature difference that generates a signal equal to the RMS noise. Both signals must be measured at the same output, i.e., at the video output or off the display screen. Unless otherwise specified, NETD is usually measured at the video output.

The value obtained for the NEDT of a thermal imager will of course depend on the exact camera settings under which it is measured. Most important is the *f*/number setting for the lens system. This should therefore be specified. If it is not, one can usually assume that it is measured for the lowest *f*/number setting (i.e., the largest aperture) of the lens system, where this is adjustable, or the fixed setting, where it is not adjustable. In cameras where the user has a choice of lenses it is normally assumed that unless otherwise specified, the quoted NETD is for a lens with an aperture of *f*/1.

5.3.6 Minimum Resolvable Temperature Difference (MRTD): The Johnson Criterion

Johnson[2] made a series of contrast threshold measurements with image intensifier sights using images of objects such as tanks, jeeps, howitzer guns, soldiers, etc. He compared these with the threshold contrast levels for periodic patterns viewed through the same instruments and found a correlation between the ability to perform specified tasks (such as detecting or identifying a target) and the ability to resolve a periodic pattern that extended over the minimum dimension of the target and had the same contrast as the target. The number of bars required in the periodic pattern was a function of the task to be performed (see Figure 5.6). The results of his comparison are summarized in Table 5.1.

© 2009 by Taylor & Francis Group, LLC

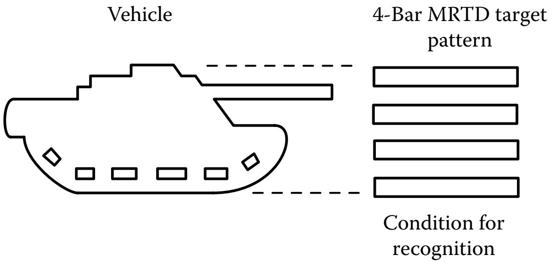

FIGURE 5.6 The Johnson criterion for recognition of a target (tank).

These experiments form the basis of the MRTD criterion that is used as one measure of performance for thermal imagers. A four-bar target with an equal mark-to-space ratio and a bar length equal to 3.5 bar periods is used (see Figure 5.7). Measurements are made with a range of targets of different spatial frequency, and for each target the MRTD is the smallest temperature difference between bars and background that enables the four bars of the target to be just resolved. The results are usually plotted as a curve of MRTD versus spatial frequency, as shown in Figure 5.7. An important aspect of measuring MRTD is that the observer is required to adjust the distance at which he or she views each target in order to optimize his ability to resolve the bars.

MRTD is assumed to relate to the ability to recognize a target (i.e., tell the difference between a tank and a jeep) so that in principle an MRTD curve allows one to predict the range at which a target will be recognized. If we know the small dimension of the target and its temperature difference with respect to the background,

TABLE 5.1
Results of the Correlation between Threshold Tasks for Selected Targets and the Ability to Resolve Periodic Bar Patterns

Target	**Number of Bars per Minimum Dimension**			
Broadside View	**Detection**	**Orientation**	**Recognition**	**Identification**
Truck	0.90	1.25	4.5	8.0
M-48 tank	.75	1.2	3.5	7.0
Stalin tank	.75	1.2	3.3	6.0
Centurion tank	.75	1.2	3.5	6.0
Half-track	1.0	1.50	4.0	5.0
Jeep	1.2	1.50	4.5	5.5
Command car	1.2	1.5	4.3	5.5
Soldier (standing)	1.5	1.8	3.8	8.0
105 howitzer	1.0	1.5	4.8	6.0
Average	1.0 ± 0.25	1.4 ± 0.35	4.0 ± 0.8	6.4 ± 1.5

© 2009 by Taylor & Francis Group, LLC

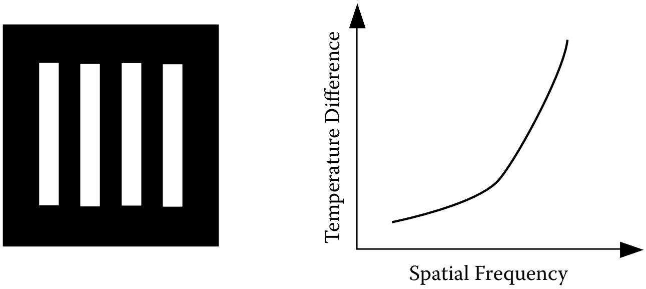

FIGURE 5.7 Typical four-bar MRTD target and an MRTD plot.

we can predict the range in the manner illustrated in Figure 5.8. The relationship between spatial frequency and range is given by

$$\text{Range} = 0.001s.h/3.5 \tag{5.2}$$

where the range is measured in meters, h is the minimum dimension of the target, also measured in meters, and s is spatial frequency in c/mrad.

We note that atmospheric attenuation will in fact reduce the effective temperature difference between target and background that the imager sees, and this should be taken into account for a more accurate range prediction.

If we assume that Beer's law holds, then the apparent temperature difference at a distance m is given by

$$\Delta T = \Delta T_0.e^{-k(\lambda).m} \tag{5.3}$$

where ΔT_0 is the temperature difference at the target and $k(\lambda)$ is a characteristic constant for a particular set of ambient conditions and a particular wavelength λ.

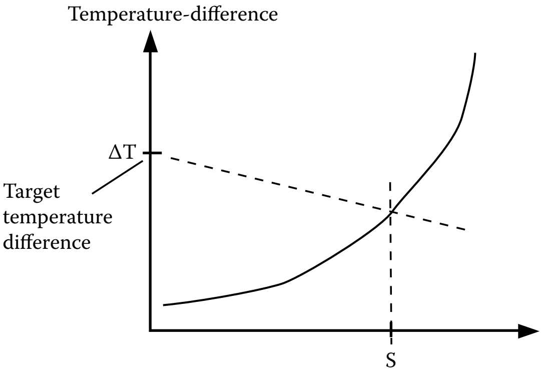

FIGURE 5.8 Determining range from the MRTD curve and the target ΔT and including the effects of atmospheric attenuation.

© 2009 by Taylor & Francis Group, LLC

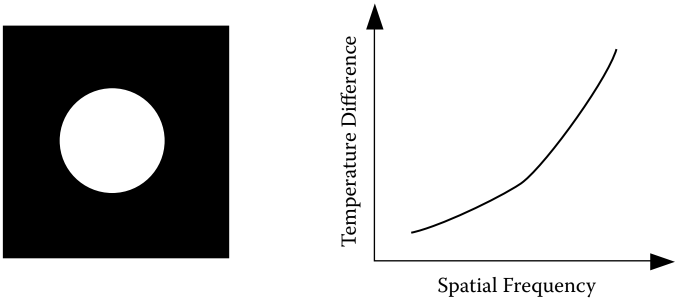

FIGURE 5.9 Typical MDTD target and an MDTD plot.

Commercial software is available* that allows one to compute values for $k(\lambda)$ for different ambient conditions.

MRTD is a measure of performance that is extremely relevant in a surveillance application, but its usefulness is questionable in applications where temperature measurement is a priority. Other parameters, such as SRF (slit response function), are of far greater use in this case.

5.3.7 Minimum Detectable Temperature Difference (MDTD)

This is similar to MRTD but uses a circular target instead of a four-bar target (see Figure 5.9). It relates to the ability to detect a target rather than recognize it. The shapes of the MRTD and MDTD curves are fundamentally different. The MRTD curve becomes asymptotic at a certain spatial frequency, reflecting the fact that there is a maximum spatial frequency that a system can resolve, however large the temperature difference. The MDTD curve is not asymptotic since in principle detection of a target should always be possible if it has a sufficiently large temperature difference with respect to the background.

MDTD can be used to predict the range at which a given target can be detected in the same way as MRTD is used to predict the recognition range. In this case the conversion from spatial frequency (i.e., the reciprocal of the MDTD target diameter) to range is given by

$$\text{Range} = 0.001 s.h \tag{5.4}$$

where again range and h are in meters and s is in c/mrad.

5.3.8 Objective MRTD

MRTD is to a large extent a subjective measurement, and results can vary significantly from one observer to the next. This variation can be minimized by training

---

* The ONTAR Corporation of North Andover, Massachusetts, produces a range of software for predicting transmission for different wavelength bands and atmospheric conditions.

© 2009 by Taylor & Francis Group, LLC

observers and by using more than one observer and averaging the results of their measurements. The concept of an objective MRTD is to replace this subjective measurement by an MRTD value that is calculated from objectively measured parameters using a suitable model for the performance of a human observer. The main parameters that determine the MRTD are the MTF of the system that determines the contrast with which the targets appear in the image, the RMS noise that influences the visibility of the image, and finally, the ability of the observer to resolve targets of different spatial frequency and contrast in the presence of noise. A model that can accurately predict performance under all circumstances could be very complex and, one can argue, is not in fact currently available. There are, however, several relatively simple models that produce a relatively good match to the subjectively measured MRTD. Two of these are described in this section, and one or the other, we propose, could be used by manufacturers, in particular where they wish to agree to a performance specification between themselves and a specific customer. The two methods are further divided in two, depending on whether the measurements are made directly on the video output from the thermal imager or off the display. These types of measurement will produce far more repeatable and reliable results than the subjective measurements. They can initially be compared with subjective measurements made on a representative sample of the imager in order to establish a constant of proportionality.

5.3.8.1 MRTD Model A (Video or Display)

In this model the video signal from the imager is captured in a frame store in a PC and appropriate software is used to measure the MTF, SiTF, NPS, and RMS noise. The procedures and the types of target required for measuring each of these parameters are described above. We note that for measuring MTF and SiTF the measurements should be made on the result of averaging several video frames together in order to improve accuracy. For the NPS and RMS noise each measurement should be made on single video frames (two successive frames being subtracted in order to remove the effects of a fixed pedestal, as well as fixed-pattern noise; see Section 7.4.3), but the results of many measurements should then be averaged together. The MTF should be measured for both the horizontal direction (i.e., a vertical slit) and the vertical direction (i.e., a horizontal slit).

This model is based on the premise that the target will just be resolved when the target temperature difference generates a target contrast that is equal to some fraction of the NETD and will be approximated by an equation of the form

$$\mathrm{MRTD}(s) = k.\mathrm{NETD}/\mathrm{contrast}(s) \tag{5.5}$$

The NETD is of course calculated from the RMS noise, NPS, and SiTF, while the contrast is calculated from the MTF of the imager. The constant k is a measure of signal/noise ratio required by an observer in order to just resolve a four-bar target. We note that k may be a function of spatial frequency s in cases where the observing distance is fixed (e.g., with an eyepiece display). Methods of computing MRTD using this approach are described in detail in Appendix A.

© 2009 by Taylor & Francis Group, LLC

5.3.8.2 MRTD Model B

The main difference between this approach and that described above is that the MRTD is based on measuring the target contrast directly rather than calculating it from the measured MTF. The target contrast is measured using a relatively large temperature difference, and on the basis that the contrast is linearly proportional to temperature difference, the temperature difference (i.e., the MRTD) that gives a contrast equal to k.NETD can be calculated from a measurement of the SiTF. The basic equation is the same as Equation (5.5), but the contrast is now given by the equation

$$\text{Contrast}(s) = C(s, \Delta T)/\Delta T \tag{5.6}$$

where $C(s, \Delta T)$ is the contrast in the image of the target when the temperature difference is ΔT.

The main concern with this approach is measuring the contrast in the image of the target, particularly at the higher values of s, where the contrast is very low even with relatively large values of ΔT. Some techniques for doing this are described in Appendix A. In practice the author has found this technique to yield results that agree very closely with subjective measurements, although it can be very difficult to obtain measurements for the higher spatial frequencies.

5.3.9 OBJECTIVE MDTD

The concept here is similar to that discussed above for objective MRTD. The model used for predicting MDTD from objectively measured parameters uses the same variables, but in a slightly different algorithm. This is a result of the difference between being able to recognize a target (i.e., resolve the bar pattern) and being able to detect the presence of a target.

The model is based on the premise that the target will just be detected when the target temperature difference generates an intensity in the image of the target that is equal to some fraction of the NETD and will be approximated by an equation of the form

$$\text{MDTD}(s) = k.\text{NETD}.\text{TR}(s) \tag{5.7}$$

where TR(s) is the ratio (actual target temperature difference)/(apparent target temperature difference) for a target of dimensions ($1/s$). Methods of computing MDTD using this approach are described in detail in Appendix A.

5.3.10 SLIT RESPONSE FUNCTION (SRF)

This is a measure of how the size of an object affects its apparent temperature when measured with a thermal imager. It is defined as the maximum video signal level in the image of a slit target (with a constant temperature difference with respect to the background), measured as a function of the width of the slit and normalized to the level for a very wide slit. A typical slit target and SRF curve are illustrated in Figure 5.10.

© 2009 by Taylor & Francis Group, LLC

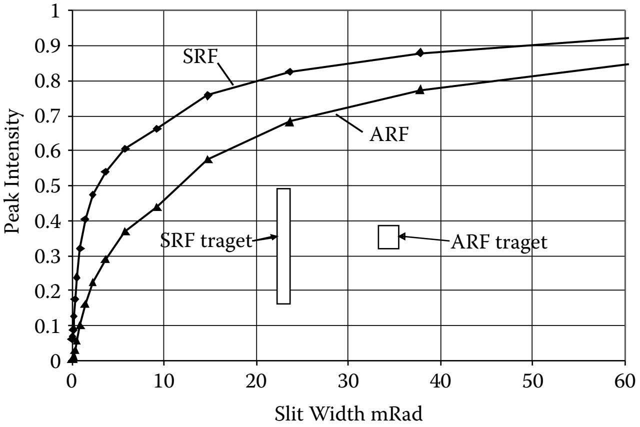

FIGURE 5.10 Theoretical SRF and ARF curves for a thermal imager with an *f*/2, 100 mm lens, and pixels with a 0.05 mm width and spacing.

The curve provides information about the magnitude of the errors in measurement of temperature that will arise with small objects and also provides an indication of the minimum width that an object must have to minimize this type of error. Strictly speaking, the SRF curve is only applicable for objects that approximate to slits.

The SRF can be predicted from the MTF of the system using the following equation:

$$\mathrm{SRF}(\theta) = \int [|\sin(\pi.\theta.s)/(\pi.\theta.s)|\,\mathrm{MTF}(s)].ds / \int |\sin(\pi.\theta.s)/(\pi.\theta.s)|\,ds \tag{5.8}$$

where θ is the angle subtended by the slit at the imager, s is spatial frequency (in the reciprocal units used for θ), and the integrations are over all values of s.[3]

5.3.11 APERTURE RESPONSE FUNCTION (ARF)

This is similar to SRF except that the target is a square aperture rather than a slit (see Figure 5.10). This will provide a better indication of temperature errors for objects that have similar dimensions vertically and horizontally, although it is a more difficult parameter to measure than SRF.

ARF can also be predicted from the MTF of the system and is given by

$$\mathrm{ARF}\,(\theta) = (\mathrm{SRF}(\theta))^2 \tag{5.9}$$

where θ is now the angle subtended by the width or height of the square aperture.

5.3.12 ABSOLUTE TEMPERATURE RANGE

A thermal imager designed for absolute measurement of temperature will have a range of temperatures, in the external scene, that can be accommodated within the linear

© 2009 by Taylor & Francis Group, LLC

range of the imager (i.e., without signal saturation occurring). The absolute temperature range should be specified in terms of the absolute minimum and absolute maximum temperature that the imager can measure. Most imagers will be designed to cover this full range in a number of smaller ranges, and these should also be specified.

Note that the absolute temperature range is directly related to the SiTF, and that both temperatures above and below ambient will normally be included in the range. In some cases the range may be specified relative to ambient temperature.

5.3.13 MAXIMUM AND MINIMUM TEMPERATURE DIFFERENCE RANGE AND OFFSET TEMPERATURE RANGE

For surveillance and other applications of an imager it is useful to be able to adjust the total temperature difference that can be accommodated in an image without saturation occurring, and also to be able to offset the mean value of the absolute temperature over which this temperature difference range is available. Adjusting the temperature difference range and the mean temperature over which this range exists allows the user to set the controls so that the full range of temperatures in the scene are accommodated without saturation and with maximum contrast. This parameter should define what these ranges are.

A similar facility is provided in imagers designed primarily for temperature measurement. However, in this case the actual temperature range over which the imager is operating will normally be one of the fixed ranges of the instrument, and the facility only adjusts the video signal going to the display to optimize the latter.

Here again note the direct relationship to SiTF.

5.3.14 TEMPERATURE MEASUREMENT UNCERTAINTY

This specifies the uncertainty in the value of a temperature measurement. It should include the effects of both random and nonrandom sources of uncertainty calculated in accordance with the ISO's *Guide to Expression of Uncertainty in Measurement (GUM)* (see also Birch[4]). The uncertainty can be specified as a temperature or as a percentage of the measured temperature. The maximum uncertainty for each measurement range should be specified.

5.3.15 EMISSIVITY RANGE

For true temperature measurement a correction must be applied to the apparent temperature of an object to allow for its emissivity. This should specify the range of emissivities that can be corrected as well as the smallest step change in emissivity that can be applied.

The correction for emissivity is normally achieved by multiplying the apparent temperature by the reciprocal of the emissivity. We note that correcting for emissivity in this way does not necessarily lead to a correct temperature measurement (see Section 3.2.2).

5.3.16 NARCISSUS

This is the dip in apparent scene temperature that occurs in some imagers, usually at the center of the image frame. It is measured as the actual maximum temperature

© 2009 by Taylor & Francis Group, LLC

difference that this effect produces when viewing a scene of uniform ambient temperature (the value of the latter should be specified). Narcissus is a special case of what more generally may be referred to as veiling glare (see next section). It is special in the sense that it usually produces a very visible effect in the image; however, where very accurate temperature measurement is concerned, it may still have an unwanted effect, even though it may not be obvious visually. Its main cause is one or more surfaces in the optical system (including any external plane windows) that in combination, or alone, reflect a nearly in-focus image of a very cold area of the image plane back on itself. The cold area is normally the cooled detector.

5.3.17 Veiling Glare Index (VGI) and Uniformity Index (VGUI)

Veiling glare is a term borrowed from visible wavelength optical systems and is a measure of the light that falls on the image plane, but is not image forming.[5,6] It arises from scatter in optical components, scatter and reflections from the edges of optical components and from the barrel and other mechanical parts of an optical system, multiple reflections in the optical system, light reflected from the image plane back to the camera body and the lens and then back to the image plane, etc. Similar effects will occur in a thermal imager, but provided the glare radiation is uniformly distributed over the image plane, the importance is relatively insignificant. The main reason for this is that the thermal image of interest is the result of relatively small variations in radiance that sit on a high background level that the imager has to ignore. A uniform veiling glare is simply a small perturbation on this background. A nonuniform glare distribution can in principle affect a temperature reading, but most importantly, it can limit the smallest temperature range that can be displayed without parts of the image reaching saturation.

The most straightforward means of assessing veiling glare that is relevant to thermal imagers is to measure the scene temperature uniformity when the imager sees a complete scene of uniform temperature. With the scene at ambient temperatures we define (for the purposes of this book) the largest measured temperature difference as the veiling glare uniformity index (VGUI). We note that this will include glare from the narcissus effect.

Methods of measuring the veiling glare index (VGI) of visible optical systems are described in ISO[5] and Williams.[6] They are not easy to implement in the case of a thermal image, but methods of doing this are described in Section 8.16.

5.3.18 Scene Influence Factor (SIF)

The temperature of all objects in an external scene can in principle affect the value of the measured temperature of a specific object in the scene. For a particular operating temperature range SIF is defined as the change in indicated temperature of a target in the center of the image, which is maintained at a temperature equal approximately to the mean of the range, as the temperature of the area surrounding the central target is changed from being the minimum temperature covered by the range to the maximum temperature covered by the range. The central target should have a diameter equal to ¼ of the width of the image. The indicated temperature of the target should

© 2009 by Taylor & Francis Group, LLC

be taken as that at the center of the target. SIF is expressed as a percentage of the average indicated temperature of the central target, i.e.,

$$\text{SIF\%} = 2(T_{\text{max}} - T_{\text{min}}).100/(T_{\text{max}} + T_{\text{min}}) \tag{5.10}$$

where T_{max} is the indicated temperature of the central target when the temperature of the surround is at the maximum of its range and T_{min} is the same temperature when the surround is at the minimum of the range. Where an imager has several set temperature ranges, a different value of SIF will be associated with each range.

5.3.19 Field of View (FOV)

The FOV is the angle subtended at the entrance aperture of the lens objective of a thermal imager by the total scene accommodated in the imager display. There will be a value for the horizontal FOV and the vertical FOV, although this can be expressed as the horizontal FOV together with the image aspect ratio (i.e., horizontal dimension:vertical dimension). Where the imager has a zoom lens, the FOVs for the two extremes of the zoom are required. Where the imager has a facility for switching between two or more FOVs, the FOVs for each switch position are required.

An alternative method of providing the same information when the imager uses a staring array is to quote the focal length(*s*) of the lens objective together with the vertical and horizontal dimensions of the sensitive area of the detector array. We then have (assuming the whole detector area is used):

$$\text{FOV} = 2.\tan^{-1}((\text{array dimension})/2(\text{focal length})) \tag{5.11}$$

5.3.20 Close Focus Distance

Normally all thermal imagers have the ability to focus on an object at infinity. The close focus distance is the shortest distance in front of the lens for which a sharp focus can be achieved. It is usually expressed in meters and is measured from the front surface of the lens objective to the close focus position.

5.3.21 Spectral Response

The full spectral response characteristics of an imager are given by a plot, or table, showing how the video signal output varies with the wavelength of the radiation from the source/target it is imaging. As indicated earlier, this information is normally provided in terms of the atmospheric window in which it is intended to operate (i.e., 3–5 μm, 8–12 μm, or 8–14 μm), or by the approximate cut-on and cut-off wavelengths that characterize its spectral response. However, there are situations where a true spectral response curve is required, particularly where measurements are made on sources/targets that have spectral characteristics that deviate significantly from the uniform characteristics of a blackbody and one may wish to use the performance data obtained using blackbody sources.

5.4 FRAME RATES AND READOUT TIMING

In some of the more advanced applications (see Chapter 10), it is important to have information about the maximum frame rates at which the imager can operate. In some imagers the use of higher frame rates is achieved by reducing the area of the array that is used, and hence reducing the field of view. Users should be aware that this and other techniques can change some of the performance parameters.[7] In some applications where, for instance, phase synchronous detection is used, the timings of the exposure and read-out stages in an imager may not be as straightforward as the user may assume.[7] In fact, in most uncooled arrays the exposure period is very short compared with the readout period.

5.5 OTHER FACTORS

In considering the suitability of a thermal imager for a given application there are several other factors that can affect one's choice (see also Section 3.6). Very briefly some of these are as follows:

- Size and weight, including any associated items of equipment, such as separate displays, computers, cylinders of dry nitrogen, etc.
- Is it designed to be handheld or supported on a tripod?
- Is it mains driven or battery driven?
- If mains driven, how convenient are the voltage and current requirements? If additional voltage conversion units are required, these could present a problem.
- If battery driven, the type (i.e., rechargeable or not) and general availability as well as the operational duration.
- If the detector is bulk cooled or cooled with a Joule–Thomson cooler, what are the associated logistical problems? (E.g., How long does the Dewar last before having to be refilled? How long will a cylinder of dry nitrogen last with a Joule–Thomson cooler? Is liquid nitrogen readily available?)

REFERENCES

1. *ISO 15529: 2007 Optics and photonics—Optical transfer function—Principles of measurement of modulation transfer function (MTF) of sampled imaging systems.*
2. Johnson, J. 1958. Paper presented at Image Intensifier Symposium, Fort Belvoir. Results summarized in Chapter 1 of Biberman, L. M. 1973. *Perception of displayed information*. New York: Plenum Press.
3. Williams, T. L. 1992. The MFT of thermal imaging cameras. Its relevance and measurement. In *Proceedings of the QIRT Conference*, No. 27, pp. 51–56.
4. Birch, K. 2001. *Estimating uncertainties in testing*. Measurement Good Practice Guide 36. Teddington, UK: National Physical Laboratory.
5. *ISO 9358: 1994 Optics and optical instruments; Veiling glare of image-forming systems; Definitions and methods of measurement.*
6. Williams, T. L. 1999. *The optical transfer function of imaging systems*. Bristol and Philadelphia: IOP Publishing.
7. Pron, H., et al. 2002. Focal plane array infrared cameras as research tools. *QIRT Journal* 1:229–40.

6 Basic Equipment for Testing and Calibrating at Thermal Wavelengths

6.1 INTRODUCTION

The basic items of equipment, such as sources of radiation, optical materials, etc., used at thermal wavelengths generally differ from those used at the shorter visible and near-infrared (IR) wavelengths. This chapter lists and describes some of the devices and instruments that can be used for making measurements at these wavelengths and outline some of the special experimental techniques that must be used.

A major factor that differentiates measurement techniques at thermal wavelengths from those made at shorter wavelengths is that at ambient temperatures all objects are radiating large amounts of thermal radiation, whereas virtually no radiation is emitted at visible and near-infrared wavelengths. The primary result of this is that in order to distinguish the radiation from a specific source from other ambient radiation, the former needs to be modulated and any system intended to detect this radiation must be designed to respond only to this modulated radiation.

The need to modulate the radiation brings with it certain advantages associated in particular with processing of the signals from the detectors used to measure the radiation. For example, alternating current (ac) preamplifiers can be used to amplify the signal from the detectors, while narrowband electrical filters, in conjunction with phase-sensitive detection circuits, will greatly reduce noise levels. The basic components of an arrangement for making measurements in the thermal IR are illustrated in Figure 6.1.

Another important consideration in making measurements in this region of the spectrum is the relative ease with which a radiation source of known characteristics can be created. We refer here to what is known as a blackbody source (or just a blackbody). This usually takes the form of a heated cavity whose temperature is accurately controlled. However, it can take other forms (see Section 6.2.6). The important properties of a blackbody are that it has an emissivity of close to unity over the appropriate spectral range and that its temperature is known. Under those conditions the radiation it emits is accurately predicted by Planck's equation (see Section 1.2).

6.2 RADIATION SOURCES

6.2.1 TUNGSTEN FILAMENT LAMPS

Traditional light sources such as tungsten filament lamps are not suitable as intense sources of radiation in the thermal infrared bands largely because the normal glass envelopes do not transmit infrared radiation. The glass envelopes themselves emit

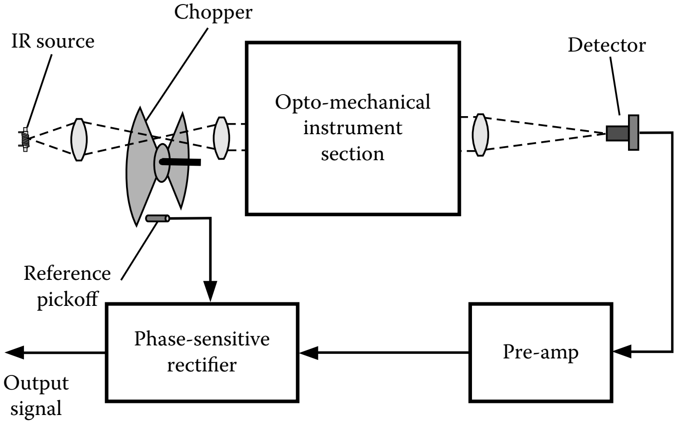

FIGURE 6.1 Typical IR measurement system.

some radiation, but because of their relatively low temperature compared with that of the filament, they constitute a very weak infrared source. It is, of course, possible to use lamps with envelopes that do transmit at least some infrared, and examples of this are the quartz halogen lamps. Quartz transmits out to approximately 4 μm, so such lamps can only just be useful at the very short end of the thermal spectrum. However, the envelopes of quartz halogen lamps do run at a higher temperature than normal glass envelopes and are therefore slightly more useful as infrared sources.

Another approach is to either weld a window of a transmitting material onto the glass envelope or make a sealable enclosure for the tungsten filament that is fitted with a transmitting window and is suitably evacuated or filled with an inert gas. The first of these options is somewhat limited since the window must be of a material that can be welded to a normal glass envelope. None of the materials that transmit in the 8–14 μm band are suitable for this purpose. In the 3–5 μm band it is possible to use sapphire (Al_2O_3), or periclase (MgO). The author has used old-style car head lamp bulbs fitted with sapphire windows as sources for the 3–5 μm band, but these were specially made by a skilled glass blower.

The second option has in principle no limitations, but would require careful design to deal in particular with problems of temperature. One should note that the emissivity of tungsten is relatively low at these wavelengths, being approximately 10 to 15% at typical filament temperatures. However, the effective emissivity will be somewhat greater than this as a result of the normal geometry of a coiled filament.

6.2.2 NICHROME WIRE OR STRIP SOURCES

Nichrome wire can be heated to approximately 1,100K in air (exact temperature will depend on the other constituents of the wire) without severe oxidization and can be used either on its own, in the form of a flat strip, or wound around a ceramic former,

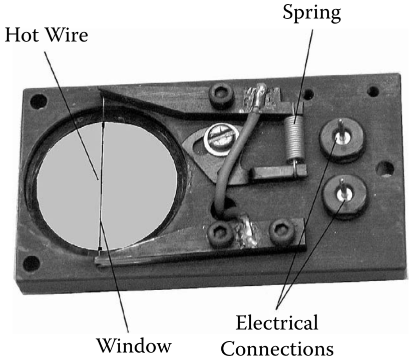

FIGURE 6.2 Hot-wire IR source.

as a very convenient source of thermal radiation in both the 3–5 and 8–14 μm bands. On its own, nichrome wire has proved useful as a line source for spectrophotometers and in equipment for testing infrared lenses and complete thermal imagers. Such sources have been used extensively by the author in place of an illuminated slit, in equipment for measuring the MTF and other parameters of infrared optical systems.[1] A photograph of such an arrangement that uses a spring-loaded lever to keep the wire stretched as it is heated is shown in Figure 6.2. Simpler arrangements, more specifically for use in spectrophotometers, are available commercially.

The great advantage of using plain nichrome wire as a line source, in addition to its simplicity, is the relatively low heat generated in comparison with an arrangement where a larger source is imaged onto a slit.

With the sources that consist of wire wound around a ceramic former, the ceramic is heated and also acts as part of the source of radiation. Several different shapes and sizes of this type of source are available commercially and are now widely used in infrared spectrophotometers. These sources usually have a significantly higher emissivity than pure wire or thin-film sources. Devices are available commercially with integral reflectors.

Generally speaking, sources based on the use of nichrome wire, or strip, are one of the most useful forms of infrared source. This is a result of their simplicity, long life, relatively low power requirements, and high radiation output. Nichrome wire sources on their own typically have emissivities of the order of 40% to 60%, with higher emissivities of the order of 70% to 90% when in the form of wire wound around a ceramic former.

6.2.3 NERNST GLOWER

This is one of the earliest forms of infrared source and was used particularly in spectrophotometers. It is made of a ceramic-like mix of alkali halides, which has to be heated above a certain temperature before its electrical resistance is such that it can be heated directly by passing a current through it. It is one of the best sources of infrared radiation from the point of view that it has a very high emissivity and runs at a temperature of approximately 2,100K. However, it is fragile, has a short lifetime, and requires a relatively complex arrangement to power it because of the need to heat it before it will run normally.

New forms of ceramic sources have been developed that have properties similar to those of the original Nernst glowers, but do not require preheating to function. Such sources are available commercially.

6.2.4 Globar (SiC/Carborundum Rod)

Silicon carbide, otherwise referred to as carborundum, in the form of rods, has been widely used as an infrared source. These rods have a relatively good emissivity (of the order of 60% to 80%) and can run at temperatures of the order of 1,500K. They tend to be brittle and easily broken, but their main disadvantage is the very large current they require to run. However, they generally have a large emitting area and are particularly useful where this is a requirement.

6.2.5 Opperman Source

Named after its designer, Kurt Opperman, this source consists of a ceramic tube with an internal platinum/rhodium heater. In this respect it is similar in principle to some of the sources described in Section 6.2.2 that comprise a heated ceramic rod.

6.2.6 Blackbody

Blackbody sources are used primarily for calibration purposes where a source of accurately known radiance is required. They are also useful where a high emissivity and very uniform area source is a requirement.

A blackbody needs to have a very high emissivity (e.g., >99%) and a very uniform temperature over its working area if it is being used for calibration purposes. Its effective temperature must also be accurately known so that its radiance can be predicted from Planck's equation (see Section 1.2). Blackbodies typically take the form of a uniformly heated or cooled cavity, with the internal surface of the cavity itself having a high emissivity, and with one or more temperature sensors that effectively measure the temperature of the surface of the cavity. The purpose of using a cavity is to increase the effective emissivity beyond that which can be achieved simply by the finish on the heated or cooled surface. The shape of the cavity is important, and some typical shapes for blackbody cavities are illustrated in Figure 6.3 (e.g., see Prokhorov[2] for information on

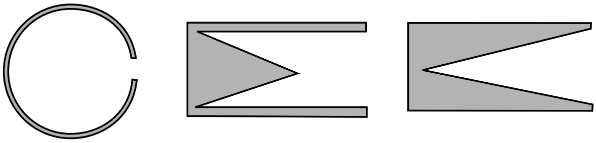

FIGURE 6.3 Typical blackbody cavity shapes.

the modern approach to design of blackbody cavities). Heating can be achieved electrically using resistive heating and cooling and heating by means of thermoelectric (Peltier effect) devices, or by circulating a liquid around the cavity from a temperature-controlled fluid bath.

Electrically heated blackbodies are readily available commercially that go to temperatures as high as 1,500K. More specialized units are available that can achieve temperatures as high as 3,000K and can be used for calibration at visible and near-infrared wavelengths. However, these may need special facilities to operate.

For blackbodies that operate at temperatures below ambient, precautions may be necessary to prevent not only condensation but also the formation of frost and ice. One way of overcoming this is to purge the cavity with dry nitrogen that has been cooled to approximately the same temperature as the cavity. In one system designed and used by the author for achieving temperatures below −40°C the cavity was cooled by immersion in a bath through which an alcohol/water mixture from a temperature-controlled water bath was circulated. The dry nitrogen was cooled by passing it through a copper tube coil in the same bath before going into the cavity.

Blackbodies are used to provide not only a calibrated source of radiance but also calibrated sources of irradiance. In the latter case they are used with very precisely measured apertures positioned in front of the output port. Blackbodies are available commercially with turret wheels containing a number of different diameter apertures.

6.2.7 High-Emissivity Plates

In many systems where large-area uniform sources are required it is convenient to use a plate that has a surface with a high emissivity, rather than using a blackbody cavity. Uniformity of temperature is obtained by making the plate from a material such as copper or aluminum that has a high thermal conductivity. Heating and cooling can be achieved by the use of thermoelectric devices, or pipes circulated with liquids from a temperature-controlled bath, or simply by attaching a number of high-wattage resistors to the back of the plate.

Several proprietary paints and chemical finishes are available commercially for producing a surface with a high emissivity. Note that the emissivity of the surface can also be improved by giving the surface a V groove structure.

The use of high-emissivity plates rather than blackbody cavities allows one not only to produce a large-area uniform source without the bulk associated with a cavity, but also, more importantly, to design sources with a relatively fast response to a demand in temperature change (for example, see Williams[3]).

6.2.8 Modulated IR Sources

In many applications an IR source is required that can be pulsed or modulated. This can be achieved very efficiently by using a mechanical chopper, particularly when one needs to modulate a relatively large source. However, several small sources have been developed that can be modulated or pulsed by modulating or pulsing the current that drives them. These are usually made up of very thin metal films with a low heat capacity, which can therefore be very rapidly heated by the electric current.

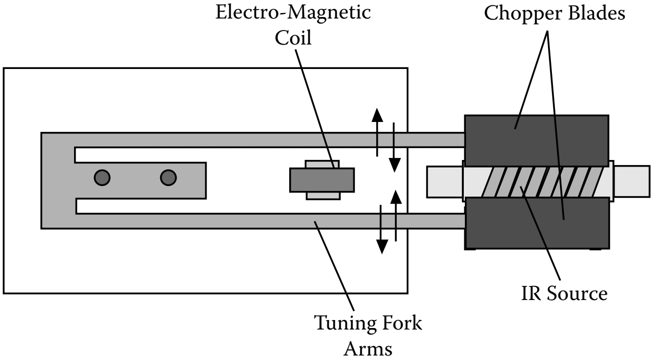

FIGURE 6.4 Example of a tuning fork chopper.

Many of the commercial devices are built into standard transistor cans and can be modulated at frequencies as high as 100 Hz.

Another approach to producing a small source that can be modulated is to use a small-diameter ceramic rod with a nichrome wire wound around it, positioned immediately behind a tuning fork chopper (see Figure 6.4).

6.2.9 Laser, Laser Diode, and LED Sources

The main gas lasers operating at wavelengths in the thermal band are the following:

- Helium-neon (HeNe) operating at a wavelength of 3.39 μm
- Carbon monoxide (CO) operating at a wavelength in the range 5.5–6.0 μm
- Carbon dioxide (CO_2) operating at a wavelength in the range 9.0–11.0 μm (normally run at a wavelength of 10.6 μm)

From the point of view of testing thermal imagers, most of these lasers are primarily useful as coherent sources in interferometers for testing lenses and windows.

A number of laser diodes are also available for the thermal band, some of which are designed to be tunable over a range of wavelengths. They are mainly of two types, lead salt or quantum cascade. The former generate very narrowband radiation but require cooling to liquid nitrogen temperatures, or even lower temperatures for the longer wavelengths. The latter will operate at temperatures generated by Peltier coolers, but are normally run in pulsed mode.

Light-emitting diodes (LEDs) are also available that generate radiation in the thermal band. These can be operated in either continuous wave (CW) or pulsed mode and generate radiation with full width half height (FWHH) of the order of 10% of the central wavelength.

The characteristics and properties of gas lasers, laser diodes, and LEDs vary considerably, and for more information, prospective users should consult the manufacturer's literature.

6.3 INFRARED DETECTORS

Detectors of thermal radiation will form part of some types of equipment for testing particular components of a thermal imager. These will frequently consist of a single element but may also be 1D or 2D arrays. For a description of the range of available detectors see Section 2.5.

6.4 COOLING DETECTORS

Methods of cooling detectors are described in Section 2.6. We note here that using detectors mounted in vacuum Dewars that are filled with liquid nitrogen is a very convenient technique for laboratory equipment, although not so convenient for a portable thermal imager.

6.5 OPTICAL SYSTEMS AND COLLIMATORS

6.5.1 General

The optical materials available for making lenses, prisms, etc., that can be used in the thermal band have been described in Section 2.2. These are also the materials used in test equipment, although the actual lens designs may be different, depending on the particular application.

6.5.2 Off-Axis Paraboloid Collimators

One of the important components of some test facilities is a collimator. This is an optical system that is interposed between a test target and the test piece to make the former appear to be at infinity. In most applications the collimator needs to be effectively free from any optical aberrations, usually referred to as being diffraction limited. In many applications an off-axis section of a parabolic mirror (usually referred to as an off-axis paraboloid) is used as a collimator (see Figure 6.5). In principle, a parabola, provided it is made correctly, is free of optical aberrations for a point at its on-axis focus. However,

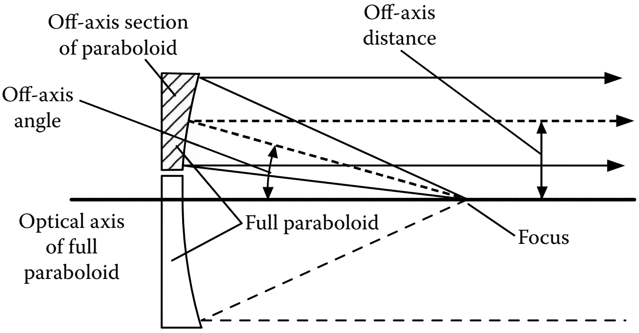
Off-axis section of paraboloid
Off-axis distance
Off-axis angle
Optical axis of full paraboloid
Full paraboloid
Focus

FIGURE 6.5 Off-axis paraboloid collimator.

once one moves off-axis away from this position, aberrations appear that get greater the further off-axis one goes. When using such a collimator it is very important that the test target be correctly positioned at the on-axis focus, and that when using an extended (e.g., a four-bar minimum resolvable temperature difference [MRTD] target), the aberrations that will be present over the outer parts of the test target are compatible with the resolution requirements of the test facility.

The position of the on-axis focus of an off-axis paraboloid is usually specified by the manufacturer in terms of the actual focal length of the collimator and the off-axis distance. The latter is the distance between the central optical axis of the collimated beam and the on-axis focus (see Figure 6.5). The user should beware, however, since some manufacturers refer to the distance from the outer edge of the mirror to the on-axis focus as the off-axis distance. Rather than specifying the off-axis distance manufacturers may quote the off-axis angle. This is the angle between the ray of light that goes from the on-axis focus to the center of the mirror and its reflection off the mirror (see Figure 6.5).

Although the aberrations of an off-axis paraboloid are zero when it is being used at the on-axis focus, the aberrations will increase as one goes off-axis (i.e., away from this position). The rate at which these increase will depend on the *f*/number (i.e., the ratio of the focal length to the diameter) and the off-axis angle, and these should be optimized for the particular application. For very small test targets the diameter of the collimator needs only be slightly larger than the aperture of the test piece; however, for extended targets the diameter must be sufficiently large that radiation from the edge of the target will still fill the aperture of the test piece (see Figure 6.6), i.e., no vignetting should occur. In most test configurations this usually implies that the diameter of the collimator must be slightly larger than the combined diameters of the test target and the test piece aperture. The choice of focal length will depend on several factors, including the path length that can be accommodated within a reasonable

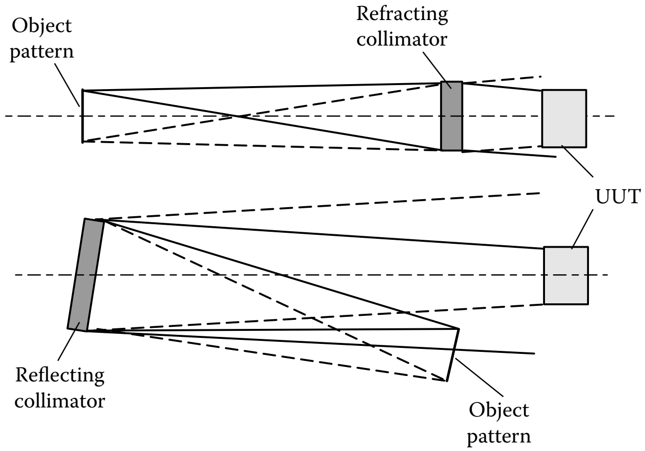

FIGURE 6.6 Comparison of relative diameters of a refracting and a reflecting collimator with a finite-size object pattern.

size for the equipment (optical paths can be folded using plane mirrors), the dimension and properties of the test target(s), the range of spatial resolutions that must be covered, and finally, the acceptable optical aberrations over the extent of the test target dimensions. The off-axis angle or off-axis distance should be kept to a minimum compatible with an optical arrangement that will not obstruct the light paths. Note that Section 9.2 describes methods of focusing and aligning collimators.

To demonstrate the process involved in the choice of parameters we take as an example the case of a collimator for use in a system for measuring the MRTD of a thermal imager with an entrance pupil diameter of 150 mm. The requirement is to measure MRTD over a spatial frequency range of 0.2 to 4 c/mrad. If we assume that the smallest practical width for one bar of a four-bar target is 0.2 mm, then the focal length of the collimator must be greater than

$$\begin{aligned} f &= (\text{spatial freqency in c/mrad}) \times 1{,}000 \times (\text{bar width}) \times 2 \\ &= 4 \times 1{,}000 \times 0.2 \times 2 = 1{,}600 \text{ mm} \end{aligned} \tag{6.1}$$

The width and height of the largest target will be given by

$$\begin{aligned} w &= 3.5 \times f/([\text{spatial frequency in c/mrad}]) \times 1{,}000) \\ &= 3.5 \times 1{,}600/(0.2 \times 1{,}000) = 28 \text{ mm} \end{aligned} \tag{6.2}$$

With the arrangement illustrated in Figure 6.7, where the collimator is approximately at a distance from the test piece equal to the collimator's focal length, the diameter of the collimator will need to be greater than 150 + 28 × $\sqrt{2}$ = 189.6 mm. If we assume that a diameter of 220 mm will therefore be appropriate, we would find, as illustrated in Figure 6.7, that an off-axis distance of 160 mm allows one to have a suitable optical arrangement where the light from any part of the target is unobstructed. The off-axis angle under these circumstances is approximately 5.7°. Ray tracing this configuration indicates that light from the extreme corner of the largest four-bar target has a root mean square (RMS) angular spread of approximately 0.05 mrad compared with the width of a bar on this target of 2.5 mrad, i.e., only 1/50 of the width. This would certainly introduce negligible errors in a measurement of MRTD. We note that for optimum performance the test target should be in a plane orthogonal to the line joining the center of the test target to the center of the collimator mirror.

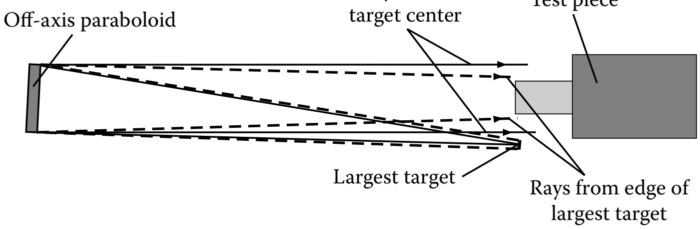

FIGURE 6.7 Scale drawing of a typical reflecting collimator arrangement.

As mentioned earlier, it is important that the collimator mirror be used at the correct off-axis distance, and methods of achieving this are described in Chapter 9.

A collimator is not always necessary for making an MRTD measurement. Direct observation of the test target can be used, provided a suitable measurement configuration is possible. This would need one to take into consideration the close focus distance of the imager, the dimensions of the test targets, and the available laboratory space. The results will be affected by less than 4% by making measurements at what are finite rather than infinite conjugates, provided the distance of the test target from the imager is not less than ×40 the focal length of the lens objective used on the test piece.

6.5.3 MULTIMIRROR COLLIMATORS

Mirror systems that use several mirrors, one or more of which are aspheric, can be designed to have a high degree of aberration correction both on-axis and off-axis (several unobstructed mirror systems that could be modified for use as collimators are described in Smith[4]). It may be necessary to use such arrangements in special circumstances, e.g., when good aberration correction is required over a relatively large field of view (FOV), or where a collimator with a small *f*/number is a requirement. In general, multimirror collimators will require very precise positioning of the mirrors relative to each other if the systems are to achieve their theoretical performance. This will almost certainly involve elaborate alignment procedures.

6.5.4 REFRACTING COLLIMATORS

The main disadvantage of refracting collimators, compared to mirror collimators, is that they will only be suitable for use over a limited spectral range, although the range will usually be sufficient to cover one of the thermal bands (i.e., 3–5 μm or 8–14 μm) but not both. Their advantages are that they can be of smaller diameter (see Figure 6.6) to cover the same aperture test piece since they can be positioned immediately in front of the entrance aperture of the test piece, and in general they will have a larger usable FOV than the equivalent off-axis paraboloid. They are particularly useful as de-collimators (see Section 7.3.10.2) when testing afocal optical systems, largely because of the very convenient optical and mechanical configuration in which they can be used.

6.5.4.1 3–5 μm Collimators

One of the principal materials used in this wavelength band is silicon. However, silicon has a relatively large change of refractive index with wavelength, which makes it difficult to provide good chromatic correction with a single Si element. If we consider the same application as discussed in Section 6.5.2, we find that the optimum lens has an RMS angular spread of approximately 0.12 mrad on-axis, compared with the width of a bar on the smallest target of 0.125 mrad, i.e., approximately the width of a bar. This would not be acceptable in this situation.

An application where a single-element Si lens could be suitable would be as a decollimator in a system for measuring the MTF of an infrared telescope (i.e., an afocal optical system). For example, if we have a telescope with an entrance pupil of 150 mm and a magnification of ×10, the exit pupil would have a diameter of 15 mm. A Si lens for the 3–5 μm wavelength range with a diameter of 15 mm and a focal length of 150 mm is virtually diffraction limited on-axis and over a FOV of approximately ±1.5° and would be very suitable for such an application where it could effectively be used only on-axis, even when making off-axis measurements on the telescope (see Section 7.3.10.2).

For large collimators, doublet lenses are required to correct the chromatic aberrations over this wavelength band. A silicon/germanium combination for this wavelength range, with a focal length of 1,600 mm and an aperture of 160 mm, is virtually diffraction limited on-axis. At an off-axis field position equivalent to being at one corner of a 28 × 28 mm four-bar target, the RMS angular spread is approximately 0.035 mrad, i.e., approximately 1/70 of the width of the relevant bar. This is better than the equivalent off-axis paraboloid (see Section 6.5.2).

6.5.4.2 8–14 μm Collimators

A single germanium element can be used as an effective collimator for this wavelength band. A suitably optimized lens with a diameter of 160 mm and a focal length of 1,600 mm is effectively diffraction limited on-axis and very close to being diffraction limited at an off-axis field position equivalent to being at one corner of a 28 × 28 mm four-bar target. Some small improvement can be obtained by using a doublet instead of a single element. In this case the best combination is probably a germanium/zinc selenide doublet.

6.5.5 High-Magnification Objectives

For certain applications infrared objectives with properties similar to those of visible wavelength microscope objectives are required, often including having a large NA. An example of one of these applications is where one needs to project a very small infrared spot on, say, a detector chip, in order to scan the area of the chip to measure its uniformity. In such an application the objective needs to be very highly corrected. An application where a very high degree of correction is not required is where the objective is used to collect the radiation passing through a pinhole or slit and focus it onto a detector. Mirror objectives are available commercially that would satisfy the first of these applications. The central obstruction in such an objective would not be a problem in this case, and the broad spectral bandwidth over which such an objective can be used is a decided advantage. The central obstruction would exclude the use of such an objective in the second of the applications, and a purely refracting optical system would be required. Such objectives would normally require a minimum of three elements, and a different objective would be required for each of the thermal bands.

6.6 INTEGRATING SPHERES

A typical integrating sphere is illustrated in Figure 6.8. It consists of a hollow sphere with one or more small ports, which is coated internally with a diffusely reflecting surface having a very high reflectance. Integrating spheres have several different applications, some of which are described in Chapter 7. The main property of an

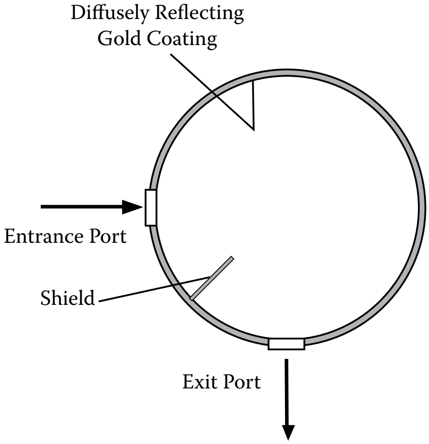

FIGURE 6.8 Section through an integrating sphere.

integrating sphere is that radiation entering one port (the input port) generates a uniform irradiance over any port that is at a position on the sphere 90° to the first (a small shield is usually incorporated into the sphere to prevent radiation from the input port reaching the output port directly). In addition to this, the irradiance at the output port is linearly related to the total radiant flux entering the input port, independent of the diameter of the input beam, or whether it is a converging, diverging, or collimated beam (hence the name integrating sphere). If a detector is positioned at the output port of an integrating sphere, its signal will be linearly related to the total radiation entering the sphere, provided of course that the detector has a linear response to radiation.

The principal requirement of an integrating sphere is that the internal coating should have a very high uniform reflectance and be an almost perfect diffuser (i.e., a Lambertian diffuser). Spheres used at visible and near-IR wavelengths are usually coated with barium sulfate, or are made from a special plastic. For the thermal IR bands, special diffuse gold coatings are normally used. Each sphere manufacturer will usually have a special name for its particular version of the different coatings.

The main disadvantage of an integrating sphere is that the irradiance level at the output port is in general a small fraction of the irradiance that could be generated if all the input radiation were used to directly irradiate the output port. The mathematical relationship between the radiant flux entering the sphere and the total flux exiting the port is

$$F_o = (F_i.\rho.\alpha_e)/(1 - \rho[1 - \alpha_a]) \tag{6.3}$$

where F_o is the total output flux in watts, F_i is the total input flux in watts, ρ is the sphere wall reflectance (where $\rho = 1$ represents 100% reflectance), α_e is the ratio of the area of the output port to the surface area of the sphere, and α_a is the ratio of the sum of all port areas to the surface area of the sphere.

From Equation (6.3) we can derive the radiance of the exit port, which will be given by

$$R_e = F_o/(\pi.A_e) \tag{6.4}$$

where R_e is the radiance of the exit port in watts m^{-2} steradian^{-1} and A_e is the area of the exit port in m^2.

In fact, the radiance of the output port is the same as the radiance of the sphere wall, so that from Equations (6.3) and (6.4) we have

$$R_s = (F_i.\rho)/(\pi.A_s[1 - \rho(1 - \alpha_a]) \tag{6.5}$$

where R_s is the radiance of the sphere wall in watts m^{-2} steradian^{-1} and A_s is the area of the sphere wall in m^2.

As an example, if we consider a 0.1 m diameter sphere with $\rho = 0.94$, having an entrance port of 0.03 m diameter and an exit (detector) port of 0.01 m diameter, then for $F_i = 1$ watt we have

$$F_o = 0.028 \text{ watts}$$

$$R_s = 114 \text{ watts m}^{-2} \text{ steradian}^{-1}$$

6.7 SPECTRAL FILTERS

For many measurements it is necessary to isolate a specific broadband spectral region, or to make measurements using a narrow band of wavelengths. There are several ways in which this can be achieved:

Multilayer dielectric long-pass filters: These are filters that do not transmit wavelengths shorter than a specified value (the cut-on wavelength) but transmit longer wavelengths. In practice, there will be a cutoff wavelength that will be determined by either the substrate on which the filter is made or the actual design of the multilayers.

Multilayer dielectric short-pass filters: Similar to long-pass filters except that they transmit wavelengths shorter than a cutoff wavelength. Again, in practice, there will be a cut-on wavelength that will be determined by either the substrate on which the filter is made or the actual design of the multilayer.

Multilayer dielectric bandpass filters: These filters transmit wavelengths within a specified band only. The actual bandwidth is usually specified in terms of full width half height (FWHH). This is the width of the spectral transmission curve for the filter, at a transmission level equal to half the peak transmission. The FWHH is specified either in wavelength units or as a percentage of the center wavelength.

Infrared materials: Many of the materials used in the thermal wavelength band do not transmit wavelengths across the complete 3–14 μm band, but have a cutoff or cut-on within the band that can be used as a filtering mechanism and whose characteristics can be controlled to a certain extent by adjusting the thickness of the material.

The bulk transmission (i.e., the transmission resulting from absorption in the material and ignoring the effects of reflection) of a plate of a material of thickness d is given by

$$t = e^{-k(\lambda).d} \tag{6.6}$$

where $k(\lambda)$ is the bulk absorption constant at a wavelength λ. Equation (6.6) is known as Beer's law. A result of this relationship is that the effective cut-on or cutoff wavelength can be manipulated to a certain extent by selecting the correct thickness of material.

Information about the transmission characteristics of different material can be found in the published literature (e.g., Klocek[5]) and in manufacturers' data sheets. Examples of some useful materials are as follows (note that there are many others):

Calcium fluoride: Transmits in the visible and has a transmission that effectively starts falling at about 5.5 μm, but in a sufficiently thin window will transmit out to 12 μm. Adjusting the thickness of the material allows one to change the transmission characteristics significantly in this region of the spectrum.

Germanium: Does not transmit any visible radiation and has a relatively sharp cut-on at 1.8 μm, with good transmission over the full 3–14 μm band.

Lithium fluoride: Transmits in the visible and has a transmission that effectively starts falling at about 4.8 μm, but in a sufficiently thin window will transmit out to 9 μm. Here again, adjusting the thickness of the material allows one to change the transmission characteristics significantly in this region of the spectrum.

Magnesium oxide (periclase): Transmits in the visible and has a transmission that effectively starts falling at about 5.8 μm, but in a sufficiently thin window will transmit out to about 8.5 μm.

Aluminum oxide (sapphire): Transmits in the visible and has a transmission that effectively starts falling at about 4.2 μm, but in a sufficiently thin window will transmit out to about 6.5 μm.

Detectors: The spectral response characteristics of the detectors used for making measurements in the thermal bands will themselves behave as filters and determine the overall spectral characteristics of a system. This is particularly so with photon detectors, where the cut-on and cutoff wavelengths are usually well defined and can be adjusted within fairly broad limits by varying the chemical makeup of the detector material.

Sources: The spectral output of a source will of course play an important part in determining the spectral response characteristics of a measurement system. In principle, the characteristics of broadband sources can be varied by adjusting their temperature. The need is usually to reduce the temperature, and this unfortunately means reducing radiation levels and hence signal levels. Where a narrow spectral band is required, one can of course use sources such as lasers, laser diodes, and LEDs (see Section 6.2.9).

Monochromators: These can be used in conjunction with either the source or detector to provide an alternative to bandpass filters. They have the advantage of allowing both central wavelength and bandwidth to be easily adjusted. Grating, prism, and variable wavelength filter monochromators have the disadvantage of having inputs and outputs in the form of narrow slits. However, this does not apply to Fourier transform spectrophotometers. Monochromator-based instruments have been built that allow wideband spectral characteristics to be closely simulated.[6] The concept is to place a suitably shaped mask in the plane of the full spectrum generated by the monochromator, and then to recombine the transmitted wavelengths using either a monochromator in reverse, an integrating sphere, or some other method of mixing the radiation, such as a random fiber bundle.

In general, the correct spectral characteristics for a particular measurement system are generated by combining one or more of the above devices. Perhaps the easiest, but not necessarily the most accurate, is to use a detector that is the same as that used in the arrangement one wishes to simulate, to provide the long wavelength cutoff and a multilayer cut-on filter to provide the cut-on characteristic. For some types of measurement (e.g., MTF[6]) it is possible to do the measurement at several monochromatic wavelengths and from these to compute the result that would have been obtained using the correct broadband characteristic. The measurements are done by recording the LSFs for each wavelength and then combining them, after having normalized the area under the LSF and applied the appropriate weighting function for each wavelength, into a single LSF and computing the MTF from this. It is important to note that the LSFs must be combined with respect to their positions relative to each other.

REFERENCES

1. Williams, T. L. 1983. Equipment for automatic testing of infrared telescopes. In *IEE Conference Proceedings*, No. 228, pp. 79–83.
2. Prokhorov, A. V. 1998. Monte Carlo method in optical radiometry. *Metrologia* 35:465–71.
3. Williams, T. L. 1985. Assessing the performance of complete thermal imaging systems. *SPIE Conference Proceedings* 590:172–78.
4. Smith, W. J. 1992. *Modern lens design*. New York: McGraw-Hill.
5. Klocek, P. 1991. *Handbook of infrared optical materials*. New York: Marcel Dekker.
6. Williams, T. L. 1999. *The optical transfer function of imaging systems*. Bristol and Philadelphia: IOP Publishing.

7 Measurement Procedures and Techniques for the Principal Components That Make Up a Thermal Imager

7.1 INTRODUCTION

This chapter describes various techniques and the associated equipment for measuring the main performance parameters connected with some of the basic components and subsystems that make up a thermal imager. These parameters have been described and defined in Chapter 4. This will be of primary interest to companies manufacturing these components and subsystems as well as the manufacturer of complete thermal imagers. However, an understanding of how these parameters are specified and assessed should also prove valuable to the user of thermal imagers in providing a better understanding of the instrument he or she uses.

7.2 GENERAL MEASUREMENT PROCEDURES

Most measurement techniques have at least two components in common, a source of radiation and a detector of radiation. The optimum arrangement in most situations is to modulate the source and demodulate the detector signal using a reference signal from the source modulator (for example, using phase-sensitive demodulation). In addition to this the detector electronics can include a bandpass filter that is centered round the modulation frequency. Such an arrangement is illustrated diagrammatically in Figure 6.1 of Chapter 6. The need to modulate the source is mainly to differentiate it from all other ambient thermal sources. The suggested electronic processing also helps to do this in that it is basically only responsive to the modulated radiation, and moreover optimizes the ratio of signal to noise. In such arrangements the modulation frequency also needs to be held stable in order to eliminate effects that are frequency dependent.

In systems that include a computer, the detector signal can be digitized at an early stage and most of the processing, including control of the modulation frequency, can be done in software. Modulation of the source is normally achieved by using a slotted disc driven either by a synchronous motor or by a direct current (dc) motor whose

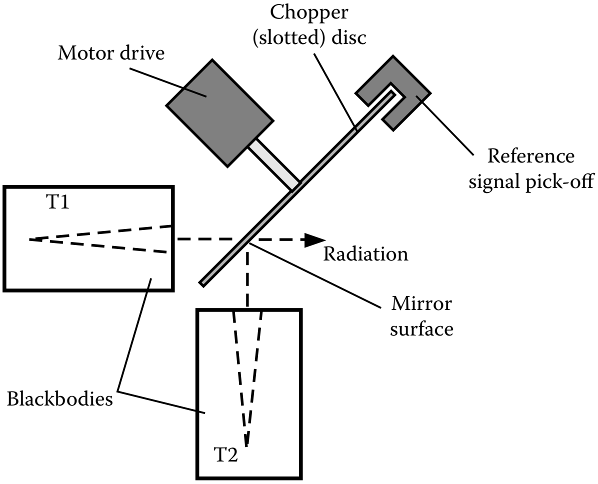

FIGURE 7.1 Modulated source arrangement using a reflecting chopper disc.

speed is controlled by a servo system (that can be implemented in software) to keep the frequency of the reference pick-off constant.

If a simple slotted disc (chopper) is used to modulate the source, the magnitude of the modulation will depend on the difference between the radiation from the source and that from the parts of the disc that obscure the source. The modulated radiation will only be constant if both the radiation from the source and that from the disc are constant. Assuming that the disc is blackened (i.e., has a high emissivity), the radiation it emits will depend on its temperature. In practice this will change relatively slowly and will not normally have much effect on the accuracy of a measurement, particularly if the source temperature is much higher than that of the chopper disc. However, there are situations where a higher stability is required. Since it is very difficult to keep the temperature of a rotating disc constant, a solution is to use a chopper disc, with a mirror surface on one side, arranged, as illustrated in Figure 7.1, so that the detector alternately sees the hot source and a colder source, both of which can be temperature-controlled blackbodies.

In situations where the detector is an array, the radiation source is not usually modulated in the normal sense of the word. However, measurements should in most circumstances be the result of determining the difference between the signal pattern when the source is on and when it is obscured by a plate or shutter that is close to ambient temperature. The temperature of a plate or shutter can of course be controlled much more easily than a rotating chopper blade.

7.3 LENSES AND OPTICAL SYSTEMS (see also Section 4.2)

7.3.1 Focal Length

Focal length is a parameter associated with an image-forming lens (i.e., the lens objective on most thermal imagers). There are two main methods of measuring focal length. The first of these relies on the use of a nodal slide and is illustrated in

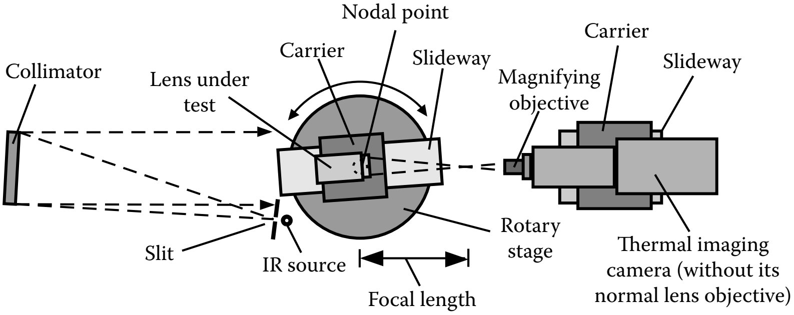

FIGURE 7.2 Nodal slide method of measuring focal length.

Figure 7.2 (see also Williams[1]). The focal length of a lens is in fact the distance from the rear nodal point to the image plane. The nodal points are defined as points of unit angular magnification on the optical axis of the lens. What this means is that a ray of light incident on the front nodal point, making an angle θ with the optical axis, effectively emerges from the rear nodal point also at an angle θ. The measurement technique depends on the principle that when a lens that is imaging an object at infinity is rotated about its rear nodal point, the position of the image is stationary. The nodal slide enables the lens to be rotated about a vertical axis whose position of intersection with the axis of the lens can be altered by a fine adjusting device in order to locate the nodal point. For an infrared lens the image is most conveniently viewed using a thermal imaging camera, with the image either formed directly on the detector array (if the camera objective can be removed to allow this) or, as illustrated in Figure 7.2, via a suitable close-focus objective (see Section 6.5.5) fitted to the camera, to provide the required magnification. The position of the lens on the nodal slide is adjusted until rotation of the lens through a small angle produces no shift of the image (the object can most conveniently be a hot wire or a slit illuminated by a suitable infrared (IR) source at the focus of a collimator). The distance from the axis of rotation (i.e., the rear nodal point) to the image is then measured as the focal length.

An alternative arrangement that could prove more convenient since it uses a thermal imager with its normal infinity focus objective is illustrated in Figure 7.3. In this case the test target (i.e., illuminated slit or hot wire—see Section 6.2) is positioned at the focus of the test piece. The measurement procedure is basically the same as before.

We note that since relatively small movements of the image are involved in the measurement, a small detector array comprising in the limit just two detectors at the focus of the test piece could be used in the first configuration and in conjunction with a simple lens objective in the second configuration. The main problem would be in determining accurately when the detector was at the best focus. However, this could be arrived at by measuring the slope of the difference signal as the image is moved from one detector to the other.

Probably the more usual method of measuring focal length is to use what is referred to as a camera bench[1,2] in conjunction with an illuminated target at the focus

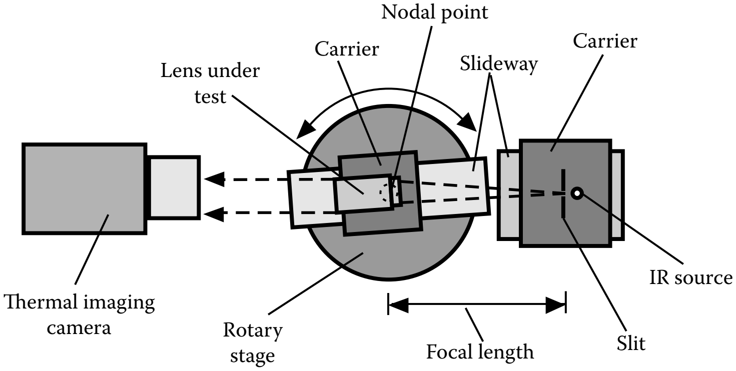

FIGURE 7.3 Alternative nodal slide arrangement.

of a collimator. Such an arrangement is illustrated in Figure 7.4 and is the basis of a test facility that permits one to evaluate most of the performance parameters associated with a lens system and in particular its modulation transfer function (MTF).

The camera bench is a mechanical optical bench assembly that allows a test target that is effectively at infinity to be positioned in different parts of the field of view of a lens objective, and for a detector system for analyzing the image to be moved to any position over a flat focal plane. The main components of such a bench are a slideway (the focal slide), pivoted about a vertical axis at its forward end, on which is supported the test piece, and a cross slide (the field slide), which in turn supports the image analyzer

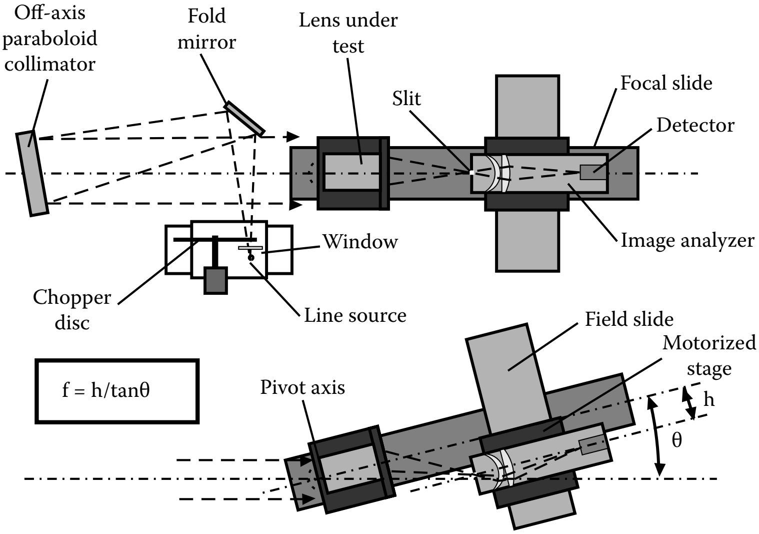

FIGURE 7.4 Illustration of a camera bench used for measuring focal length, showing the on-axis and off-axis positions.

(i.e., the detector system). The test piece will be positioned along the focal slide so that its entrance pupil is approximately over the axis of rotation of the slideway so that the pupil remains in the collimated beam as the camera bench is rotated, and the field slide will support the image analyzer via a micrometer stage (that could be motorized) to allow fine focusing adjustments to be made. The field slide itself can in most situations consist only of a micrometer stage since the image format diagonal associated with most test pieces is normally less than 50 mm. Camera benches, as indicated above, are widely used for measuring a whole range of performance parameters of a lens objective.

The method of measurement (see Section 4.2.1) uses the relationship $f = h/\tan\phi$ to determine the focal length, where h is the shift in position of the image along the field slide (that defines the focal plane) when the effective position of a target at infinity changes from being on-axis to being at an angle ϕ to the axis of the lens. The position and correct focus of the image can once again be measured using a thermal camera fitted with a close-focus objective as the image analyzer. Alternately and more usually, equipment capable of measuring line spread functions (LSFs) as a means of determining MTF can be used to determine precisely the position of the focal plane (i.e., the position where the MTF is a maximum) as well as the position of the image along the field slide (see Section 7.3.10 and Williams[1]). A facility for measuring the angle ϕ must be incorporated in the camera bench.

Many commercial MTF test facilities include software that provides a means of automatically measuring focal length using the technique described above.

It is of course possible to measure focal length using a finite conjugate bench arrangement, and one method of doing this is described in Section 7.3.10.

7.3.2 ANGULAR MAGNIFICATION

Angular magnification is a parameter associated with afocal systems (i.e., telescopic systems that do not form images directly). It is defined as $\tan\theta'/\tan\theta$, where θ is the angle the object at infinity makes with the optical axis of the system and θ' is the angle the image at infinity makes with the optical axis (see Section 4.2.2). Magnification can be measured using the camera bench described in Section 7.3.1 with the addition of a lens (the de-collimator) placed at the exit pupil of the test piece. The arrangement is illustrated in Figure 7.5. The measurement is made by determining the shift h of the image of the test object (i.e., the line or slit source at the focus of the collimator) formed by the de-collimator lens, as the camera bench is rotated away from the on-axis position by an angle θ. The angular magnification will be given by

$$M = h/(f_{dc}.\tan\theta) \tag{7.1}$$

where f_{dc} is the focal length of the de-collimator lens (where $h/f_{dc} = \tan\theta'$). We note that for accurate results the de-collimator lens must be designed to be relatively free from distortion and have a flat image field, over the distance h used for the measurement. The form of image analyzer used for locating the image will be as described in Section 7.3.10.

Commercial bench facilities for measuring the MTF of afocal systems will frequently have a software option for measuring angular magnification.

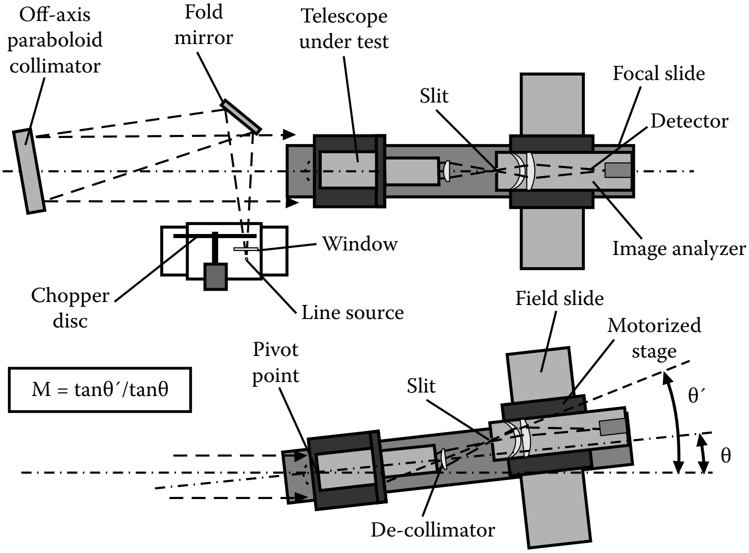

FIGURE 7.5 Camera bench used for measuring the magnification of a telescope.

However, the optical bench configuration is usual slightly different from that described above, mainly because the requirement can be to measure MTF at relatively large image angles and to have a de-collimator lens that is effectively diffraction limited (i.e., with no aberrations) over the image angles that will be used. This can be very difficult to achieve, so that the more usual bench arrangement is similar to that illustrated in Figure 7.6, where the de-collimator lens is always used in its on-axis position.

The system again uses a slideway, pivoted at its front end so that it can rotate about a vertical axis, a carrier with a bracket for supporting the test piece, and a second carrier on which is mounted a rotary bearing or stage (that can be motorized), which in turn supports the de-collimator lens and the image analyzer. The mechanical configuration must be such that the entrance pupil of the de-collimator lens can be positioned close to the axis of rotation of the bearing, with both positioned close to the exit pupil of the test piece. The coincidence of the axis of rotation, the entrance pupil of the de-collimator, and the exit pupil of the test piece must be such that the exit pupil of the test piece is always within the boundaries of the entrance pupil of the de-collimator, as the bearing is rotated.

Measurements are made by measuring the angle θ' through which the de-collimator and image analyzer have to be rotated to locate the image of the test object (i.e., the line or slit source at the focus of the collimator) formed by the de-collimator lens, when the camera bench is rotated through an angle θ. The magnification is given by

$$M = \tan\theta'/\tan\theta \tag{7.2}$$

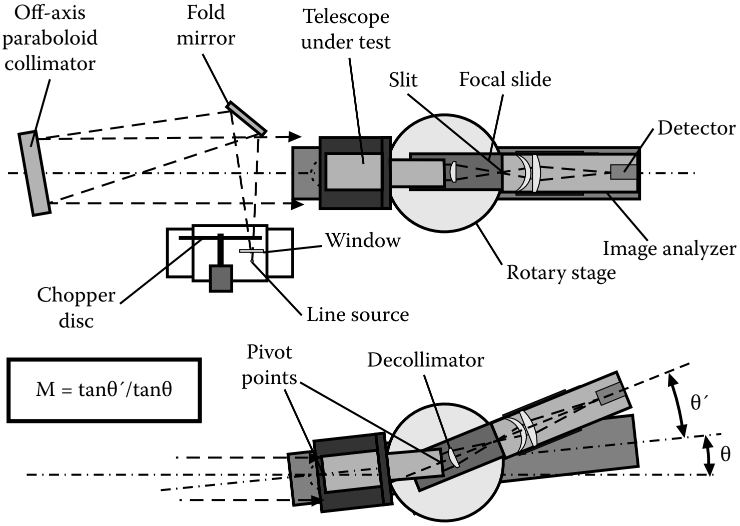

FIGURE 7.6 Modified camera bench for measuring magnification of telescopes.

The de-collimator used in this arrangement need only be well corrected over a very small image field and can in most cases be a single-element Ge or Si lens depending on whether measurements are in the 8–14 μm or 3–5 μm band. When the system is designed for measuring MTF, the de-collimator needs to be diffraction limited and may need to be a doublet depending on the pupil size, etc.

7.3.3 *f*/NUMBER OR NA

The *f*/number is generally taken as the ratio of focal length to entrance pupil diameter. Strictly speaking, it is the ratio 1/(2.NA)—see Equations (4.8) and (4.9) of Section 4.3—where

$$\mathrm{NA} = \sin[\tan^{-1}\{(\text{entrance pupil diameter})/(2.f)\}] \tag{7.3}$$

If the focal length f is known, or has been measured as described in Section 7.3.1, determining the *f*/number or numerical aperture (NA) requires the entrance pupil diameter D to be measured. One method of doing this is illustrated in Figure 7.7. The technique consists in placing the test piece in the collimated beam from a small circular or rectangular source so that its optical axis coincides with the axis of the beam, and placing a detector at the image of the source that is sufficiently large to collect all the radiation in the image, or alternately to use a combination of a small integrating sphere and detector to provide a sufficiently large collection area with a uniform response. The measurement procedure is to position an iris diaphragm in front of the entrance aperture of the test piece and coaxial with it, and to close it down until the detector signal just

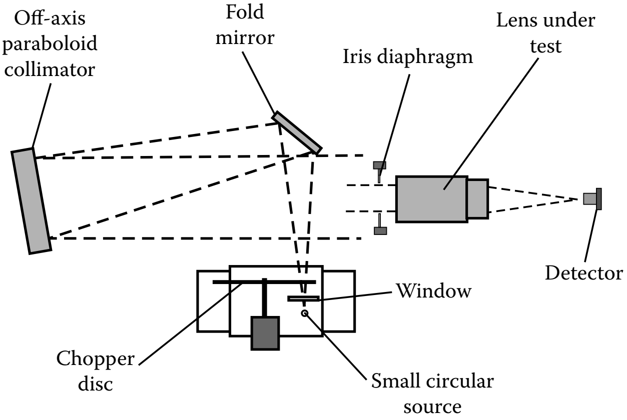

FIGURE 7.7 Arrangement for measuring the entrance pupil diameter.

begins to drop. The diameter of the iris at that point can be assumed to be that of the entrance pupil of the test piece. As an alternative to using an iris diaphragm a plate can be introduced at each side of the aperture and adjusted in each case until the detector signal starts to drop. The positions of the edge of the plate will define the edges of the entrance pupil.

A further alternative is to replace the collimated beam by the beam from an appropriate laser mounted on a precision slideway that allows it to be moved at right angles to its beam, which would also be at right angles to the optical axis of the test piece (see Figure 7.8). With the system set so that the laser beam moves across a diameter of the test piece aperture, the two positions where the detector signal falls to 50% of its maximum value can be assumed to define the edges of the entrance pupil. A HeNe laser (working at 3.39 μm) can be used for the 3–5 μm band and a CO_2 laser for the 8–14 μm band. We note that low-power versions of these lasers are not generally available, and that for convenience and safety it will be necessary to attenuate the beam from the laser.

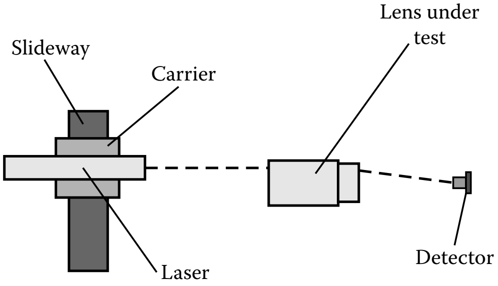

FIGURE 7.8 Measuring entrance pupil diameter using a laser.

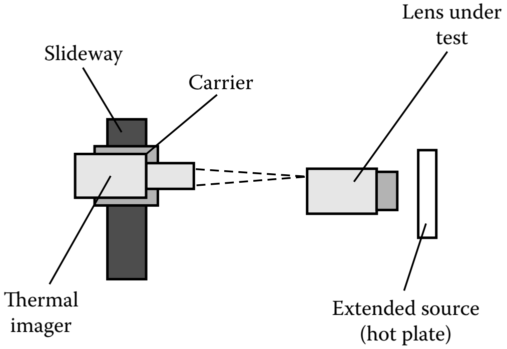

FIGURE 7.9 Measuring the entrance pupil diameter using a thermal imager.

The entrance pupil diameter can also be measured using a thermal imager, and the arrangement is illustrated in Figure 7.9. A large-area source such as a heated high-emissivity plate or a blackbody with a suitably large cavity diameter is positioned on the image side of the lens and close to its exit aperture. The thermal imager is positioned on a calibrated slideway and focused, to view the entrance aperture of the test piece. In fact, it must be focused to give a sharp-edged image of the bright aperture that it should see. The diameter of the entrance pupil is in fact the diameter of this image and is best measured by moving the thermal imager along the calibrated slideway so that first one edge of the image is positioned on a central fiducial mark (or equivalent) on the thermal imager display, and then doing the same for the second edge and measuring the distance moved between the two positions. Alternately, if the full image of the entrance pupil can be seen on the display, the diameter can be measured by viewing a suitable scale to calibrate the display. Note that the scale has to be placed so that it is in focus on the display without refocusing the thermal imager. Note also that a suitable scale will be a series of slots in a metal plate at ambient temperature, placed in front of a large-area heated source.

7.3.4 Entrance and Exit Pupil Diameters of Afocal Systems

The entrance and exit pupils of an afocal system are both significant parameters of these devices. They can be measured using techniques similar to those described in Section 7.3.3. Since afocal systems do not form images on their own, a lens (decollimating lens) is required to form an image of the source on the detector. The entrance pupil can then be measured as described above, while the exit pupil can be measured by placing the iris diaphragm, obscuring plates, or laser on the exit pupil side of the test piece. Alternately, if the entrance pupil diameter D has been measured as well as the angular magnification M of the system, the diameter of the exit pupil d can be calculated from the relationship

$$d = D/M \tag{7.4}$$

The entrance pupil diameter can also be measured using a thermal imager in exactly the manner described above. The same procedure can be used to measure the exit pupil diameter, except the source is now placed at the entrance aperture and the thermal image now looks at the exit aperture of the test piece and focuses on the image of the exit pupil.

If the entrance and exit pupil diameters are measured, Equation (7.4) can be rearranged to give the value for the magnification.

7.3.5 DISTORTION

For an image-forming lens objective, this is a measure of the departure from the linear relationship (see Section 4.2.10)

$$h' = k.\tan\theta \tag{7.5}$$

where h' is the distance along the image plane from the position of the image of a point object when it is in the center of the field of view (FOV) and when it is at an off-axis angle θ, and k is a constant. When there is no distortion, k is equal to the focal length of the lens (see Section 7.3.2). Distortion is determined by measuring values of h' for a range of values of θ. Distortion is usually expressed as a percentage and is given by the relationship

$$\text{Distortion}\% = (h' - k.\tan\theta).100/h' \tag{7.6}$$

The constant k can be taken as being equal to the focal length f, which will make the values of distortion small for small values of θ. Alternately, it can be taken as that value that makes the root mean square (RMS) distortion over the full FOV a minimum.

Measurement techniques are the same as those described in Section 7.3.1 for measuring focal length using a camera bench.

For an afocal optical system, distortion is a measure of the departure from the linear relationship (see Section 4.2.10)

$$\tan\theta' = k.\tan\theta \tag{7.7}$$

where θ is the angle subtended by the object with the optical axis and θ' is the angle subtended by the image with the optical axis. When there is no distortion, k is equal to the magnification of the afocal system (see Section 7.3.2). Distortion is determined by measuring values of θ' for a range of values of θ. Distortion expressed as a percentage is given by the relationship

$$\text{distortion}\% = (\tan\theta' - k.\tan\theta).100/\tan\theta' \tag{7.8}$$

As indicated in Section 4.2.10, some afocal systems are specifically designed so that

$$\theta' = k\theta \tag{7.9}$$

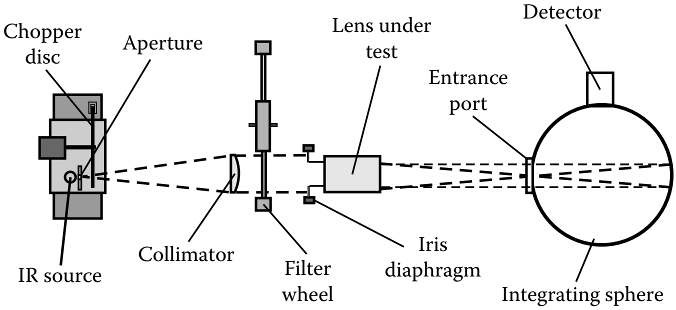

FIGURE 7.10 Arrangement for measuring spectral transmission.

so that in this case distortion is measured as

$$\text{Distortion\%} = (\theta' - k.\theta).100/\theta' \tag{7.10}$$

7.3.6 Spectral Transmission

Transmission has been defined in Section 4.2.7. There are two main techniques for its measurement, the first of which is illustrated in Figure 7.10. The arrangement consists of a small source at the focus of a collimator, a spectral filter (ideally a set of filters that are in a turret wheel and can be positioned in the collimated beam as required), an adjustable iris diaphragm, and finally, an integrating sphere (see Section 6.6) with an appropriate detector and signal readout electronics. A mechanical chopper is shown in the diagram with a reference signal pick-off that in conjunction with the signal processing system optimizes signal processing (see Section 7.2).

The procedure is to first set the diameter of the iris so that the diameter of the collimated beam is such that it will pass through the entrance port of the integrating sphere and through the aperture of the test piece without obstruction. The detector signal is then measured both with and without the test piece in the collimated beam. The ratio of the signal with test piece to the signal without test piece is the transmission for the wavelength in question. The measurement can then be repeated for other wavelengths. In some situations it is sufficient to make measurements at a single wavelength in order to characterize the transmission sufficiently well. In such circumstances it is an advantage to use one of the laser wavelengths so that a single laser and chopper can replace the broadband source, collimator, filter, and iris diaphragm. This will allow better signal levels to be achieved and will increase the accuracy of measurement.

An alternative technique is illustrated in Figure 7.11(a) and (b) (see Williams[3]). In this arrangement a modulated blackbody cavity is used as a very uniform source with a relatively large area. Figure 7.11(a) shows the configuration for the measurement without the test piece, and Figure 7.11(b) shows the configuration for the measurement with the test piece. When the test piece is not present the lens next to the detector is set to form an image of the blackbody cavity on the detector via an

© 2009 by Taylor & Francis Group, LLC

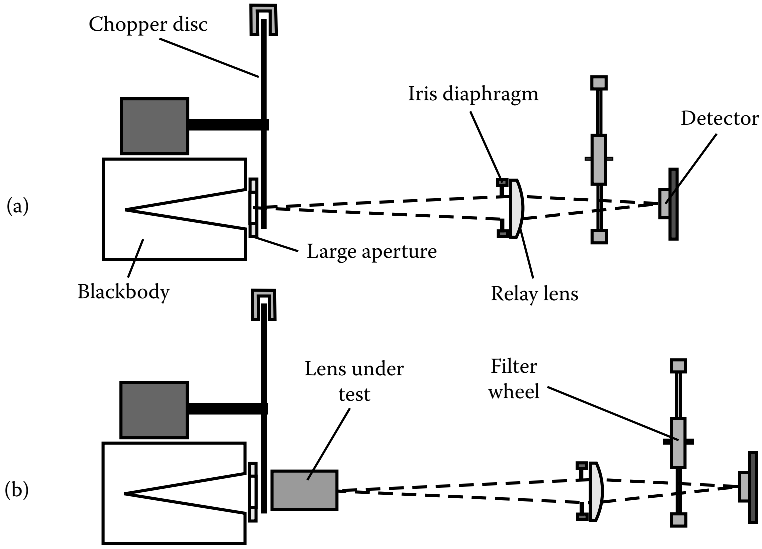

FIGURE 7.11 Arrangement for measuring spectral transmission using a large-area uniform source (e.g., a blackbody). (a) Without the test piece. (b) With the test piece.

appropriate spectral filter. For the measurement with the test piece, the latter is positioned with its normal exit aperture close to the blackbody source, and the two are moved along a slideway so that the lens next to the detector now focuses an image of the entrance aperture of the test piece on the detector. The ratio of the detector signals in these two situations is, as noted earlier, equal to the transmission for the wavelength in question.

There are several conditions that must be satisfied in order to obtain a correct measurement with this technique. These are as follows:

- In theory, for both measurements, an image of the blackbody cavity is imaged on the detector, and this must be larger than the area of the detector.
- The diameter of the iris diaphragm must be the same for both measurements.
- The focus position of the relay lens relative to the detector must be the same for both measurements.

Ideally the aperture of the blackbody should be positioned at the exit pupil of the test piece, so that there will be an image of this aperture at the entrance pupil (the entrance and exit pupils are conjugate image planes), and in the ideal arrangement this is then imaged onto the detector (see Figure 7.11(a) and (b)). If the source has a radiance $R(\lambda)$ and the lens close to the detector in combination with the iris diaphragm has an NA = sin(u), then the detector signal with the test lens out will be given by

$$S_0 = R.k(\lambda).\sin^2(u) \tag{7.11}$$

© 2009 by Taylor & Francis Group, LLC

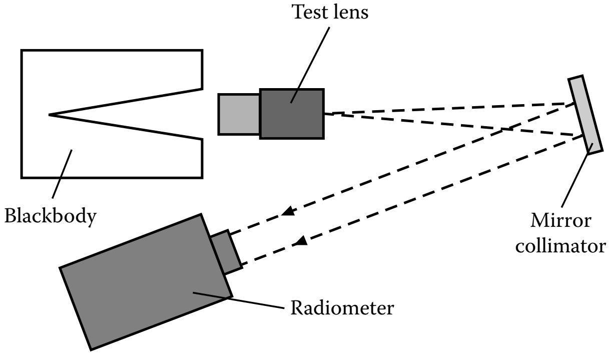

FIGURE 7.12 Measuring lens transmission using a radiometer.

where $k(\lambda)$ is a constant that includes the effect of the transmission of the lens and filter. With the test lens in place the signal will be

$$S_m = t(\lambda).R.k(\lambda).\sin^2(u) \tag{7.12}$$

where $t(\lambda)$ is the transmission of the test lens at wavelength λ. We see from these two equations that

$$t(\lambda) = S_m/S_0 \tag{7.13}$$

In a practical system the blackbody aperture needs to be variable (e.g., by having a turret with a selection of different size apertures). The smallest aperture is used to adjust focus by maximizing the detector signal. The other apertures are used to check that for both measurements there is a point where increasing the diameter of the aperture does not increase the detector signal. The next largest aperture should be used for the measurements.

This technique can be modified for use with a radiometer or preferably a spectraradiometer.[3] The modification to the technique is required in order to take into account the fact that a radiometer measures all the radiation it sees within the chosen spectral band, which will include any radiation emitted by the test piece itself and not just the radiation from the blackbody source. The arrangement is illustrated in Figure 7.12. This shows a radiometer designed to take in a collimated beam, which must therefore be used in conjunction with an additional lens or mirror to focus down the area it looks at. Note that a chopper is no longer required, since this will be part of the radiometer, depending on the latter's design.

The radiometer signal needs to be measured under four separate conditions:

1. S_1 = the signal when the radiometer sees the blackbody source directly and the latter is at ambient temperature; i.e., the radiance it measures is only that of the source $R_{s,0}(\lambda)$.

© 2009 by Taylor & Francis Group, LLC

2. S_2 = the signal when the radiometer sees the blackbody source through the test piece and the source is again at ambient temperature; i.e., the radiance it measures is that of the source reduced by the transmission factor $t(\lambda)$ of the lens = $t(\lambda).R_{s,0}(\lambda)$, plus the effective radiance of the test piece itself, $R_{TP}(\lambda)$.
3. S_3 = the signal when the radiometer sees the blackbody source directly and the latter is at a higher than ambient temperature T; i.e., the radiance it measures is only that of the source $R_{s,T}(\lambda)$.
4. S_4 = the signal when the radiometer sees the blackbody source through the test piece and the source is still at temperature T; i.e., the radiance it measures is that of the source reduced by the transmission factor $t(\lambda)$ of the lens = $t(\lambda).R_{s,T}(\lambda)$, plus the effective radiance of the test piece itself, $R_{TP}(\lambda)$.

The lens transmission can then be calculated as

$$\begin{aligned} t(\lambda) &= [(t(\lambda).R_{s,T}(\lambda) + R_{TP}(\lambda)) - (t(\lambda).R_{s,0}(\lambda) + R_{TP}(\lambda))]/[R_{s,T}(\lambda) - R_{s,0}(\lambda)] \\ &= (S_4 - S_2)/(S_3 - S_1) \end{aligned} \tag{7.14}$$

If the area that the radiometer sees is sufficiently small, this technique provides a convenient method of measuring the uniformity of transmission over the aperture of the test piece. All that this requires is a convenient method of scanning this small area across the aperture of the test piece. Examples of such scans are shown in Figure 7.13. These were obtained using a radiometer that had a motorized scanning base.[4]

We note that in practice it will be more convenient not to change the temperature of the blackbody, but to leave it at the above ambient temperature T. To do this, it will be sufficient to use a plate at ambient temperature, that has a high-emissivity surface, as the ambient source and to position it in front of the blackbody as required.

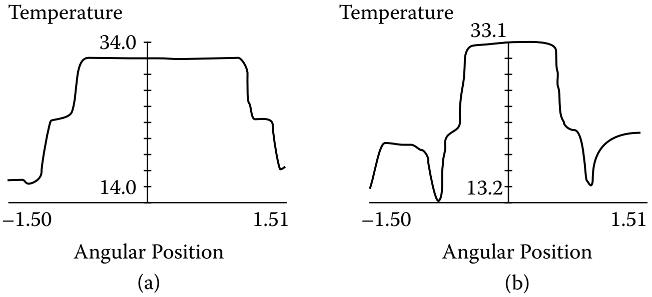

FIGURE 7.13 Examples of transmission scans across the aperture of two infrared optical systems using a radiometer. The central portion is the lens aperture. (a) 50 mm objective. (b) ×3.75 telescope.

© 2009 by Taylor & Francis Group, LLC

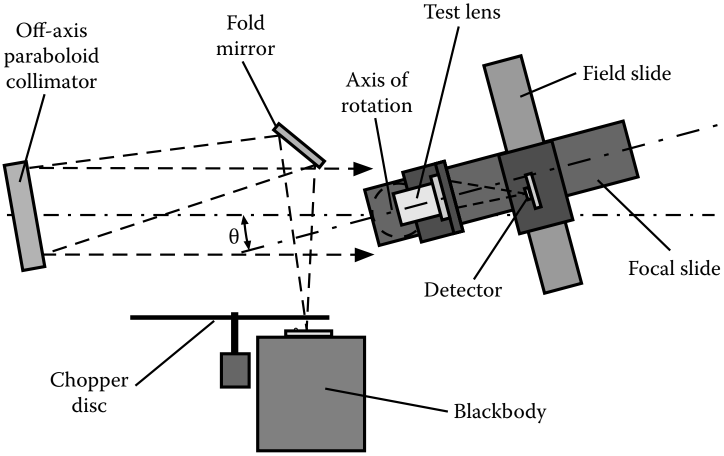

FIGURE 7.14 Arrangement for measuring relative field irradiance using a camera bench.

7.3.7 RELATIVE FIELD IRRADIANCE

This is defined in Section 4.2.6. An arrangement using a camera bench for measuring this parameter is illustrated in Figure 7.14. The detector is placed at the focus of the test lens and a small blackbody source is positioned at the focus of the collimator. The image of the source at the detector must overfill the latter. Measurements are made by recording the detector signal as the field angle θ is varied in steps over the full FOV of the test piece. As θ is varied the source will have to be moved to different positions along the field slide so that its image remains coincident with the detector. If the signal at a field angle θ is given by $S(\theta)$, then the relative field irradiance is given by

$$I(\theta) = S(\theta).\cos(\theta)/S(0) \tag{7.15}$$

An alternative arrangement for measuring relative field irradiance is illustrated in Figure 7.15. In this case the arrangement is similar to that used for making

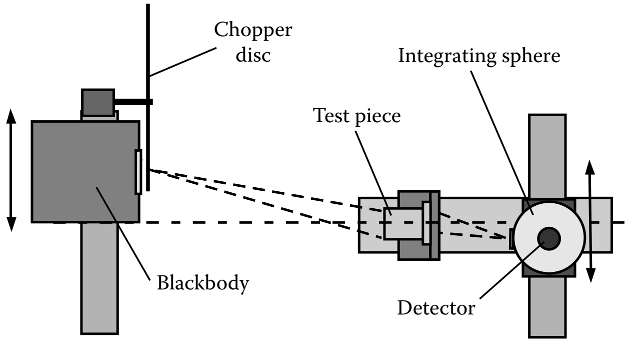

FIGURE 7.15 Arrangement for measuring relative field irradiance.

© 2009 by Taylor & Francis Group, LLC

measurement of other parameters at finite conjugates and consists of two slideways parallel to each other, on one of which is supported a blackbody cavity source and on the other an integrating sphere and detector combination. The test piece is supported between the two slideways, arranged so the image of the source is in focus at the input port of the integrating sphere. Measurements are made by recording the detector signal as the object field position h and corresponding image position h' are varied in steps over the full FOV of the test piece. As the position of the source is varied, the integrating sphere will have to be moved along the field slide so that it remains in coincidence with the image of the source.

For the situation where the input port of the integrating sphere is always larger than the image of the source and the detector signal at an image position h' is given by $S(h')$, the relative field irradiance is given by

$$I(h') = S(h').\cos(\theta)/S(0) \tag{7.16}$$

where θ is the angle the source makes with the optical axis of the test piece, i.e., $\theta = \tan^{-1}(h/(\text{object conjugate}))$.

For the situation where the input port of the integrating sphere is always smaller than the image of the source, and if the detector signal at an image position h' is given by $S(h')$, the relative field irradiance is given by

$$I(h') = S(h')/S(0) \tag{7.17}$$

7.3.8 VEILING GLARE

The veiling glare of optical systems is traditionally measured using the black spot technique and characterized by the veiling glare index.[1,5] The concept is to have as an object a central spot or area that emits no radiation surrounded by a large area that radiates uniformly. The veiling glare index (VGI) is a measure of the irradiance in the image of the black spot as a percentage of the irradiance in the image of the surrounding area (see Figure 7.16). As far as the author is aware, no equipment for measuring VGI at thermal wavelengths has been described in the literature. Some possible techniques are described here.

The first of these is illustrated in Figure 7.16. The black spot is effectively the aperture of a blackbody cavity designed to have an emissivity at the wavelength of interest >99.9% (i.e., an effective reflectance <0.001). This is surrounded by a metal screen coated with a diffusely and highly reflecting surface (e.g., gold, aluminum, or silver) and occupying the full FOV of the test piece. The screen is irradiated as uniformly as possible by radiation from either a bank of synchronously modulated infrared sources or a more powerful chopped source via a suitable optical system, and serves as the radiating surround. The irradiance in the image of the black spot and that in the image of the surround is measured using a suitable aperture, collecting optics (if necessary), and detector. Typically the image of the black spot should have a diameter of approximately 1/6 of the image format diagonal, and the diameter of the measuring aperture should be of the order of 1/5 the image of the black spot.

© 2009 by Taylor & Francis Group, LLC

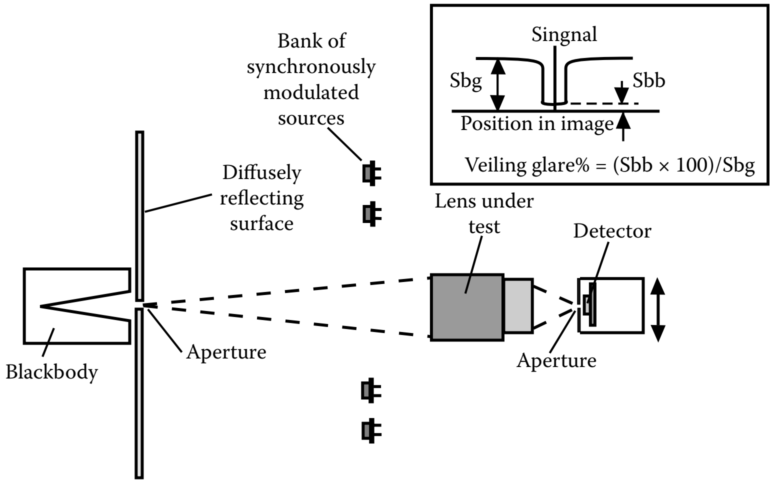
Bank of synchronously modulated sources
Singnal
Sbg
Sbb
Position in image
Veiling glare% = (Sbb × 100)/Sbg
Diffusely reflecting surface
Lens under test
Detector
Blackbody
Aperture
Aperture

FIGURE 7.16 Arrangement for measuring veiling glare index.

In a modification of this method, the test target again consists of a small circular area of high emissivity (e.g., a blackbody cavity) that is maintained at a constant temperature and is now surrounded and insulated from a large high-emissivity area that fills the FOV of the imager and whose temperature one can change within a fairly short time period.

There are several ways in which a suitable arrangement can be configured. One of these is to have two separate background plates that are sequentially interchanged. A further alternative is to use a single background plate whose temperature can be varied. The technique would be to measure the relative irradiance (i.e., detector signal) in the image of the black spot and then in that of the surround, as the temperature of the surround is increased. The two curves of relative irradiance (i.e., for the blackbody cavity and the heated surround) versus temperature of the surround should be very nearly linear, and their ratio, expressed as a percentage, will be the VGI.

In all cases the technique consists in measuring the difference of the apparent radiance (or temperature) in the image of the central cavity as the temperature of the surround is varied from one close to that of the central cavity to some much higher temperature. The ratio (usually expressed as a percentage) of this difference to the radiance of the background is referred to as the veiling glare index, i.e.,

$$\mathrm{VGI\%} = (S_2 - S_1)*100/(S_4 - S_3) \tag{7.18}$$

where S_1 and S_2 are the relevant radiances (or simply the detector signals) of the central cavity, and S_3 and S_4 are those of the surround.

7.3.9 NARCISSUS

This is usually characterized in a thermal image by a dark central region of the image when viewing an object that has a uniform radiance. It is a function of the design of

© 2009 by Taylor & Francis Group, LLC

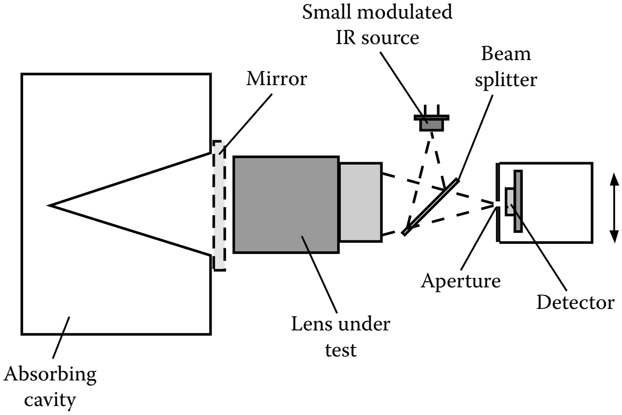

FIGURE 7.17 Arrangement for measuring narcissus index.

the optical system that forms the image and of the quality of the coatings on the optical surfaces, as well as the characteristics of the detector. The effect can be thought of as arising from reflections at one or more of the optical surfaces producing an image of the cold detector back onto the image plane. The magnitude of the effect will depend on how close to focus on the image plane the one or more reflections are and how intense the reflections are. The causes are in fact similar to those that give rise to veiling glare, and as far as the author is aware, no equipment for measuring narcissus has been described in the literature. A possible and untried technique for evaluating the contribution of a lens to this parameter is described briefly here.

The arrangement is illustrated in Figure 7.17; it uses a small modulated infrared source that, via a beam splitter, is effectively at the focus and on the optical axis of the test piece, and an aperture and detector arrangement that is directly in the image plane of the test piece. Measurements are made by first placing an absorbing surface at the entrance aperture of the test piece and scanning the detector across the image plane and recording the maximum and minimum signal values, and then repeating the procedure with a mirror surface placed at the entrance aperture of the test piece with its surface at right angles to the optical axis. For the purpose of this technique the narcissus index (NI) is defined as

$$\mathrm{NI} = (S_{\max} - S_{\min})/(S_{\max,0} - S_{\min,0}) \tag{7.19}$$

where $S_{\max}$ and $S_{\min}$ are the maximum and minimum signals with the absorbing surface at the entrance aperture of the test piece, and $S_{\max,0}$ and $S_{\min,0}$ are the same values when a mirror surface is placed at the entrance aperture of the test piece.

7.3.10 MTF (SEE ALSO SECTION 4.2.7)

This is one of the most important performance parameters of an optical system, and there are several different techniques that can be used for its measurement.[1] The

© 2009 by Taylor & Francis Group, LLC

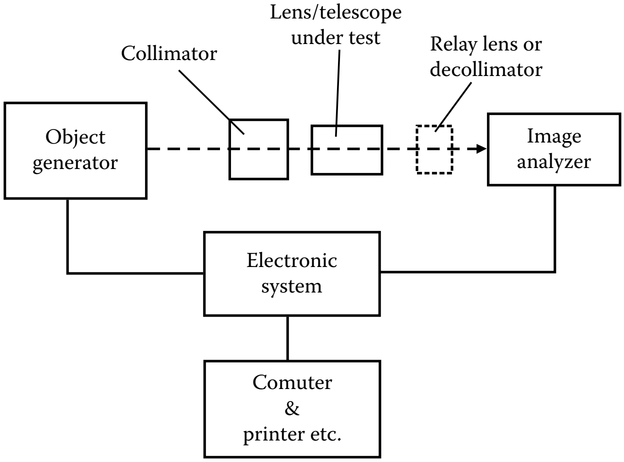

FIGURE 7.18 Block diagram of a typical MTF system.

simplest and most reliable of these is to use a narrow illuminated slit, or equivalent, as the test object and measure the distribution of radiation across the image of the slit (i.e., the LSF) by scanning the image with another slit (parallel to the first) followed by a detector system to measure the radiation passing through the latter. The measured LSF is then digitized and processed in a PC to arrive at the MTF.

The processing basically does a Fourier transform of the LSF and then corrects this for the finite widths of the two slits by applying the reciprocal of their own Fourier transforms to that of the LSF. The basic arrangement is illustrated in Figure 7.18; it includes an *object generator* that provides the slit object (normally with a chopper disc to modulate the radiation from the slit), a *collimator* so that the measurement is made with an infinite object conjugate, and the *lens* under test that forms an image of the slit target on the input slit of the image analyzer (via a de-collimator if testing a telescopic objective). The LSF is measured by scanning the *image analyzer* assembly (this incorporates the image slit and the detector). Measurements can of course be made at finite conjugates, particularly if this is representative of how the test piece will be used, and rather than scanning the slit in the image plane, the measurement can be made by scanning the object slit. The latter has the advantage that the required scan steps can be coarser in this position than in the image plane, but the disadvantage that if one requires the spatial frequency scale to be expressed in units in the image plane, the relationship between distance measured in each plane must be calibrated. The spatial frequency scale for afocal systems is usually expressed in angular units in object space, and in this case scanning the object slit is an advantage.

7.3.10.1 Testing Image-Forming Objectives

A complete test facility designed to measure MTF at various positions in the field of view must include a precise mechanical arrangement for varying the field angle, for moving the image analyzer over a flat image plane at right angles to the optical axis

© 2009 by Taylor & Francis Group, LLC

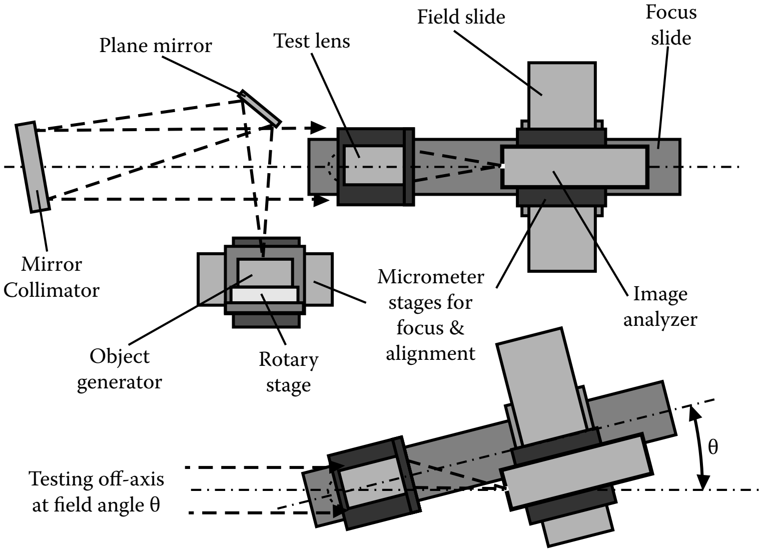

FIGURE 7.19 Typical MTF bench arrangement for testing on-axis and off-axis.

of the test piece, and finally, for accurately adjusting the focus. Such a facility for testing with an infinite object conjugate is the camera bench, described in Section 7.3.1 and illustrated in Figure 7.4. Figure 7.19 is a more detailed illustration of the complete optical bench arrangement, while Figure 7.20 is a photograph of an actual optical bench system. It consists of the assembly referred to as the object generator at the focus of an off-axis mirror collimator (see Section 6.5.2) and the camera bench on which are mounted the test piece and the assembly referred to as the image analyzer.

A typical object generator will consist of a slit, or a set of interchangeable slits, illuminated with appropriate infrared radiation, a chopper disc and motor to modulate the radiation and including a reference signal pick-off, a means of scanning the slit controlled from the PC, and finally, a means for varying the orientation of the slit. The complete assembly will be mounted on a slideway to allow it to be correctly set with respect to collimator focus. Figure 7.21 illustrates the arrangement of an object generator designed by the author[1] that has proved very successful for measuring MTF and other performance parameters of infrared lenses over many years. Rather than a slit, the system uses a nichrome wire heated by an electric current as the source (see Figure 6.2). The source is mounted on a linear bearing and can be scanned using a stepper motor that drives a micrometer thread. The orientation of the slit is varied by rotating the complete assembly about a horizontal axis passing through the center of the hot wire (when the wire is in the center of its scan position). The rotation can either be achieved manually or be driven by another stepper motor controlled from the PC.

The image analyzer used in the same system is illustrated in Figure 7.22. It consists of an interchangeable slit with a large NA multielement optical system that

© 2009 by Taylor & Francis Group, LLC

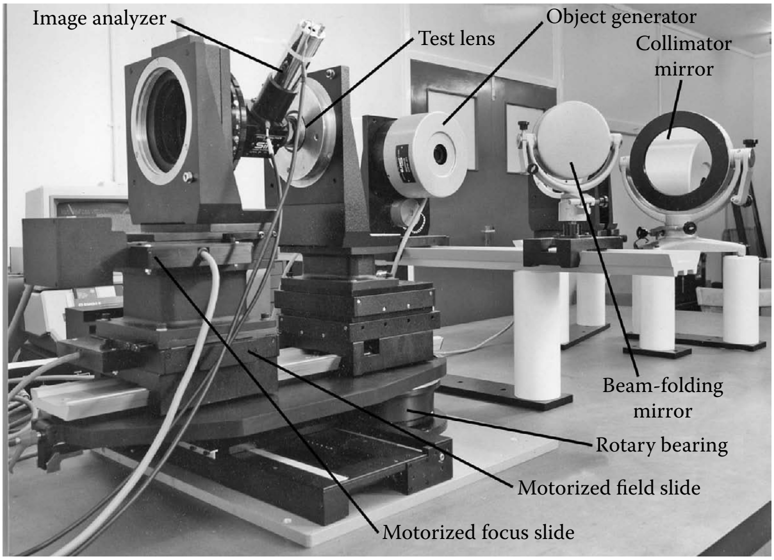

FIGURE 7.20 An optical bench system for measuring MTF of thermal imaging camera objectives.

collects the radiation passing through the slit and images it onto an infrared detector. For the 3–5 μm range a thermoelectrically cooled cadmium mercury telluride (CMT) detector is used and the lens elements are all made from Si. For the 8–12 μm range a liquid nitrogen (LN_2)-cooled CMT detector is used and the lens elements

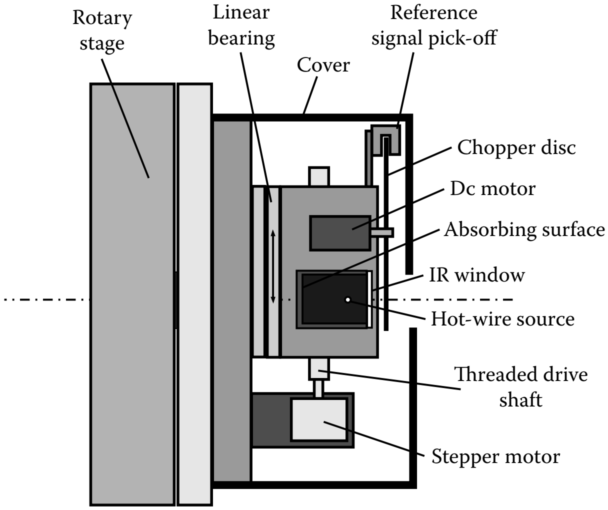

FIGURE 7.21 Diagrammatic illustration of the arrangement of an object generator.

© 2009 by Taylor & Francis Group, LLC

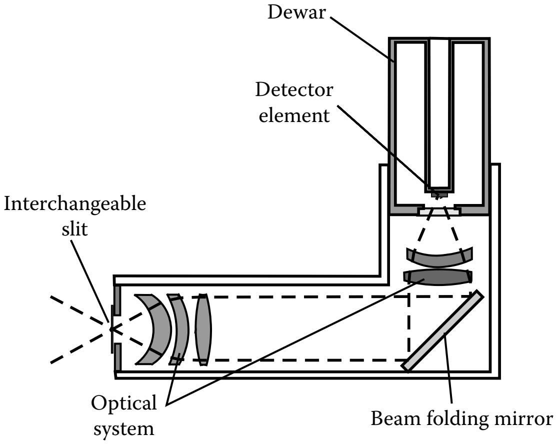

FIGURE 7.22 Example of an image analyzer using a bulk-cooled IR detector.

are all made from Ge. The collecting optics needs to have a high NA since not only must it be greater than the NA of the test piece, but it must allow for the fact that for off-axis measurements the radiation will enter the slit at an angle. The arrangement described above had an NA of approximately 0.85. A particular feature of this optical system is that it is designed to have a long tube length in order, when necessary, to reach images that would normally be difficult to access. The means for rotating the slit was to rotate the complete assembly in a bearing with its axis horizontal and passing through the center of the slit. Rotation could be manual or motorized using a stepper motor controlled from the PC. A point to note is that when a detector with an LN_2 Dewar is used, the slit can be mounted at 45° to the Dewar, so that when the slit is rotated from the vertical to the horizontal position, the Dewar tilts from 45° in one direction to 45° in the other direction and the LN_2 does not spill out of the top.

The image analyzer is mounted on the field slide via a micrometer stage that can be manual or motorized and is used for fine focus adjustment. Since, as mentioned earlier, the image format diagonal for most test pieces is less than 50 mm, it is convenient to use a micrometer stage for the latter. If this is motorized, it can be used for measuring the LSF using a scan in image space.

It is usual to test lens systems in the on-axis position and, in at least one or two positions either side of the axis (e.g., at 1/3 and 2/3 the full FOV), and to do measurements with the slits both vertical (i.e., the tangential MTF) and horizontal (i.e., the radial or sagital MTF). For a more comprehensive evaluation of the test piece the unit should be evaluated across more than one image diagonal (e.g., two diagonals at right angles to each other). This can be done by mounting the test piece in a precision bearing that allows it to be rotated about its optical axis, or by using a periscopic mirror system between collimator and test piece, with the second mirror in the periscope adjustable about a horizontal axis so that the collimator beam can be rotated in a vertical direction. The image analyzer then also needs to be adjustable about a vertical direction.

© 2009 by Taylor & Francis Group, LLC

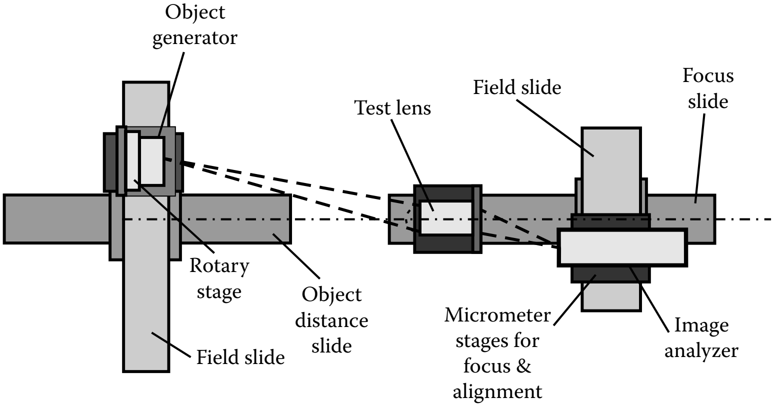

FIGURE 7.23 Testing at finite conjugates.

For making measurements at finite conjugates the bench arrangement shown in Figure 7.23 can be used. The object generator and image analyzer are now supported on two parallel slideways that can themselves be supported on a single long slideway running orthogonal to both of them and on which the test piece itself can be supported. Alternately, as shown in the diagram, two separate slideways can replace the single slideway, with the test piece supported on the same slideway as the cross slide that carries the image analyzer. Other details of the arrangement are similar to those for the infinite conjugate bench.

The finite conjugate bench arrangement will frequently be suitable for testing lenses designed for use at infinite conjugates provided the object conjugate is greater than about ×20 the focal length of the lens, although a shorter object conjugate may be sufficient for some lens designs. This has the advantage that no collimator is required. One disadvantage is that in order to measure focal length accurately with such an arrangement, a more complicated procedure must be adopted. One of these is based on the use of what is referred to as Newton's equation, which is usually written as

$$x.x' = f.f' \tag{7.20}$$

where x and x' are the distance of the object and image from their respective infinite focus positions, and f and f' are the respective focal lengths (both the same in air, except for the sign). This equation can be rewritten as

$$x' + \Delta x' = -f^2[1/x + \Delta(1/x)] \tag{7.21}$$

where $\Delta(1/x)$ is a change in the value $1/x$, and $\Delta x'$ is the change in x' that this produces. A plot of $\Delta x'$ as a function of $\Delta(1/x)$ will yield a straight line with a slope equal to $-f^2$. This procedure allows the focal length to be measured without knowing the object or image distances, but merely accurately measuring the change in the image distance produced by a measured change in the object distance.

© 2009 by Taylor & Francis Group, LLC

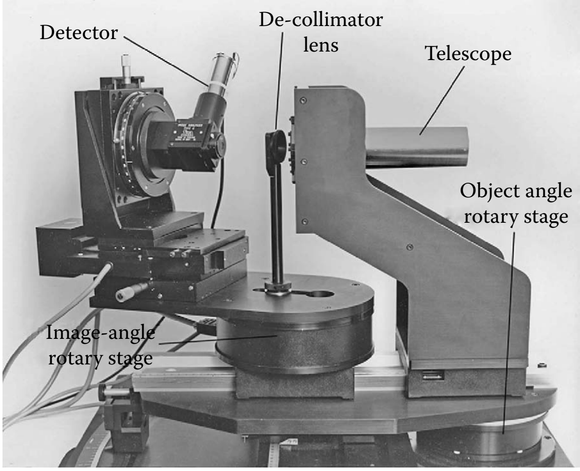

FIGURE 7.24 Bench arrangement for test afocal systems both on-axis and off-axis.

7.3.10.2 Testing Afocal Systems

The bench arrangement for testing this type of optical system will be different from that used for testing image-forming objectives, although the object generator and image analyzer assemblies will be the same. The arrangement is virtually the same as that described in Section 7.3.2 for measuring angular magnification, and illustrated in Figures 7.5 and 7.6. Figure 7.24 shows an actual bench arrangement for testing a telescope both on-axis and off-axis.

There are several alternative techniques and bench arrangements for measuring MTF, and a comprehensive description of these will be found in Williams.[1]

7.3.10.3 Measuring MTF with a Detector Array or Thermal Imager

The equipment described above measures the LSF by mechanical scanning of either the image analyzer or the object generator line source. The mechanical scanning requirement can be removed by using either a linear or two-dimensional (2D) detector array (i.e., a thermal imager) to scan the image of the slit to obtain the LSF. If the array or imager is positioned at the image, or short conjugate, side of the test piece, a well-corrected (i.e., diffraction-limited) lens objective with a high NA is required to relay a magnified image of the LSF onto the detector array since most arrays will not on their own have a sufficiently high resolution.

This has the advantages listed above for scanning the image analyzer, but the big disadvantage of requiring a high NA lens with the necessary performance at the desired wavelength. A better solution is to place the detector array (i.e., the image analyzer) at the focus of the collimator and place the illuminated (the object generator) slit in the focal plane of the test piece. The design of the latter would be similar to that of the image analyzer described above, but with a small heated ceramic source replacing the detector and including a remotely operated shutter. The detector array could be used without a lens or in conjunction with a low-magnification objective, with an NA slightly greater than that

© 2009 by Taylor & Francis Group, LLC

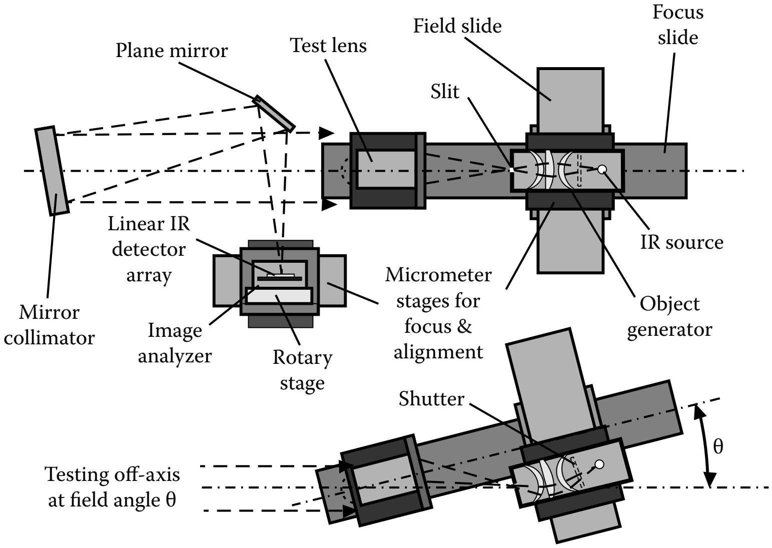

FIGURE 7.25 MTF system using a detector array.

of the collimator and corrected for use only on-axis. We note that an array with pixels 50 μm apart would have a Nyquist limit (i.e., the highest spatial frequency it can theoretically resolve) of 10 c/mm. In practice, it would not be used for measurements up to this frequency, partly because the corrections that would have to be applied for the MTF of the array would be very great, and partly to avoid significant problems with aliasing (see Appendix B). If a 2D array is used, aliasing problems can be avoided by using a sloping slit technique,[1,6,7] and this should allow measurement up to about 6 c/mm. With linear arrays, or where the sloping slit technique is not implemented, the practical limit will be about 3 c/mm. If the focal length of the collimator was ×10 that of the test piece, this would represent a spatial frequency of 30 c/mm at the focus of the test piece. Figure 7.25 illustrates this technique for measuring MTF. A point to note with this technique is that the array will record the image of the slit surround, so that it will be necessary to record an array output with the source on and effectively off (hence the need for a shutter to be included in the source unit) and subtract the two to get the true LSF.

We note that rather than using an illuminated slit as the target for measuring MTF it is possible to use a sharp edge. The edge trace from the detector array is then processed in software to convert it to an LSF before computing the MTF. The conversion process is one of differentiating the edge trace and will tend to increase signal noise. Procedures for doing this in relation to digital still cameras and using a sloping edge technique can be found in ISO 12233[8] (2000) and can be adapted for IR measurements. A requirement will be to irradiate the edge target uniformly over an extended area.

7.3.10.4 Removing a Pedestal or dc Offset from the LSF

In many situations the measured LSF will sit on a pedestal that can be the result of a chopper with blades that are not exactly at the same temperature as the background

© 2009 by Taylor & Francis Group, LLC

to the slit target, or the result of a dc offset due to dark current in a scanning array or a residual offset in the processing electronics. This should be subtracted from the measured LSF before processing the latter to determine the MTF. In most cases it is sufficient to determine the best-fit line that passes through a small percentage of the measured points at each end of the measured LSF and to subtract this from the latter. In certain cases the pedestal may be very nonlinear and can be measured in the same way that the LSF is measured, but with the source switched off.

When removing a pedestal it is necessary to ensure that it is a pedestal and not part of the real LSF. Poorly corrected lens systems can have an LSF with a very extended skirt. The effect of a positive pedestal will be to produce a rapid drop in MTF at low spatial frequencies, while a negative pedestal will produce a rise in MTF at low frequencies.

7.4 DETECTORS AND DETECTOR ARRAYS

7.4.1 Responsivity

The responsivity, R, of a detector is a measure of the output signal for an incident energy of 1 watt. Its value will depend on a number of variables, including the wavelength of the radiation, the characteristics of the electrical circuit used to read out the detector signal, and the frequency of modulation of the input radiation, if in fact modulated radiation is used (in practice measurements will almost always be made with modulated radiation, although this may be at very low frequencies, particularly where detector arrays are concerned). These variables must all be stated if a value of responsivity is to be meaningful.

The *absolute spectral response* is a curve showing the value of the responsivity over a range of different wavelengths, while the *relative spectral response* is the same curve normalized to unity at some specific wavelength, which is usually the wavelength of peak response. Rather than specify responsivity as a function of wavelength, we sometimes identify it as the response to the broadband radiation from a blackbody at a specified temperature (normally 500K).

To measure responsivity one requires a source that produces a known uniform irradiance at the detector. An infrared monochromator can be used as a source, but will need to be used in conjunction with a calibrated irradiance meter that preferably has a flat spectral response over the wavelength range of interest. The alternative is to use a blackbody source to irradiate the detector directly if the broadband response is being measured, or in conjunction with a set of calibrated spectral filters (calibrated for their integrated transmission) if the spectral characteristics are required.

An arrangement using a double monochromator[9] is illustrated in Figure 7.26. The arrangement incorporates several different sources that allow a large spectral range to be covered (including visible and thermal wavelengths) and includes a motorized stage on which the detector under test and the calibrated detector that measures the irradiance are mounted, so that they can easily be interchanged. The radiation can be modulated using a chopper disc placed between the source and the monochromator. If, as is frequently the case, the detector measuring irradiance has a slow response, it may be necessary to use a chopper disc whose speed of rotation can be varied over the required speed range. We note that the relevant irradiance for these measurements is that corresponding

© 2009 by Taylor & Francis Group, LLC

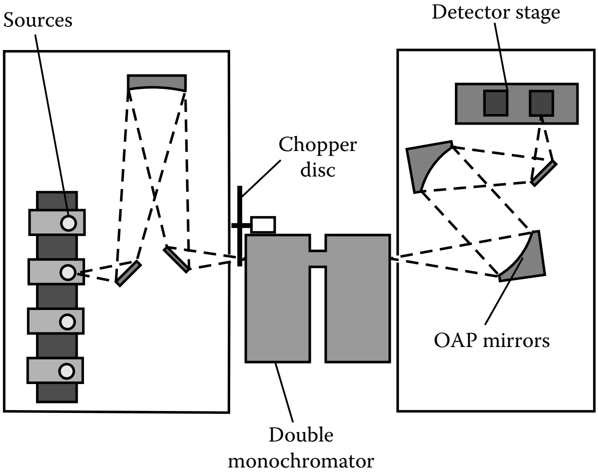

FIGURE 7.26 System for measuring the spectral response of detectors.

to the difference in radiance between seeing the source and seeing a chopper blade (or shutter, if virtually dc measurements are being made on, for instance, a detector array). For the most precise measurements this requires the temperature of the chopper blade to remain constant or the arrangement described in Section 7.2 to be used. The lens at the output aperture of the monochromator serves to image the effective exit pupil of the system onto the detector. When testing a detector array it may be necessary to test limited areas of the array at a time, so that the motorized stage may also be used for this.

An arrangement using a blackbody is illustrated in Figure 7.27. The radiance $\mathbf{W}(\lambda.T_{BB})$ of the blackbody can be calculated using Planck's equation (see Section 1.2) from a knowledge of the temperature T_{BB} of the blackbody. The maximum irradiance at the detector will be given by the equation

$$I(\lambda, T_{BB}) = \mathbf{W}(\lambda.T_{BB}).A/d^2 \tag{7.22}$$

where A is the area of the aperture placed in front of the blackbody and d is the distance between this aperture and the detector. The irradiance will be in the same units

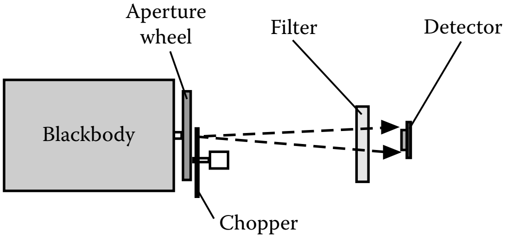

FIGURE 7.27 Measuring spectral response of detectors using a blackbody source.

© 2009 by Taylor & Francis Group, LLC

as the radiance of the blackbody, provided A and d^2 are in the same units. If, as is shown in the diagram, a spectral filter with transmission characteristics $t(\lambda)$ is positioned in front of the detector, then the total irradiance at the detector is given by

$$I_{\text{total}} = \int_{\lambda} I(\lambda, T_{\text{BB}}).t(\lambda).d\lambda \tag{7.23}$$

where the integral is over all wavelengths transmitted by the filter, and where the units of I_{total} will be watts m^{-2}, assuming these are the units used in calculating the radiance. The total number of watts falling on the detector will of course be I_{total} multiplied by the area of the detector in m^2.

The actual alternating current (ac) radiation that the detector sees will be the difference between the radiation it receives from the blackbody and the radiation it receives from the chopper blade. The radiation it receives from the chopper blade can be calculated in the same way by replacing the blackbody temperature by that of the chopper blade, which in most situations will be very approximately ambient temperature. Although the plate in which the aperture is located will not contribute to the ac signal, since the radiation from it will not be modulated, the dc radiation can affect the operating characteristics of the detector, particularly if it gets heated by the blackbody. To prevent this, the plate can be kept at ambient temperature by circulating water from a temperature-controlled water bath through a pipe attached to the back of the plate. Using a chopper blade, or shutter, that has a low emissivity on the surface facing the blackbody and a high emissivity on the other side will help to keep the temperature of the chopper blade, or shutter, constant. The full spectral characteristics of the detector responsivity can be determined by using a set of narrowband spectral filters of different central wavelengths.

Points to note about the measurement are that the modulation should be close to being square wave, which implies that the chopper blades will be large compared to the diameter of the aperture in front of the blackbody, and that the calculations described above relate to the amplitude of the ac signal and not its average value.

7.4.2 DETECTIVE QUANTUM EFFICIENCY (DQE)

DQE is defined in Section 4.3.1. It is calculated from the same data that are used to determine the responsivity, except that the incident radiation on the detector has to be converted to photons per second and the basic signal from the detector to electrons per second. Watts convert to photons per second using the relationship

$$\text{Photons/s} = \text{watts}.\lambda/h.c \tag{7.24}$$

where c is the velocity of light and h is Planck's constant. The latter has a value of 6.626×10^{-34} Joules/s, while $c = 2.998 \times 10^8$ meters/s. The units used for λ must be meters in this case. Electric current in amps converts to electrons/s using the relationship

$$\text{Electrons}/s = \text{amps}/e \tag{7.25}$$

where e is the charge on the electron in units of Coulombs ($e = 1.602 \times 10^{-19}$).

© 2009 by Taylor & Francis Group, LLC

7.4.3 RMS Noise

This is defined in Section 4.3.2. It is normally measured with the detector exposed to unmodulated ambient radiation. Measurements are made using a voltmeter or ammeter equipped to measure RMS values. To measure the noise spectrum one can again use a suitable voltmeter or ammeter equipped to measure this quantity. Suitable instruments frequently come in the form of digital scopes. Alternately, both parameters can be measured on a PC equipped with suitable software, together with a means of digitizing the detector signal. The noise spectrum is derived from the noise signal by doing a Fourier transform of the latter.

When dealing with arrays, one may need to differentiate between two forms of noise. One of these is the time-varying or temporal noise, while the other is the result of the different responsivity and dark signal characteristics of individual detectors and is usually referred to as fixed-pattern noise. A technique used by the author for differentiating between the two is to measure temporal noise by grabbing two frames of data from the array in a PC frame store and subtracting them from each other and then performing the noise analysis on the result. Subtracting the two frames will remove the fixed-pattern noise; however, the noise in the resulting frame will be increased by a factor of $\sqrt{2}$, and this must be allowed for in the computations. Fixed-pattern noise can be measured by averaging together a large number of frames to remove the temporal noise.

Measurements of noise will in practice show relatively large differences from one measurement to the next, and a large number of measurements must be averaged together to obtain consistent results.

Important points to note in measuring noise are that a very low noise preamplifier of known gain is required, and that it must have a sufficiently large bandwidth to cover the range of frequencies necessary.

7.4.4 Noise-Equivalent Power (NEP)

This is an important parameter of a detector and is defined in Section 4.3.4. If the responsivity, R, of the detector and the RMS noise are known, then the NEP is simply given by

$$\mathrm{NEP} = (\mathrm{RMS\ noise})/R \tag{7.26}$$

Since R is a function of wavelength as well as modulation frequency, and since the RMS noise will be a function of frequency and frequency bandwidth, a value for the NEP must be characterized by these variables.

7.4.5 Frequency Response

This is a measure of how the responsivity varies with the frequency of modulation of the incident radiation. There are several ways in which this can be determined. Probably the most straightforward is to irradiate the detector with a very short pulse of radiation and then to do a Fourier transform of the detector signal measured as

© 2009 by Taylor & Francis Group, LLC

a function of time. The process is similar to that of measuring the MTF of an optical system using a slit object and then doing a Fourier transform of the image of the slit (see Section 7.3.10). The calculated amplitude response can be corrected for the width of the pulse (assuming it is a rectangular-shaped pulse) by dividing the calculated transform by $\sin(\pi.w.\upsilon)/(\pi.w.\upsilon)$, where w is the width of the input pulse in seconds and υ is frequency in Hz. If the preamplifier does not have a flat frequency response over the frequency range required, then a similar correction can be applied for this. We note that the width of the pulse must be sufficiently narrow for $1/w > \upsilon_{\mathrm{max}}$, where the latter is the maximum frequency of interest

Since the frequency response will not normally be a function of wavelength, a source such as a pulsed light-emitting diode (LED), pulsed laser diode, or pulsed laser can be used. Obviously, these sources must operate at a wavelength within the spectral response range of the detector (see Section 6.2.9 for suitable devices). Where measurements are required up to very high frequencies a special arrangement may be needed to achieve a suitably short pulse. An electro-optic or acousto-optic modulator can be used to generate very short pulses in a laser beam. Alternately, one can consider using a galvanometer mirror or rotating mirror to sweep the laser beam across a narrow slit aperture positioned ahead of the detector. A similar technique could also be used with other sources, but a suitable optical system will normally be needed both to focus the source on the slit and to focus the slit into the plane of the detector, to ensure that the pulse contains sufficient energy.

When measuring frequency response, care should be taken not to operate the detector in a region where it is reaching saturation.

7.4.6 MTF

The various aspects of the MTFs of detectors are discussed in Section 4.3.10. The technique for measuring the MTF of a detector will depend to a certain extent on whether it is a single-element detector, a linear array, a linear array with time delay and integration (TDI), a SPRITE detector, or a 2D staring array. Common to all measurements is the requirement to project the image of a narrow illuminated slit onto the detector. The width w' of the image of the slit projected onto the detector must be such that $w' << 1/s$ ($1/s$ is the width of a slit whose MTF goes to zero at a frequency s), where s is the maximum spatial frequency for the measurement. In practice one would wish to have $w' \leq 1/(2.s)$, so that to measure up to, say, 25 c/mm a width of 20 μm or less would be acceptable. In addition to this the lens that projects the image onto the detector must have an MTF with a cutoff well above the maximum frequency s. If we assume that it is acceptable to have a lens with a cutoff frequency that must be greater than twice s, then the NA of the lens on the image side will be given by $\mathrm{NA} > s.\lambda$. Taking the same example we used above and assuming $\lambda = 0.01$ mm, we find that $\mathrm{NA} > 0.25$ is required; i.e., the lens must have an aperture equivalent to at least *f*/2 on the image side.

7.4.6.1 Slit Scan While Monitoring the Output of a Single Element

An arrangement for measuring the LSF of single-element detectors and linear, or 2D, detector arrays, and overcoming any problems associated with aliasing, is illustrated

© 2009 by Taylor & Francis Group, LLC

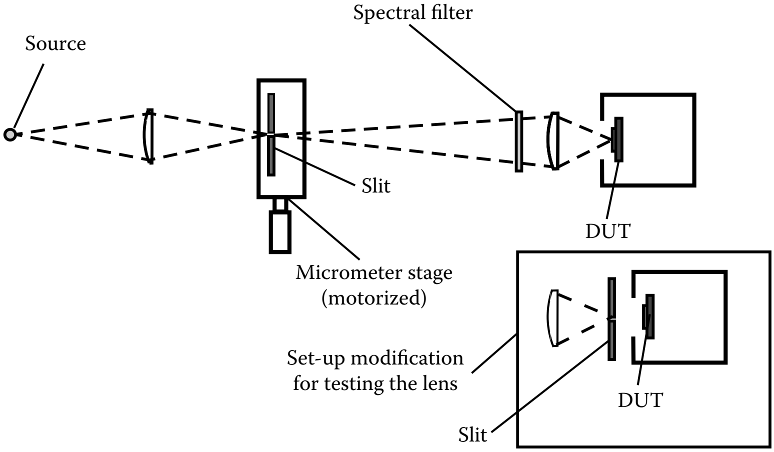

FIGURE 7.28 Arrangement for measuring the MTF of a detector/detector array.

in Figure 7.28. The technique is to monitor the signal of the single-element detector, or that of a single element of the linear or 2D array, as the image of a slit is scanned in steps across the detector or detector element. In fact, the scan will need to extend over a distance greater than the extent of the element in question, since cross talk between detector elements will affect the LSF. The criterion for deciding how far to scan is that the scan must extend far enough that the signal at each end of the scan must be at the signal level obtained when the source is off (strictly speaking, when the source temperature is the same as ambient temperature). A further requirement of the measurement is that the step size used for the scan must in theory be less than half the width of the element, although in practice it should not be greater than approximately 1/6 the width, but preferably not greater than 1/10 the width. A check that the step size is sufficiently small is to vary the position of the steps relative to the detector element. This should not change the MTF calculated from the LSF. The MTF must of course be corrected in all cases for the effective width of the image of the slit on the detector, as well as the MTF of the lens that forms the image.

The insert in Figure 7.28 illustrates how the combined MTF of the lens and object slit can be measured by a small modification of the arrangement using the same detector and with the addition of another slit.

7.4.6.2 Slit and Array Scan Technique for Linear and 2D Arrays

We note that where an array is concerned, an LSF can be measured by reading out the signal from each of the elements along a line of the array, using a stationary slit image. However, because of the aliasing problems associated with the undersampling that occurs in this case, the measured LSF and the MTF calculated from it will vary depending on the exact position of the slit image with respect to the array elements. The technique described above overcomes this problem by scanning the slit image across a detector element. However, this only measures the MTF of a single element

© 2009 by Taylor & Francis Group, LLC

of an array, and this may not be representative of the average MTF of the array. This can be overcome using the same arrangement used above (see Figure 7.28), except that rather than monitoring the output of a single element of the array, the LSF obtained by reading out the array is recorded for each position of the slit scan. These LSFs are then averaged together after applying a lateral shift to each one equal to the number and size of the steps taken for that particular LSF. This effectively lines up all the LSFs and measures their average shape. The MTF is determined from this, with corrections applied as above, for the width of the slit and the MTF of the lens.

7.4.6.3 Tilted (Sloping) Slit Technique for 2D Arrays

There is a method of being able to use a stationery slit image for measuring the MTF of 2D arrays. The technique is to use a slit image that extends in length over a number of rows or columns (depending on whether the slit is vertical or horizontal, respectively) and to carry out the measurement with the slit image slightly tilted with respect to the columns or rows, as illustrated in Figure 7.29.[6,7] The idea is to measure separately the LSF associated with each row (assuming the slit image is vertical) over which the slit image extends, then to calculate the position of the centroid of each LSF and, from this data (using, say, a least squares fit), determine the slope of the slit image. From knowledge of the slope each LSF is then shifted laterally to bring all the centroids into line, and the LSFs are then averaged together. The LSF obtained in this way can then be used to calculate a unique MTF that will be the same as that calculated by the slit scanning techniques described above. Here again corrections have to be applied for the MTF of the lens and the width of the slit. The same procedure is used when the slit is horizontal, except that the LSFs are measured down columns rather than along rows. Strictly speaking, the width of the slit used for calculating the correction must itself have a correction made to it for the angle of tilt used. If the actual width of the slit in the image plane is w, the slit width to use for calculating the correction will be given by

$$w' = w/\cos\phi + p.\tan\phi \tag{7.27}$$

where ϕ is the tilt angle and p is the height or width of the pixel, depending on whether the slit is vertical or horizontal, respectively. The difference this makes can be significant, particularly if ϕ is large, e.g., if $\phi = 5°$, $w = .020$ mm, and $p = .050$ mm, then $w' = 0.024$ mm. In the worst case, this could make the measured MTF lower than it should be by 0.025, a value that can be considered as just significant.

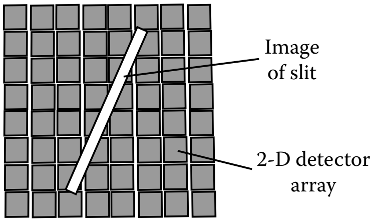

FIGURE 7.29 Sloping slit technique for measuring MTF.

© 2009 by Taylor & Francis Group, LLC

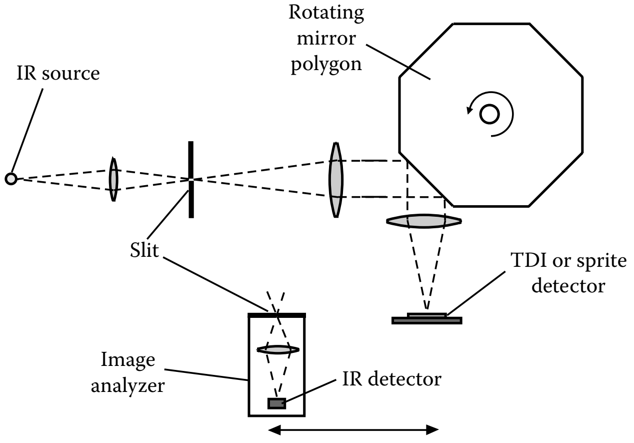

FIGURE 7.30 Arrangement for measuring the MTF of TDI and SPRITE detectors.

When using this technique the tilt and length of the slit must be sufficient that the slit image passes across several columns if the slit is vertical, and several rows if the slit is horizontal, and at a sufficient number of different relative positions across an element. A check that the arrangement is satisfactory can be made by varying the length and tilt of the slit. This should not change the MTF calculated from the final LSF.

The technique can be used with a sloping edge target rather than a sloping slit (see Section 7.3.10 and ISO 12233[8] (2000)).

7.4.6.4 SPRITE or Detector with TDI

The MTF in the scan direction of this type of detector must be measured using the image of a moving slit that simulates the same speed as the scanner will produce in the final thermal imager. Several papers have described scanning arrangements for doing this type of measurement.[1,10,11] In principle, the scanner system of a thermal imager can be adapted as a test bed for this type of detector. Figure 7.30 shows the essentials of a system for doing this type of measurement, parts of which are those of an imager that employs a mirror polygon scanner. The latter, in conjunction with two relay lenses, scans the image of a slit across the detector at a speed that can be controlled by adjusting the speed of rotation of the polygon. The system uses a commercial digital transient recorder that is triggered by pulses from the drive electronics of the rotating polygon to measure and store the output from the detector. The LSF obtained in this way goes to a computer, where the analysis to get the MTF is carried out. As usual, corrections have to be applied for the MTF of the object slit and the relay lenses. As Figure 7.30 shows, the latter can be measured by replacing the test piece with a second slit and a single-element detector (e.g., the image analyzer described in Section 7.3.10).

7.4.6.5 Random Pattern Technique

Other methods of measuring the MTF of detector arrays have been described in the literature.[1] Of particular interest are those using a random pattern as the test

© 2009 by Taylor & Francis Group, LLC

target, since these overcome the problems associated with aliasing. A method of doing this for thermal imaging lenses is described in Daniels.[12] The random target is produced in a metal film on a ZnSe substrate and is generated by a computer. The power spectrum of the original pattern and that measured by the detector array of the image of the pattern projected on it are related by the equation

$$\Phi_m(s) = \Phi_i(s).(\mathrm{MTF}_a(s))^2 \tag{7.28}$$

where $\Phi_m(s)$ is the spatial frequency power spectrum as measured by the array, $\Phi_i(s)$ is the spatial frequency power spectrum of the image of the test pattern formed on the array, and $\mathrm{MTF}_a(s)$ is the MTF of the array. We also have that

$$\Phi_i(s) = \Phi_o(s).(\mathrm{MTF}_o(s))^2 \tag{7.29}$$

where $\Phi_o(s)$ is the power spectrum of the original test pattern and $\mathrm{MTF}_o(s)$ is the MTF of the lens objective that relays an image of the test pattern onto the detector. All values of the spatial frequency s must be for image space (i.e., allowance made for magnification between target and its image).

7.4.6.6 Software Requirements

In all techniques that involve measuring an LSF by using the scan facility provided by a linear or 2D array, it is useful to have a facility that allows the operator to select what part of the array output to use for the measurement. In the case of a linear array this would be the ability to set a cursor at the start and end points on a display of the full output of the array. For a 2D linear array the cursor should be a rectangle that can be positioned around the image of the slit and whose size and shape can be adjusted to select the length and width of the area that will be used for the measurement. In all cases a facility is required for removing a background pedestal from the measured LSF (see Section 7.3.10).

Note: For all measurements made on detectors it is very important to ensure that the bandwidth of any signal processing or sampling electronics is sufficiently great so as not to affect the result of a measurement. For example, a frame grabber used to capture the output from a 2D array operating with a video bandwidth of, say, 5 MHz should have a bandwidth/sampling rate of at least 50 MHz, but preferably 100 MHz or more.

7.5 SCANNERS

Some of the performance characteristics that are relevant to scanner systems have been described in Section 4.4. To measure these it is necessary to have virtually all the elements of a complete thermal imager. For this reason, measurement techniques are the same as those for complete thermal imagers and are described in Section 8.2.

© 2009 by Taylor & Francis Group, LLC

7.6 DISPLAYS

7.6.1 LUMINANCE AND SPECTRAL CHARACTERISTICS

The luminance of a display is measured using a calibrated photometer/luminance meter. A simple photometer/luminance meter is illustrated in Figure 7.31. It comprises a lens objective that images part of the display onto an aperture behind which is a detector (usually a Si detector), which in conjunction with a special filter has a spectral response that corresponds to the photopic response of the eye, as formally defined by the Committee International d'Eclairage (CIE). A chopper can be included in the system so that the output from the detector is an ac signal, and usually a choice of several diameter apertures is provided.

If the spectral characteristics of the display are needed, a spectrophotometer is required. This can take the form of a photometer, as illustrated in Figure 7.31, but with the addition of a set of spectral filters on some form of turret. If three of these filters have the characteristics of the red/green/blue (RGB) spectral response curves (as defined by the CIE), then it will be possible to determine the RGB color coordinates of the light from the display. Alternately, a photometer with the arrangement illustrated in Figure 7.32 can be used. Here the light passing through the aperture goes to a fiber optic light guide and then onto a grating spectrometer with a linear detector array in the plane of the spectrum. The output from the array goes to a PC where the output is calibrated and can then be used to compute and display a variety of data, including watts/nm, or lumens/nm as a function of wavelength, total lumens, RGB color coordinates, etc. Both photometers and spectrophotometers are widely available commercially.

In addition to the photometer a video signal generator is required. This should have a facility for varying the luminance of the display, and if a color display is being evaluated, a facility for separately controlling the three color channels.

7.6.2 POLAR LUMINANCE DISTRIBUTION

One of the instruments described in Section 7.6.1 can form the basis of a facility for measuring how the luminance of a screen varies with the viewing angle. The only

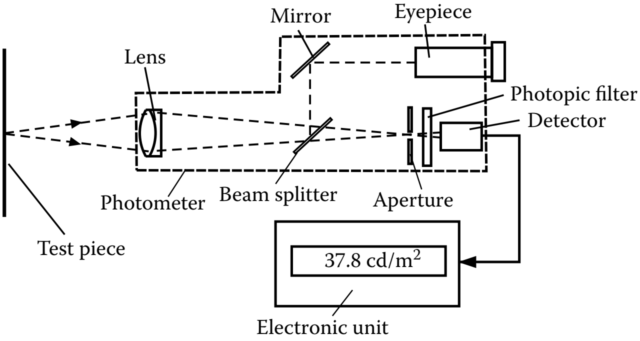

FIGURE 7.31 Basic photometer.

© 2009 by Taylor & Francis Group, LLC

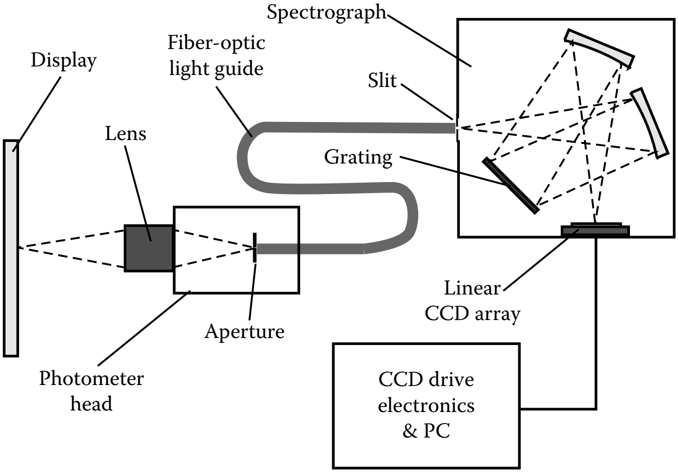

FIGURE 7.32 Spectrophotometer arrangement.

additional requirement is a facility for either rotating the screen so that the photometer views it at different angles, or rotating the photometer so that it looks at the screen at different angles. The polar characteristics can be very important, particularly in the case of liquid crystal display (LCD) and if more than one observer is required to view the display at the same time, or where one observer needs to view the display from different positions.

7.6.3 GREY SCALE/LINEARITY

Here again a photometer is required to measure the luminance of the display as well as a video signal generator. The latter should be calibrated to allow the level of the video signal to be varied in a measurable fashion. Measurements consist simply of recording luminance levels as a function of the video signal level.

7.6.4 MTF

A suitable arrangement for measuring the MTF of a display is illustrated in Figure 7.33. It includes a pattern generator that can generate a slit image on the display, a digital video camera fitted with a microscope objective and photopic filter, and finally, a PC that can capture one or more images from the camera and process them to obtain initially an LSF (for example, a plot of the luminance across the image of the slit), and from this to compute the MTF.

The exact procedure required for measuring the LSF will depend on whether the display is a cathode ray tube (CRT) or an LCD or equivalent. For the MTF of a CRT in the direction of the scan lines the pattern generator only needs to generate a stationery slit whose width at the video signal stage is known and is sufficiently narrow to allow the MTF to be measured up to the maximum spatial frequency required

© 2009 by Taylor & Francis Group, LLC

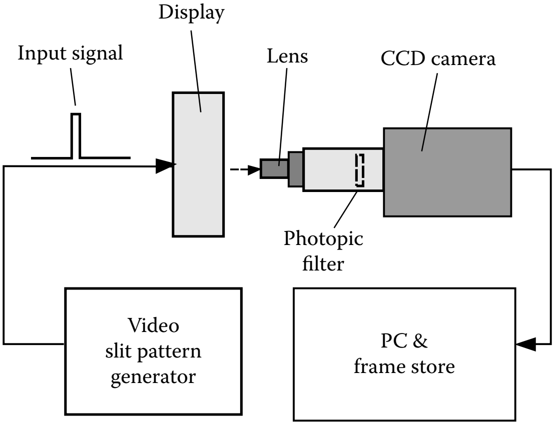

FIGURE 7.33 Arrangement for measuring the MTF of a display.

(i.e., the width $w \ll 1/s$, where s is the maximum spatial frequency). Corrections are required in the normal way for the width of the slit produced by the pattern generator and for the combined MTF of the microscope objective and video camera. The former can be measured using a calibrated scope and its temporal width then converted to a linear distance on the display, while the latter can be determined by replacing the display by an illuminated slit of known width and measuring the resulting LSF, and then computing the MTF, with the latter being corrected for the known width of the slit.

For measurements on a CRT display in the direction orthogonal to the scan lines, and for both directions on an LCD type of display, different procedures are required. The procedures are somewhat similar to those described in Section 7.4.6 for the MTF of detector arrays. In the first of these the pattern generator produces a slit of known width that can be moved in steps in the direction in which the MTF is being measured (i.e., in the direction orthogonal to the slit), while at each step the video camera measures the LSF. The LSFs are then all averaged together after applying a lateral shift to each LSF that corresponds to the number and size of the steps taken to that position. The MTF is calculated from this LSF and is corrected for the effective width of the video slit and for the MTF of the lens and camera. The alternative is to have a pattern generator that produces a stationery tilted slit and, as described in Section 7.4.6, to measure separately the LSF associated with each row (assuming the slit image is vertical) over which the slit image extends, then to calculate the position of the centroid of each LSF and from these data (using, say, a least squares fit) to determine the slope of the slit image. From a knowledge of the slope each LSF is shifted laterally to bring all the centroids into line and the LSFs are then averaged together. The LSF obtained in this way can then be used to calculate the MTF. Here again corrections have to be applied for the MTF of the lens and the width of the slit. The same procedure is used when the slit is horizontal, except that the LSFs are measured down columns rather than along rows.

A technique that can be used with all types of display for both the vertical and horizontal directions is to use a pattern generator that can produce a grating pattern on the

© 2009 by Taylor & Francis Group, LLC

display, where the video signal in the direction orthogonal to the grating lines varies sinusoidally, and where the spatial frequency of the signal can be changed, but where the amplitude of the video signal input remains constant. The arrangement is the same as that shown in Figure 7.33, except the signal generator produces a sinewave pattern rather than a slit. The MTF is determined by measuring the contrast in the sinewave pattern generated on the display, using the digital video camera. The focal length of the lens on the camera will have to be selected in order to provide a FOV that covers at least one period of the lowest spatial frequency one wishes to measure and also, in conjunction with the camera array, to have a sufficiently high MTF to be able to easily resolve the highest required spatial frequency. For normalization purposes, the contrast for zero spatial frequency is generated by measuring the display luminance with the video signal being changed between the maximum and minimum levels used for the sinewaves. For this type of measurement corrections have to be applied for the contrast of the video input signal (assuming it is not unity) and for the combined MTF of the camera and lens.

The MTF of a display can vary over its area, particularly in the case of a CRT display, and this should be considered when carrying out an evaluation. In addition to this the luminance response may be nonlinear, which means that the MTF will vary with the amplitude of the sinewave input and where on the response curve the input signal lies.

We note that whether the target on the display is a slit or sinewave (an edge can also be used), the video camera can be replaced by a suitable digital still camera (see Sections 7.3.10 and 7.4.6 and Williams[11]).

7.6.4.1 Eyepiece Displays

When the display is designed for viewing through an eyepiece or is collimated by an optical system so that it can be viewed at close quarters by the eye (e.g., in a helmet-mounted display), the same measurement procedures can be used, except that instead of using a microscope objective with the video camera, one requires an objective that will focus on an object effectively at infinity. This objective should in fact have an entrance pupil that is similar in size to that of the eye (ideally variable from 2 to 7 mm), has a performance that is virtually diffraction limited (since it is not valid to apply a correction for such a lens), and can be focused over a range of at least 1 to −4 dioptres. In addition to this, it should be possible to position the entrance pupil of the objective to coincide with the exit pupil of the display eyepiece. Finally, the focal length of the lens must be sufficiently long that the maximum spatial frequency one wishes to resolve is well within the capability of the camera. Typically, one may wish to resolve something like 2.29 c/mrad (40 c/°) at the output of the eyepiece. If the camera has an array of 0.008 mm elements the corresponding Nyquist limit will be 62.5 c/mm, and to avoid aliasing problems, it should not be used beyond a maximum of, say, 6 c/mm (for a possible error of no more than 1% in the measured MTF). The focal length of the lens should therefore be greater than $1{,}000/(6 \times 2.29) = 72.8$ mm.

A lens (de-collimator) that satisfies these requirements is likely to be something like a color-corrected doublet that would only be corrected for use over a very small field angle. If measurements are to be made both on-axis and off-axis, a mechanical facility is required to allow the camera and de-collimator lens to be rotated about an axis that passes through the exit pupil of the eyepiece. More information about testing this type of display can be found in Williams[1] and Mouroulis.[13]

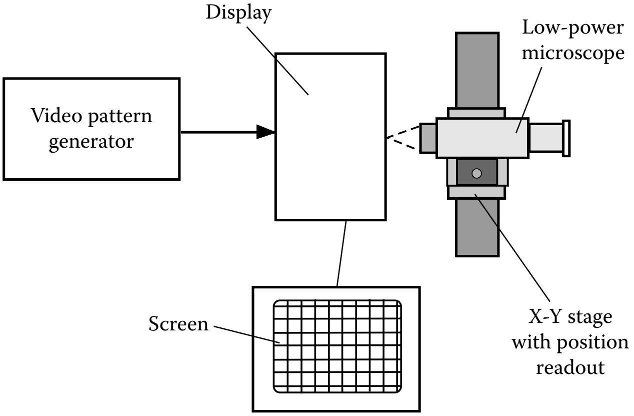

FIGURE 7.34 Technique for measuring linear distortion of a display.

7.6.5 DISTORTION

Methods of defining distortion can be found in Section 4.5.6.

This can be measured using the arrangement illustrated in Figure 7.34. It consists of a micrometer stage, which carries either a low-power microscope or a microphotometer, and enables them to moved in a plane parallel to the surface of the display and to be positioned to view any part of the latter. The input to the display should be from either a pattern generator that produces a square array of equally spaced lines or one that has controls that enable the *x*, *y* coordinates of a marker pattern to be accurately set. Distortion is determined by measuring the *x*, *y* coordinates of line intersections or marker positions as a function of the equivalent input signals.

When measuring distortion of a display that includes an eyepiece, an arrangement such as that illustrated in Figure 7.35 is required. This allows the angular position of the image to be measured as a function of the equivalent input signals.

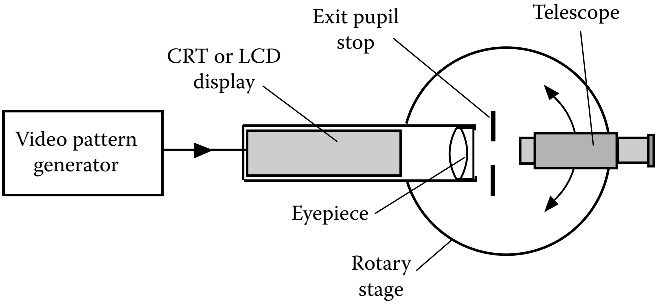

FIGURE 7.35 Measuring the distortion for an eyepiece display.

7.6.6 VEILING GLARE

The measurement technique for glare depends on whether one is measuring the glare that is generated by the display itself or the glare that comes from ambient lighting. In the former case, the method normally used is what is sometimes referred to as the black spot or black patch technique. The concept (illustrated in Figure 7.16) is to generate a pattern on the display (usually in the center) that consists of an area that, in principle, should be completely black, surrounded by a uniform bright area covering the remainder of the display area. The veiling glare index is defined as

$$\mathrm{VGI\%} = (L_{\mathrm{spot}}/L_{\mathrm{bground}}).100 \tag{7.30}$$

where L_{spot} is the luminance of the center of the black area and L_{bground} is the luminance of the bright background. The black area can be either a circular spot, a square spot, or a stripe running down the length of the display (see Figure 7.36). The major dimension of the spot or square and the width of the stripe should be approximately equal to ×0.1 the width of the display. The dimensions of the area in the black spot over which luminance is measured should be of the order of ×0.2 the major dimension of the circle or square and the width of the stripe. The exact value obtained for a measurement of VGI will depend to some extent on the shape and size of the black patch and the area of the patch used for measuring L_{spot}. These should be carefully specified when making measurements.

When assessing the glare produced by ambient lighting a different technique is required. Basically, one needs to simulate the conditions of use as far as the ambient light is concerned and, in particular, the directions from which it will be incident on the display and the relative illuminance from each of these directions. In practice, some nominal arrangement of sources will need to be defined and the glare measured on that basis.

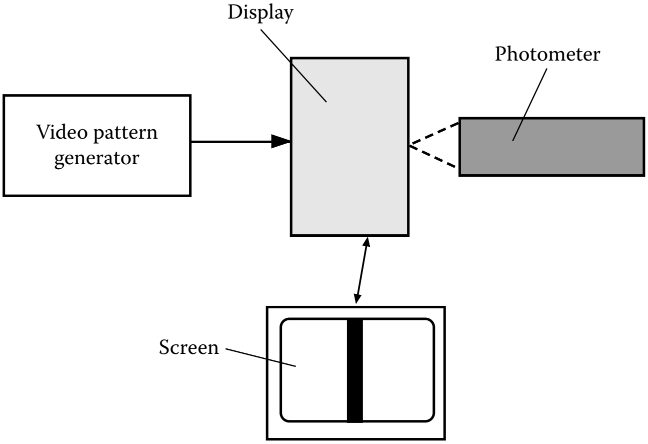

FIGURE 7.36 Measurement of VGI of a display.

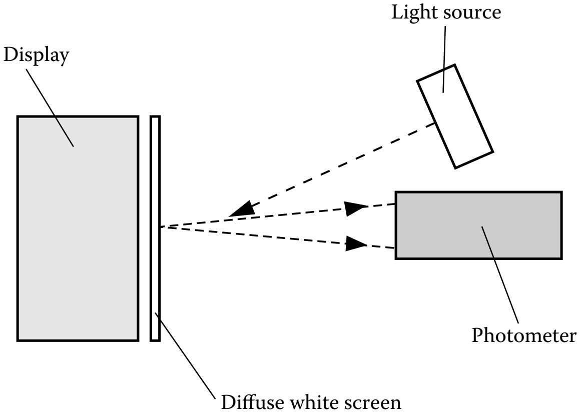

FIGURE 7.37 Measuring the AGI of a display.

The measurement technique is illustrated in Figure 7.37. The luminance of the display screen is measured with the external source on, but the display itself off. A white diffusely reflecting screen is then placed over the front of the display and its luminance measured. If the two measured luminances are L_{display} and L_{screen}, respectively, the display can be characterized by an ambient light glare index (AGI) given by

$$\text{AGI}\% = L_{\text{display}}.100/L_{\text{screen}} \tag{7.31}$$

The source should be relatively uniform and diffuse and should have an area subtending at least 10° at the display. The white screen should have a reflectance greater than, say, 95% and be close to a perfect diffuser (i.e., a Lambertian diffuser).

It is important to note that the value of AGI will depend on the angular position of the source with respect to the display as well as the angular direction in which the luminance is being measured. It may be necessary to make measurements for several source and photometer positions, but these should be typical of real conditions of use and should include worst-case configurations.

REFERENCES

1. Williams, T. L. 2000. *The optical transfer function of imaging systems*. Bristol and Philadelphia: IOP Publishing.
2. *ISO 9335: 2007 Optics and photonics—Optical transfer function—Principles and procedures of measurement.*
3. Williams, T. L. 1985. Measurement of spectral transmission of infrared lenses. *SPIE Conference Proceedings* 590:116–21.
4. Williams, T. L. 1982. Scanning radiometer for calibrating thermal imager test targets. *SPIE Conference Proceedings* 369:51–55.
5. *ISO 9358: 1994 Optics and optical instruments; Veiling glare of image forming systems; Definitions and methods of measurement.*

6. *ISO 15529: 2007 Optics and photonics—Optical transfer function—Principles of measurement of modulation transfer function (MTF) of sampled imaging systems*.
7. Williams, T. L. 1992. Measurement of the MTF of staring array imaging systems. *SPIE Conference Proceedings* 1781:347–58.
8. *ISO 12233: 2000 Photography–Electronic still-picture cameras–Resolution measurements*.
9. Theocharous, E., et al. 2003. Latest measurement techniques at NPL for characterization of infrared detectors and materials. *SPIE Conference Proceedings* 5209:228–39.
10. Braim, S. P., et al. 1983. TED (SPRITE) detector MTF. In *IEE Conference Publication*, No. 228, pp. 63–66.
11. Williams, T. L., et al. 1989. Recent advances in testing thermal imagers. *SPIE Conference Proceedings* 1110:220–31.
12. Daniels, A. D., et al. 1995. Random transparency targets for modulation transfer function measurement in the visible and infrared regions. *Optical Engineering* 34:860–68.
13. Mouroulis, P. 1999. *Visual instrumentation*. New York: McGraw-Hill.

8 Measurement Techniques and Procedures for Complete Thermal Imagers

8.1 INTRODUCTION

This section describes the techniques that can be used to measure the performance parameters of complete thermal imagers as described and defined in Chapter 5. As already indicated in the first chapter of this book, the relevance of each of these performance parameters will to some extent depend on the application intended for the imager, and in particular whether it is to be used for surveillance or temperature measurement. The techniques described in this chapter can be used by both the manufacturer of an imager in order to characterize his or her product and by the user who wishes to check that the performance of his or her imager has not deteriorated, and that it is still suitable for the intended application. Invariably, individual users may find that they need to modify the techniques that are described here, either to make use of facilities that already exist or because the actual imagers they are testing dictate the use of a modified arrangement.

Most of the measurements that are made on a thermal imager can make use of a common test facility. The essential parts of such a facility (see Figure 8.1) are a temperature-controlled blackbody or high-emissivity source, a test target arrangement where the exact nature of the test pattern will depend on the type of measurement being made, a mirror or refracting collimator, and finally, a mechanical support for the test piece that provides facilities for varying the orientation of the test piece about a vertical and a horizontal axis. In addition to this, some of the measurements will require specific software for analyzing the output from the test piece. Details of the exact requirement for each type of measurement are provided below.

We note that a collimator is not essential provided a sufficiently long throw is available in the laboratory (e.g., greater than at least ×40 the focal length of the lens objective on the thermal imager) and that the thermal imager has a facility to focus to this distance. However, a different equipment configuration is required if measurements are to be made for off-axis as well as on-axis target positions. If the imager is simply rotated about the entrance pupil of the lens objective (as shown in Figure 8.1), the object distance, and hence the best focus setting, will vary with the field angle. What is required is to mount the target and high-emissivity source on a slideway set perpendicular to the optical axis of the imager and to vary the field angle by moving the target and source along the slideway (see, for example, Figure 7.23).

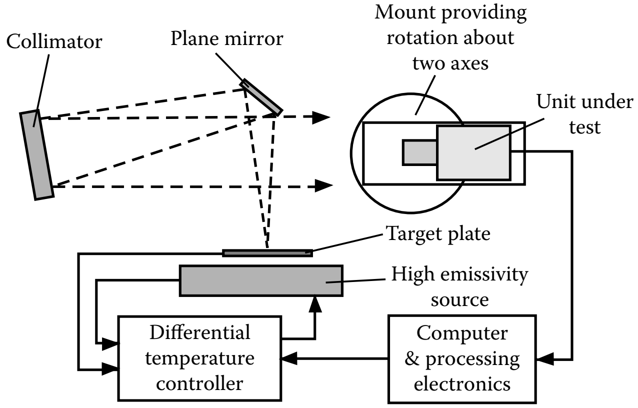
Collimator
Plane mirror
Mount providing rotation about two axes
Unit under test
Target plate
High emissivity source
Differential temperature controller
Computer & processing electronics

FIGURE 8.1 General arrangement for testing complete thermal imagers.

8.2 MTF

8.2.1 GENERAL

As indicated in earlier chapters, this is a measure of the ability of an imaging system to generate high-contrast images with fine detail (more detailed information on modulation transfer function [MTF] can be found in Williams[1]). It is a fundamental performance parameter and is one of the defining factors in some of the other performance parameters used in connection with thermal imagers and whose measurements are described below. These include MRTD, MDTD, SRF, and ARF.

The MTF of a thermal imager can be measured at the video output of the imager or off the display associated with the imager. It is frequently more meaningful to measure the MTF at the video output since the actual final working display is often not supplied as part of the imager and can be the screen of a computer, where the important processing has already been done on the video signal. The situation where it becomes relevant and important to measure the MTF off the display is when an imager is being used for surveillance purposes, or where the purpose of the imager is to generate an image that will be viewed by the eye, such as when it is used as a night flying or driving aid. Nevertheless, for a full evaluation of a thermal imager, a measure of the MTF of the system, including any display that forms part of it, will be relevant. The MTF of the imager and display can be measured separately, and the results combined to give a measure of the complete MTF.

8.2.2 MEASUREMENT FROM THE VIDEO OUTPUT

The relevant procedures are similar to those described in Section 7.4.6 for measuring the MTF of detectors. The main difference (see Figure 8.1) is that the lens is now part of the imager and contributes to its MTF and the test configuration will normally include a collimator so that the MTF measurement is effectively for an object at infinity (although, as indicated above, measurements can be made at finite conjugates if a sufficiently long throw is available between imager and target). An additional part of the measurement facility is a rotary stage on which the imager can be supported and that allows the MTF to be measured in different parts of the horizontal FOV. This should include a facility for making small adjustments in a vertical plane, but can include a facility for rotating the imager through larger angles in a vertical plane to allow the full FOV to be accessed. If accurate angle measurements are not required, the imager can be mounted on a standard tripod with the usual adjustment facilities. A display of the thermal image will show the position of the test target in the FOV. If a collimator is not used, a different optical bench arrangement, i.e., one designed for testing at finite conjugates, may be required (see Section 8.1).

The three techniques described in Section 7.4.6—slit scan while monitoring the output of a single element, slit and array scan technique for linear and two-dimensional (2D) arrays, and tilted (sloping) slit technique for 2D arrays—are all relevant. The only difference is that no correction has to be applied for the lens of the imager. In some instances the design of the imager will be such that there is, in fact, no aliasing, or that any aliasing that exists is very small. In such cases the MTF can be determined from the line spread function (LSF) of a stationery slit aligned vertically or horizontally as required. This will always be so in the scan direction for imagers that use scanners.

The need to remove a pedestal from the measured LSF (see Section 4.3.10) is particularly important when measuring the MTF of a thermal imager since the latter will virtually always generate a nonzero signal from the background to the illuminated slit target. It is also important to reiterate the warning given in Section 7.4.6 that the frame store must have a frequency bandwidth significantly greater than that of the video output from the imager, so that it will have no effect on the measured MTF.

In the arrangement shown in Figure 8.1, the computer uses a frame grabber to capture a whole video frame, part or even all of which is processed to arrive at the LSF, and from that the MTF. However, instead of a frame grabber it is possible to use a scope that has facilities for capturing and storing a single video line, or part of a single video line, and then transmitting it to a computer.[2,3] The advantage of this is that it may be easier to obtain a scope with the high bandwidth required for MTF measurements, rather than obtain a similar frame grabber. Although the use of a scope is best if one only requires data along a single video line, it can be used to obtain 2D data by having a line selector that can be controlled from the computer (this may already be part of the scope, or may be a separate item).

Edge targets may also be used for measuring the MTF of complete imagers (see Section 7.3.10), as also, in principle, can be random pattern targets (see Section 7.4.6).

8.2.3 MEASUREMENT OFF THE DISPLAY

The MTF of a thermal imager that includes the display can be determined by calculating the product of the MTF measured from the video output and the separately measured MTF of the display. Alternately, it can be measured directly off the display. The measurement techniques will be the same as those described in Section 7.6.4,

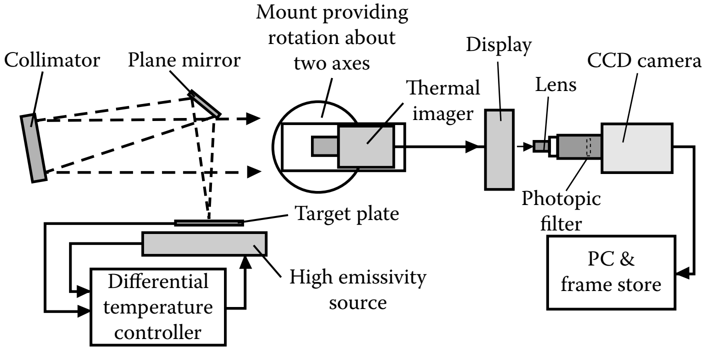

FIGURE 8.2 Arrangement for measuring the combined MTF of imager and display.

with the main difference being that the video pattern generator is now replaced by the thermal imager, collimator, and illuminated slit system (i.e., the object generator), as described in Section 8.2.2. The arrangement is illustrated in Figure 8.2.

The MTF, as usual, needs to be corrected for the width of the slit object, and it is also of particular importance in this case to remove any pedestal on which the LSF sits. In some cases the pedestal can be significantly nonuniform and should be measured by switching off the source that illuminates the slit (i.e., having zero temperature difference between target and source). Removal of any residual linear pedestal, after the measured pedestal has been removed, is recommended.

For displays viewed through an eyepiece the techniques described in Section 7.6.4 are also applicable.

8.3 NYQUIST LIMIT

The Nyquist limit is defined in Section 5.3.2. It is not normally a parameter one measures, since it can be calculated from the design data of the imager.

8.4 ALIASING

In an ideal situation the design of an imager should be such that it does not suffer from aliasing. However, it is difficult to reduce aliasing in a design without also reducing the MTF (see Appendix B), and usually a compromise is arrived at that reduces aliasing to an acceptable level while not too greatly affecting the MTF. It can be important to know the level of any residual aliasing in an imager since it can produce unwanted effects in the final image, the most obvious of which are the moiré fringes that appear when viewing periodic structures. As far as the use of a thermal imager for surveillance purposes is concerned, aliasing could produce artifacts in the small detail of the image that may lead to a misinterpretation of the image. Where temperature is being measured aliasing could produce small changes in the temperature profile of image detail that would vary with the exact position of the detail in the image.

Three measures of aliasing are defined in Section 5.3.3; here we only describe how each can be measured (see also ISO 15529[4] and Williams[5]).

Aliasing function: This parameter is determined by measuring the LSF for a static slit aligned vertically or horizontally (depending on the direction in which aliasing is being measured) and repeating the measurement as the slit is moved in small steps in the direction orthogonal to its length. The maximum and minimum values of the MTF calculated from these LSFs must then be identified. The aliasing function is a plot of the difference between the two MTFs plotted as a function of spatial frequency.

Aliasing ratio: This parameter is just the aliasing function, as measured above, but converted to a ratio by dividing half the difference between the maximum and minimum MTFs by their average value; i.e., if the maximum MTF at a spatial frequency s is $\mathrm{MTF}_{\max}(s)$ and the minimum MTF is $\mathrm{MTF}_{\max}(s)$, then we have

$$\text{Aliasing ratio} = \mathrm{AR}(s) = (\mathrm{MTF}_{\max}(s) - \mathrm{MTF}_{\max}(s))/(\mathrm{MTF}_{\max}(s) + \mathrm{MTF}_{\max}(s)) \quad (8.1)$$

Aliasing potential: Measuring this parameter again requires one to measure the LSF with a slit aligned vertically or horizontally to the detector array (depending on the direction in which aliasing is being measured). However, in this case the measured LSF is obtained by recording the output from a single detector element, or the average output from a number of elements in the same column or row (i.e., along and within the length of the slit image), as the slit is scanned in a direction orthogonal to its length. The MTF calculated from this MTF (after applying a correction for the width of the slit) is then used to calculate the aliasing potential (see definition in Section 5.3.3). The method of measurement described here is similar to that described in Section 7.4.6 as slit scan while monitoring the output of a single element. The precautions required to ensure that a sufficient length of scan is used will be the same here.

Equipment for making the measurements described above will be the same as that described in Section 8.2.2

8.5 SIGNAL TRANSFER FUNCTION (SiTF)

To measure SiTF one requires a calibrated source whose temperature can be varied. This can be viewed directly by the imager or via a collimator. In the latter case calibration of the source must include the effect of the collimator (see Chapter 9 for calibration techniques). The source can be a full-temperature-controlled blackbody cavity or a flat plate coated with a high-emissivity paint, in front of which is a large circular aperture. Generally speaking, the temperature-controlled flat plate is the better option since it can be heated and cooled using thermoelectric devices and will normally respond to a demand for a temperature change much more rapidly than most blackbody cavities. Some accuracy may be sacrificed in this way, as the emissivity will always be less than that of a full cavity, although calibration of the source can make the errors insignificant. Measurements are made by monitoring the level of the video signal, or the luminance of the display, in the area of the image of the source. Both types of measurement can be made with the type of equipment used for measuring MTF. The procedure can be automated using software that controls the temperature of the source and records the video signal level, or the display luminance. The arrangement will be similar to those shown in Figures 8.1 and 8.2.

8.6 NOISE-EQUIVALENT TEMPERATURE DIFFERENCE (NETD)

To determine the NETD one needs to have measured the SiTF and the RMS noise associated with the imager. The RMS noise is measured with the imager seeing a uniform field (e.g., a metal plate coated with a high-emissivity paint) that is at ambient temperature. The noise can be measured from the video signal using any of the techniques described in Section 7.4.3. The preferred method is to carry out the measurement on all, or at least a large area, of the 2D image by storing two frames of data in the PC and then subtracting them from each other. The RMS noise is calculated as

$$N_{\mathrm{RMS}} = \sqrt{}(\Sigma_n (S_i - \mathrm{S}_{av})^2)/\sqrt{}2 \tag{8.2}$$

where S_i is the signal from the i^{th} point of the array of measurement points in the image, n is the total number of points in the array, and

$$S_{av} = (\Sigma_n S_i)/n \tag{8.3}$$

The NETD is given by

$$\mathrm{NETD} = N_{\mathrm{RMS}}/(dS/dT) \tag{8.4}$$

where dS/dT is the slope of the SiTF curve (i.e., the increase in signal for a 1° increase in temperature).

NEDT is normally measured at the video signal; however, a value can be determined at the display using a value for the SiTF measured off the display and a measure of the RMS noise also measured off the display. The latter can be determined by using the video camera system used to measure the MTF off the display (see Section 8.2) and analyzing the output from this by storing frames of data in a PC in the same way as is described above for measuring the noise from the video signal of the thermal imager. The video camera would have to be calibrated to determine the relationship between its signal output and image luminance. Since the noise of the video camera may itself be significant, this would need to be evaluated separately and subtracted from the noise measured off the display using the equation

$$N_{\mathrm{RMS}} = \sqrt{}((N_{\mathrm{meas}})^2 - (N_{\mathrm{cam}})^2) \tag{8.5}$$

where N_{meas} is the uncorrected value of the RMS noise measured from the display and N_{cam} is the RMS noise of the video camera on its own.

We note that the value of NETD determined from the video signal and that from the display will not necessarily be the same.

8.7 MINIMUM RESOLVABLE TEMPERATURE DIFFERENCE (MRTD)

The target for measuring MRTD consists of four equally spaced bars, where the space between bars is equal to the bar width, and the length of the bars is equal to seven bar widths (see Section 5.3.6 and Figure 5.7). MRTD is normally measured as a function of spatial frequency, where the spatial frequency is taken as the reciprocal of the angle subtended at the thermal imager by one period (i.e., the angular distance between the centers of the bars) of the four-bar test pattern. In order to measure MRTD, one requires a set of four-bar test patterns covering the range of spatial frequencies one wishes to use, and for convenience, these are frequently mounted on a turret wheel so that it is easy to change from one target to another. The bars are usually in the form of slots in a metal plate coated with high-emissivity paint, and these are positioned in front of a temperature-controlled source that is either a blackbody cavity or a plate coated with a high-emissivity paint (or finish). The target plate is usually left at ambient temperature, and the temperature of the source is controlled to maintain a set temperature difference between it and the target plate. For some special types of test the temperature of the target plate itself may be controlled at temperatures other than ambient.

The source and target plate will in most instances be mounted with the target plate at the focus of a collimator, and the test piece will be mounted in the collimated beam, either on a tripod with the normal adjustments, or on a stage that provides adjustment about both a vertical and a horizontal axis. The arrangement will generally be similar to that shown in Figure 8.3.

The targets used for measuring MRTD will generally range from being relatively large to being very small, and this can give rise to problems with respect to resolution and vignetting. These problems are fully discussed in Sections 6.5.2 and 6.5.4 in

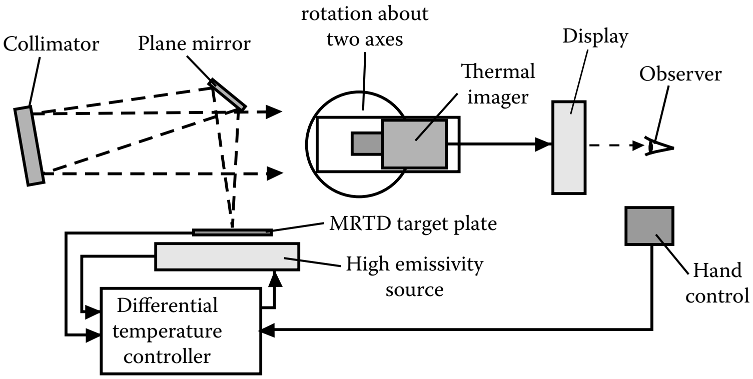

FIGURE 8.3 Arrangement for measuring MRTD.

relation to off-axis paraboloid mirror collimators, as well as refracting collimators. Measurements can of course be made without a collimator, by viewing the target directly. This has the great advantage of avoiding the problems associated with a collimator. However, it has some problems of its own. One of these is that many imagers, and particularly the ones used for surveillance, where MRTD is most relevant, will not focus at a close distance. This means not only having a sufficiently long throw to do the measurements, but having a set of targets suitable for this longer throw. In principle, the performance of the imager may be different when used at its close focus distance, although provided the close focus distance is greater than ×40 the focal length of the lens on the imager, this should not be a problem.

The measured value of the MRTD for the medium and larger targets can be less than one hundredth of a degree, so that very precise and sensitive setting and control of temperature differences is required. The ability to generate both positive and negative temperature differences is necessary, largely to overcome the zero temperature difference offset that invariably occurs with such test facilities and which can give rise to significant errors where small temperature differences are concerned. There are several possible reasons for this offset, including residual errors in the calibration of temperature sensors, temperature gradients between the position of the temperature sensor and the target (possibly caused by convection currents), emissivities of source and target that are not unity, so that their apparent temperature will depend to a small extent on the temperature of surrounding structures, etc. If the zero offset remains constant, it can of course be calibrated (see Section 9.3.5) and corrected. However, in the author's experience there are always small day-to-day and target-to-target variations in the offset.

The recommended procedure for each target is to measure the MRTD for a positive temperature difference (ΔT_+) and the temperature difference for a negative temperature difference (ΔT_-), and then calculate the correct MRTD as

$$\Delta T = (\Delta T_+ - \Delta T_-)/2 \tag{8.6}$$

Because of the partly subjective nature of MRTD, several sets of measurements should be made and the average of the results taken as the actual MRTD. Moreover, operators should have had training in making the measurements and, where possible, more than one operator should be used for the measurements on each test piece.

A point to note when measuring MRTD is that it is generally accepted that, unless otherwise specified, the operator can vary the distance at which he or she views the display in order to optimize his or her visibility of the target. In practice this means that he or she will move away from the screen to view the largest targets (the effect is very significant). Another point to note is that the target is accepted as being resolved if approximately 75% of the bar lengths are resolvable. With thermal imagers where the image is viewed through an eyepiece, the position of the eye will be fixed, and this could lead to a different MRTD being obtained, by measurement through the eyepiece and by viewing the image on an external display.

The results of a measurement of MRTD can be presented either in tabular form (e.g., spatial frequency and MRTD in two columns) or as a plot of MRTD as ordinate (usually plotted on a log scale) versus spatial frequency as abscissa (plotted on

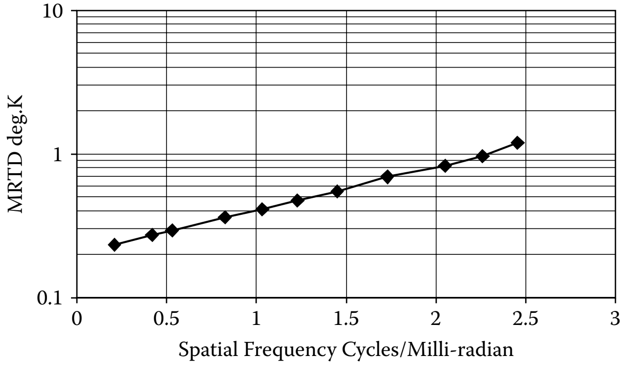

FIGURE 8.4 Example of MRTD plotted on a log/linear scale.

a linear scale). The spatial frequencies to cover the desired spatial frequency range are best chosen to follow an approximately geometrical progression, e.g., s, $k.s$, $k^2.s$, $k^3.s$, …, where s is spatial frequency and k is a suitably chosen constant to provide the desired number of measurement points within the required spatial frequency range. Using such a selection for the spatial frequencies, the operator will find that if the MRTD is plotted on a log scale and the spatial frequency on a linear scale, the spacing of the points on the MRTD scale will be nearly equal, and all the points will fit approximately on a straight line, at least for part of the curve (see Figure 8.4). MRTD is measured in degrees Kelvin and spatial frequency in either cycles/degree (c/deg) or cycles/milliradian (c/mrad).

8.8 MINIMUM DETECTABLE TEMPERATURE DIFFERENCE (MDTD)

The difference between making MDTD and MRTD measurements is that MDTD measurements are made with circular targets of varying diameter rather than four-bar targets of varying spatial frequency. The equipment (see Section 8.7) is otherwise the same. MDTD data are usually presented in the same format as MRTD data, with spatial frequency replaced by the reciprocal of the target diameter measured in degrees or milliradians.

As explained in Chapter 5, a fundamental difference between MRTD and MDTD is that an imager will have a limit to the maximum spatial frequency of target that can be resolved, however large the temperature difference becomes, while in theory, for the MDTD, there is no limit to how small a target can be detected, provided the temperature difference is sufficiently large.

We note that some laboratories have used a square rather than circular target for MDTD measurements. This will not have any great effect for relatively coarse targets (i.e., targets that are clearly resolved), but for smaller targets the critical factor will not be the diameter or width of a target so much as its area. So at the higher spatial frequencies (i.e., for the smaller targets), a given value of MDTD will occur at a lower spatial frequency for a circular target than it will for the equivalent square target (i.e., the target whose width is the same as the circle's diameter) by a factor of $\pi/4$ (0.785).

8.9 OBJECTIVE MRTD

This is an alternative to the subjective measurement of MRTD and is described and discussed in Section 5.3.8. It involves measuring several objective performance parameters of an imager and then calculating MRTD from these parameters using an appropriate mathematical model. Since there is currently no generally accepted mathematical model for this calculation, it is not a performance parameter one can quote without indicating what model is being used. However, it is now accepted that such an approach provides a far more repeatable and reliable assessment of this aspect of a thermal imager and is a sounder basis for an agreed acceptance test between customer and manufacturer.

In Section 5.3.8 two models are described, and the associated mathematical models are described in Appendix A.

8.10 OBJECTIVE MDTD

The comments made in Section 8.9 also apply in this case (see also Section 5.3.9). The mathematical models associated with computing MDTD are described in Appendix A.

8.11 SLIT RESPONSE FUNCTION (SRF)

This is defined in Section 5.3.10 (see also Williams[6]), which also indicates how a value for this performance criterion can be calculated from the measured MTF of the imager and display (if the latter is included as part of the system). The arrangement illustrated in Figures 8.1 and 8.3 can be used for measuring SRF directly, depending on whether the measurement does or does not include the display. For making the measurement the temperature difference between source and target is kept constant at a level that will provide a reasonably large signal from the imager, but will not saturate its output under any measurement conditions. The target should consist of either a slit whose width can be varied or a set of fixed slits of known width. The procedure is to record the indicated temperature at the center of the image of the slit as a function of the width of the slit. The temperature indication will be that determined by the particular facility provided for doing this on the imager, and may be different if different facilities are provided for doing this.

Imagers provided for surveillance purposes may not include a facility for measuring temperature. If one wishes to measure an SRF for such an imager, this can be done by measuring the video signal level corresponding to the center of the slit image as a function of the slit width, or by measuring the luminance at the center of the image of the slit using a photometer. However, one should be aware that the effective MTF of the video signal analyzer, or the photometer, will affect the result. This must be minimized by applying an appropriate correction or by using devices with a relatively high MTF, or both.

8.12 APERTURE RESPONSE FUNCTION (ARF)

This is defined in Section 5.3.11. The measurement procedure and equipment are the same as for SRF, except that the targets are now either a variable dimension square aperture or a set of square apertures of varying size.

8.13 TEMPERATURE MEASUREMENT PERFORMANCE CHARACTERISTICS

A number of these are defined in Chapter 5, as follows:

- Absolute temperature range (Section 5.3.12)
- Maximum and minimum temperature difference ranges and offset temperature range (Section 5.3.13)
- Temperature measurement uncertainty (Section 5.3.14)

All these characteristics can be measured using the arrangement shown in Figure 8.5. An accurate (or accurately calibrated) blackbody source is required with a relatively large aperture (i.e., an aperture that occupies approximately 1/5 of the horizontal FOV). If possible, it is preferable not to use a collimator, although if it is necessary to do so, the combination of blackbody source and collimator must be calibrated (see Section 9.3.5). All measurements are done by comparing and recording the blackbody temperature and the temperature indication given by the thermal imager, under the conditions specified in the relevant sections of Chapter 5.

An important point to note when attempting to achieve the highest accuracies is the effect of atmospheric absorption. This will be particularly marked in the 3–5 μm band, where there is a large CO_2 absorption. Its effect can be decreased by reducing the optical path between blackbody and thermal imager, provided adequate focus of the source aperture can be achieved. Another approach is to place the test equipment in an enclosure filled with dry nitrogen. Normally, a polythene tent into which dry nitrogen is fed from a nitrogen bottle is adequate for this purpose.

Another point to note is that the closer the focus setting on the lens of the imager, the smaller will be the NA at which it is working, and this will affect the temperature

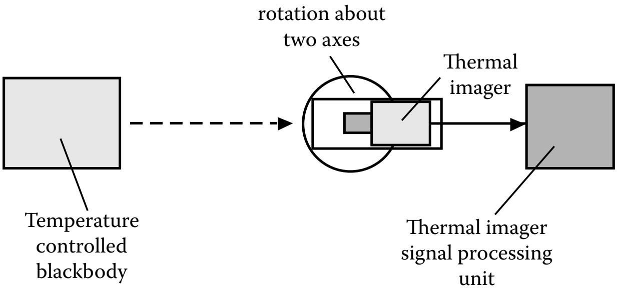
Mount providing rotation about two axes
Thermal imager
Temperature controlled blackbody
Thermal imager signal processing unit

FIGURE 8.5 Arrangement for measuring the temperature characteristics.

TABLE 8.1
Attenuation Factor as a Function of Object Distance

Object Distance, mm	Attenuation Factor, γ
200	0.56
400	0.77
800	0.88
1,600	0.94
3,200	0.97
6,400	0.98
12,800	0.99
Infinity	1.00

readings. The relationship between the indicated temperature, T_{ind}, and the actual temperature, T_{actual}, will be given by the equation

$$T_{\text{ind}} = \gamma . T_{\text{actual}} \tag{8.7}$$

where the attenuation factor γ for an object distance L is given by the equation

$$\gamma = [(L - f)/L]^2 \tag{8.8}$$

Table 8.1 illustrates how this varies for a lens of focal length 50 mm.

The effect of both the atmospheric absorption and the focus setting can be assessed in practice by altering the optical path length between blackbody and imager.

8.14 EMISSIVITY RANGE

A thermal imager intended to provide accurate temperature measurement will have a switch or other device that allows the operator to correct temperature measurements for the nonunity emissivity of the object whose temperature is being measured. As discussed in Section 3.2.2, accurate compensation for emissivity is difficult to achieve for several reasons, the most important of which are that if the emissivity is not unity, the apparent temperature of the object will depend on not only its temperature, but also that of the surround, and that the distance between the object and the imager will affect the degree of radiation attenuation caused by the atmosphere.

A simple assessment of the accuracy of the emissivity correction and its nominal range is to record the temperature indication $T_{e=1}$ given by the thermal imager (using the equipment shown in Figure 8.5) with no emissivity correction (i.e., emissivity, e, set to unity) and with the emissivity set to some other value, β. The new temperature reading should be

$$T_{\beta} = \beta . T_{e=1} \tag{8.9}$$

In principle, the emissivity correction may be more sophisticated than this and may make some allowance for ambient temperature. In this case, the relationship could be given by

$$T_\beta = \beta . T_{e=1} + (1 - \beta) . T_{\text{ambient}} \tag{8.10}$$

8.15 NARCISSUS

This can be assessed using an arrangement similar to that shown in Figure 8.5, but with the big difference that the uniform source area should now cover all the FOV of the imager, and can be positioned next to or close to the front of the imager. The source can be either a blackbody cavity with an aperture larger than the diameter of the entrance aperture of the lens on the imager, or a uniform high-emissivity plate. This external source should be at a uniform ambient temperature (i.e., 20°C). Where the imager has a facility for measuring temperature in different parts of the FOV, the minimum temperature in the area around the center of the FOV should be recorded as T_{center} and that toward the edge of the FOV as T_{outer}. The Narcissus index (as a percent) should be taken as

$$\text{NI}_{20} = (T_{\text{outer}} - T_{\text{center}}) . 100/T_{\text{outer}} \tag{8.11}$$

The index will in principle be different if the temperature of the external source is not the specified 20°C.

8.16 VEILING GLARE INDEX (VGI) AND UNIFORMITY INDEX (VGUI)

These are defined in Section 5.3.17. As discussed there, veiling glare is not usually a problem with thermal imagers provided it produces a uniform level of irradiation over the image field. The narcissus effect is in fact one example of a nonuniform distribution of veiling glare that is of significance to the performance of a thermal imager and that arises from reflections in the lens that generate a roughly in-focus image of the cooled detector back into the image plane. In general, therefore, it is sufficient to make a measurement of narcissus as described in Section 8.16 in order to assess the detrimental effects of veiling glare. Where Narcissus is not present, the same technique can be used for measuring the VGUI, as defined in Section 5.3.17.

If one wishes to measure the veiling glare index (VGI), from both internal and external sources, the arrangement described in Section 7.3.8 and illustrated in Figure 7.16 can be modified for this purpose. The modification would consist of replacing the lens by the complete thermal imager and a means for effectively measuring the video signal level over the image (this can in principle be done by using the facility for measuring temperature, when this is available). The other modification would be that rather than modulating the external sources at a constant frequency, one would merely switch them on and off, with the difference in the video signal level in the image of the central cavity, compared to that in the uniform surround, being the measure of veiling glare index. The measurement obtained in this way would only represent the glare from external sources, but would include internal effects such as the reflection of radiation off the detector, back to the camera body, and then back to the detector. To investigate the effect of internally generated radiation sources, it would be sufficient to measure the image uniformity with a high-emissivity plate placed immediately over the front of the lens aperture, or preferably over the aperture of the imager with the lens removed, if that is possible.

As described in Section 7.3.8, the VGI is determined by measuring the difference of the apparent temperature in the image of the central cavity as the temperature of the surround is varied from one close to that of the central cavity to some much higher temperature. The ratio (usually expressed as a percentage) of this difference to the temperature difference of the background is referred to as the veiling glare index, i.e.,

$$\mathrm{VGI}\% = (T_2 - T_1)*100/(T_4 - T_3) \tag{8.12}$$

where T_1 and T_2 are the relevant temperatures of the central cavity and T_3 and T_4 are those of the surround.

We note that test conditions must be chosen so that both the temperature of the central cavity and that of the surround are within the linear operating range of the thermal imager.

8.17 SCENE INFLUENCE FACTOR (SIF)

This is defined in Section 5.3.18, and an arrangement for measuring SIF is illustrated in Figure 8.6. The target consists of a temperature-controlled blackbody with an aperture slightly larger than 1/4 of the width of the FOV of the imager, with a plate mounted in front of it that has dimensions approximately equal to the FOV of the imager and has a central aperture equal to 1/4 of the width of the FOV. The plate would have a high-emissivity coating and would have a facility for being heated or cooled uniformly over its area to a controlled temperature. In most circumstances a copper or aluminum plate coated with a high-emissivity paint, heated and cooled either by a temperature-controlled fluid bath or by means of thermoelectric devices,

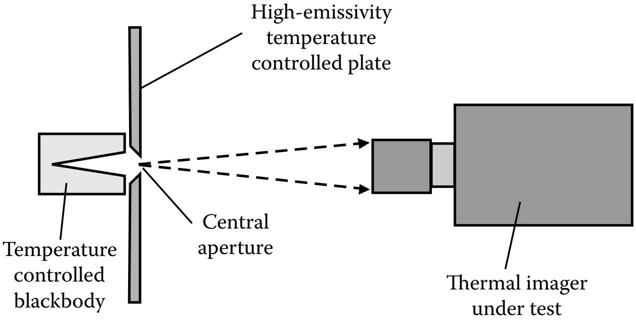
High-emissivity temperature controlled plate
Central aperture
Temperature controlled blackbody
Thermal imager under test

FIGURE 8.6 Arrangement for measuring SIF.

would be adequate. The imager should preferably view the target directly, provided the target distance and size allow the imager to focus on the central aperture. If a collimator is used, there could be problems in covering the full FOV. In this respect, it may be preferable to use a refracting collimator rather than a reflecting one.

A measure of SIF can be important as an indicator of possible errors if accurate temperature measurements are required when viewing a scene that may include some high- or low-temperature objects. In this respect, even a measurement of SIF using a target that did not cover the full FOV can be useful.

8.18 FIELD OF VIEW (FOV)

This is defined in Section 5.3.19. A suitable arrangement for measuring the FOV would be that illustrated in Figure 8.1. A suitable target pattern would be a slit perpendicular to the direction in which the FOV is being measured. Two crossed slits would be suitable for measurements of both the angular width and height of the FOV. The rotary mount on which the imager is supported would need to have an angular scale for measuring rotations about both a horizontal and vertical axis. As it is frequently the case that a scale and sufficiently large rotation are only available about a vertical axis, the imager can be mounted on its side for measuring the vertical FOV.

Measurements are made simply by noting the angular readings in both directions, when the target is just on the edge of the image on the display.

It is, of course, possible to make measurements without a collimator, but with the target viewed directly. In principle, a small error could arise unless the axis of rotation passed through the front nodal point of the thermal imager lens. In practice, if the axis of rotation passes approximately through the front aperture of the lens and the target is at a large distance (e.g., ×40 the focal length of the lens), the errors would be negligible.

8.19 CLOSE FOCUS DISTANCE

This is defined in Section 5.3.20. Two situations arise for this type of measurement. The first is when the close focus distance is of the order of a few meters. Measurements can be made by mounting a suitable target pattern and source on a slideway and viewing it directly with the thermal imager. The source and target are moved along the slideway toward the imager, until the image of the target pattern, as seen on the display, is just in focus.

The second of these is when the close focus distance is so long that the distance cannot be accommodated in the laboratory. It may, of course, be possible to make such measurements outdoors when a sufficiently long and convenient throw is available. However, a similar effect can be achieved by using a collimator and mounting the target and source on a micrometer stage that allows them to be moved in and out of the collimator focus position. If the target is moved a distance Δx away from the infinity focus position of the collimator in order to produce an in-focus image on the display, then the close focus distance will be given by the equation

$$d = f(f + \Delta x)/\Delta x \tag{8.13}$$

TABLE 8.2
Close Focus Distance, *d*, as a Function of Collimator Defocus, Δ*x*

Δ*x* Meters	*d* Meters
0.01	101
0.02	51
0.03	34
0.04	26
0.05	21

where f is the focal length of the collimator. Table 8.2 shows values of d for a collimator of 1 m focal length and a range of values of Δx.

The target pattern for this type of measurement could be a slit or a suitably small MRTD target. Although for most purposes it will be sufficient to judge focus by viewing the display, greater precision can be achieved by displaying the intensity profile across the target. A facility for doing this may be available on the imager, or it may be necessary to use a computer with a frame grabber and software that enables the profile to be displayed on the computer screen.

8.20 SPECTRAL RESPONSE

In some special applications it may be necessary to know in detail the spectral response characteristics of an imager. This is not an easy function to measure, largely because it requires measurements to be made using relatively narrow spectral bands of radiation, which result in low signal levels.

There are several techniques that can be used for doing such measurements, the choice depending to a large extent on how fine a spectral resolution is required. Figure 8.7 illustrates an arrangement that makes use of a number of bandpass filters that would be chosen to cover the spectral range of interest. A high-temperature (e.g., >1,000°C) blackbody is used and is viewed by the imager via a bandpass filter.

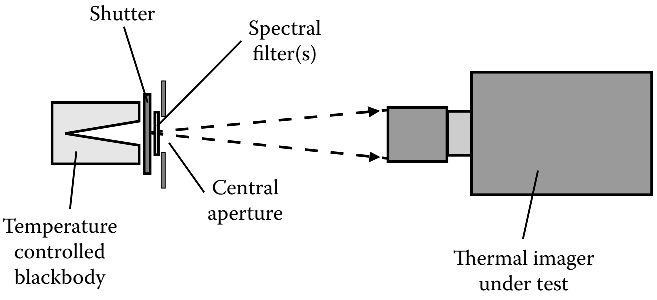

FIGURE 8.7 Measurement of spectral response using filters.

Included in the arrangement is a shutter (coated with a high-emissivity paint) at ambient temperature. The video signal level, or the indicated temperature, in the image of the blackbody aperture is measured for each filter in turn, with and without the shutter closed. The same measurements can then be made using a calibrated radiometer. The spectral response of the imager is then given by

$$R(\lambda) = (S_{\text{img}}(\lambda, T_2) - S_{\text{img}}(\lambda, T_1))/(S_{\text{rad}}(\lambda, T_2) - S_{\text{rad}}(\lambda, T_1)) \tag{8.14}$$

where $S_{\text{img}}(\lambda, T_2)$ is the imager signal, or temperature indication, for the filter with a central wavelength λ and the blackbody at a temperature T_2, and $S_{\text{img}}(\lambda, T_1)$ is the signal with the shutter, at an ambient temperature T_1, closed. $S_{\text{rad}}(\lambda, T_2)$ and $S_{\text{rad}}(\lambda, T_1)$ are the equivalent signals, or temperatures, for the calibrated radiometer.

An alternative approach is to measure the absolute spectral transmission of each of the spectral filters on a spectrometer. The integral under the product of this spectral transmission curve with the blackbody radiance calculated from Planck's equation (see Section 1.2) can be taken as the equivalent of the radiometer measurements, i.e.,

$$S_{\text{rad}}(\lambda, T) = \int R(\lambda, T).t(\lambda).d\lambda \tag{8.15}$$

where $R(\lambda, T)$ is the radiance of a blackbody at a temperature T and for a wavelength λ, and $t(\lambda)$ is the filter transmission at a wavelength λ. The integral is over the full-wavelength bandpass of the filter.

We note that for various reasons it may be necessary to use a collimator between the imager and the blackbody. This should not significantly affect the results, provided that a mirror collimator is used and that both the measurements with the imager and radiometer are made using the collimator. We also note that the accuracy of the measurements will be improved by averaging several frames of the imager video signal.

If measurements are required with relatively small steps between wavelengths, it may be necessary to use a monochromator instead of a set of spectral filters, and a suitable configuration is illustrated in Figure 8.8. In this case, a high-temperature

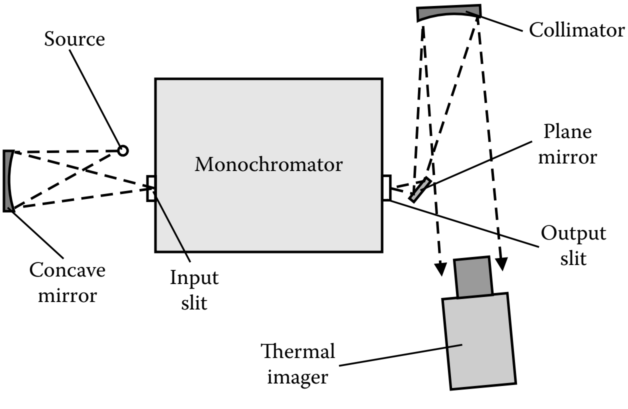

FIGURE 8.8 Measurement of spectral response using a monochromator.

source such as a Nernst Glower (see Section 6.2.3) may be used instead of a blackbody, and the monochromator output will need to be measured with a calibrated radiometer. One of the main problems is that of using slits that are sufficiently wide to be resolved by the imager, while at the same time achieving a sufficiently narrow passband—some compromise will be necessary. Unless the imager has a close focus capability, a collimator will almost certainly be required.

The measurement procedure is the same as that described above.

REFERENCES

1. Williams, T. L. 1999. *The optical transfer function of imaging systems*. Bristol and Philadelphia: Institute of Physics Publishing.
2. Williams, T. L. 1985. Measurement of the MTF of thermal and other video systems. *SPIE Conference Proceedings* 549:151–56.
3. Williams, T. L. 1985. Assessing the performance of complete thermal imaging systems. *SPIE Conference Proceedings* 590:172–78.
4. *ISO 15529: 2007 Optics and optical instruments—Optical and photonic—Optical transfer function—Principles of measurement of modulation transfer function (MTF) of sampled imaging systems*.
5. Williams, T. L., and Davidson, N. T. 1992. Measurement of the MTF of IR staring array imagers. *SPIE Conference Proceedings* 1689:53–63.
6. Williams, T. L. 1992. The MFT of thermal imaging cameras. Its relevance and measurement. In *Proceedings of the Eurotherm Seminar*, No. 27, pp. 51–56.

9 Calibration and Alignment of Test Facilities

9.1 INTRODUCTION

Most of the measurements described in this book use equipment that needs to be calibrated or carefully aligned, either on a regular basis or on a one-off basis. In this chapter we describe some of the methods and equipment that can be used for doing this. The calibration techniques described here do not include such parameters as linear and angular scales and the dimensions of test targets (e.g., four-bar minimum resolvable temperature difference [MRTD] targets). Although these are important, they make use of well-established techniques. Here we are concerned mainly with radiometric measurements and important optical characteristics.

9.2 CALIBRATING AND ALIGNING A COLLIMATOR

9.2.1 WAVEFRONT DEFORMATION (ABERRATION)

The perfect collimator has an emerging wavefront that is a plane surface, when the source is a point positioned at its focus. In the ideal situation, the wavefront should remain plane as the source is moved over the focal plane and if the wavelength of the radiation is changed. In practice this condition is never completely achieved, even with the theoretical design. Acceptable departures from planarity are only those that will not significantly affect the result of a measurement. Refracting collimators can usually be designed so that the wavefront deformation is minimal over a useful angular field and does not change significantly over a useful range of wavelengths (see Section 6.5.4). Reflecting collimators do not, of course, suffer from the effects of a change in wavelength; however, a single spherical surface will produce significant wavefront deformation, even in the on-axis focus position, while an off-axis paraboloid mirror is only free of wavefront deformation at its on-axis focus position (see Section 6.5.2).

In practice the actual collimator will have manufacturing errors that will introduce wavefront errors beyond those that are predicted theoretically. The actual wavefront deformation can be measured using either an interferometer or a noninterferometric device such as a Shack-Hartmann wavefront sensor. Figure 9.1 shows the testing configuration for an off-axis paraboloid using a Fizeau interferometer.[1] A visible wavelength interferometer can be used in this case, but an infrared interferometer would be required for a refracting collimator. A Fizeau interferometer operates by making measurements on the fringe pattern produced by interference between a

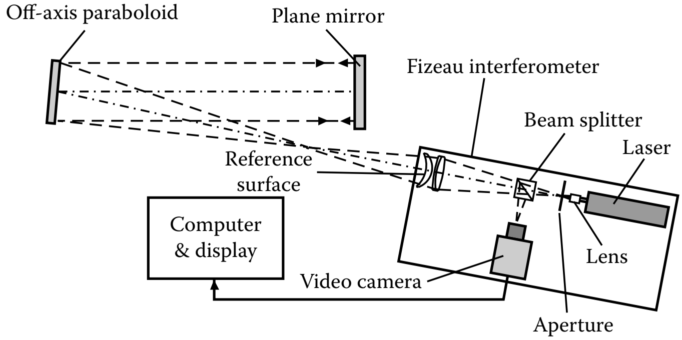

FIGURE 9.1 Testing an off-axis paraboloid collimator with a Fizeau interferometer.

coherent reference wavefront produced by reflection from a reference surface (see Figure 9.1) and the wavefront that has been transmitted through, or reflected from, the test piece. Both visible and infrared interferometers of this type are available commercially. The interferometers normally operate at a single wavelength using a laser source, which for visible wavelengths is usually a HeNe laser working at 0.63 μm, and in the infrared is either a HeNe laser operating at 3.39 μm or a CO_2 laser at 10.6 μm. The use of a single wavelength makes it difficult to assess the effect of wavelength changes in refracting collimators. Lasers are, however, available working at a few other wavelengths in the thermal band (see Section 6.2.9).

Various wavefront sensors such as the Shack-Hartmann[2,3] are also available commercially. They effectively function by measuring the relative deflections of a set of pencils or rays of light transmitted through, or reflected from, the aperture of the test piece. They can be used in a configuration similar to that illustrated in Figure 9.2, where the radiation goes twice through the collimator as a result of reflection from a plane mirror. The wavefront sensor has the advantage that it does not necessarily use a laser, and as a result, it is relatively easy to use a broadband source and change wavelengths using appropriate filters. A further advantage of wavefront sensors is that they are less sensitive to vibrations than interferometers.

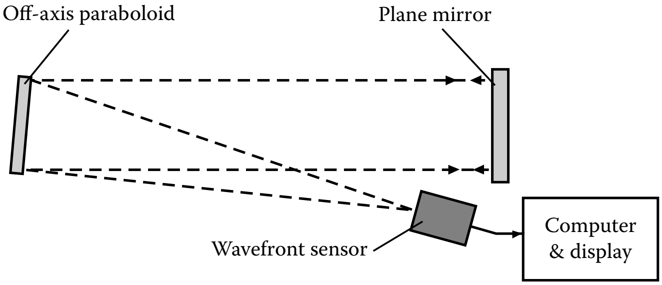

FIGURE 9.2 Testing an off-axis paraboloid collimator with a wavefront sensor.

The degree of correction one would wish to achieve for the most demanding applications (e.g., measuring modulation transfer function [MTF] or MRTD) would be a departure from planarity of better than $\pm\lambda/4$, but preferably better than $\pm\lambda/8$, where λ is the wavelength of the thermal radiation with which the collimator will be used, and the figure quoted is for a single pass through the collimator (i.e., for a double-pass measurement the above values should be doubled).

9.2.2 CALIBRATING FOCAL LENGTH

An accurate knowledge of the focal length of the collimator may be required for certain measurements. Accurate data may be available from the supplier of the collimator; otherwise, the user may have to measure it.

The simplest method is to measure the angle subtended in the collimated beam by a target of known width in the focal plane of the collimator. The relevant equation for calculating the focal length is

$$f = h/\tan\theta \tag{9.1}$$

where $2h$ is the full width of the target and 2θ is the angle subtended by the full width of the target.

The target could be a four-bar MRTD target of suitable and very precisely measured width, or could be a slit mounted on a micrometer stage that was moved over a precisely measured distance. The angle θ can be measured in several different ways. For a reflecting collimator one can use a telescope (a standard autocollimator can be used as a telescope), with cross-wires in its eyepiece, mounted on a rotary stage with an angular readout. Instead of a telescope, it is possible to mount a laser on the rotary stage and rotate the stage so that the laser beam was incident at the required positions on the target. For a refracting collimator the telescope could be replaced by a thermal imager (see Figure 9.3) with a fiduciary mark on its display, or simply by an assembly consisting of a lens with a narrow slit and thermal detector at its focus. In this case the target will need to be a slit

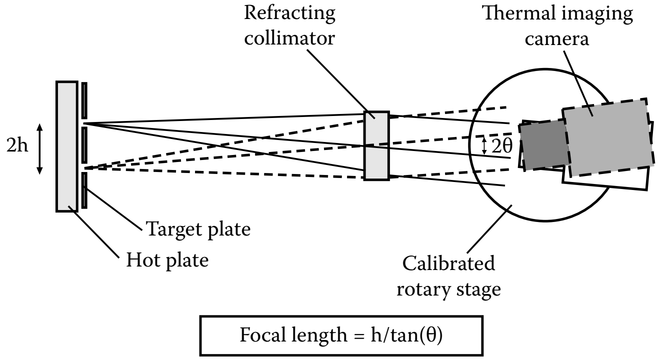

FIGURE 9.3 Arrangement for measuring the focal length of a refracting collimator.

with a hot source behind it, or simply a hot wire (see Section 6.2.2). This latter procedure would be easy to implement on an MTF bench since these components are basically the same as those used for MTF measurement on a lens. Many commercial MTF systems will include such a procedure for measuring focal length in their software.

9.2.3 COLLIMATOR ALIGNMENT AND FOCUS

As indicated earlier, collimators are normally only corrected for a limited field of view (FOV), which in the case of an off-axis paraboloid is very small. It is important, therefore, that the source and target in any test system be placed at the center of the FOV of the collimator, and that for extended targets consideration be given to how adequate the performance of the collimator is over the FOV occupied by the target. Where a fixed target, with more than one test pattern on it, is used, the smallest target should be positioned at the center of the FOV.

With an off-axis paraboloid one way of locating the center of the FOV is by dead reckoning, where one uses a knowledge of the off-axis distance (OAD) or the off-axis angle (OAA), provided by the manufacturer of the mirror, or measured by the user with an interferometer or wavefront sensor (the center of the FOV is where the wavefront aberrations are a minimum). The OAD is either the distance from the on-axis focus of the paraboloid to the central axis of what will be the collimated beam, or the distance from the on-axis focus of the paraboloid to the adjacent edge of what will be the collimated beam (see Figure 9.4). The user needs to establish exactly which of these is being quoted as the OAD. The OAA is the angle between the ray incident at the center of the off-axis section and the central ray of what will be the collimated beam. We note that it is of course important that the orientation of the mirror is set so that the position of the focus is correct. The direction of this focus is usually indicated by a mark on the rim of the mirror, or an arrow drawn on the back surface of the mirror.

The most convenient way of correctly aligning the collimator using this information is illustrated in Figure 9.5. It uses a HeNe laser that is adjusted so that the beam is incident at the center of the off-axis paraboloid, and then adjusting the angle of the collimator mirror so that the beam is reflected from the mirror at the correct OAA or OAD. There are various ways of doing this. One of these is to mount suitable jigs on the optical

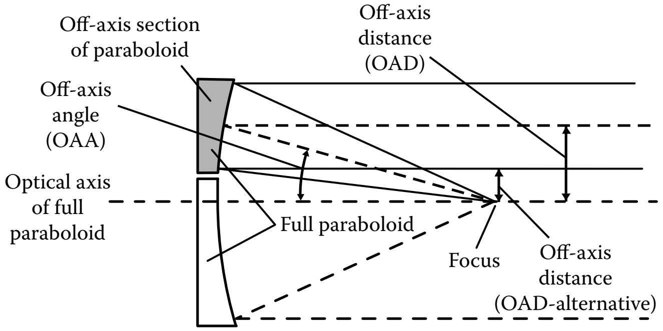
Off-axis section of paraboloid
Off-axis distance (OAD)
Off-axis angle (OAA)
Optical axis of full paraboloid
Full paraboloid
Focus
Off-axis distance (OAD-alternative)

FIGURE 9.4 Parameters of an off-axis paraboloid.

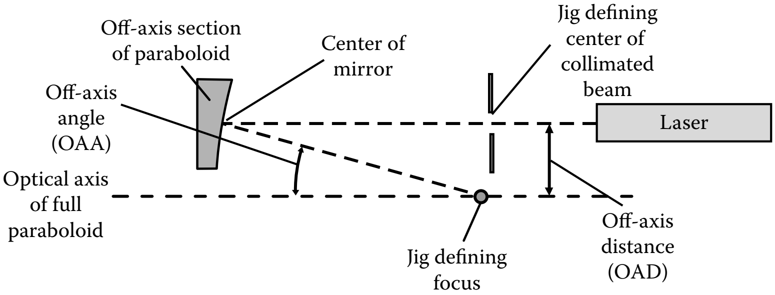
Off-axis section of paraboloid
Center of mirror
Jig defining center of collimated beam
Off-axis angle (OAA)
Laser
Optical axis of full paraboloid
Jig defining focus
Off-axis distance (OAD)

FIGURE 9.5 Method of setting up the off-axis paraboloid collimator using jigs.

bench that have been positioned correctly by mechanical measurement. So, for example, there would be a jig with a small aperture at the correct horizontal and vertical positions placed in front of the laser and through which the beam would be directed, a plate or mask mounted on the mirror to indicate its center, to which the laser beam would go, and finally, a jig that had a mark on it to indicate where the laser beam should fall when the vertical and horizontal angles of the mirror are set correctly. If these jigs are designed so that they can easily be removed and replaced on the optical bench in their correct positions, regular checks can be made that the system is still in alignment.

Another technique is illustrated in Figure 9.6. In this method a plane mirror in an adjustable mount is supported on a goniometer stage, which in turn is mounted on a carrier and linear stage. The laser beam is first directed to the center of the mirror after having adjusted the vertical and horizontal positions of the beam, at the laser end, to be correct (a suitable jig can be used for this purpose). The plane mirror assembly is then moved along the slideway to intercept the laser beam (before it is incident on the collimator mirror), and its angular orientation adjusted so that the laser beam is reflected back on itself. Using the angular readings on the goniometer stage, one rotates the mirror to the correct OAA angle and moves it to a position along the linear stage where it intersects the beam reflected off the collimator. Finally, the angle of the collimator is adjusted so that the laser beam is reflected back on itself. Note that the angular setting of the plane mirror will need to include the 180° required for it to face the beam reflected off the collimator.

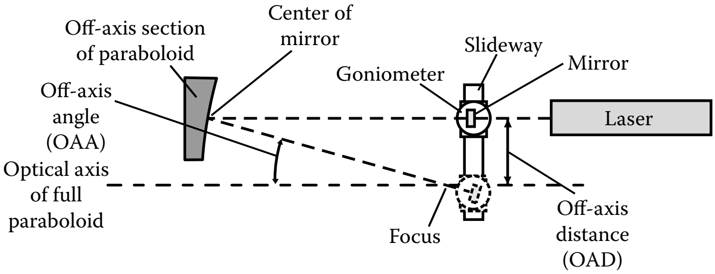

FIGURE 9.6 Method of setting up the off-axis paraboloid collimator using correct off-axis angle.

With a refracting collimator it is also important to position the target on the optical axis. A refracting collimator should have been assembled into a metal mount that has a reference surface that is exactly perpendicular to the optical axis of the collimator (methods of lens mounting can be found in Yoder[4]). The collimator will usually be supported in a mount with a plane surface against which the reference surface of the collimator will normally be placed. Therefore, aligning the mount correctly will ensure that when the collimator is in position, it will also be correctly aligned. A suitable technique is therefore to align a laser so that it passes through the center of the lens mount and is incident on the center of the target, and then to place a plane mirror on the mount that locates against the reference face of the mount and to adjust the mount so that the laser beam is reflected back on itself. In the same way, the target can be adjusted so that it is perpendicular to the laser beam.

The next important setting is to position the target at the correct focus distance. There are several ways of determining when the target is in focus. With a mirror collimator, the simplest technique is to illuminate the target with a visible wavelength source and use a film or digital single-lens reflex (SLR) camera, with its focus set to infinity, to view the target via the collimator, and use the focus setting facilities provided on the camera to determine when the target is in focus. The technique will be more sensitive the longer the focal length of the camera lens. The target pattern will also affect the sensitivity of the method, and, for example, a small MRTD target should give a good result. The camera infinity setting can be checked beforehand by using it to view a very distant object. Alternately, one can use a telescope with a cross-wire in its eyepiece and determine when the image of the target is in the same focal plane as the cross-wire. To achieve a suitable accuracy with this technique, it will be necessary to determine when there is no parallax between the cross-wire and the image of the target. This is achieved by moving one's eye from one side of the telescope exit pupil to the other and determining the focus position of the target where the relative movement of the two images is a minimum. A similar technique must be used initially to set the focus of the telescope to infinity by viewing a distant object.

Techniques similar to these can be used with a refracting collimator, except that in this case it will be necessary to use a thermal imager operating at a suitable wavelength. The accuracy of judging correct focus will usually be improved by viewing a line of the video output that shows the signal profile across the target, rather than the normal image produced on the imager display. Another method for improving accuracy is to mount the thermal imager firmly on a high-precision slideway that allows it to be moved across the beam from the collimator. Correct focus is achieved when the position of the image of the target, in the FOV of the imager, is static as the imager is moved across the collimated beam.

Another technique that can be used with a mirror collimator is illustrated in Figure 9.7. Here again the target is illuminated with a visible wavelength source, and a plane mirror is placed in the collimated beam and adjusted to reflect the beam back to the target. A beam divider and ground glass screen arrangement at the target allow the return beam to produce an image of the target on the screen, and the operator can judge when it is in focus. The beam divider and screen arrangement must be designed and adjusted so that the optical path between target and beam divider is the same as that between beam divider and screen. The technique, as described here, would not

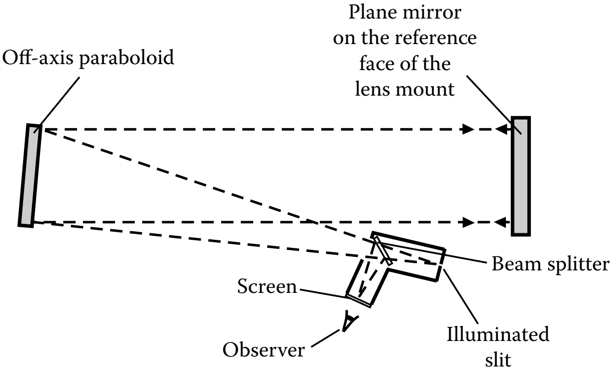

FIGURE 9.7 Focusing an off-axis paraboloid by retro-reflection off a plane mirror.

be suitable for a refracting collimator. However, more sophisticated arrangements can make use of this technique for such collimators. For example, a thermal imager with its lens removed can be used to view the return image. The effective image plane of the thermal imager would need to be positioned where the glass screen is in the arrangement shown in Figure 9.7. Alternately, the thermal imager could be replaced by a slit and IR detector (e.g., the image analyzer of an MTF system—see Section 7.3.10) that was scanned across the return image of the target, with the suitably displayed detector output being used to judge the best focus.

It is important to note that with an off-axis paraboloid collimator, the plane of the target should be perpendicular to a line drawn from the center of the target to the center of the actual mirror and not, as one might believe, perpendicular to a line drawn from the center of the target to the center of what would be the full paraboloid. This is a result of the curved nature of the focal plane of a parabolic or spherical mirror and minimizes the aberrations that occur as one moves away from the on-axis position. This is illustrated in Table 9.1, which shows how the RMS spot diameter varies as one goes off-axis, for the two settings.

TABLE 9.1
RMS Spot Diameters in the Focal Plane of an Off-Axis Paraboloid Mirror

Position in the Focal Plane, mm	RMS Spot Diameter for No Tilt of the Focal Plane, μm	RMS Spot Diameter for an Optimized Tilt of the Focal Plane, μm
0	3	3
8	40	18
–8	36	18
16	74	35
–16	77	36

Finally, we reiterate the fact that collimators are not always necessary and that, provided the thermal imager, or other device under test, can focus down to distances that can easily be accommodated in the laboratory, and that these distances are at least ×20, but preferably ×40, the focal length of the lens, tests at finite conjugates will give results similar to those at infinite conjugates. However, very long distances can give rise to problems with turbulence that may affect the results. For similar reasons, if the thermal imager has a focusing facility, the accuracy with which the correct collimator focus has to be set can be reduced.

9.2.4 TEST PIECE ALIGNMENT

9.2.4.1 Lens System

Lenses are normally mounted on a camera bench (see Section 7.3) in order to measure their performance characteristics, and correct alignment of the lens normally implies correct alignment of the camera bench. The basic requirements are that with the bench set at zero field angle, the reference face of the mount, which will support the test piece, should be perpendicular to the incident collimated beam and, if measurements are to be made off-axis, that lateral movement of the image analyzer should be in a plane parallel to the reference face of the lens mount (see Figure 9.8). A less critical requirement for off-axis measurements is that the front aperture (strictly speaking, the entrance pupil) of the lens should be approximately over the axis of rotation of the camera bench, so that in off-axis positions the aperture remains approximately central to the collimated beam.

When a reflecting collimator is used, the reference face of the lens mount can be aligned by initially setting up a laser so that the beam is approximately central on the mirror aperture and incident on the center of the target (see Figure 9.9(a)). A plane mirror is then mounted against the reference face of the mount facing the laser,

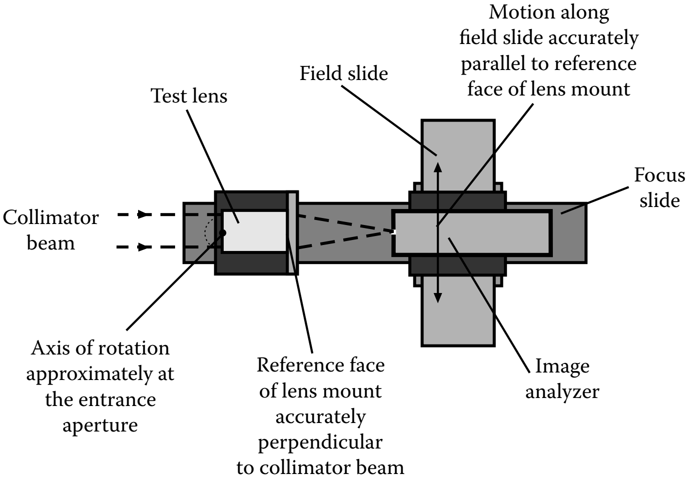
Motion along field slide accurately parallel to reference face of lens mount
Field slide
Test lens
Focus slide
Collimator beam
Axis of rotation approximately at the entrance aperture
Reference face of lens mount accurately perpendicular to collimator beam
Image analyzer

FIGURE 9.8 Alignment requirements with the camera bench in its on-axis position.

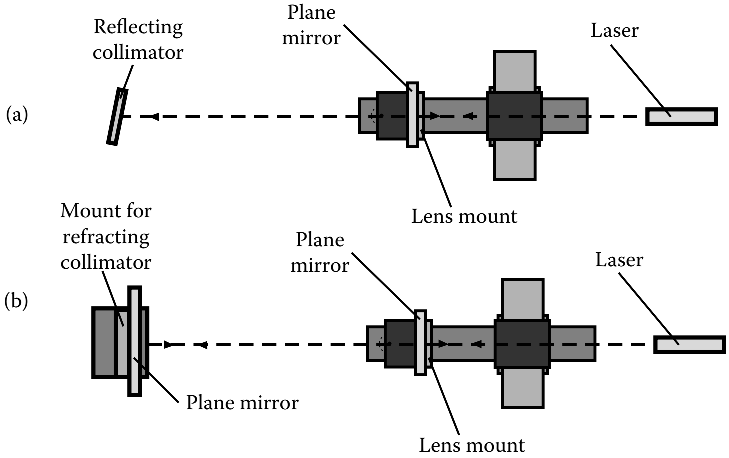

FIGURE 9.9 Using a laser to align the camera bench and collimator.

and the mount (or complete camera bench) is adjusted so that the mirror reflects the laser beam back on itself. The laser can be replaced by an autocollimating telescope, which is first adjusted to have an image of the center of the target on the center of its eyepiece cross-wires, and then with the plane mirror in position, the bench is adjusted so that the autocollimated image of the cross-wires is coincident with the actual cross-wires. It is important to note that the autocollimating telescope must have been set up so that the telescopic axis coincides exactly with the autocollimating axis.

A rather similar technique can be used with a refracting collimator, except that in this case the laser beam is adjusted to fall on the center of the collimator and to be perpendicular to the reference surface on the collimator mount (see Figure 9.9(b)). A plane mirror mounted against this surface can be used to reflect the laser beam back on itself to set this condition.

A technique for achieving the second of the above objectives is to replace the image analyzer with a suitably mounted electronic or mechanical measuring probe that will measure the change in distance between image analyzer mount and a flat metal surface that replaces the plane mirror on the reference face of the lens mount (see Figure 9.10). The camera bench should be adjusted so that this distance does not change as the image analyzer mount moves laterally. On some camera benches the adjustment would be to the lens mount, and in this case this alignment should be performed first. Aligning the reference face of the lens mount to the collimated beam is then usually done by adjusting the zero field angle setting of the camera bench. Other adjustments may be necessary to the full camera bench, or just to the lens mount, to ensure the reference face is perpendicular to the collimated beam about a horizontal as well as vertical axis.

9.2.4.2 Thermal Imager

Alignment is much simpler in this case, since zero field angle is determined simply by the settings on the bench support for the imager (see Section 8.1), when the image

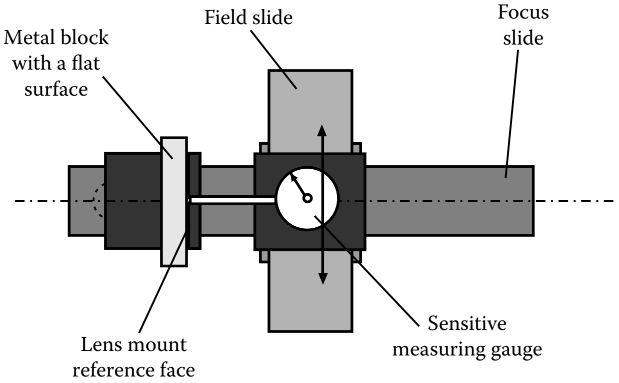
Field slide
Focus slide
Metal block with a flat surface
Lens mount reference face
Sensitive measuring gauge

FIGURE 9.10 Use of dial gauge or electronic gauge for adjusting parallelism of field slide and lens mount reference face.

of the target is in the center of the imager display. However, if measurements will be made off-axis, it is also necessary to mount the imager so that the aperture of the lens is approximately central in the collimated beam and coincident with the axis, or axes, of rotation of the imager support.

9.2.5 CHECKING AN MTF TEST FACILITY

An MTF test facility cannot be calibrated. There is no way to allow for errors in the results of a measurement. However, there are ways of checking that the system is functioning correctly and giving answers that are correct within acceptable limits. A full description of the checks that can be made on an MTF system and its subunits can be found in Williams[5] and ISO11421.[6] Here we only describe some of the simpler overall checks of a system.

9.2.5.1 Audit Lenses

For an MTF system set up for lens testing, one approach is to get a lens that is typical of the lenses that will be tested (e.g., with respect to *f*/number, FOV, focal length, and performance) and to have its MTF measured under closely specified conditions in a reputable laboratory (this could be a national standards laboratory, where they provide such a service). This can then be used to check that similar results are obtained on one's own system. The conditions that must be specified are lens orientation, *f*/number, method of focus (usually on-axis by maximizing the MTF at a specified spatial frequency), field positions, test azimuths (i.e., radial or tangential), wavelength, and spatial frequency range.

9.2.5.2 Standard Lenses

Standard lenses are made under sufficiently well-controlled and measured conditions, for their MTF to be the same as that predicted from theory, within close limits. Unfortunately, to achieve this, the lenses need to be of single-element, or at most two-element, construction. This usually means that they have a limited NA and FOV, so that although they provide for a more certain check within their performance range, they will usually need to be supplemented by audit lenses. The test conditions also need to be fully specified (see above), although in this case the orientation of the lens should not matter.

Standard lenses that operate at thermal wavelengths are described in Williams.[5]

9.2.5.3 Slits

An MTF system set up for testing displays, or for testing complete thermal imaging systems off the display, can be checked by using a slit of known width attached to the front of the display, so that the latter effectively illuminates it from the rear. The slit is used as though it is a slit image on the display and its MTF measured. If the width of the slit is w, the MTF is given by the equation

$$\mathrm{MTF}(s) = \sin(\pi.s.w)/(\pi.s.w) \tag{9.2}$$

where s is spatial frequency in the reciprocal of the units used for w (i.e., if w is in mm, s will be in c/mm). Several slits of different widths should be used, with the widths chosen to cover the spatial frequency range that would be used for the actual measurements (note that the first zero of the MTF curve of a slit will be at a spatial frequency equal to $1/w$).

9.2.5.4 Square-Topped Pulses

An MTF system designed to measure MTF off the video output of a thermal imager can be checked by replacing the output from the imager with a synthetically generated square pulse or series of pulses that simulate the image of a slit of well-defined width. A video pattern generator intended, for example, for testing TV displays can be used for this purpose, with, if necessary, some additional electronic circuitry.[7] The effective width of the pulse(s) can be measured using a suitable calibrated oscilloscope. The oscilloscope will measure pulse width in terms of time, which then has to be converted to a distance on the display. For example, if the effective length of a video line is Y seconds, the pulse duration y seconds, and the width of the image on the display W mm, the value of w to use in Equation (9.2) for calculating the MTF will be $W.y/Y$ mm. The measured MTF in this example will be in c/mm; however, if instead of the width W of the display one uses the horizontal angular width of the FOV of the imager, in, say, milliradians, the measured MTF will be in c/mrad.

9.3 RADIOMETRIC CHARACTERISTICS

9.3.1 General

Almost all the tests on a thermal imager require the operator to know what the effective temperatures or temperature differences are over an aperture or target pattern. Even though the main source of radiation may be a well-characterized blackbody cavity, the effective temperature that the thermal imager sees will be affected by any optical components (e.g., collimators) between it and the source. In addition to this,

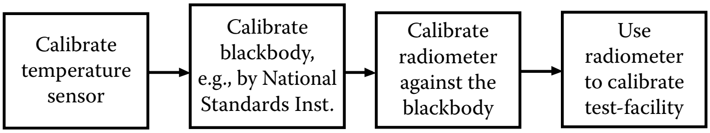
Calibrate temperature sensor
Calibrate blackbody, e.g., by National Standards Inst.
Calibrate radiometer against the blackbody
Use radiometer to calibrate test-facility

FIGURE 9.11 Scheme for calibrating a test facility.

where temperature differences between the source and a target plate are concerned, the emissivity of the target plate may not be unity, and its effective temperature may be affected by the temperature of its surrounds. Another factor that can significantly affect the radiometric characteristics of a test facility is atmospheric absorption, although, if necessary, this can be eliminated by enclosing equipment in a polythene tent that is filled with pure dry nitrogen. For these reasons, calibration of a complete test facility is important.

The equipment involved in calibrating test facilities can include blackbodies, temperature sensors, radiometers, and spectraradiometers. Calibrated blackbodies serve to convert the temperature measured by calibrated temperature sensors to sources of known radiance, while radiometers and spectraradiometers serve as radiance transfer standards after calibration against a blackbody. The scheme is illustrated in Figure 9.11.

Another item of equipment that plays an important part in any test facility is a temperature controller, which will be part of any blackbody system and of any other source whose temperature needs to be kept stable.

The calibration procedures, in each case, are briefly described below.

9.3.2 TEMPERATURE SENSORS

There are various types of temperature sensors, with the two most important being platinum resistance (PtR) thermometers and thermocouples. However, there are various types of semiconductor sensors that are useful in many situations because of their small size and fast response, although they may not be as good from the point of view of linearity and stability. However, even PtR and thermocouple thermometers may change their properties if subjected to mechanical strain or temperatures outside their intended ranges. All these sensors also involve associated equipment for measuring voltage, resistance, or current, and their accuracy and stability are of equal importance where accuracy of temperature measurement is concerned.

PtR sensors are the most accurate, and different devices are available that allow one to cover a temperature range of approximately –250 to 850°C. Temperatures can be sensed to better than 0.01°C. Thermocouples are less sensitive, but allow one to cover a much larger temperature range of approximately –200 to 2,000°C, by appropriate choice of metal combinations. Temperature sensing for thermocouples, however, is not usually better than 0.5°C. Semiconductor devices are available that have a sensitivity similar to that of PtR thermometers, but the temperature range one can cover with this type of device is only approximately −40 to 150°C (a range that is probably suitable for most thermal imager targets).

The accurate calibration of temperature sensors requires special equipment and skilled operators. A national standards laboratory will usually offer such a facility, but there are other certified laboratories that also do so.

9.3.3 BLACKBODIES

Blackbodies are carefully designed, heated or cooled cavities that have an exit aperture with a radiant emittance that is given to a very close approximation by Planck's equation (see Sections 1.2 and 6.2.6) where the effective emissivity is unity. The radiance of the blackbody is calculated from a knowledge of its temperature—hence the importance of having calibrated temperature sensors. The theoretical concept for a blackbody is that the walls of the cavity will themselves have a high emissivity, but that the effective emissivity is increased because the design of the cavity ensures that any radiation emitted by the cavity has undergone several reflections off the cavity walls. For this reason, it is important that the walls of the cavity are at the same uniform temperature and that this is the temperature indicated by the temperature sensor(s).

Here again, the accurate calibration of blackbodies requires special equipment and skilled operators. A national standards laboratory will usually offer such a facility, but there may be certified laboratories that also do so.

The calibration process at this level usually involves comparing the radiance of the blackbody against the radiance of a standard blackbody using some form of radiometer. The standard blackbody is one that normally will have undergone careful analysis of the design, as well as calibration, by a national standards laboratory.

We note that in practice, blackbodies may have a limited range of wavelengths over which they function with the required accuracy (i.e., wavelengths where their effective emissivity is close to unity). It is also the case that the angle of the cone of radiation they emit may be limited where their effective emissivity is close to unity.

9.3.4 RADIOMETERS

Radiometers are instruments that measure the radiance of a source, but can also be calibrated to measure the effective temperature, specifically of blackbody, or pseudo-blackbody (e.g., target plates coated with a high-emissivity paint), sources. They normally find a use for calibrating complete test facilities that can include one or more mirrors or lenses that have a reflectance or transmittance that is less than unity.

Very simply, a radiometer can consist of a lens that projects an image of the source onto a detector, or simply a detector placed at a known distance from the source. In the former instance, the size of the detector and the object and image conjugates that are used determine the area of the source over which the radiance is being measured, and the spectral response of the detector, plus any filters included in the system, defines the spectral characteristics of the radiometer. In the latter arrangement the detector output is, strictly speaking, a measure of the irradiance the source generates at the detector. If the source has a uniform radiance, the latter can be calculated from irradiance using data about the area of the source and its distance from the detector, i.e.,

$$\text{Radiance} = \text{irradiance}.A/d^2 \tag{9.3}$$

where A is the source area and d is the distance between source and detector.

The irradiance will be proportional to the detector signal (for a detector with a linear response), the constant of proportionality being determined by using a source of known area and radiance (i.e., a calibrated blackbody).

Rather than using the area of the detector to define the area whose radiance is being measured, it may be preferable to use an aperture positioned at the focus of the lens to do this, with the detector arranged to collect all the radiation that passes through the aperture. An additional optical system (i.e., a lens or mirror arrangement that images the aperture onto the detector) may be necessary to ensure that all the radiation passing through the aperture is incident on the detector.

In all the arrangements described above it is important to note that the detector will respond to all the radiation falling on it, and that this will include radiation from its immediate surrounds, as well as the radiation from external sources that are within its FOV. The detector should therefore have some form of surround that is at a constant temperature, with an aperture that defines its FOV. Figure 9.12 illustrates two possible arrangements. In both cases the first lens images the test piece onto aperture 1, and this defines the area over which the radiance will be measured. In the simple arrangement the detector is placed close to this aperture to receive all the radiation passing through the aperture. In the more complex arrangement the second lens images the first lens onto aperture 2, and this defines the area of the first lens from which radiation will pass onto the detector, and finally the third lens images aperture 1 onto the detector. When the radiometer uses chopped radiation the requirements are slightly different and these are discussed below.

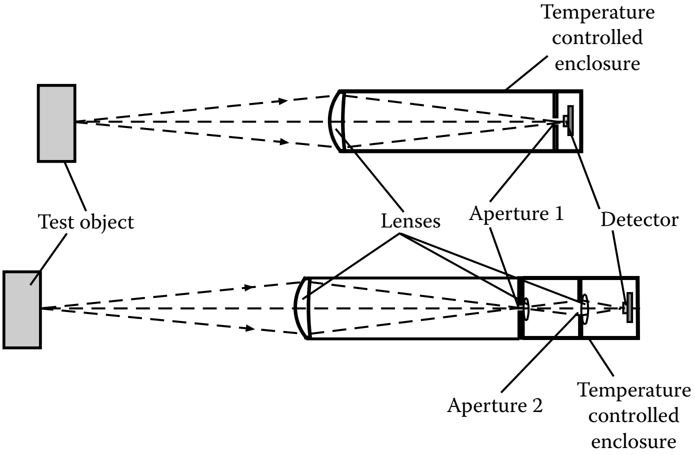
Temperature controlled enclosure
Test object
Lenses
Aperture 1
Detector
Aperture 2
Temperature controlled enclosure

FIGURE 9.12 Arrangement for a radiometer.

There are several important facts to note about the design of radiometers:

- The detector is a major consideration in the design of a radiometer. The highest-sensitivity detectors normally operate best when the radiation one wishes to measure is chopped. If the chopping occurs at the source whose radiance or temperature is being measured, radiation from the internal parts of a radiometer, including the lens, will not significantly affect the results of a measurement. However, all chopped radiation will be included in a measurement, so that care is required to chop only the radiation one wishes to measure.
- As indicated in Section 7.2, when a chopper is used the detector responds to the difference in radiation between source and chopper blade, and this must be taken into consideration, either by using a chopper that reflects a temperature-controlled reference source or by keeping the temperature of the chopper constant. In one design of radiometer that used a reflecting chopper (described below and in Williams[8]), the temperature of the reference source was not controlled, but was monitored, and a correction was applied to the detector output for the radiation produced by this source.
- The ideal detector to use in a radiometer is one that absorbs and responds to all the radiation falling on it over a wide band of wavelengths (i.e., has a uniform response over the band of wavelengths one requires to use in the measurement). This is normally only achieved using a bolometer type of detector coated with high absorptance material. However, there are additional methods of increasing the effective absorptance, and Theocharous[9] describes an arrangement using a pyroelectric detector with a black absorbing coating, where the effective absorption is further enhanced by mounting a small hemispherical mirror above the detector with a suitable aperture for the radiation to enter. The radiation is incident on the detector at an angle, and any radiation that is diffusely or specularly reflected off the detector is reflected back to the detector by the mirror.
- As indicated above, the most sensitive detectors do not generally have a flat spectral response, and their use requires more careful consideration. Provided they are equipped with one or more narrow passband filters, they can be calibrated with each filter and will give a true measure of radiance at each of the filter wavelengths. With a sufficient number of filters the instrument effectively becomes a spectraradiometer, and it is then possible to study the spectral radiance characteristics of a source and calculate the total radiance over the range of wavelengths covered by the filters. Rather than use filters, it is of course possible to incorporate what is effectively a monochromater or spectrograph into the instrument, including Fourier transform infrared (FTIR) systems.
- A radiometer with a broadband spectral response that is nonuniform (i.e., one determined by the spectral response of the detector) is normally an adequate tool for measuring the effective temperature of a near blackbody, when the spectral response of the detector covers the same wavelength band as the thermal imager that will be tested with that source (e.g., a blackbody source and collimator system for measuring MRTD).

9.3.5 RADIOMETRIC CALIBRATION OF AN MRTD OR SIMILAR TEST FACILITY

In Chapter 8, Figure 8.1 shows a typical MRTD or other test facility where the calibration information of significance is the temperature difference between the source and the target. The calibration is done by comparing the temperature difference between target and source as measured by the calibrated radiometer and the temperature difference indicated by the test facility system. There are several points to note when undertaking such a calibration:

- The calibration is done either by scanning the small measurement area of the radiometer across a suitable target (some radiometers have a built-in motorized scanning facility), or by taking several readings covering a suitable area of the target background and the target patterns.
- The dimensions of the chosen target pattern must be large compared with the instantaneous measurement area of the radiometer; otherwise, the temperature difference readings will be less than they should be. A suitable check is to see that the reading is constant over an area of the target pattern that is at least half its smallest dimension (e.g., the width of a bar in an MRTD target). In many cases it may be necessary to make a special target with suitably large dimensions to achieve this. However, the target must have the same emissivity and other properties of the actual targets.
- A series of measurements should be made that cover the full range of temperature difference settings that will be used in practice. The temperature difference indicated by the radiometer for the center of the target should be the value to record.
- The central portion of a typical graph of set temperature difference versus measured temperature difference is shown in Figure 9.13. A point to note is that almost invariably there will be a zero offset (i.e., there will be a small measured temperature difference when the set temperature difference is zero). The value of this offset can depend on the ambient conditions that exist at the time of the calibration and is the reason for following the MRTD measurement procedure described in Section 8.7, where the MRTD is determined by making measurements at both positive and negative temperature differences. If we assume that the relationship between the measured temperature difference, ΔT_{meas}, and the set temperature difference, ΔT_{set}, is

$$\Delta T_{\text{meas}} = k.\Delta T_{\text{set}} + \Delta T_0 \tag{9.4}$$

where ΔT_0 is the zero offset and k is the slope of the curve, then we have, using the recommended procedure, that

$$\begin{aligned}\text{MRTD} &= [(\Delta T_{\text{meas}})_+ - (\Delta T_{\text{meas}})_-]/2 = [(k(\Delta T_{\text{set}})_+ + \Delta T_0) - (k(\Delta T_{\text{set}})_- + \Delta T_0)]/2 \\ &= k[(\Delta T_{\text{set}})_+ - (\Delta T_{\text{set}})_-]/2 \end{aligned} \tag{9.5}$$

where $(\Delta T_{\text{set}})_+$ is the positive temperature difference value and $(\Delta T_{\text{set}})_-$ is the negative temperature difference value. We see from this that the important calibration constant is the value of the slope k.

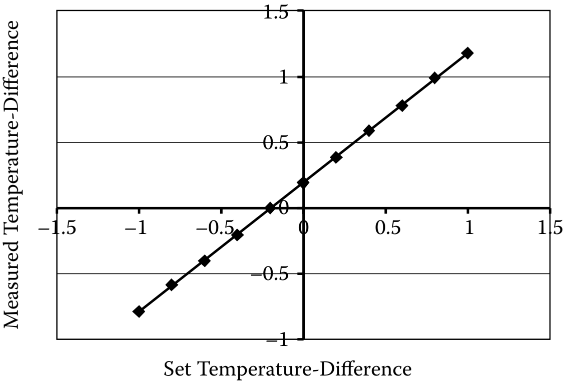

FIGURE 9.13 Example of a temperature difference calibration curve for an MRTD target system (central portion only).

The same considerations also apply to MDTD measurement and to any other measurements where temperature difference is the relevant variable.

9.3.6 SPECTRAL CHARACTERISTICS

Although in principle a test facility that uses a blackbody cavity as a source should have a spectral characteristic that is predictable from knowledge of its temperature, in practice the overall spectral characteristics of the facility may be affected by atmospheric absorption as well as the characteristics of any transmissive or reflective components in the system. The spectral characteristics of any windows, lenses, or mirrors can be calibrated separately using the techniques described in Section 7.3.6, and then combined with the blackbody characteristics to determine the overall system characteristics. To include the atmospheric transmission characteristics, a similar technique could be employed, where a collimated beam was used and the path length was first set to a very close distance, and then to that of the test facility.

Where the source has a relatively large area, a direct measurement of the spectral characteristics can be made using a spectraradiometer, as described in Section 9.3.4. However, a problem will arise with small sources such as slits or hot wires. A solution to this is to make two radiometric measurements, the first with the source on and the second with the source off, and to subtract the one from the other.

REFERENCES

1. Malacara, D., ed. 1992. *Optical shop testing*. 2nd ed. New York: Wiley-Interscience.
2. Platt, B. C., and Shack, R. 2001. History and principles of Shack-Hartmann wavefront sensing. *Journal of Refractive Surgery* 17:S573–77.
3. Williams, T. L., and Cormier, A. J. 2003. Wavefront sensing for testing spherical surfaces and lens systems: A new approach. *SPIE Proceedings* 5252:346–57.
4. Yoder, P. R. 2008. *Mounting optics in optical instruments*. SPIE Press Monograph, Vol. PM181.

5. Williams, T. L. 1999. *The optical transfer function of imaging systems*. Bristol and Philadelphia: Institute of Physics Publishing.
6. *ISO 11421: 1997 Optics and optical instruments—Optical transfer function—Accuracy of OTF measurement*.
7. Williams, T. L., et al. 1989. Recent advances in testing thermal imagers. *SPIE Conference Proceedings* 1110:220–31.
8. Williams, T. L. 1982. Scanning radiometer for calibrating thermal imager test targets. *SPIE Conference Proceedings* 369:51–55.
9. Theocharous, E. 2006. The establishment of the NPL infrared relative spectral responsivity scale using cavity pyroelectric detectors. *Metrologia* 43:S115–19.

10 Applications of Thermal Imaging Cameras

10.1 INTRODUCTION

Thermal imaging may be applied wherever there is a need to see or measure the apparent temperature differences (i.e., due to real differences or differences in emissivity) in a scene. Such temperature differences may arise from normal causes (for example, the heating due to the malfunction of an electronic component), or may be deliberately generated in order to measure a specific effect (such as measuring de-lamination in a composite panel). Most of the physical properties of materials or structures can, by the use of appropriate arrangements, be converted into thermal patterns that are a measure of these physical properties or structures. Many of the applications show a very considerable degree of ingenuity, and this book may help to generate many more.

Thermal imaging has the big advantage over other methods of measuring temperature, or temperature differences, in that it provides a two-dimensional image of temperature distribution whose variation with time can be followed dynamically. These advantages permit the user to assess temperatures over a large scene while using a single instrument from one position in the scene, and to visualize temperature patterns and the changes in these patterns as well as to follow moving objects.

This chapter briefly describes some of these applications, with the idea of demonstrating some of the ways in which thermal imaging has and can be applied, but without going into great detail. Many of these applications have been in use for many years, but over the years advances in the thermal imagers themselves and the development of digital processing systems and software have greatly increased the sensitivity, accuracy, and convenience of the techniques. Those interested in pursuing any particular application can follow up with some of the references that are provided. The list of references is by no means comprehensive, but is only intended to give a lead into each of the topics covered.

10.2 INDUSTRIAL APPLICATIONS

10.2.1 BUILDINGS AND STRUCTURES

Thermal imaging has been used in a number of different ways for inspecting buildings and structures. One of the most obvious is for investigating areas of high heat loss, which can be caused by poor design of the building, missing insulation, or incorrect or faulty construction.[1–3] Temperature differences between the inside and outside of a building will generate a heat flow that will increase the temperature of the colder side (usually the outer side) and reduce the temperature of the warmer side. The temperature distribution on the walls, windows, and roofs will produce thermal images that show the heat conducted through different parts of the building and any areas where insulation is poor or missing. Differences in heat conduction will also be a result of different materials in different parts of the building and can produce images of the internal structure of walls, etc. Unnecessary loss of heat is an important consideration in the fight against global warming.

Buildings can suffer from air leakage from various causes, and this can be a particular problem for those constructed from precast panels where the seal between panels is not adequate. One method that has been used to locate such leaks[4,5] is to pressurize (both positively and negatively) the air inside the building, and after a sufficiently long period (of the order of hours) to use a thermal imager to view the outside of the building to determine where the leaking air has changed the temperature of the joins or other leakage paths. A significant temperature difference between the inside and outside of the building is helpful, and account must be taken of the reflected radiation from adjacent buildings (see Section 3.2.2).

Some structures are not necessarily parts of buildings and may not have an inside and an outside, so that temperature effects must be generated either by providing some special form of heating on one side of the structure or by relying on the heat produced by the sun. Structural patterns and anomalies such as voids will show up when, for example, a structure has been heated by the sun during the day and then cools down at night.[6] The thermal pattern will not only depend on the thermal conductivity of parts of the structure, but also on their heat capacity. In this type of measurement the user must be aware of the possible effects of emissivity differences (see Section 3.2.2) on the surface being viewed by the imager. The emissivity affects not only the thermal image but also the original heating or cooling effects.

One of the applications of thermal imaging has been to inspect for the presence of moisture as a result of either leaks or other causes.[6] One such application has been to inspect sites, with several flat-roofed buildings, for leaks, using a helicopter-borne thermal imager.[7] Where leaks occur the roof insulation becomes saturated with water and, because of its relatively higher heat capacity, will show up as a relatively warmer area when flown over at night, having been heated by the sun during the day. Leaks can also be detected from the inside of a building as illustrated in the thermal image of Figure 10.1.

Thermal imaging has been used to study the airflow from vents and other warm or cold air sources in a room. One technique for visualizing the airflow is to stretch a plastic sheet along the section of interest and to observe the heat pattern produced, by the airflow, over the plastic sheet.[5]

10.2.2 INSPECTION OF COMPOSITE PANELS AND STRUCTURES

Composite panels and structures are widely used in various industries and in particular in the construction of aircraft where strength and lightness are important.[8,9] Safety is paramount and a thorough inspection is required to ensure that there are no areas of de-lamination, voids, or unwanted buried artifacts. Thermal imaging has been widely used for this type of inspection, where heat from lamps (or some other source) is applied on one side of the panel and the imager is used to see the resulting thermal pattern on the other side. De-lamination and voids will be regions of poor thermal conductivity and will show up as cooler areas on the opposite side of the panel.

This type of inspection can be useful not only for inspecting structures in the manufacturing and construction stages, but also during service as a means of discovering damage that has resulted at a later date in the use of the structure.[10,11]

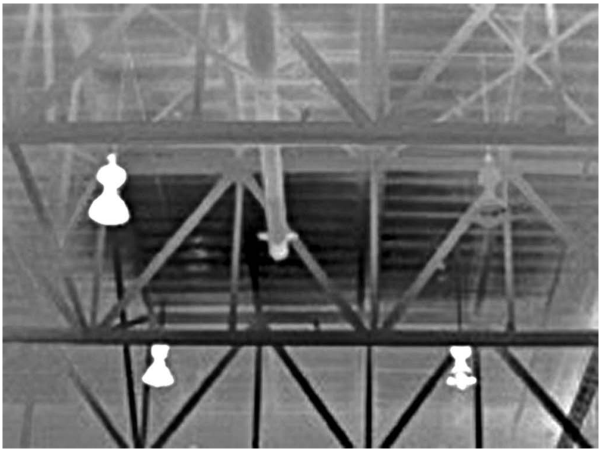

FIGURE 10.1 Thermal image showing an area of leakage in a roof. (With kind permission of FLIR Systems Ltd.)

10.2.3 INSPECTION OF FURNACE AND OTHER HIGH-TEMPERATURE CONSTRUCTIONS

An important aspect of furnaces and ladles for transporting molten metals (see Figure 10.2) is the functionality of the insulation. A thermal imager will very quickly show up areas where insulation is breaking down or has become less efficient.

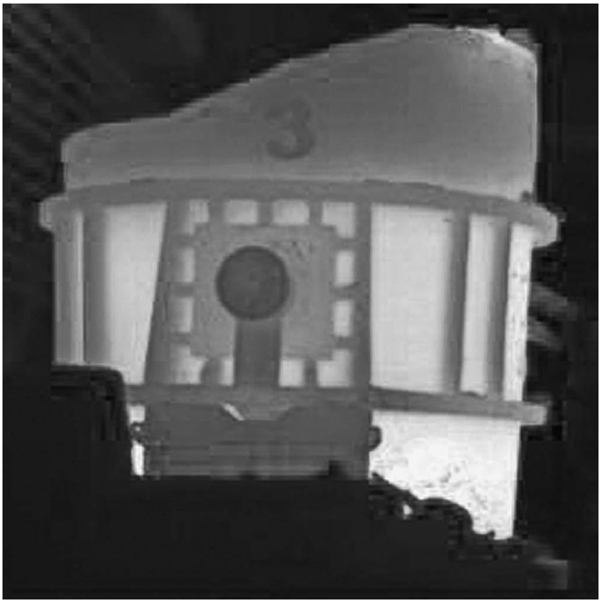

FIGURE 10.2 Thermal image of a ladle carrying molten metal. (With kind permission of Land Instruments International.)

10.2.4 PLANT AND SITE INSPECTION

One of the largest applications of thermal imagers is as a means of inspecting various types of industrial plants and sites, both for maintenance purposes (i.e., to identify equipment that is developing faults that could lead to failure) and as a means of determining the cause of actual failures. This type of application embraces most industries, including chemical, engineering, and electric power. Applications such as monitoring the temperature of bearings, and of various types of motors as well as electric fuses and electric wiring, are common to all these industries. In chemical plants thermal imaging can be used for monitoring pipework for blockages, corrosion, and underground leaks, checking the fill level of large storage tanks,[12] the abnormal operating temperatures of a processing plant, etc.[13,14] In the electric power industry[15] thermal imaging can be used for checking high-voltage insulators (these will get hot if they are no longer functioning as they should—Figure 10.3 shows a faulty bushing connector), power lines for finding thickness changes, malfunction of transformers, etc. It is quite common to use helicopters for this type of inspection, to allow extensive distances and areas to be conveniently covered.

Figure 10.4 illustrates some thermal images and their associated visual images that are relevant to industrial inspection.

In addition to its use for monitoring plants, thermal imaging can play an important role in quality control during manufacture. Its use for inspection of composite structures is covered in other sections of this chapter; however, there are many other ways in which it can be applied,[16] for example, monitoring temperatures in temperature-sensitive processes. Figure 10.5 illustrates the use of a thermal imager to inspect an internal car-seat heater.

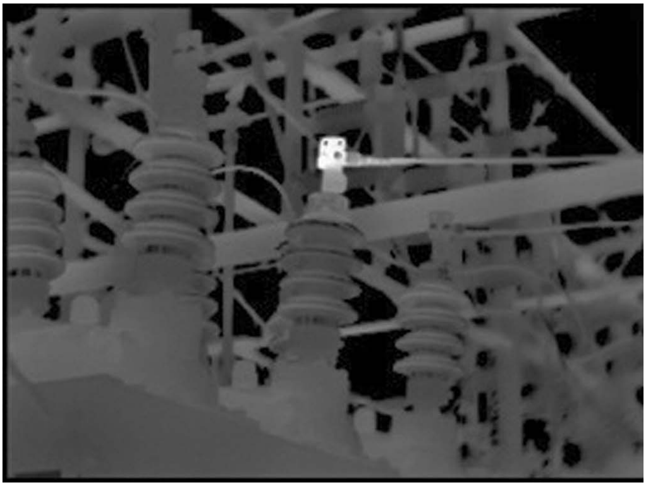

FIGURE 10.3 Thermal image of a faulty bushing connector. (By kind permission of FLIR Systems Ltd.)

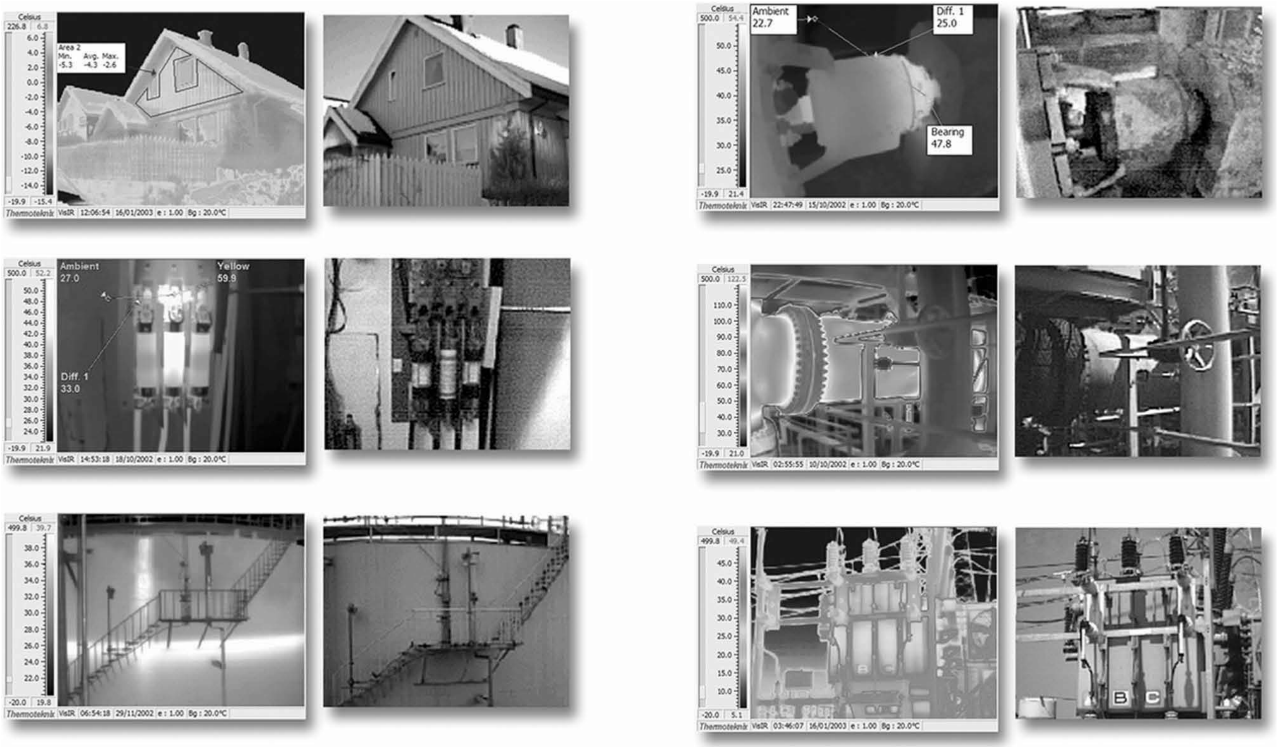
Celsius
Area 2
Min. Avg. Max.
-5.3 -4.3 -2.6
Thermoteknix VisIR 12:06:54 16/01/2003 e : 1.00 Bg : 20.0°C
Ambient
27.0
Yellow
59.9
Diff. 1
33.0
Thermoteknix VisIR 14:53:18 18/10/2002 e : 1.00 Bg : 20.0°C
Thermoteknix VisIR 06:54:18 29/11/2002 e : 1.00 Bg : 20.0°C
Ambient
22.7
Diff. 1
25.0
Bearing
47.8
Thermoteknix VisIR 22:47:49 15/10/2002 e : 1.00 Bg : 20.0°C
Thermoteknix VisIR 02:55:55 10/10/2002 e : 1.00 Bg : 20.0°C
B C
Thermoteknix VisIR 03:46:07 16/01/2003 e : 1.00 Bg : 20.0°C

FIGURE 10.4 Some industrial thermal images and their associated visual images. (With kind permission of Thermoteknix Systems Ltd.)

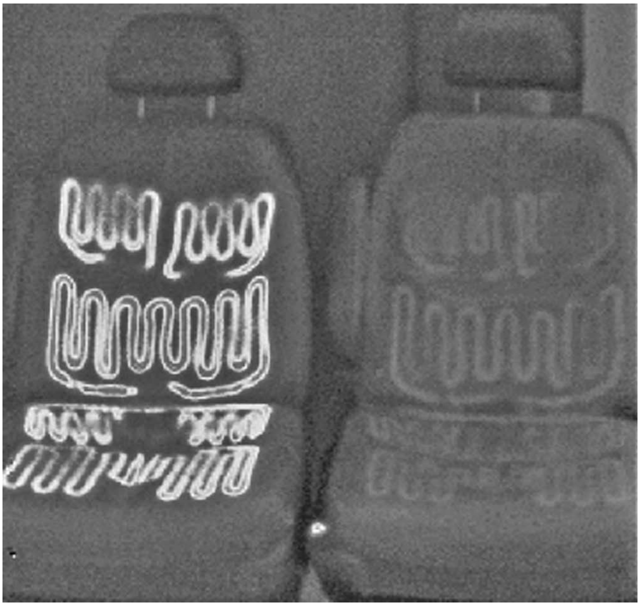

FIGURE 10.5 Thermal image used for inspecting an internal car-seat heater. (With kind permission of FLIR Systems Ltd.)

10.3 ADVANCED AND SPECIALIST APPLICATIONS

10.3.1 Detection of Buried Objects

The ability to detect objects buried underground is a valuable application of thermal imaging. It can readily be used for detecting pipework, where the contents of the pipe are hotter or colder than the ground in which it is buried. The greater challenge is to detect passive objects that have been buried for some time.[17] This could be useful for locating not only objects of archeological interest, but also objects such as mines. The feasibility of such detection depends on being able to see local temperature differences that can be produced as the object, and the ground in which it is buried, cools after being heated by the sun. Where the object has different thermal properties to its surrounds one can expect to see a different surface temperature, although the temperature differences may be very small and require the application of special image processing techniques to make them visible.

10.3.2 Studying and Preserving Works of Art

Most works of art are basically films of various thicknesses on some form of more homogeneous backing. As such, one would correctly expect many of the techniques described in this chapter for looking at films and sheets of material to be applicable to studying paintings and frescoes. Particularly successful has been the location and monitoring of de-lamination in frescoes.[18–20] One of the problems in dealing with works of art is the different emissivities of the external paint surfaces, which results in differential heating when attempting to generate heating of the work using lamps. To overcome this, one of the techniques is to use hot air to heat the surface.[19,20]

10.3.3 FIRE DETECTION AND VOLCANO MONITORING

Forest fires and fires on industrial sites can cause an enormous amount of damage unless they are detected at an early stage. Surveillance with a thermal imager provides a means of early detection that can function over large areas, long distances, and both during daylight and nighttime.

For these and many additional reasons, thermal imagers have proved useful in monitoring and analyzing several different aspects of volcanoes.[21] These include detection of magna movements within the summit, distinguishing lava flows of different ages, detecting instabilities on the flanks of active volcanoes, detection of danger conditions early, etc.

10.3.4 VISUALIZING ELECTRIC AND MAGNETIC FIELDS

Electric and magnetic fields can be visualized by using a thermal imager to view the heating effects they generate in sheets of suitable materials. For visualizing electric fields, use has been made of thin planar sheets of lossy carbon-loaded material, and for magnetic fields, thin planar sheets of lossy ferrite-loaded material.[22]

10.3.5 THERMAL WAVE IMAGING (TWI) AND TIME-RESOLVED INFRARED RADIOMETRY (TRIR)

TWI is a dynamic technique where the internal structure of a sheet of material or similar structure is investigated.[23–29] The concept is to create a thermal wave at one point or line on the surface, and then to record the thermal image of the rest of the surface as a function of time. The wave is produced by a heat pulse from one or more lamps and travels through the body of the material (see Figure 10.6). It is reflected back to the surface from an internal body, void, or surface in the material and generates a heat pattern on the surface that can be observed in the thermal image. The time taken for a part of the pattern to reach a maximum temperature will depend on the characteristics of the main body of the structure and the depth and position of the body or surface producing the reflection. The shape and size of the pattern will be an indication of the shape and size of the body.

TRIR is not dissimilar from TWI, but relies on the time taken for the heat pulse to be reflected or transmitted to a surface rather than its magnitude. The advantage of this is that the method is not very sensitive to surface emissivity. Frequently the technique uses a step increase in the applied heating rather than a pulse.[30]

These techniques are suitable for observing not only effects due to internal structures in the material, but also thickness changes in the material arising from recesses and other departures from planarity (intentional or otherwise) on the remote surface of the sheet. The technique can also be used for assessing the thickness and uniformity of coatings.[31]

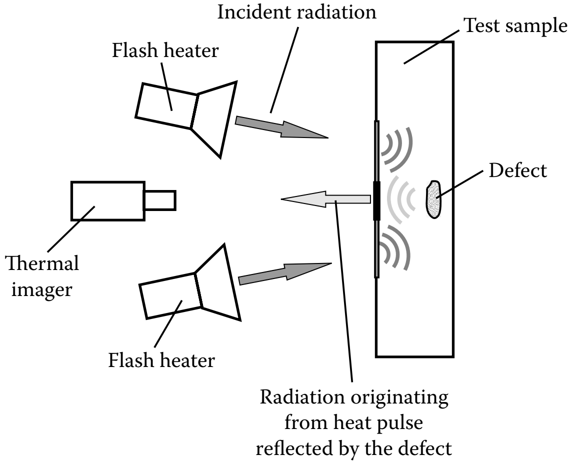

FIGURE 10.6 Illustration of the principle of thermal wave imaging.

TWI and TRIR are also applicable to inspection where the sheet is viewed on the opposite side of the heat source, although this is sometimes referred to simply as thermal imaging nondestructive testing (NDT), or TNDT.[32,33] There are many different ways of implementing both types of measurement. The chosen technique will depend on the material being inspected and the defects that are being searched for.

10.3.6 SONIC THERMAL NDT

A method of inspection for cracks and other defects is to transmit sonic waves through the structure and use a thermal imager to detect the heating effect that this produces at the sites of cracks or some similar defects (see Figure 10.7). The heating effects can be small, and the technique will normally require some special form of processing to be effective,[34–36] such as synchronous image capture.

10.3.7 THERMOELASTIC STRESS ANALYSIS

When a solid is compressed or stretched adiabatically it generates small temperature changes that are localized and proportional to the stress at that point in the structure. The temperature changes are very small, and to detect them, an imaging system is required that can ideally resolve as little as 0.01K. This was originally achieved[37] using a special form of thermal imager that scanned the structure slowly on a point-by-point basis. The structure under test was stressed cyclically, and the signal from the detector was processed by a form of lock-in amplifier that used a lock-in signal from the equipment that stressed the structure. The final output was a thermal image that showed the level and pattern of stress in the structure. The arrangement was very successful and was used for analyzing and developing a wide variety of structures, such as car suspensions. Later developments allowed the use of this technique on structures that could only be stressed transiently, such as bridges.

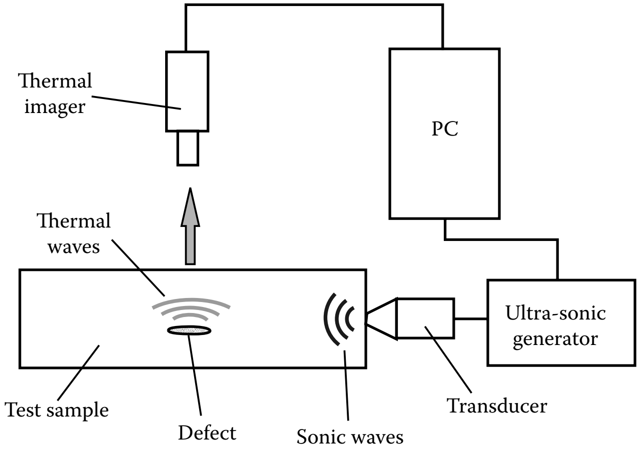

FIGURE 10.7 Illustration of the principle of sonic thermal NDT.

With the current availability of high-sensitivity thermal imagers that use large detector arrays, plus the processing power of modern computers, it is possible to do similar measurements using relatively standard commercial imagers. To achieve the required sensitivity the structures will normally still need to be stressed cyclically, and capture and processing of the images synchronized with the latter.[38–40]

10.4 MEDICAL AND BIOLOGICAL APPLICATIONS

Normal human skin has a relatively high emissivity (e.g., 98%), making it a good medium for allowing a thermal imager to measure its temperature fairly accurately. The temperature of the external surface of the skin will to some extent depend on the temperature and characteristics of the environment, and successful use of thermal imaging in such applications does require the environment to be carefully controlled. Apart from this, the temperature of the skin surface will depend on the temperature of the underlying parts of the body, which can deviate from normality as a result of many medical conditions.[41] Conditions producing fever will of course produce a rise in the body's temperature, and we have the example of the SARS epidemic, when airports were fitted with thermal imaging cameras to detect incoming passengers who had a high fever and might have been infected with the virus.[42,43] Figure 10.8 illustrates how a thermal imager can be used to show the fine details of the temperature distribution in a human hand.

There are situations where the emissivity of the skin can be changed by medical conditions or by the application of medical or cosmetic substances to the skin. Some of these conditions exhibit fluorescence in the infrared when the skin is illuminated with visible or ultraviolet light. These effects can be wavelength dependent and are best measured using a thermal imager that can measure the spectral characteristics of the thermal radiation. This can be done by using an imager fitted internally or

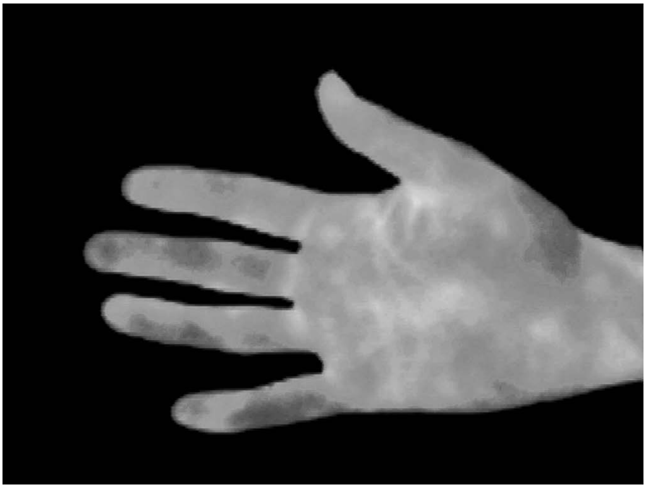

FIGURE 10.8 Temperature distribution in a human hand. (With kind permission of Land Instruments International.)

externally with a set of bandpass filters[44] that can be switched between frames to generate a set of thermal imagers taken at different wavelengths.

Some of the medical conditions that thermal imaging has helped to diagnose, locate, or monitor are:

- Obesity: Not only is subcutaneous fat a good insulator, but it also changes the blood flow.
- Hypothermia and hyperthermia: The body is dangerously too cold or too hot.
- Inflammation due to some form of infection: Such areas are usually hotter than normal.
- The state of tumors: The temperature at the site of a tumor can indicate the stage of its development.
- Vascular problems: Local temperatures will be a good indication of changes or abnormalities in blood flow, and thermal images can show varicose veins and dangerous conditions such as deep-vein thrombosis, as well as other vascular and arterial conditions.[45]
- Muscle temperature: The muscles that have been used in exercising will show up as relatively hot areas on a thermal image, and this could be useful for a physiotherapist working on restoring muscle condition and to athletes as an aid to training for a sport.

A related application has been to check the integrity of face masks used in medical applications, including preventing the transmission of viruses.[46] The method uses a thermal imager to generate images of hot breath leaking from the mask.

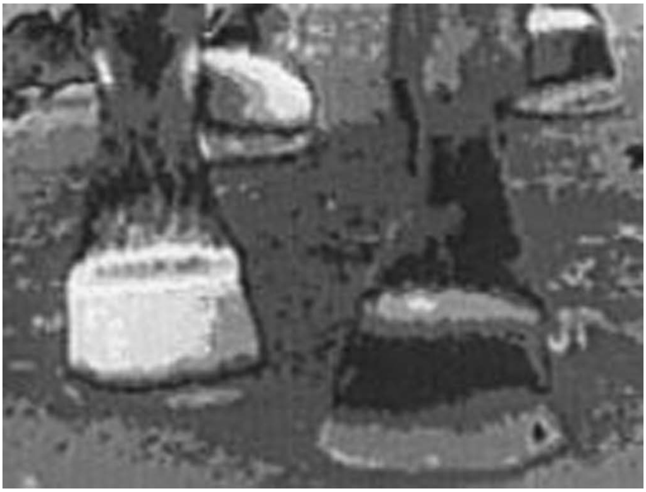

FIGURE 10.9 Thermal image showing medical problems of imbalance in an equine hoof. (With kind permission of FLIR Systems Ltd.)

Thermal imaging is equally applicable in the field of animal medicine, and Figure 10.9 illustrates the use of a thermal image to detect problems of imbalance in an equine hoof.

10.5 MILITARY AND CIVIL SURVEILLANCE AND OTHER APPLICATIONS

The development of high-sensitivity and high-resolution thermal imagers is largely due to their application for military surveillance and target detection and tracking. The advantages of thermal imaging that make them invaluable in this type of application are their ability to easily pick out objects that are hotter than their surround, and this includes humans and animals, as well as most vehicles and aircraft that are, or have recently been, in use. Equally important are the facts that the thermal wavelengths allow one to see through smoke, mist, and light fog, that no form of external lighting is required, and that normal camouflage is not effective at these wavelengths and effective camouflage is difficult to implement.

These advantages are also invaluable in surveillance of all types of nonmilitary sites (Figure 10.10 is an example of a thermal image of a car park). One of the civil applications that we have become very familiar with from various TV shows is that of tracking criminals from helicopters. Outdoors it is very difficult to hide from a thermal imager even in woodland, unless it is very thick. The same properties make it very useful for picking out life forms in various rescue missions.

Another useful property of a thermal imager is that it can allow one to reconstruct the moderately recent location of humans in a room. So, for example, a recently

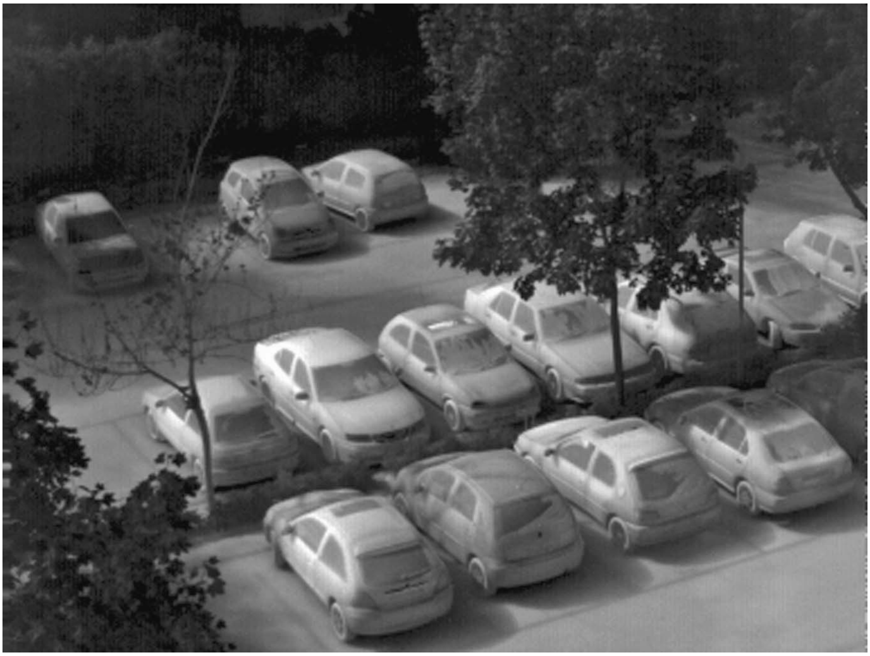

FIGURE 10.10 Thermal image of a car park. (With kind permission of Thermoteknix Systems Ltd.)

occupied chair will show the heat imprint of the occupier. The past position of hands or feet, etc., may also be detectable.

In recent years thermal imaging has been used in several nature films, not only to show the activities of animals in darkness and to detect their presence in woodland or undergrowth, but also to demonstrate the body temperature cycles of animals such as reptiles in contrast to those of mammals.

A rather different application that has been investigated is the use of a thermal imager for lie detection.[47] The idea here is that the temperature pattern and the actual temperatures on the face of an individual will change if he or she is lying.

REFERENCES

1. Hart, J. 1988. The use of thermography in the thermal performance testing of buildings. In *Applications of thermal imaging*, eds. S. G. Burney, T. L. Williams, and C. H. N. Jones, chap. 4. Bristol and Philadelphia: IOP Publishing Ltd.
2. McMullan, P. C. 1993. Masonry building envelope analysis. *SPIE Conference Proceedings* 1933:43–54.
3. Allinson, D., et al. 2005. Towards quantitative aerial thermal infrared thermography for energy conservation in the built environment. *SPIE Conference Proceedings* 5782:133–44.
4. Colantonio, A. 1995. Air leakage effects on stone cladding panels. *SPIE Conference Proceedings* 2473:27–35.

5. Sundberg, J. 1992. Visualizing airflow using IR—Techniques. *QIRT Seminar Proceedings* 27:333–37.
6. Lyberg, M. D., et al. 1990. Detection of moisture damage in buildings using thermography. *SPIE Conference Proceedings* 1313:100–5.
7. Knehans, A. 1993. The impact of aerial infrared roof moisture scans on the US Army's ROOFER program. *SPIE Conference Proceedings* 1933:67–73.
8. Cramer, K. E. 1995. Quantitative thermal imaging of aircraft structures. *SPIE Conference Proceedings* 2473:226–32.
9. Plotnikov, Y. A., and Winfree, W. P. 1999. Visualization of subsurface defects in composites using a focal plane array infrared camera. *SPIE Conference Proceedings* 3700:26–31.
10. Jones, T. S. 1995. Infrared inspection of advanced army composites. *SPIE Conference Proceedings* 2473:214–18.
12. Qin, Y. W. 1995. Thermographic NDT technique for delamination defects in composite structures. *SPIE Conference Proceedings* 2473:219–23.
12. Snell, J. 2004. Locating levels in tanks and silos using infrared thermography. *SPIE Conference Proceedings* 5405:245–48.
13. Weigle, R. K. 2005. Applications of infrared thermography for petrochemical process heaters. *SPIE Conference Proceedings* 5782:100–8.
14. Williams, T. L. 1988. Industrial and civil applications of thermography. In *Applications of thermal imaging*, eds. S. G. Burney, T. L. Williams, and C. H. N. Jones, chap. 2. Bristol and Philadelphia: IOP Publishing Ltd.
15. Funnell, I. R. 1988. Thermography in the electricity supply industry. In *Applications of thermal imaging*, eds. S. G. Burney, T. L. Williams, and C. H. N. Jones, chap. 3. Bristol and Philadelphia: IOP Publishing Ltd.
16. Meola, C., et al. 2002. Infrared thermography in the quality assurance of manufacturing systems. *Nondestructive Testing and Evaluation* 18:83–90.
17. Castro, E. H., et al. 2005. Thermographic detection of buried objects. *SPIE Conference Proceedings* 5782:145–52.
18. Grinzato, E., et al. 1998. NDE of frescoes by infrared thermography and lateral heating. *QIRT* 60:64–67.
19. Grinzato, E., et al. 1994. Non-destructive evaluation of delaminations in fresco plaster using transient infrared thermography. *Research in Nondestructive Evaluation* 5:257–71.
20. Bison, P. G., et al. 1998. Fresco thermographic inspection by convective heating technique. In *Review of progress in Quantitative Non-Destructive Evaluation*, eds. D. O. Thompson and D. E. Chimenti, 1769–76. Vol. 17. New York: Plenum Press.
21. Calvari, S. 1998. Monitoring active volcanoes using a handheld thermal camera. *SPIE Conference Proceedings* 5405:199–209.
22. Norgard, J. 1995. Empirical calibration of infrared images of electromagnetic fields. *SPIE Conference Proceedings* 2473:332–37.
23. Almond, D. P., et al. 1988. Thermal wave imaging and testing. In *Applications of thermal imaging*, eds. S. G. Burney, T. L. Williams, and C. H. N. Jones, chap. 8. Bristol and Philadelphia: IOP Publishing Ltd.
24. Selman, J. J., et al. 1993. Evaluation of a prototype thermal wave imaging system for non-destructive evaluation of composite and aluminium aerospace structures. *SPIE Conference Proceedings* 1933:178–87.
25. Favro, L. D., et al. 1995. Imaging the early time behaviour of reflected thermal-wave pulses. *SPIE Conference Proceedings* 2473:162–66.
26. Shepard, S. M., et al. 2005. Flash duration and timing effects in thermographic NDT. *SPIE Conference Proceedings* 5782:352–58.
27. Zalameda, J. N., et al. 2004. Improved sampling of thermal transients using focal plane array infrared imagers. *SPIE Conference Proceedings* 5405:374–81.

28. Marinetti, S., et al. 1999. Pulse phase thermography for defect detection and visualization. *SPIE Conference Proceedings* 3586:230–38.
29. Vavilov, V., et al. 1992. Dynamic thermal tomography: New NDE technique to reconstruct inner solids structure using multiple IR image processing.In *Review of progress in Quantitative Non-Destructive Evaluation*, eds. D. O. Thompson and D. E. Chimenti, 425–32. Vol. 11A. New York: Plenum Press.
30. Spicer, J. W. M., et al. 1993. Time-resolved infrared radiometry (TRIR) using a focal plane array for characterisation of hidden corrosion. *SPIE Conference Proceedings* 1933:148–59.
31. Shepard, S. M., et al. 1995. Thermal wave NDT of ceramic coatings. *SPIE Conference Proceedings* 2473:190–93.
32. Vavilov, V. 1992. Thermal non-destructive testing: Short history and state-of-art. *QIRT Seminar Proceedings* 27:179–94.
33. Grinzato, E. 1995. Methodolgy of processing experimental data in transient thermal NDT. *SPIE Conference Proceedings* 2473:167–78.
34. Miller, W. O., et al. 2003. Defining the envelope for sonic IR: Detection limits and damage limits. *SPIE Conference Proceedings* 5073:406–16.
35. Zweschper, T., et al. 2003. Frequency modulated elastic wave thermography. *SPIE Conference Proceedings* 5073:386–91.
36. Shepard, S. M., et al. 2004. Experimental considerations in vibrothermography. *SPIE Conference Proceedings* 5405:332–35.
37. Webber, J. M. B. 1988. Techniques and applications for thermoelastic stress analysis. In *Applications of thermal imaging*, eds. S. G. Burney, T. L. Williams, and C. H. N. Jones, chap. 7. Bristol and Philadelphia: IOP Publishing Ltd.
38. Lesniak, J. R. 1995. Differential thermography applied to structural integrity assessment. *SPIE Conference Proceedings* 2473:179–89.
39. Gyekenyesi, A. L. 2004. Evaluating the mechanical behaviour of notched SiC/SiC composites using thermoelastic stress analysis. *SPIE Conference Proceedings* 5405:456–65.
40. Sakagami, T., et al. 2005. Development of a self-reference lock-in thermography and its application to crack monitoring. *SPIE Conference Proceedings* 5782:379–87.
41. Jones, C. H., et al. 1988. Medical thermography. In *Applications of thermal imaging*, eds. S. G. Burney, T. L. Williams, and C. H. N. Jones, chap. 6. Bristol and Philadelphia: IOP Publishing Ltd.
42. Peacock, G. R. 2004. Human radiation thermometry and screening for elevated body temperature in humans. *SPIE Conference Proceedings* 5405:48–53.
43. Tan, Y. H., et al. 2004. Development and deployment of infrared fever screening systems. *SPIE Conference Proceedings* 5405:68–78.
44. Anbar, M. 1995. Multiple wavelength infrared cameras and their biomedical applications. *SPIE Conference Proceedings* 2473:323–31.
45. Wang, H. 2004. IR imaging of blood circulation of patients with vascular disease. *SPIE Conference Proceedings* 5405:115–23.
46. Dowdall, J., et al. 2005. Thermal image analysis for detecting facemask leakage. *SPIE Conference Proceedings* 5782:46–53.
47. Pavlidis, I. T. 2004. Lie detection using thermal imaging. *SPIE Conference Proceedings* 5405:270–79.

Appendix A: Objective Measurement of MRTD and MDTD

A.1 PERFORMANCE PARAMETERS THAT DETERMINE MRTD AND MDTD

The performance of a thermal imager, as far as its ability to allow the user to detect and recognize targets, will be largely determined by how high a resolution it provides, how good its sensitivity is to temperature differences, and finally, what the level of noise is in the final image. The resolution of an imager is best measured by its modulation transfer function (MTF), while its relative sensitivity and noise are measured by its noise-equivalent temperature difference (NETD) (see Sections 5.3.5 and 8.6).

As a result of experimental work carried out by Johnson,[1] two measures of performance have been used to designate the ability of the observer to detect and recognize targets: the minimum detectable temperature difference (MDTD) and the minimum resolvable temperature difference (MRTD) (see Sections 5.3.6 and 5.3.7). Both measures of performance are, strictly speaking, subjective measurements using one or more observers to determine the temperature differences required to just detect circular or square targets of varying angular subtense (MDTD), or the temperature differences required to just resolve four-bar targets of varying angular subtense (MRTD). As one might expect, subjective measurements of this type do not produce results that are very repeatable between different observers. In this appendix we describe some alternatives to the subjective measurements that depend only on performance measurements that can be made completely objectively. The equations given in this appendix are approximations that have been found to work and to give repeatable results. For this and other reasons, it is currently necessary to use some constant of proportionality to match the objective measurements to the subjective measurements, although this is probably not necessary where a purchaser places an acceptance specification on a manufacturer. Further information about objective MRTD and MDTD can be found in Chapter 9 of Williams.[2]

A.2 THEORY FOR MRTD MEASUREMENT

In Section 5.3.8 two approaches to measuring MRTD objectively are described. In this appendix we expand on these descriptions.

A.2.1 MRTD MODEL A (VIDEO OR DISPLAY)

In Section 5.3.8 the equation for calculating MRTD from objectively measured parameters is given as

$$\text{MRTD}(s) = k.\text{NETD}/\text{Mod}(s) \tag{A.1}$$

where k is a constant, NETD is the noise-equivalent temperature difference calculated from measurements of the root mean square (RMS) noise, the noise power spectrum (NPS), and the signal transfer function (SiTF), while Mod(s), the modulation, is calculated from the MTF of the imager. The constant k is a measure of signal/noise ratio required by an observer in order to just resolve a four-bar target. For comparison of objective results with subjective measurements taken where the observer can position himself or herself to best resolve the four-bar target, k is best assumed to be a constant independent of the spatial frequency. However, where the position of the observer is fixed (e.g., with an eyepiece display), better agreement may be obtained by making k a function of spatial frequency expressed in angular terms, to accommodate the fact that the contrast required by the eye to resolve a target varies with the angular spatial frequency subtended by the target at the eye.

Methods of measuring noise, NPS, and SiTF, and calculating NETD from these parameters are described in Chapter 8, where methods of measuring MTF are also described. The task here is to provide a relationship for calculating Mod(s) from the measured MTF. The simplified approach used here, which appears to be more than adequate for its purpose, is to assume that the profile of the four-bar targets is given by the profile of a repetitive bar pattern at the appropriate spatial frequency (Trgt(s)) multiplied by the profile of a repetitive bar pattern equivalent to the width of the four-bar pattern ($\text{Env}(s)_a$) and multiplied by a similar pattern for the height of the four-bar pattern ($\text{Env}(s)_b$). The last two profiles may be the same if the MTF in both directions is the same, but could in principle be different. The relevant equations are

$$\text{Trgt}(x, s) = \{\textstyle\sum_n [(\sin(\pi.n/2)/(\pi.n/2))].\cos(2.\pi.x.s + \pi).\text{MTF}_a(s)\} + 0.5 \tag{A.2}$$

$$\text{Env}(x, s)_a = \{\textstyle\sum_n [(\sin(\pi.n/2)/(\pi.n/2))].\cos(2.\pi.x.s/7 + \pi).\text{MTF}_a(s/7)\} + 0.5 \tag{A.3}$$

$$\text{Env}(x, s)_b = \{\textstyle\sum_n [(\sin(\pi.n/2)/(\pi.n/2))].\cos(2.\pi.x.s/7 + \pi).\text{MTF}_b(s/7)\} + 0.5 \tag{A.4}$$

where s is the spatial frequency of the four-bar pattern, x is linear distance, and $\text{MTF}_a(s)$ and $\text{MTF}_b(s)$ are the MTFs of the system in the two orthogonal directions. The value of n should be sufficiently high to ensure that any increase in its value will not significantly change the result.

From these equations we can calculate the profile of the four-bar targets as

$$\text{Bars}(x, s) = \text{Trgt}(x, s).\text{Env}(x, s)_a.\text{Env}(x, s)_b \tag{A.5}$$

The modulation is given by

$$\text{Mod}(s) = [\text{Bars}(3/(2.s),s) - \text{Bars}(0, s)] \tag{A.6}$$

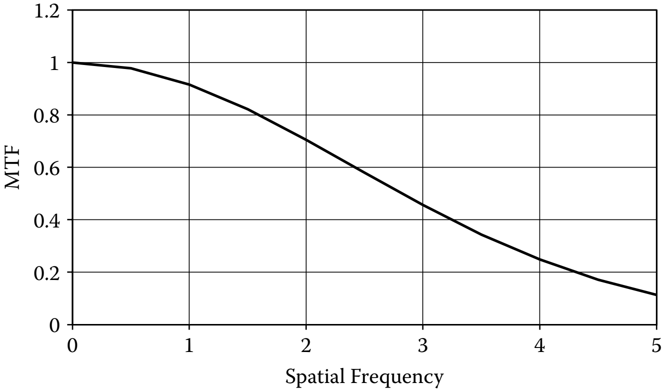

FIGURE A.1 Gaussian MTF curve used for predicting the MRTD curves in this appendix.

In order to simplify the calculation procedure it can be helpful to approximate the MTF of the system by a Gaussian curve or a polynomial. Figure A.1 is an example of a Gaussian MTF curve given by the equation

$$\mathrm{MTF}(s) = \exp[-\pi(0.7s)^2] \tag{A.7}$$

Figure A.2 shows plots of $\mathrm{Bars}(x,s)$ for $s = 3.0$, 5.8, and 8.0, while Figure A.3 is a plot of the resulting MRTD curve, assuming that NEDT = 0.1°C and $k = 1$.

A.2.2 MRTD Model B

As explained in Section 5.3.8, the technique used here is that of measuring the modulation directly in the image of the four-bar target using a large temperature

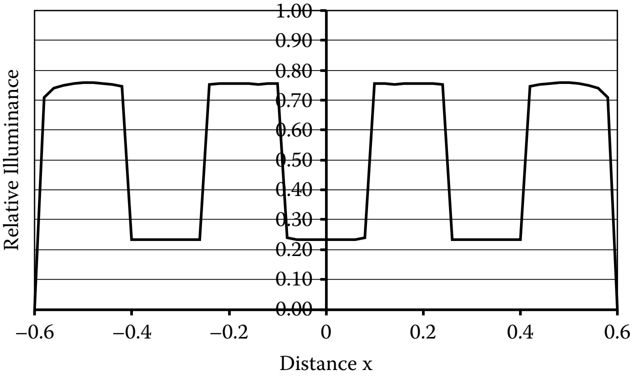

(a)

FIGURE A.2 (a to c) Plots of the luminance profiles for different MRTD target spatial frequencies as predicted by model A. *(Continued)*

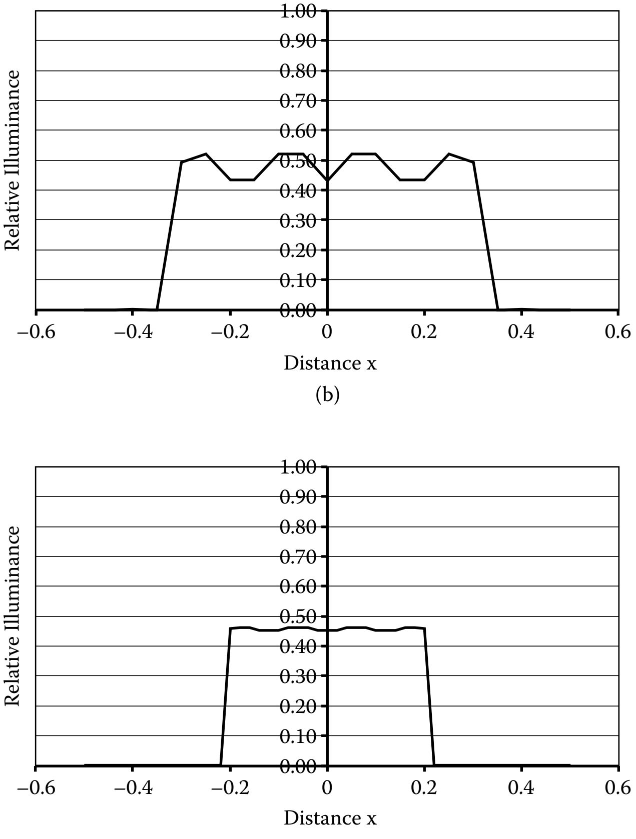

(b)

(c)

FIGURE A.2 *(Continued)*

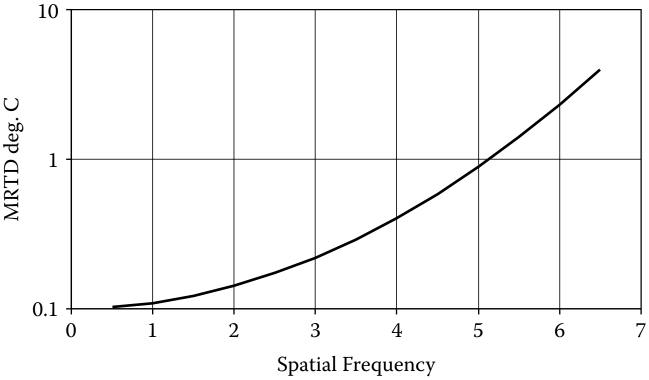

FIGURE A.3 MRTD calculated using model A.

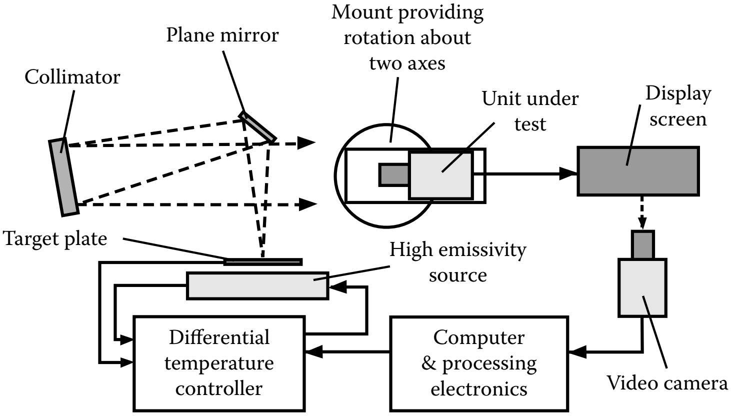
Mount providing rotation about two axes
Plane mirror
Collimator
Unit under test
Display screen
Target plate
High emissivity source
Differential temperature controller
Computer & processing electronics
Video camera

FIGURE A.4 Arrangement for measuring MRTD using model B.

difference, and then to calculate the temperature difference ΔT (i.e., the MRTD) for which

$$\mathrm{Mod}(s, \Delta T) = k.\mathrm{NETD} \tag{A.8}$$

where

$$\mathrm{Mod}(s, \Delta T) = (\Delta T/\Delta T_m).\mathrm{Mod}(s, \Delta T_m) \tag{A.9}$$

where $\mathrm{Mod}(s, \Delta T_m)$ is the modulation depth in the image of the target when the temperature difference is ΔT_m (i.e., the high temperature difference where the modulation was measured).

The measurements can be made off the display of the thermal imager using the arrangement illustrated in Figure A.4. In this arrangement a charge-coupled device (CCD) camera is used to capture the image of the four-bar target and transfer it to a frame store in a PC. Suitable software can be used to control the thermal source automatically in order to measure NETD and SiTF (using appropriate targets; see Chapter 8) as well as $\mathrm{Mod}(s, \Delta T_m)$ for the various four-bar targets. The main problem is in developing software for measuring the latter, particularly at the higher spatial frequencies, where the modulation depth can be very small even at relatively high temperature differences. In our experience the best solution is for the software to have knowledge of the size and position of the four-bar target on the display, and from that to make measurements of the luminance in the areas it knows to be the image of the bars and measurements in the areas that it knows are the spaces in between, in order to determine the modulation depth. This method of measuring an objective MRTD was found to give results that agreed very well with subjective measurements.

A.3 THEORY FOR MDTD MEASUREMENT

Objective techniques for measuring MDTD are similar to those described above for measuring MRTD, except that the equations are different. Three approaches are described here. Two of these use equations involve the measured MTF and NETD to predict the signal level in the image of square targets of different dimensions, while the third involves a direct measure of the signal level in the image of the target at a high temperature difference, which is then used to predict the MDTD from a measurement of the SiTF.

A.3.1 MDTD Model A

In Section 5.3.9 the equation for determining MDTD objectively is given as

$$\mathrm{MDTD}(s) = k.\mathrm{NETD}.\mathrm{TR}(s) \tag{A.10}$$

where TR(s) is the ratio (actual target temperature difference)/(apparent target temperature difference) for a target of dimensions (1/s).

The theory applied here is that the peak intensity in the image is proportional to the integral under the modulus of the Fourier transform of the image, so that we have

$$\mathrm{TR}(s) = \{\int[\sin(\pi.f/s)/(\pi.f/s)].|\mathrm{MTF}(f)|.df\}^2/\{\int[\sin(\pi.f/s)/(\pi.f/s)].df\}^2 \tag{A.11}$$

where the integral is over a positive range sufficiently large not to significantly affect the result, and f is spatial frequency in the same units used for the reciprocal of the target dimensions (i.e., 1/s). MTF(f) is the MTF of the system assumed to be the same in both the horizontal and vertical directions.

The graph of Figure A.5 shows a plot of the MDTD using this equation and assuming that NETD = 0.1°C, k =1, and $|\mathrm{MTF}(f)| = \exp[-\pi(0.1f)^2]$.

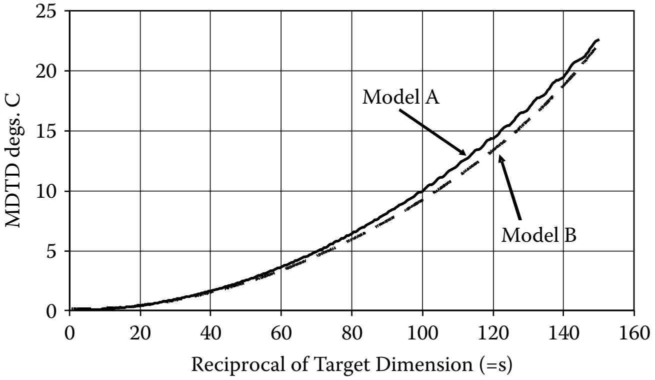

FIGURE A.5 Plot of MDTD using models A and B.

A.3.2 MDTD Model B

The assumption here is that the signal peak is given by the peak in the image of one square wave of a repetitive square-wave pattern that has a markspace ratio that is not unity, so that we have

$$V(x, f) = 1/a + \sum_n \{(a/2).\sin(\pi.n/a).\mathrm{MTF}(n.f).\cos(2.\pi.x.n.f)/(\pi.n/a)\} \qquad \text{(A.12)}$$

where $V(x, f)$ is the square wave of frequency f, a is the ratio of the total period to the pulse width, x is linear distance, and the value of n should be sufficiently high to ensure that any increase in its value will not significantly change the result. The pulse width is $s = a.f$, and therefore:

$$\mathrm{TR}(s) = 1/[V(0, s/a)^2 - \mathrm{V}(a/2.s, s/a)^2] \qquad \text{(A.13)}$$

The graph of Figure A.5 also shows a plot of the MDTD obtained using this equation, where NETD and MTF(f) are the same as the values used for the plot of model A, and where $a = 20$ and $k = 1.32$ (selected to give a closer match between the two curves).

A.3.3 MDTD Model C

The technique used here is similar to that used in the MRTD model B method. It involves measuring directly the difference S between the peak signal in the image of the target and the background signal, and then to calculate the temperature difference ΔT (i.e., the MDTD) for which

$$S(\Delta T) = k.\mathrm{NETD} \qquad \text{(A.14)}$$

where $S(\Delta T)$ is the difference signal for a temperature difference ΔT, and where

$$S(\Delta T) = (\Delta T/\Delta T_m).S(\Delta T_m) \qquad \text{(A.15)}$$

where $S(\Delta T_m)$ is the signal difference in the image of the target when the temperature difference is ΔT_m (i.e., the high temperature difference where the signal peak was measured). Finally, we have from these equations that

$$\mathrm{MDTD}(s) = \Delta T_s = k.\mathrm{NETD}.\Delta T_{m,s}/S(\Delta T_{m,s}) \qquad \text{(A.16)}$$

where the temperature differences all refer to the target of spatial frequency s.

REFERENCES

1. Johnson, J. 1958. Paper presented at Image Intensifier Symposium, Fort Belvoir. Results summarized in Chapter 1 of Biberman, L. M. 1973. *Perception of displayed information*. New York: Plenum Press.
2. Williams, T. L. 1999. *The optical transfer function of imaging systems*. Philadelphia: IOP Publishing.

Appendix B: Sampled Imaging Systems and Aliasing

B.1 WHAT ARE SAMPLED IMAGING SYSTEMS?

ISO 15529[1] defines a sampled imaging system as an "imaging system or device, where the image is generated by sampling the object at an array of discrete points, or along a set of discrete lines, rather than a continuum of points." The two-dimensional (2D) detector arrays used in most thermal imagers are such devices, as are imagers that scan the image in a series of lines, although in the latter case the effects of sampling only occur in the direction perpendicular to the scan direction.

One of the more obvious effects of sampling is the moiré fringes that are seen on TV programs when viewing the image of an object with a regular line pattern, such as the weave in certain types of cloth. However, less obvious effects, which may nevertheless generate artifacts in an image, can result from sampling. The effects in an image of under-sampling are usually referred to as aliasing (see also Section 5.3.3).

In practice, any system where the sampling period is significantly less than the combined resolution of the lens system and the detector array (i.e., the spacing of the bars of a repetitive pattern that the camera can only just resolve, or more strictly, the spatial frequency where the modulation transfer function [MTF] falls to zero) can be considered a system where the image is sampled over a continuum of points, and where therefore the effects of sampling are insignificant and there will be no aliasing.

If and when sampling effects are present in a thermal imager, they will generate errors in temperature readings, which could be significant when very accurate temperature readings are required. This appendix will illustrate the effects of aliasing and outline the conditions under which it occurs and the conditions for eliminating it, without going into a detailed description of the theory. Readers who wish to follow the theory in more detail will find a comprehensive explanation in ISO 15529,[1] Williams,[2] and Wittenstein.[3]

B.2 IMAGE FORMATION BY SAMPLED IMAGING SYSTEM

The critical dimension in a sampled imaging system is the **Nyquist frequency**, which is the spatial frequency equal to half the reciprocal of the spacing between sampling points. So if the spacing between the pixels of a detector array is a, the Nyquist frequency for that array is $1/2a$. The Nyquist frequency is the maximum sinewave spatial frequency that can be resolved by the detector array. However, there are other important effects that can result from using a sampled imaging system, some of which are illustrated in Figures B.1 to B.3. These figures show the image of a square wave pattern generated by a detector array. Figure B.1(a) shows the image of a pattern where the spatial frequency is low compared to the Nyquist frequency, while Figure B.1(b) and (c) show the image of the same spatial frequency pattern,

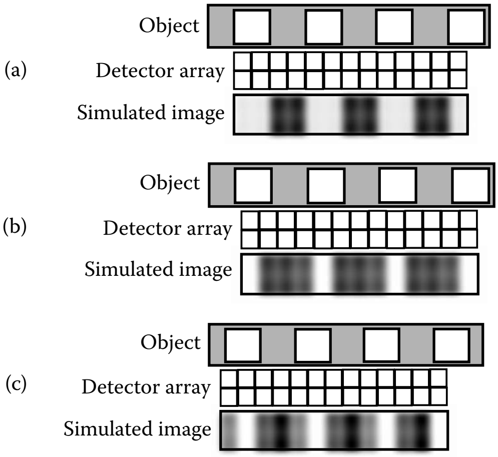

FIGURE B.1 (a to c) Illustration of the effect on the image of altering the relative phase of the latter with respect to the detector array—spatial frequency less than the Nyquist limit.

which has been shifted along its length so that it has a different phase with respect to the detector array. Although the image has the same spatial frequency as the original pattern in all cases, it differs significantly in shape. Figure B.2(a) and (b) show a pattern where the spatial frequency is close to the Nyquist frequency, where again the pattern has been shifted along its length. In this example the image still has the same spatial frequency as the original pattern, but the amplitude has changed significantly. Figure B.3(a) and (b) show the images of two patterns with a frequency higher than

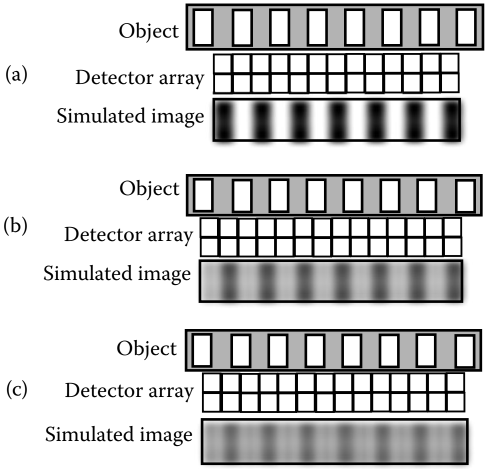

FIGURE B.2 (a to c) Illustration of the effect on the image of altering the relative phase of the latter with respect to the detector array—spatial frequency close to the Nyquist limit.

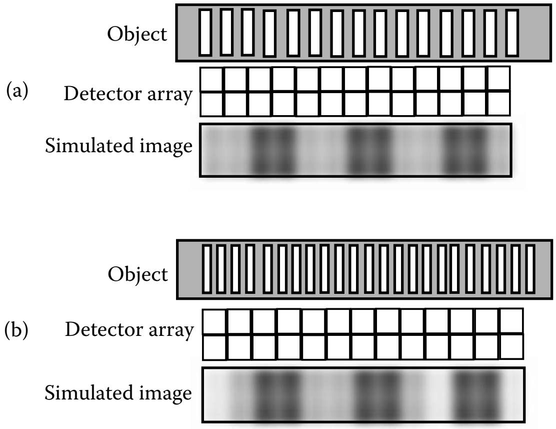

FIGURE B.3 (a and b) Illustration of the effect on the image when the spatial frequency is higher than the Nyquist limit of the detector array.

the Nyquist frequency. In this case the image does not have the same spatial frequency as the original pattern, but a frequency less than the Nyquist limit.

These illustrations are only approximate and are used here to demonstrate the types of effect that can arise with sampled imaging systems. If the variation in intensity along the pattern followed a sinewave rather than a square wave, then the effects illustrated in Figures B.1(a) to (c) and B.2(a) and (b) would be different and the images would all approximate to sinewaves of the same spatial frequency as the original pattern, and their amplitude would be independent of the relative phases of the pattern and the array. In the case of Figure B.3(a) and (b) the image would also be a sinewave of fixed amplitude, but the frequency would not be the same as that of the original pattern, but would be less than the Nyquist frequency. For patterns intermediate between a square wave and a sinewave, the effects would also be intermediate between the two extremes.

We see from these illustrations that sampled imaging systems are potential sources of temperature measurement errors, at least where finer detail is concerned. However, there are conditions where errors do not arise from this source or, if they do, are negligible. This situation is discussed in the next section.

B.3 BASIC THEORY

Figure B.4 shows a typical train of the units that make up an imaging system such as a thermal imager, as well as symbols for the OTF (Optical Transfer Function[2]—this is a more complete description of how a sinewave target is reproduced by an imaging system and includes the MTF as well as a term describing the relative phases with which the sinewaves are reproduced. The latter is referred to as the PTF (Phase Transfer Function) and is usually ignored except in special circumstances) and the MTF of each unit. Each of the sampling apertures (pixels) will provide a single signal that is proportional to the total radiant energy falling on that aperture, and the reconstruction function is the electronically generated function that converts this to a spatial distribution that prevents

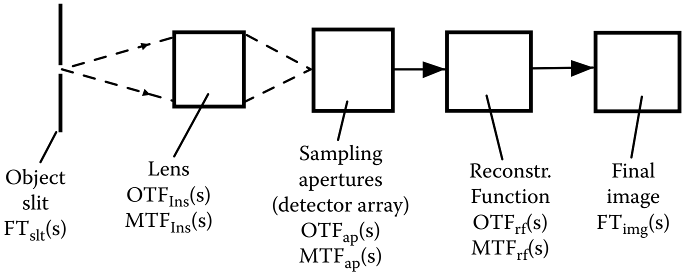

FIGURE B.4 Block diagram of a typical imaging system.

the image from being made up of a series of points and includes the effect of the display. If the sampling apertures and their spacing are sufficiently small so that they act effectively as a continuum of sampling points, then the image of a narrow slit formed by the system (i.e., the line spread function [LSF]) will be given by the equation

$$\mathrm{LSF}_{\mathrm{img}}(x) = \mathrm{LSF}_{\mathrm{slt}}(x) \copyright \mathrm{LSF}_{\mathrm{lns}}(x) \copyright \mathrm{LSF}_{\mathrm{ap}}(x) \copyright \mathrm{LSF}_{\mathrm{rf}}(x) \qquad \text{(B.1)}$$

where the symbol © is used here to designate the process of convolution, and x is the linear distance variable. The Fourier transform of the intensity distribution in the final image will be given by the equation

$$\mathrm{FT}_{\mathrm{img}}(s) = \mathrm{FT}_{\mathrm{slt}}(s).\mathrm{OTF}_{\mathrm{lns}}(s).\mathrm{OTF}_{\mathrm{ap}}(s).\mathrm{OTF}_{\mathrm{rf}}(s) \qquad \text{(B.2)}$$

where s is the spatial frequency variable.

The OTF of each unit is in fact the Fourier transform of the LSF associated with that unit. The MTF of the camera system will be given by the equation

$$\mathrm{MTF}_{\mathrm{cam}}(s) = |\mathrm{FT}_{\mathrm{img}}(s)|/|\mathrm{FT}_{\mathrm{slt}}(s)| = \mathrm{MTF}_{\mathrm{lns}}(s).\mathrm{MTF}_{\mathrm{ap}}(s).\mathrm{MTF}_{\mathrm{rf}}(s) \qquad \text{(B.3)}$$

Normal OTF theory such as that represented by Equations (B.1) to (B.3) only applies to imaging systems where the LSF of the system does not change significantly if it is shifted laterally. This is referred to as the principle of stationarity, and such systems are referred to as being isoplanatic.[4] Figure B.5 illustrates why a sampled imaging system does not satisfy this condition. For such systems, where the spacing between pixels of the array is a, the following equation holds:

$$\mathrm{LSF}_{\mathrm{img}}(x) = [\mathrm{LSF}_{\mathrm{in}}(x)\{\textstyle\sum_k \delta(x - \phi - k.a\}] \copyright \mathrm{LSF}_{\mathrm{rf}}(x) \qquad \text{(B.4)}$$

where $\mathrm{LSF}_{\mathrm{in}}(x) = \mathrm{LSF}_{\mathrm{slt}}(x) \copyright \mathrm{LSF}_{\mathrm{lns}}(x) \copyright \mathrm{LSF}_{\mathrm{ap}}(x)$ and can be considered as the input to the sampling stage. The function $\{\sum_k \delta(x - \phi - k.a\}$ represents the sampling comb, where δ is the Dirac delta function, ϕ is a term that describes the relative position or phase of the sampling comb with respect to the image, and k is an integer denoting the number of a pixel in the array. Because the comb function is periodic, the values of ϕ can be limited to $0 < \phi < a$. More details of how Equation (B.4) is derived will be found in ISO 15529,[1] Willaims,[2] and Wittenstein.[3]

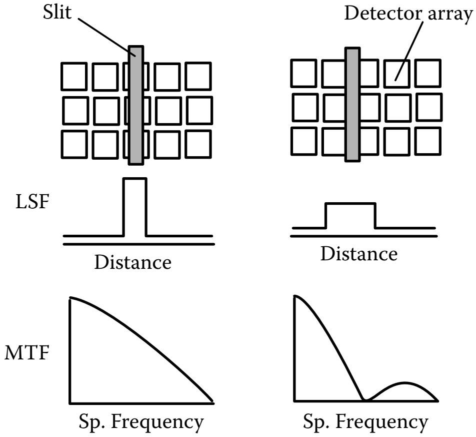

FIGURE B.5 Illustration of how stationarity does not hold for sampled systems.

The Fourier transform of $\mathrm{LSF}_{\mathrm{img}}(x)$ will be given by

$$\mathrm{FT}_{\mathrm{img}}(s) = [\mathrm{FT}_{\mathrm{in}}(s) © \{\textstyle\sum_k \delta(s - k.a\}.\mathrm{exp} i2\pi\phi s\}].\mathrm{OTF}_{\mathrm{rf}}(s) \qquad \text{(B.5)}$$

After performing the convolution this becomes

$$\mathrm{FT}_{\mathrm{img}}(s) = [\textstyle\sum_k \mathrm{FT}_{\mathrm{in}}(s - k.a).\mathrm{exp}(i2\pi\phi(k/a))\}].\mathrm{OTF}_{\mathrm{rf}}(s) \qquad \text{(B.6)}$$

What this means is that if the target is a slit, the Fourier transform of the slit image will be given by the sum of similar Fourier transforms replicated at spatial frequency intervals of $1/a$ with a phase difference of $2\pi\phi(k/a)$, multiplied finally by the OTF of the reconstruction function. This means that we no longer have a unique Fourier transform of the image of a slit, and hence the OTF of the imaging system (if we are using this method of measuring OTF). Instead, we have a value that depends on the position of the slit image on the sampling array. This is illustrated in Figure B.6(a) and (b). In Figure B.6(a) curve 1 is $\mathrm{FT}_{\mathrm{in}}(s)$, which is the product $\mathrm{FT}_{\mathrm{slt}}(s).\mathrm{MTF}_{\mathrm{lns}}(s).\mathrm{MTF}_{\mathrm{ap}}(s)$ for $k = 0$, and curve 2 is the same Fourier transform, but with $k = 1$. Figure B.6(b) shows the $\mathrm{FT}_{\mathrm{img}}(s)$ (but without including the reconstruction function), which is the combination of the two curves of Figure B.6(a), for two different relative phases (i.e., positions of the slit image on the sampling array). In this case curve 3 is for zero phase difference and curve 4 is for a 180° phase difference (i.e., the two extreme cases). Figure B.6(c) shows the reconstruction function and the effect of including it in these two curves. These are basically the two MTF curves one would have obtained on the basis that the Fourier transform of a narrow slit image is the MTF of the imaging system.

There are two special situations worth describing. The first is where $\mathrm{FT}_{\mathrm{in}}(s)$ falls to zero, or is very small, for spatial frequencies beyond the Nyquist limit. This is illustrated in Figure B.7(a) to (c), where the curve numbers have the same meaning as

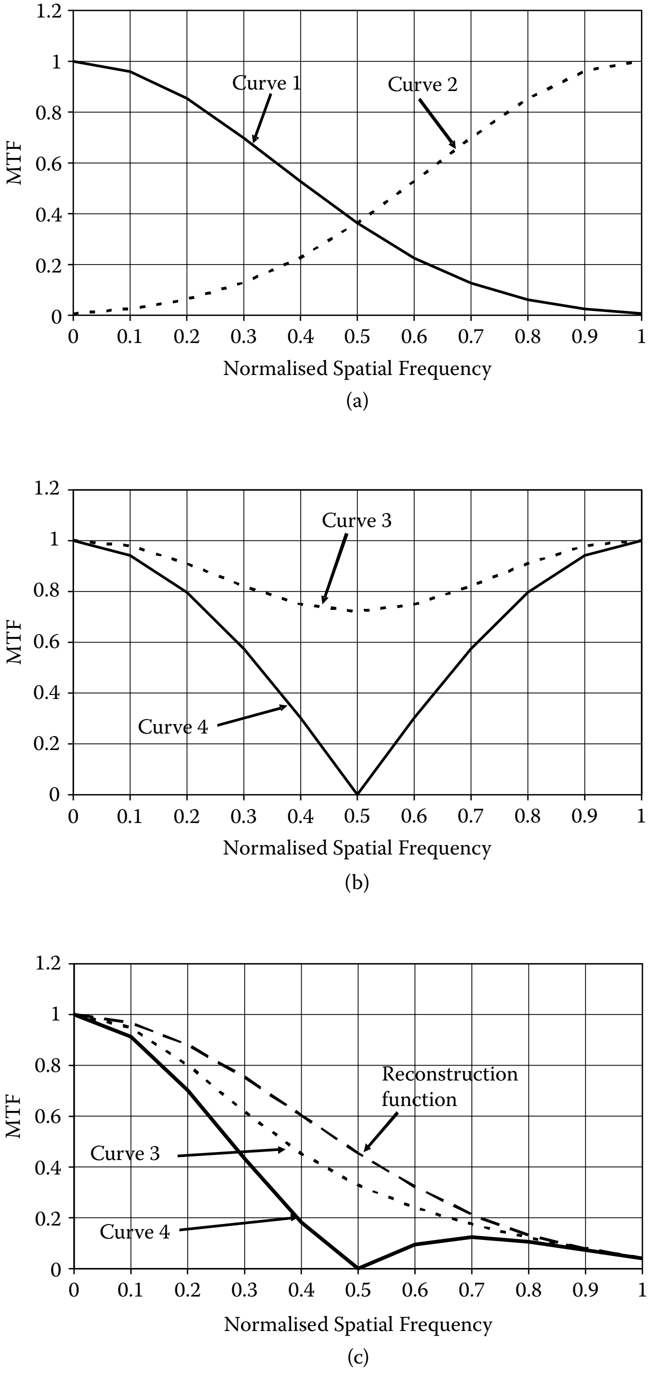

(a)

(b)

(c)

FIGURE B.6 (a to c) Illustration of the results of measuring the MTF of a sampled system using a narrow slit target.

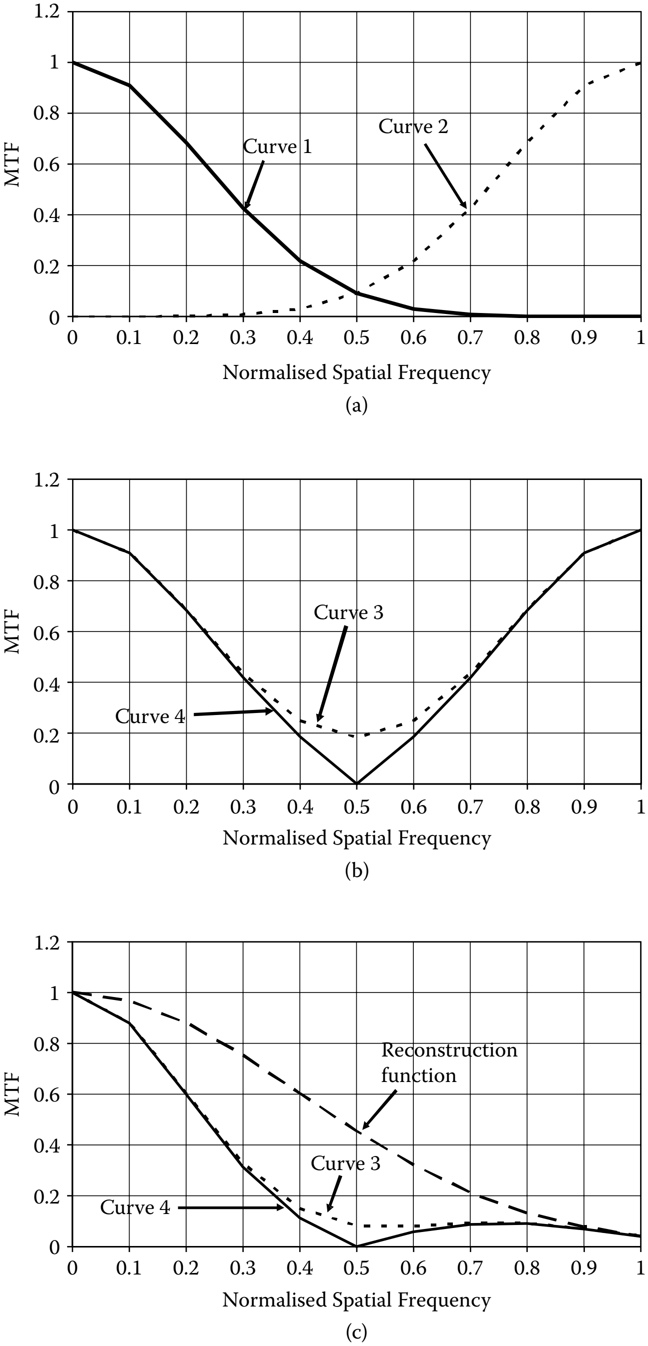

FIGURE B.7 (a to c) Illustration of the results of measuring the MTF of a sampled system using a narrow slit target when the Fourier transform of the input function is low for frequencies above the Nyquist limit.

in the earlier figures. We see here that the MTF of the imaging system has virtually a unique value independent of relative phases. In this situation no aliasing occurs, and the fact that the imaging system is a sampled system will not introduce any sources of error, such as moiré fringes. This is a situation that the designer will aim for, preferably by using a combination of lens and detector array that have a combined Fourier transform that is very low at spatial frequencies beyond the Nyquist limit.

Although one might expect the spatial response of a single pixel of a detector array to have the shape of a top hat with a width equal to the width of the sensitive area of the pixel, in practice there will usually be cross talk between pixels that will both alter their shape and increase their effective width. The result of this is to reduce the value of a pixel's Fourier transform and lower the spatial frequency where the value falls to zero. This will help to reduce the designer's task of removing aliasing, although it may have other undesirable effects.

The second special situation is where the object being imaged is a grating where the intensity varies sinusoidally. In this case the final image will also be a sinusoidal grating, with a contrast that is independent of the relative phase of the sinusoid and the sampling array. The spatial frequency of the grating image will be the same as that of the original object (allowing, of course, for the magnification of the imaging system) for all grating spatial frequencies less than the Nyquist frequency. For frequencies greater than this the spatial frequency will be given by

$$S_{\mathrm{img}} = 1/a - S_{\mathrm{obj}} \tag{B.7}$$

where S_{obj} is the spatial frequency of the original object and, as before, a is the spacing of the pixels (sampling apertures). The modulation at that spatial frequency will be given by the MTF at that spatial frequency multiplied by the MTF of the reconstruction function.

B.4 MEASURES OF ALIASING

It is useful to be able to characterize the potential for aliasing in a sampled imaging system, and this can be done using three parameters defined by ISO15529[1] (see also Section 5.3.3). The first of these is the *aliasing function*. It is based on the fact that if we measure the Fourier transform of the image of a narrow slit with a sampled imaging system we get values that depend on the position of the slit image (i.e., its phase) relative to the sampling array. The aliasing function is defined as

$$\mathrm{AF}(s) = (|\mathrm{FT}_{\mathrm{img}}(s)|_{\mathrm{max}} - |\mathrm{FT}_{\mathrm{img}}(s)|_{\mathrm{min}})/2 \tag{B.8}$$

where $|\mathrm{FT}_{\mathrm{img}}(s)|_{\mathrm{max}}$ is the maximum value of the modulus of the Fourier transform of the slit image and $|\mathrm{FT}_{\mathrm{img}}(s)|_{\mathrm{min}}$ is the minimum value. AF(s) is a measure of the degree to which the system responds to spatial frequencies higher than the Nyquist frequency and, as a result, produces spurious low frequencies in the image.

The second of these parameters is the *aliasing ratio*. This is defined as

$$\mathrm{AR}(s) = \mathrm{AF}(s)/(|\mathrm{FT}_{\mathrm{img}}(s)|)_{\mathrm{av}} \tag{B.9}$$

where $(|FT_{img}(s)|)_{av}$ is the average of the maximum and minimum values of the modulus of the Fourier transform of the slit image, i.e.,

$$(|FT_{img}(s)|)_{av} = (|FT_{img}(s)|_{max} + |FT_{img}(s)|_{min})/2 \qquad (B.10)$$

AR(*s*) can be thought of as a measure of the noise produced by the aliasing, and of being equivalent to a noise/signal measurement.

The last of these parameters is the *aliasing potential*, which is defined as

$$AP = \int_{s=0.5\to1} (MTF_{lns}(s)^*MTF_{ap}(s))/\int_{s=0\to0.5} (MTF_{lns}(s)^*MTF_{ap}(s)) \qquad (B.11)$$

where s is normalized so that $1/a$ becomes unity and where, as earlier, $MTF_{lns}(s)$ is the MTF of the lens and $MTF_{ap}(s)$ is the MTF of the sampling aperture (pixel) and any "blur" filters positioned between the lens and sampling aperture. As its name implies, this parameter is a measure of the potential of an imaging system to produce aliasing and is possibly most useful in the design stage of an imager.

B.5 MTF MEASUREMENT TECHNIQUES

In principle, a sampled imaging system that suffers from aliasing cannot have a true MTF associated with it since it is not isoplanatic (see above and ISO 9334[4]). However, for practical purposes, where a measure of the imaging quality of the system is required, it is very useful to have some form of MTF to characterize the system. ISO 15529[1] effectively defines the MTF of a sampled imaging system (e.g., thermal imaging camera) as the product

$$MTF_{cam}(s) = MTF_{lns}(s).MTF_{ap}(s).MTF_{rf}(s) \qquad (B.12)$$

where, as earlier, $MTF_{lns}(s)$ is the MTF of the lens, $MTF_{ap}(s)$ is the MTF of the sampling aperture (pixel) and any "blur" filters positioned between the lens and sampling aperture, and $MTF_{rf}(s)$ is the MTF of the reconstruction function, which will include the effects of the associated detector electronics and, if necessary, any display. $MTF_{ap}(s)$ is in fact the modulus of the Fourier transform of the output signal from a single pixel, as a narrow slit is scanned across the pixel and neighboring pixels, with a correction applied for the width of the slit.

ISO 11529[1] and Williams[2] describe several ways of measuring this MTF. Some of these are more convenient than others when wishing to test a thermal imaging camera. Most of the techniques described in Section 7.4.6 in connection with measuring the MTF of detector arrays can also be applied to measuring the MTF of a complete thermal imager where aliasing is a concern. Actual arrangements for doing such measurements on complete thermal imagers are covered in Chapter 8. The techniques where a slit is scanned are suitable for providing data from which the various aliasing parameters can be calculated.

An MTF measurement technique that is similar in principle to the sloping slit method described in Section 7.4.6, but using an edge rather than a slit, has been described in ISO 12233.[5] The method is specified for measuring the MTF of digital still cameras, but could be readily adapted to testing thermal imaging cameras.

REFERENCES

1. *ISO 15529: 2007 Optics and photonics—Optical transfer function—Principles of measurement of modulation transfer function (MTF) of sampled imaging systems.*
2. Williams, T. L. 1999. *The optical transfer function of imaging systems.* Bristol and Philadelphia: IOP Publishing.
3. Wittenstein, W., et al. 1982. The definition of the OTF and the measurement of aliasing for sampled imaging systems. *Optica Acta* 29:41–50.
4. *ISO 9334: 1995 Optics and photonics—Optical transfer function—Definitions and mathematical relationships.*
5. *ISO 12233: 2000 Photography—Electronic still-picture cameras—Resolution measurements.*